BIOINFORMATICS CHARACTERIZATION OF THE MOLECULAR PATHWAYS IMPACTED BY IMMUNE CHALLENGES IN THE AMYGDALA

BY

MARISSA RACHEL KEEVER-KEIGHER

DISSERTATION

Submitted in partial fulfillment of the requirements
for the degree of Doctor of Philosophy in Animal Sciences
in the Graduate College of the
University of Illinois Urbana-Champaign, 2021

Urbana, Illinois

Doctoral Committee:

Professor Sandra Rodriguez-Zas, Chair
Professor Gustavo Caetano-Anolles
Professor Matthew B. Wheeler
Associate Professor Maria Bonita Villamil

ABSTRACT

Intrauterine environment during pregnancy plays a critical role in fetal development, and environmental stressors and pathogens that elicit an immune response in the mother have the ability to influence critical processes within the fetus during development. This maternal immune activation (MIA) can have lasting effects on the fetus and has been associated with neurological and behavioral deficits often seen in neurodevelopmental, neurodegenerative, and mood disorders. The amygdala, a structure located in the forebrain, plays a central role in many processes associated with these disorders, as well as an individual's response to stressors. In these studies, high-throughput RNA sequencing along with bioinformatics approaches were used to characterize the transcriptomic changes in the amygdala of pigs subject to viral-elicited MIA compared to control pigs. We investigated how the amygdalar transcriptome between MIA and control pigs was altered with respect to sex; in the presence of a second, post-natal stressor; and how transcripts were differentially alternatively spliced between MIA and control pigs within sex. Functional enrichment analysis provided insight into affected pathways, while protein-protein interaction networks identified non-canonical relationships impacted by MIA. Additionally, complementary analyses, such as transcription factor enrichment analysis, which was performed to investigate the interaction between MIA and a post-natal stressor (i.e. weaning) aided in identifying shared transcription factors among dysregulated genes. Our approaches revealed lasting and sex-dependent changes to the transcriptome of the amygdala following MIA, altered transcription in the amygdala in response to weaning stress following MIA, and aberrant alternative splicing in the amygdala of both male and female pigs exposed to MIA. Investigation of the affected genes and pathways involved confirmed the link between MIA and neurological and behavioral disorders.

ACKNOWLEDGMENTS

I would like to thank all the people who have helped make this possible. First and foremost, I would like to thank my wife, Amy Keigher; your constant support gave me the confidence to keep going, and without you I would not be where I am today. Additionally, I am thankful for the support of my family, who have always been there to lend an ear when I needed it.

I am also immensely grateful to my advisor, Dr. Sandra Rodriguez-Zas, for allowing me to be a part of her lab. Your enthusiasm and love of research are contagious. Thank you so much for sharing your knowledge and expertise with me and for taking the time to make me a better researcher.

I would like to thank my lab mates and coworkers, who have made my time here so enjoyable, especially my dear friend Shannon Maxey. You have always been there for me from the first time I wandered into your office as an undergraduate to make copies.

Lastly, my sincerest thanks to my committee members, Dr. Gustavo Caetano-Anolles, Dr. Matthew Wheeler, and Dr. Maria Bonita Villamil.

TABLE OF CONTENTS

Chapter 1: Review of Literature

1.1 Introduction

Infectious agents and environmental stressors have the ability to elicit an immune response within the mother during gestation. The ensuing changes in cytokine signaling can alter the overall developmental trajectory of the fetus and, ultimately, brain development (Odorizzi and Feeney, 2016; Prins et al., 2018), which has been linked to increased incidence of neurodevelopmental and neurodegenerative disorders later in life.

1.2 Porcine Reproductive and Respiratory Virus

A significant stressor during gestation for pigs is the porcine reproductive and respiratory virus (PRRSV), an enveloped single-stranded RNA virus discovered in the Netherlands in the early 1990s (Wensvoort et al., 1991). This virus causes respiratory disorders in growing pigs, while inducing reproductive failure in gestating females. PRRSV increases serum levels of the proinflammatory cytokines interleukin 1 beta (IL-1β), interleukin 6 (IL-6), and tumor necrosis factor alpha (TNF-α) within the animal (Antonson et al., 2017). Today, the PRRSV affects the swine industry worldwide, and in 2013 the loss associated with pig performance, clinical effects, and pig inventory were estimated at $664 million (Holtkamp et al., 2013); however, these estimate likely underestimate the true cost of PRRSV, as studies indicate the exposure of the offspring to PRRSV-induced MIA has lasting impacts of the developmental success of the piglets (Antonson et al., 2017; Keever et al., 2020).

1.3 The Effects of Maternal Immune Activation

Two popular animal models of maternal immune activation (MIA) are elicited by administrating doses of the viral mimetic polyinosinic:polycytidylic acid [Poly(I:C)] or the bacterial endotoxin lipopolysaccharide (LPS) during gestation. Poly(I:C) is a synthetic double-stranded RNA that mimics the product of viral replication and acts as a ligand for toll-like receptor 3 (TLR3) (Alexopoulou et al., 2001), which is a mediator of the innate immune response (Schulz et al., 2005). LPS, a molecule found on the outer membrane of Gram-negative bacteria, activate the innate immune response through toll-like receptor 4 (TLR4) (Ulevitch and Tobias, 1995). These models have been confirmed to induce behaviors associated with neurodevelopmental disorders, like schizophrenia spectrum disorders (SSD) and autism spectrum disorders (ASD), and neurodegenerative disorders, such as Alzheimer's disease (AD), in offspring (Knuesel et al., 2014; Canetta et al., 2016; Mattei et al., 2017b). SSD is characterized in the fifth edition of the Diagnostic and Statistical Manual of Mental Disorders (DSM-5) by at least two of the following behaviors for a significant period of time over the course of a one-month period: 1) delusions, 2) hallucinations, 3) disorganized speech, 4) grossly disorganized/catatonic behavior, and 5) negative symptoms; at least one symptom must be of the type listed in one through three. The DSM-5 describes individuals with ASD as a) having deficits in: social reciprocity, nonverbal communication, and interpersonal relationships and b) having at least two of the following: stereotypical behavior, aversion to change, extremely restricted interests, and hyper- or hypo-reactivity to sensory stimuli. The DSM-5 currently recognizes two syndromes associated with AD: major and minor neurocognitive decline. In the former, cognitive decline is severe enough to interfere with the independence of the individual, whereas, in the latter, the cognitive decline is not marked enough to interfere with an individual's ability to function independently.

MIA models have demonstrated alterations to gene expression networks and pathways within the brains of the offspring that are associated with neural circuitry and morphological abnormalities related to SSD, ASD, and AD. Administration of LPS to gestating rats resulted in under-expression of genes related to the migration of inhibitory GABAergic interneurons and neurodevelopment within the brains of offspring (Oskvig et al., 2012). Additionally, Poly(I:C)-induced MIA in mice has resulted in deficits in central nervous system development (Ibi et al., 2013) and increased the strength of excitatory glutamatergic projections from the frontal cortex into the amygdala of mice (Li et al., 2018a), a region that is critical to an individual's response to both environmental and social stressors.

1.4 The Roles of the Amygdala

The amygdala regulates responses to pathogen infection and environmental stressors (Tian et al., 2015). This structure is an almond-shaped cluster of nuclei located in the forebrain within the medial temporal lobe of each hemisphere (LeDoux, 2007) and plays a central role in social interaction, cognition, neuroendocrine, behavior, learning, memory, emotion, and autonomic systems. The amygdala is also involved in regulation of several dimorphic functions such as aggression, sexual behavior, gonadotropin secretion, and integration of olfactory information (Hines et al., 1992), as it is connected to other sexually dimorphic nuclei and experiences high uptake of gonadal hormones. This sexually dimorphic nature of the amygdala is supported by the differential activation of the amygdala to stimuli between males and females (Killgore and Yurgelun-Todd, 2001), including differences in the sexual responses, emotional memory (Hamann, 2005), and differential vulnerability to insult (Baird et al., 2007). As the amygdala is well-connected to other brain regions and integral to many regulatory functions, interference with

normal development of this structure can affect social, locomotor, and feeding behavior (Petrovich and Gallagher, 2003); growth and reproductive physiology; health status; and immunological response to secondary stressors.

1.5 Weaning

Weaning encompasses social, physical, and environmental stresses (Curley et al., 2009; Campbell et al., 2013). The separation of the offspring from their mother and familiar littermates, the physical handling and transport, co-mingling of unfamiliar individuals, new surroundings, and new feeding strategies can all contribute to the stress experienced by weaned rodents and pigs (Curley et al., 2009; Campbell et al., 2013).

Weaning is a stressful event that is accompanied by hormonal and immunological changes (Pie et al., 2004; Gimsa et al., 2018). Marked increases in plasma lymphocytic trapping and cortisol level were detected in one day after weaning in pigs (Kick et al., 2012). Decreases in the concentrations of T cells, B cells, and natural killer cells in response to a stressful event corresponding with lymphocytic trapping were also observed in mice (Kick et al., 2012). A review of stress effects on pigs (Gimsa et al., 2018) highlighted the association of weaning with lower glucocorticoid receptor (GR) binding in the hippocampus and amygdala of one-month-old pigs (Kanitz et al., 1998). Also, weaning together with isolation was associated with lower levels of the hydroxysteroid dehydrogenase enzyme that processes glucocorticoids, GR, and mineralocorticoid receptor (MR) in the prefrontal cortex of 2-3 week old pigs (Poletto et al., 2006).

1.6 RNA Sequencing

High throughput sequencing methods have made it possible to investigate transcriptomes by generating sequence data at a depth of tens-of-millions of reads per sample. Preparation of RNA sample for next generation sequencing requires total RNA extraction from tissues, RNA purification to remove contaminants, such as proteins, depletion of ribosomal RNA, and selection of mRNA, if total RNA is not desired. RNA must be fragmented into 200-500 bp sections, and a cDNA library is created from fragments, with adapter indices ligated to the end of the cDNAs. The adapter at the end of the cDNA allow the fragment to hybridize to complementary oligos on the lane of a flow cell. Additionally, they are later used for identification of sample-of-origin so that samples may be demultiplexed after sequencing. Once cDNAs hybridize with the oligos on the flow cell via their adapters, the sequences are amplified by repeated replication and reverse strands are cleaved and washed away to created clonal clusters. The sequence of these clonal clusters are determined via sequencing by synthesis, where fluorescently labeled base pairs compete for complementary binding to the strands of the amplified cDNA, a light is used to excited the fluorescent label, and a high-speed camera records the signal from each clonal cluster. The computer records data regarding fluorescent color, corresponding to a specific nucleotide, and signal quality (Wang et al., 2009b; Zhong et al., 2011).

The large datasets created through high-throughput sequencing present a unique problem. Following the generation of this data tens of millions of reads per sample need to be evaluated, and biological significance needs to be extracted the data to understand its meaning.

1.7 Bioinformatics Approaches

Quality control

RNA sequence data from high-throughput experiments is stored by the computer reading the SBS data in a text-based file called a FASTQ file. The FASTQ files contain sequence information, as well as quality information generated for each base called by the computer. Quality information stored in the file can then be used to remove poor-quality bases using a tool that reads the coded quality scores, such as FASTQC (Andrews, 2010).

Alignment

Generating count data from RNA-seq output is a key process for downstream analysis. In this step data may be aligned to a genome using a program such as STAR (Dobin et al., 2013), or they may be analyzed for transcriptome compatibility with pseudoalignment using a program like Kallisto (Bray et al., 2016). While both methods produce similar results, pseudoalignment cuts down considerably on computation time and memory (Bray et al., 2016)

Rather than expending computational time and memory determining the exact location in the genome from where a read originated, Kallisto determines which transcripts likely produced the read. A three-step approach is employed by Kallisto. First the transcript file provided to Kallisto is broken down into short sequences of length k (k-mers). These k-mers are used to build a transcript de Bruijn graph (T-DBG), where contigs are the set of k-mers within the T-DBG belonging to the same transcript. Next, k-mers of RNA-seq reads are compared to the T-DBG to determine the intersection of the transcripts that the read-derived k-mer is compatible with. This process is able to save time by skipping nodes (i.e., transcript k-mers from T-DBG) that are

redundant in transcript origin. Lastly, Kallisto's quantification step optimizes the following likelihood function to determine transcript abundance:

$$L(\alpha) \propto \prod_{f \in F} \sum_{t \in T} \mathbf{y}_{f,t} \frac{\alpha_t}{l_t} = \prod_{e \in E} \left(\sum_{t \in e} \frac{\alpha_t}{l_t} \right)^{c_e}$$

Here, F represents the set of fragments yielded from reads, while T represents the complete set of transcripts. The $y_{f,t}$ parameter is a compatibility matrix, where 1 indicates if fragment, f, is compatible with transcript, t, and 0 indicates that they are incompatible. The value α_t is the probability of a fragment coming from a transcript, and l_t corresponds to the transcript length. The compatibility matrix is divided to equivalency classes, which is the set of all reads compatible with a same set of transcripts. Then, the expectation-maximization (EM) algorithm is used to maximize the likelihood function and converge on optimal values of α_t (Bray et al., 2016).

Differential Gene Expression Analysis

Differential gene expression (DGE) analysis is used to determine genes of interest. In the R environment, this is typically accomplished with a package, such as edgeR (Robinson et al., 2010). The edgeR package uses a negative binomial distribution for modeling overdispersed count data, and an empirical Bayes approach is used to borrow dispersion information across genes to moderate, or shrink, the degree of overdispersion across all genes (Smyth, 2004).

A critical first step in DGE analysis is count normalization, which aims to minimize the impact of technical bias in the experiment. The default method of normalization in edgeR is the trimmed mean of M-values (TMM) method, which assumes that most genes are not differentially expressed; thus, the aim is to minimize the log-fold changes of genes between samples for most genes, and

the method yields normalization factors by which the library is multiplied (Robinson and Oshlack, 2010).

Following normalization, DGE analysis can be carried out using a generalized linear model in edgeR, allowing the package to handle multifactor experimental designs, and statistical analysis can be performed using the likelihood ratio test (i.e., chi-square test) or a quasi-likelihood F-test (Lun et al., 2016).

Functional Enrichment Analyses

The aim of functional enrichment analysis is to extract biological significance from DGE analysis data and to determine which annotated categories, including biological processes, molecular functions, cellular components, and Kyoto Encyclopedia of Genes and Genomes (KEGG) pathways, are overrepresented or enriched among datasets.

For gene set enrichment analysis (GSEA), the entire list of genes analyzed for the experiment is provided along with expression values (e.g., Log(fold change)). This list is ranked by expression value and then it is determined for each set of genes in a biologically significant category, if that set of genes is distributed evenly throughout an experimental gene list or if the set is primarily found within the top or bottom of the list. An enrichment score (ES) is calculated as a running sum when a gene within the set of interest is encountered in the ranked list, and the magnitude of the sum decreases when genes that are not in the set of interest are encountered. The maximum deviation from zero in a random walk through the list corresponds to the final ES (Subramanian et al., 2005).

The significance of the ES is determined by comparing the actual ES to a null ES. The null ES is calculated by permuting phenotype data and recalculating the ES for a pre-specified number of

times (e.g. 1000). The normalized enrichment score (NES) is then calculated by dividing the actual ES for a set of genes by the mean of the ES for the permutations (Subramanian et al., 2005). Finally, determination of the false discovery rate (FDR) *q*-value is calculated for a value, NES(S), by creating a histogram of all permuted NES values, NES(S,π); finding the percentage of all NES(S,π) values greater than NES(S); finding the percentage of all actual NES greater than NES(S); and dividing the former value by the latter. This step is repeated in a similar manner for negative NESs (Subramanian et al., 2005).

Database for Annotation, Visualization and Integrated Discovery (DAVID) uses a pre-selected set of genes for analysis, which is commonly the list of differentially expressed genes. Then, using the pre-selected set of genes an expression analysis systematic explorer (EASE) value is calculated using a jackknifed one-tailed Fisher hypogeometric exact test. This statistic examines the probability of observing the distribution of a 2x2 contingency table, given all possibilities, with one data point being removed from the set of genes both in the pathway of interest and in the pre-selected gene list (Hosack et al., 2003). Functional clustering can be performed following functional analysis. This process is based on determining the occurrence of common genes between functional annotations, and clustering the annotations with the most common genes together (Huang et al., 2007).

Alternative Splicing Analysis

Along with differential expression of genes, alternative splicing of genes also affects phenotype, and is a popular aspect of the transcriptome to investigate.

RNA-seq data is typically derived from mature mRNA, and therefore, splice information needs to be reconstructed during analysis. LeafCutter is among the most popular tools for the differential

splicing analysis (Li et al., 2018b). This analysis focuses on splicing events that involve the step-wise removal of introns and skipped exons from mRNA; however, unlike other tools, it does not measure isoforms derived from alternative transcription start sites or polyadenylation, which are computationally time-consuming as it requires read assembly and inference when data is ambiguous.

After alignment of RNA-seq data to a reference genome, LeafCutter extracts split-read data from alignment files. That is, read data with a minimum of 6 bp mapped into an exon are extracted, and overlap of extracted introns are compared among reads. From this data, LeafCutter constructs a network, where nodes correspond to introns and edges correspond to shared splice junctions, and connected components of the network represent intron clusters. Introns with no shared splice junctions (i.e., singleton nodes) are discarded, and a Dirichlet-multinomial model is used to identify clusters with differentially excised introns between groups (Li et al., 2018b).

1.8 Aims of Studies

PRRSV-elicited MIA has been established as a model of MIA in pigs; a species that has greater homology to humans compared to rodents and has a high economic value. However, it is not well-known how prolonged MIA effects the molecular pathways of the amygdala with respect to sex, a secondary stressor, and alternative splicing. To address these gaps, the aim of these studies are to a) advance the understanding of the sex-dependent impact of MIA on the molecular mechanisms of the amygdala, b) understand of the effect of the double-hit paradigm on the amygdala gene networks of pigs using PRRSV-elicited MIA and weaning stress, and c) examine the impact that MIA has on alternative splicing within the amygdala.

1.9 References

Alexopoulou L, Holt AC, Medzhitov R, Flavell RA. 2001. Recognition of double-stranded rna and activation of nf-kappab by toll-like receptor 3. Nature. 413(6857):732-738.

Andrews S. 2010. Fastqc: A quality control tool for high throughput sequence data.

Antonson AM, Radlowski EC, Lawson MA, Rytych JL, Johnson RW. 2017. Maternal viral infection during pregnancy elicits anti-social behavior in neonatal piglet offspring independent of postnatal microglial cell activation. Brain Behav Immun. 59:300-312.

Baird AD, Wilson SJ, Bladin PF, Saling MM, Reutens DC. 2007. Neurological control of human sexual behaviour: Insights from lesion studies. Journal of neurology, neurosurgery, and psychiatry. 78(10):1042-1049.

Bray NL, Pimentel H, Melsted P, Pachter L. 2016. Near-optimal probabilistic rna-seq quantification (vol 34, pg 525, 2016). Nature Biotechnology. 34(8):888-888.

Campbell JM, Crenshaw JD, Polo J. 2013. The biological stress of early weaned piglets. J Anim Sci Biotechno. 4.

Canetta S, Bolkan S, Padilla-Coreano N, Song LJ, Sahn R, Harrison NL, Gordon JA, Brown A, Kellendonk C. 2016. Maternal immune activation leads to selective functional deficits in offspring parvalbumin interneurons. Mol Psychiatry. 21(7):956-968.

Curley JP, Jordan ER, Swaney WT, Izraelit A, Kammel S, Champagne FA. 2009. The meaning of weaning: Influence of the weaning period on behavioral development in mice. Dev Neurosci-Basel. 31(4):318-331.

Dobin A, Davis CA, Schlesinger F, Drenkow J, Zaleski C, Jha S, Batut P, Chaisson M, Gingeras TR. 2013. Star: Ultrafast universal rna-seq aligner. Bioinformatics. 29(1):15-21.

Gimsa U, Tuchscherer M, Kanitz E. 2018. Psychosocial stress and immunity-what can we learn from pig studies? Front Behav Neurosci. 12.

Hamann S. 2005. Sex differences in the responses of the human amygdala. Neuroscientist. 11(4):288-293.

Hines M, Allen LS, Gorski RA. 1992. Sex differences in subregions of the medial nucleus of the amygdala and the bed nucleus of the stria terminalis of the rat. Brain Res. 579(2):321-326.

Holtkamp DJ, Kliebenstein JB, Neumann EJ, Zimmerman JJ, Rotto HF, Yoder TK, Wang C, Yeske PE, Mowrer CL, Haley CA. 2013. Assessment of the economic impact of porcine reproductive and respiratory syndrome virus on united states pork producers. J Swine Health Prod. 21(2):72-84.

Hosack DA, Dennis G, Sherman BT, Lane HC, Lempicki RA. 2003. Identifying biological themes within lists of genes with ease. Genome Biol. 4(10).

Huang DW, Sherman BT, Tan Q, Collins JR, Alvord WG, Roayaei J, Stephens R, Baseler MW, Lane HC, Lempicki RA. 2007. The david gene functional classification tool: A novel biological module-centric algorithm to functionally analyze large gene lists. Genome Biol. 8(9).

Ibi D, Nagai T, Nakajima A, Mizoguchi H, Kawase T, Tsuboi D, Kano SI, Sato Y, Hayakawa M, Lange UC et al. 2013. Astroglial ifitm3 mediates neuronal impairments following neonatal immune challenge in mice. Glia. 61(5):679-693.

Kanitz E, Manteuffel G, Otten W. 1998. Effects of weaning and restraint stress on glucocorticoid receptor binding capacity in limbic areas of domestic pigs. Brain Res. 804(2):311-315.

Keever MR, Zhang P, Bolt CR, Antonson AM, Rymut HE, Caputo MP, Houser AK, Hernandez AG, Southey BR, Rund LA et al. 2020. Lasting and sex-dependent impact of maternal immune activation on molecular pathways of the amygdala. Front Neurosci-Switz. 14.

Kick AR, Tompkins MB, Flowers WL, Whisnant CS, Almond GW. 2012. Effects of stress associated with weaning on the adaptive immune system in pigs. J Anim Sci. 90(2):649-656.

Killgore WD, Yurgelun-Todd DA. 2001. Sex differences in amygdala activation during the perception of facial affect. Neuroreport. 12(11):2543-2547.

Knuesel I, Chicha L, Britschgi M, Schobel SA, Bodmer M, Hellings JA, Toovey S, Prinssen EP. 2014. Maternal immune activation and abnormal brain development across cns disorders. Nature Reviews Neurology. 10(11):643-660.

LeDoux J. 2007. The amygdala. Curr Biol. 17(20):R868-R874.

Li Y, Missig G, Finger BC, Landino SM, Alexander AJ, Mokler EL, Robbins JO, Manasian Y, Kim W, Kim KS et al. 2018a. Maternal and early postnatal immune activation produce dissociable effects on neurotransmission in mpfc-amygdala circuits. J Neurosci. 38(13):3358-3372.

Li YI, Knowles DA, Humphrey J, Barbeira AN, Dickinson SP, Im HK, Pritchard JK. 2018b. Annotation-free quantification of rna splicing using leafcutter. Nat Genet. 50(1):151-+.

Lun ATL, Chen YS, Smyth GK. 2016. It's de-licious: A recipe for differential expression analyses of rna-seq experiments using quasi-likelihood methods in edger. Methods Mol Biol. 1418:391-416.

Mattei D, Ivanov A, Ferrai C, Jordan P, Guneykaya D, Buonfiglioli A, Schaafsma W, Przanowski P, Deuther-Conrad W, Brust P et al. 2017. Maternal immune activation

results in complex microglial transcriptome signature in the adult offspring that is reversed by minocycline treatment. Transl Psychiat. 7(5):e1120-e1120.

Odorizzi PM, Feeney ME. 2016. Impact of in utero exposure to malaria on fetal t cell immunity. Trends in Molecular Medicine. 22(10):877-888.

Oskvig DB, Elkahloun AG, Johnson KR, Phillips TM, Herkenham M. 2012. Maternal immune activation by lps selectively alters specific gene expression profiles of interneuron migration and oxidative stress in the fetus without triggering a fetal immune response. Brain Behav Immun. 26(4):623-634.

Petrovich GD, Gallagher M. 2003. Amygdala subsystems and control of feeding behavior by learned cues. Amygdala in Brain Function: Bacic and Clinical Approaches. 985:251-262.

Pie S, Lalles JP, Blazy F, Laffitte J, Seve B, Oswald IP. 2004. Weaning is associated with an upregulation of expression of inflammatory cytokines in the intestine of piglets. J Nutr. 134(3):641-647.

Poletto R, Steibel JP, Siegford JM, Zanella AJ. 2006. Effects of early weaning and social isolation on the expression of glucocorticoid and mineralocorticoid receptor and 11 beta-hydroxysteroid dehydrogenase 1 and 2 mrnas in the frontal cortex and hippocampus of piglets. Brain Res. 1067(1):36-42.

Prins JR, Eskandar S, Eggen BJL, Scherjon SA. 2018. Microglia, the missing link in maternal immune activation and fetal neurodevelopment; and a possible link in preeclampsia and disturbed neurodevelopment? Journal of Reproductive Immunology. 126:18-22.

Robinson MD, McCarthy DJ, Smyth GK. 2010. Edger: A bioconductor package for differential expression analysis of digital gene expression data. Bioinformatics. 26(1):139-140.

Robinson MD, Oshlack A. 2010. A scaling normalization method for differential expression analysis of rna-seq data. Genome Biol. 11(3).

Schulz O, Diebold SS, Chen M, Naslund TI, Nolte MA, Alexopoulou L, Azuma YT, Flavell RA, Liljestrom P, Sousa CRE. 2005. Toll-like receptor 3 promotes cross-priming to virus-infected cells. Nature. 433(7028):887-892.

Smyth GK. 2004. Linear models and empirical bayes methods for assessing differential expression in microarray experiments. Stat Appl Genet Mol Biol. 3:Article3.

Subramanian A, Tamayo P, Mootha VK, Mukherjee S, Ebert BL, Gillette MA, Paulovich A, Pomeroy SL, Golub TR, Lander ES et al. 2005. Gene set enrichment analysis: A knowledge-based approach for interpreting genome-wide expression profiles. P Natl Acad Sci USA. 102(43):15545-15550.

Tian J, Dai HM, Deng YY, Zhang J, Li Y, Zhou J, Zhao MY, Zhao MW, Zhang C, Zhang YX et al. 2015. The effect of hmgb1 on sub-toxic chlorpyrifos exposure-induced neuroinflammation in amygdala of neonatal rats. Toxicology. 338:95-103.

Ulevitch RJ, Tobias PS. 1995. Receptor-dependent mechanisms of cell stimulation by bacterial-endotoxin. Annu Rev Immunol. 13:437-457.

Wang Z, Gerstein M, Snyder M. 2009. Rna-seq: A revolutionary tool for transcriptomics. Nat Rev Genet. 10(1):57-63.

Wensvoort G, Terpstra C, Pol JMA, Terlaak EA, Bloemraad M, Dekluyver EP, Kragten C, Vanbuiten L, Denbesten A, Wagenaar F et al. 1991. Mystery swine disease in the netherlands - the isolation of lelystad virus. Vet Quart. 13(3):121-130.

Zhong S, Joung JG, Zheng Y, Chen YR, Liu B, Shao Y, Xiang JZ, Fei Z, Giovannoni JJ. 2011. High-throughput illumina strand-specific rna sequencing library preparation. Cold Spring Harb Protoc. 2011(8):940-949.

Chapter 2: Lasting and sex-dependent impact of maternal immune activation on molecular pathways of the amygdala[1]

2.1 Abstract

The prolonged and sex-dependent impact of maternal immune activation (MIA) during gestation on the molecular pathways of the amygdala, a brain region that influences social, emotional, and other behaviors is only partially understood. To address this gap, we investigated the effects of viral-elicited MIA during gestation on the amygdala transcriptome of pigs, a species of high molecular and developmental homology to humans. Gene expression levels were measured using RNA-Seq on the amygdala for 3-week old female and male offspring from MIA and control groups. Among the 403 genes that exhibited significant MIA effect, a prevalence of differentially expressed genes annotated to the neuroactive ligand-receptor pathway, glutamatergic functions, neuropeptide systems, and cilium morphogenesis were uncovered. Genes in these categories included corticotropin releasing hormone receptor 2, glutamate metabotropic receptor 4, glycoprotein hormones, alpha polypeptide, parathyroid hormone 1 receptor, vasointestinal peptide receptor 2, neurotensin, proenkephalin, and gastrin releasing peptide. These categories and genes have been associated with the MIA-related human neurodevelopmental disorders including schizophrenia and autism spectrum disorders. Gene network reconstruction highlighted differential vulnerability to MIA effects between sexes. Our results advance the understanding necessary for the development of multifactorial therapies targeting immune modulation and

[1]Marissa R. Keever, Pan Zhang, Courtni R. Bolt, Adrienne M. Antonson, Haley E. Rymut, Megan P. Caputo, Alexandra K. Houser, Alvaro G. Hernandez, Bruce R. Southey, Laurie A. Rund, Rodney W. Johnson, Sandra L. Rodriguez-Zas. Frontiers in Neuroscience 14(2020): 774

neurochemical dysfunction that can ameliorate the effects of MIA on the offspring behavior later in life.

2.2 Introduction

The maternal immune response triggered by pathogens and other environmental stressors during gestation can also elicit an indirect response by the fetal immune cells (Kroismayr et al., 2004; Odorizzi and Feeney, 2016; Prins et al., 2018). Viral infection during gestation, for example, activates a cytokine-related signaling cascade, and molecules from this process can cross the placenta and reach the fetal brain. The resulting maternal immune activation (MIA) can impact fetal developmental processes and exert long-term postnatal effects in the offspring (Rutherford et al., 2014). The relationship between MIA and neurodevelopmental disorders, including schizophrenia spectrum disorders (SSD) and autism spectrum disorders (ASD), and neurodegenerative disorders, such as Alzheimer's disease (AD), in offspring has been established (Knuesel et al., 2014; Canetta et al., 2016; Mattei et al., 2017b). These diseases share some behavior symptoms, comorbidities such as eating disorders, and genetic and environmental (i.e., MIA) agents (Canitano and Pallagrosi, 2017). The previous neurological disorders have been associated with abnormal structure and dysregulation of the amygdala (Schumann et al., 2011; Fernandez-Irigoyen et al., 2014) and share genes and molecular mechanisms including histocompatibility complex (MHC) genes (Anders and Kinney, 2015), glutamatergic and GABAergic-associated genes (Bourgeron, 2009; Marin, 2012; Li et al., 2016), and mitochondrial activity processes (Pieczenik and Neustadt, 2007; Sragovich et al., 2017).

The fetal amygdala is susceptible to inflammatory signals, and the plasticity of this brain structure to MIA can lead to alterations of the developmental trajectory. These disruptions may have long-

lasting and maladaptive consequences for the offspring, due to the significant role that the amygdala plays in many neurological pathways. Located in the forebrain, the amygdala influences social interaction, cognition, neuroendocrine, behavior, learning, memory, emotion, and autonomic systems. The amygdala also modulates the response of these processes to stressors, including pathogenic infections and those resulting from management practices, such as weaning (Tian et al., 2015). The amygdala experiences high uptake of gonadal hormones and is anatomically connected to other sexually dimorphic nuclei. Therefore, this brain region is involved in regulation of several dimorphic functions such as aggression, sexual behavior, gonadotropin secretion, and integration of olfactory information (Hines et al., 1992). Evidence supports the differential activation of the amygdala to stimuli between males and females (Killgore and Yurgelun-Todd, 2001), including differences in the sexual responses and emotional memory (Hamann, 2005), and differential vulnerability to insult (Baird et al., 2007). Due to the interconnected and multi-regulatory nature of this brain structure, insults to the amygdala can impact the individual's social, locomotor, and feeding behavior (Petrovich and Gallagher, 2003); growth and reproductive physiology; health status; and immunological response to secondary stressors.

Recent studies lend support to the link between MIA and altered amygdala function (Carlezon et al., 2019). In mice, MIA elicited by polyinosinic:polycytidylic acid [Poly(I:C)] increased the synaptic strength of glutamatergic projections from the prefrontal cortex to the amygdala (Li et al., 2018a). In open-field tests, mice exposed to MIA spent less time in the center and traveled a higher distance, indicative of a higher anxiety behavior incidence than the control counterparts. These findings suggest that the change in the balance between excitation (glutamatergic) and inhibition (feedforward GABAergic) modified the spike output of amygdala neurons, therefore affecting

brain circuits that could regulate behavior in SSD and ASD. A candidate gene study of the effects of social stress during gestation reported that the expression of a corticotropin-releasing hormone receptor in the amygdala of 10-week-old pigs was higher in females than in males (Rutherford et al., 2014). This study concluded that prenatal stress substantially increased anxiety-related behaviors in female pigs. Studies of the impact of maternal stressors during gestation on specific amygdala molecular profiles and associated neurological or behavioral disorders in the offspring later in life highlight the complexity of the molecular mechanisms underlying the pathophysiology of MIA.

Research on the lasting effects of MIA in pigs complements the insights offered by rodent models (Antonson et al., 2019). The advantages of studying a pig model stem from the greater homology of humans to pigs, rather than to rodents, when considering organ physiology, size, development, and, in particular, brain growth and development processes (Murphy et al., 2014). A pig model that has offered insights into MIA employs porcine reproductive and respiratory syndrome virus (PRRSV) to elicit MIA. This immune challenge activates the microglia (i.e., macrophage-like cells in the brain) and is associated with behavioral changes in neonatal pigs (Antonson et al., 2017; Antonson et al., 2018).

The study of MIA elicited by PRRSV allows for the characterization of the impact of a live viral pathogen that self-replicates in the host, evoking extended activation of immune pathways. PRRSV challenge during gestation is a well-characterized, replicable, and effective method for inducing MIA in pigs (Antonson et al., 2017; Antonson et al., 2018). In addition, PRRSV outbreaks impose a major economic burden to the livestock industry. PRRSV is an enveloped single-stranded RNA virus that infects alveolar macrophages, causing interstitial pneumonia and increased serum

levels of the cytokines interleukin 1 beta, interleukin 6, and tumor necrosis factor alpha (Antonson et al., 2017). The persistent repercussions of MIA on the molecular pathways of the pig amygdala are yet to be investigated. Moreover, the potentially distinct vulnerability to the prolonged effects of MIA between sexes remains unknown.

The overarching goal of the present study is to advance the understanding of the impact of MIA on the molecular mechanisms of the amygdala. Three supporting objectives are explored: (a) characterization of prolonged transcriptome changes elicited by viral MIA in pigs, a species that has high neurodevelopmental homology with human, and food production value; (b) identification of molecular pathways that present differential vulnerability to MIA between sexes; and (c) understanding the effect of MIA on molecular interactions assisted by gene network inference. The findings from these complementary analyses support the use of multiple therapeutic targets to ameliorate the potential detrimental effect of MIA on the offspring physiology and behavior.

2.3 Materials and Methods

Animal Experiments

All experimental procedures used published protocols (Antonson et al., 2017; Antonson et al., 2018). The animal studies were approved by the Illinois Institutional Animal Care and Use Committee (IACUC) at the University of Illinois and are in compliance with the USDA Animal Welfare Act and the NIH Public Health Service Policy on the Humane Care and Use of Animals.

Camborough gilts born and raised at the University of Illinois at Urbana-Champaign herd were inseminated at 205 days of age using PIC 359 boar sperm (Antonson et al., 2017; Antonson et al., 2018). All gilts were PRRSV negative and were moved at gestation day 69 into disease-

containment chambers maintained at 22°C and a 12 h light/dark cycle with lights on at 7:00 AM. The gilts were fed daily 2.3 kg of a gestational diet and had *ad libitum* water access. One week after acclimation, four gilts were intranasally inoculated with live PRRSV strain P129-BV (School of Veterinary Medicine at Purdue University, West Lafayette, IN, United States) using 5 mL of 1×10^5 median tissue culture infectious dose ($TCID_{50}$) diluted in sterile Dulbecco's modified Eagle medium (DMEM; 5 mL total volume). The four gilts in the Control group were intranasally inoculated with an equal volume of sterile DMEM. PRRSV inoculation corresponded to the last third of gestation in pigs and humans, during initiation of rapid fetal brain growth (Antonson et al., 2017; Antonson et al., 2018). PRRSV and Control groups were housed in separate containment chambers.

The rectal temperatures and diet consumption of the gilts were recorded daily until farrowing (Antonson et al., 2017; Antonson et al., 2018). The PRRSV-inoculated gilts were offered the maximum fed daily, and feed refusal was measured. The Control gilts were fed the same amount consumed by the PRRSV-inoculated gilts on the previous day. The daily body temperature and feed intake levels were compared using a mixed-effects model analyzed with PROC MIXED (SAS Institute Inc., Cary, NC, United States). The model included the effects of gilt treatment and replicate while accommodating for heterogeneity of variance between MIA groups.

Farrowing was induced with an intramuscular injection of 10 mg of Lutalyse (dinoprost tromethamine, Pfizer, New York, NY, United States) on gestation day 113 in consideration that the average gestation length is approximately 114 days (Antonson et al., 2017; Antonson et al., 2018). Gilts farrowed in individual farrowing crates of standard dimensions (1.83 ×, 1.83 m). After farrowing, the gilts were fed twice a day up to 5 kg of a nutritionally complete diet for the lactating

period and water remained available *ad libitum*. Pigs received intramuscular injections of iron dextran (100 mg/pig, Butler Schein Animal Health, Dublin, OH, United States) and Excede for Swine (25 mg/pig; Zoetis, Parsippany, NJ, United States) to control for respiratory diseases. The pigs remained with their mothers until postnatal day 22. The body weight of pigs was measured daily and analyzed using a mixed-effects model in SAS, PROC MIXED (SAS Institute Inc., Cary, NC, United States). The model included the effect of MIA and the random effect of gilt, accommodating for heteroscedasticity between pig treatment and sex groups. The impact of MIA was studied at postnatal day 22 because this is a common age to wean pigs. The study of transcriptome profiles from older pigs could be confounded with changes in diet and environment associated with weaning, while profiles from younger pigs would hinder the assessment of the prolonged effects of MIA.

RNA Extraction and Sequencing

A balanced experimental design was studied, including 24 pigs evenly distributed between maternal PPRSV activated (MPA group of pigs) and Control gilts (CON group of pigs), each group encompassing males and females (denoted Ma and Fe, respectively). At postnatal day 22, pigs were removed from the farrowing crate and anesthetized intramuscularly using a telazol:ketamine:xylazine drug cocktail (50 mg of tiletamine; 50 mg of zolazepam) reconstituted with 2.5 mL ketamine (100 g/L) and 2.5 mL xylazine (100 g/L; Fort Dodge Animal Health, Fort Dodge, IA, United States) at a dose of 0.03 mL/kg body weight, following protocols (Antonson et al., 2017).

Following anesthetization, pigs were euthanized using an intracardiac injection of sodium pentobarbital (86 mg/kg body weight, Fata Plus, Vortech Pharmaceuticals, Dearborn, MI, United

States). Pig brains were extracted, the amygdalae were recognized using the stereotaxic atlas of the pig brain (Felix et al., 1999), dissected out, flash frozen on dry ice, and stored at -80ºC following published protocols (Antonson et al., 2019). RNA was isolated using EZNA isolation kit following the manufacturer's instructions (Omega Biotek, Norcross, GA, United States). The RNA integrity numbers of the samples were above 7.5, indicating low RNA degradation. The RNA-Seq libraries were prepared with TruSeq Stranded mRNAseq Sample Prep kit (Illumina Inc, San Diego, CA, United States). The libraries were quantitated by qPCR and sequenced on one lane on a NovaSeq 6000 for 151 cycles from each end of the fragments using NovaSeq S4 reagent kit. FASTQ files were generated and demultiplexed with the bcl2fastq v2.20 conversion software. Paired-end reads (150 nt long) were obtained, and the FASTQ files are available in the National Center for Biotechnology Information Gene Expression Omnibus (GEO) database (experiment accession number GSE149695).

RNA Sequence Mapping and Differential Expression Analysis

The average Phred quality score of the reads assessed using FastQC (Andrews, 2010) was > 35 across all read positions, and therefore, no reads were trimmed. The paired-end reads from the individual samples were aligned to the *Sus scrofa* genome (version Sscrofa 11.1;(Pruitt et al., 2007)) using kallisto v0.43.0 (Bray et al., 2016) with default settings. The normalized (trimmed mean of M-values) gene expression values were described using a generalized linear model encompassing the effects of the MIA group (MPA or CON levels), sex (Fe or Ma levels), and MIA-by-sex interaction and analyzed using edgeR (version 3.1 4.0) in the R v. 3.3.1 environment (Robinson et al., 2010). Genes supported by > 5 transcripts per million (TPM) by each MIA-sex combination were analyzed to ensure adequate representation across comparisons.

Orthogonal pairwise contrasts between MIA and sex groups were evaluated in addition to testing for the effects of MIA-by-sex interaction and main effects of MIA and sex. The four groups compared in the contrasts, identified by treatment followed by the sex levels, are: MPA_Fe, MPA_Ma, CON_Fe and CON_Ma. The P-values were adjusted for multiple testing using the Benjamini-Hochberg false discovery rate (FDR) approach (Benjamini and Hochberg, 1995).

Functional Enrichment and Network Inference

Two complementary approaches were used to identify over-represented functional categories among the genes exhibiting differential expression across MIA and sex groups (Caetano-Anolles et al., 2015; Caetano-Anollés et al., 2016; Gonzalez-Pena et al., 2016a; Gonzalez-Pena et al., 2016b). Functional categories investigated included Gene Ontology (GO) biological processes (BP), GO molecular functions (MF), and KEGG pathways. The Gene Set Enrichment Analysis (GSEA) approach implemented in the software package GSEA-P 2.0 (Subramanian et al., 2007) was used to identify category over-representation with gene over- and under-expressed while considering all genes analyzed. The normalized enrichment score (NES) of the categories in the Molecular Signature Database (MSigDB) was calculated using the maximum deviation of the cumulative sum based on the signed and standardized fold change. The statistical significance of the enrichment was assessed using the FDR-adjusted P-value computed from 1000 permutations.

The over-representation of functional categories was also evaluated among genes that exhibited a significant MIA-by-sex interaction or main effect using the Database for Annotation, Visualization and Integrated Discovery (DAVID 6.8) (Huang et al., 2009). The enrichment of Direct GO categories in the DAVID database was assessed. The *Sus scrofa* genome was used as the background for enrichment testing, and enrichment is reported using the Expression Analysis

Systematic Explorer (EASE) score that was computed using a one-tailed jackknifed Fisher hypergeometric exact test. Functional categories were clustered based on gene annotation, and the statistical significance of clusters is summarized as the geometric mean of the $-\log_{10}$ EASE scores of the categories (Delfino et al., 2011; Serao et al., 2011; Delfino and Rodriguez-Zas, 2013).

Weighted Gene Co-expression Network Analysis and Gene Network Visualization

An approach complementary to the identification of differentially expressed genes was used to uncover co-expression networks using Weighted Gene Co-expression Network Analysis (WGCNA) version 1.68 (Langfelder and Horvath, 2008). The input data were voom-transformed read count values generated using the limma package (version 3.40.2) (Ritchie et al., 2015) in R (version 3.6.1). Genes were filtered to remove those with low expression levels or no variation across samples per developer recommendations. The number of genes used for network analysis was 16,175 genes. Considering potential for interaction patterns, a sex-dependent soft-thresholding power was used to call for network topology analysis. The lowest power values that support a scale-free topology power used were 15 for the CON_Ma-MPA_Ma contrast and 27 for the MPA_Fe-MPA_Ma contrast. The Pearson correlation coefficient of the normalized expression values was used to identify modules of connected genes. The minimum module size was set to 30, with the deepSplit set to 2, and the mergeCutHeight set to 0.15. Module profiles were identified using the correlation between the eigengene of each module and pig group. Enrichment of functional categories among the genes in each module profile was explored with DAVID using the *Sus scrofa* genome as background, and testing included an FDR multiple test adjustment.

Further understanding of the impact of the MIA-by-sex interaction was gained through the reconstruction of gene networks using the BisoGenet package (Martin et al., 2010) in the

Cytoscape platform (Shannon et al., 2003a). Information from gene and protein interactions annotated in databases including BIOGRID, HPRD, DIP, BIND, INTACT, and MINT was used to visualize relationships between genes (Salwinski et al., 2004b; Alfarano et al., 2005; Mishra et al., 2006; Stark et al., 2006; Kerrien et al., 2007; Licata et al., 2012b). Networks highlighting differences in gene levels associated with MIA within sex (i.e., the contrasts MPA_Ma-CON_Ma and MPA_Fe-CON_Fe) were compared. The network framework includes genes that exhibited a significant MIA-by-sex interaction effect (FDR-adjusted $P < 0.1$) and are annotated to enriched functional categories. The framework genes were identified by full nodes with size reflecting the differential expression level between the MPA and CON groups. The network edges depict known molecular relationships curated in the BisoGenet databases. The framework genes were connected through correlated genes listed in the BisoGenet database of molecular interactions that did not reach significant MIA-by-sex interaction effect. The comparison of these networks offered insights into the simultaneous effect of MIA across interacting genes and enabled the detection of shared and distinct co-regulation patterns between MPA and CON pigs across sexes.

2.4 Results

Maternal Immune Activation and Sequencing Metrics

The differences between MPA and CON gilts in rectal temperatures and daily diet consumption indicated the activation of the maternal immune system in response to PRRSV. The difference in body temperature between CON and MPA gilts on gestation day 87 was -1.00°C (standard error 0.35°C; $P < 0.005$). The difference in feed refusal between CON and MPA gilts on gestation day 88 was -927.6 g (standard error 201.2 g; $P < 0.0001$). A significant increase in rectal temperatures and decrease in feed intake ($P < 0.001$) was observed within 48 h of inoculation and returned to

baseline levels within 10 days for body temperature and within 14 days for feed intake. At 21 days of age, CON pigs were 1.20 kg heavier than MPA pigs (standard error = 0.5673; $P < 0.089$) while no significant sex or interaction effects were detected.

The sequencing of the 24 RNA samples produced 6.6 billion sequenced reads, and 69 million paired-end reads per sample. The number of reads was consistent across MIA and sex groups (coefficient of variation < 0.1), and the effects of MIA, sex, and MIA-by-sex interaction were tested on 16,175 genes that surpassed the minimum number of reads per MIA-sex combination.

Transcriptome Changes Associated with Maternal Immune Activation that are Sex-Dependent

Overall, 328 genes exhibited a significant (FDR-adjusted $P < 0.1$) MIA-by-sex interaction effect, and among these, 273 genes had a significant effect at FDR-adjusted $P < 0.05$. The profile of these genes indicated that the effect of MIA differed between females and males. Forty-six genes that presented a MIA-by-sex interaction effect are listed in Table 2.1 together with their expression pattern and P. The majority of the genes in Table 2.1, including neurotensin (NTS), displayed a reversal in the expression level between CON and MPA groups across sexes (i.e., opposite Log_2[fold change] sign across sexes). An extended list including 328 genes that exhibited a MIA-by-sex interaction effect at FDR-adjusted $P < 0.1$ is provided in Table 2.11.

Another frequent pattern among the genes that displayed a MIA-by-sex interaction effect was characterized by a consistent expression profile between CON and MPA across sexes, albeit the magnitude differed between sexes (Table 2.1). For example, glycoprotein hormones, alpha polypeptide (CGA) was over-expressed in CON relative to MPA, but the differential was higher in males than in females. Other genes presenting this pattern included guanylate-binding protein 1

(GBP1), transthyretin (TTR), aldehyde dehydrogenase 1 family member A2 (ALDH1A2), hemoglobin subunit beta (HBB), and basic helix-loop-helix family member e22 (BHLHE22).

Notable is the significant MIA-by-sex interaction effect on genes associated with neuropeptides and hormones, and genes that participate in glutamatergic processes. Genes under-expressed in MPA relative to CON males while presenting the opposite pattern in females (Table 2.1) included NTS, the neuropeptide gene proenkephalin (PENK), the neuropeptide gene gastrin-releasing peptide (GRP), the neuropeptide-related gene vasoactive intestinal peptide receptor 2 (VIPR2), corticotropin releasing hormone receptor 2 (CRHR2), neuron-derived neurotrophic factor (NDNF), reelin (RELN), glutamate metabotropic receptor 4 (GRM4), solute carrier family 17 member 6 (SLC17A6), calcium voltage-gated channel auxiliary subunit alpha 2 delta 3 (CACNA2D3), EF-hand domain family member D1 (EFHD1), glutathione peroxidase 3 (GPX3), parathyroid hormone 1 receptor (PTH1R), thyroid hormone responsive (THRSP), and CGA. The CGA gene codes for the alpha subunit protein of the hormones chorionic gonadotropin (CG), luteinizing hormone (LH), follicle-stimulating hormone (FSH), and thyroid-stimulating hormone (TSH).

Functional and Network Analysis of Genes that Exhibit Sex-Dependent Associations with Maternal Immune Activation

The genes expressing significant MIA-by-sex interaction effects were analyzed for functional enrichment. Table 2.2 presents the clusters of most enriched and informative categories from the DAVID analysis, and the complete list of categories is in Table 2.12. The categories in Table 2.2 encompass genes presenting the most frequent interaction profile characterized by under-expression in CON females relative to males but over-expression in MPA females relative to

males. These genes include KEGG Autoimmune thyroid disease (Cluster 1) and BP brain development (GO:0007420) (Cluster 4).

Enrichment results from GSEA complemented the findings from DAVID. Highly enriched informative categories among genes that have a MIA-by-sex interaction effect are presented in Table 2.3, and the extended list of categories is presented in Table 2.13. The categories in Table 2.3 support pathways in Table 2.2 including ion homeostasis (Table 2.2) and regulation of voltage-gated calcium channel activity processes (Table 2.3). Notably, the enrichment of the neuroactive ligand receptor interaction pathway and the hormone and neuropeptide activity processes include genes such as CGA and VIPR2 that were identified in Table 2.1.

Network visualization furthered the understanding of the impact of MIA on the relationships among genes that exhibited a significant MIA-by-sex interaction effect. The networks in Figures 1, 2 depict the relationships between genes in the enriched neuroactive ligand receptor pathway that highlight the differential expression between CON and MPA in males and females (i.e., CON_Ma-MPA_Ma and CON_Fe-MPA_Fe contrasts), respectively. Red and blue rectangular nodes represent framework genes, and edges represent the known associations between genes based on curated databases of molecular interactions. Red and blue nodes denote over- or under-expression of the gene in CON relative to MPA, and the size is an inverse logarithmic function of the differential expression P-value. The simultaneous study of the differential expression pattern and connectivity among genes highlights the discrepancy in network modules elicited by MIA between the sexes.

Transcriptome Changes Associated with Maternal Immune Activation

Overall, 161 genes exhibited (FDR-adjusted P-value < 0.1) differential expression between MPA and CON pigs, irrespective of sex. Table 2.4 lists notable highly differentially expressed genes, and the complete list is in Table 2.14. The majority of these genes were over-expressed in MPA relative to CON pigs. Among the genes over-expressed in MPA compared to CON pigs were islet amyloid polypeptide (IAPP), ankyrin repeat domain 24 (ANKRD24), interferon-induced transmembrane protein 1 (IFITM1) and 3 (IFITM3), cathepsin C (CTSC), mitogen-activated protein kinase kinase 7 (MAP2K7), heparan sulfate-glucosamine 3-sulfotransferase 5 (HS3ST5), secreted phosphoprotein 1 (SPP1), immunoglobulin heavy chain (IGHG), and transforming acidic coiled-coil-containing protein 1 (TACC1). Among the genes under-expressed in MPA relative to CON pigs are insulin-like growth factor 2 (IGF2), cellular retinoic acid-binding protein 2 (CRABP2), and aldehyde dehydrogenase 1 family member A1 (ALDH1A1).

Functional Analysis of Genes Associated with Maternal Immune Activation

Table 2.5 presents the top significant clusters of informative enriched categories from the DAVID analysis of genes differentially expressed between MPA and CON groups across sexes (the extended list of categories is presented in Table 2.15). Some categories identified by the DAVID analysis are consistent with the categories detected at more significant levels among the genes presenting an MIA-by-sex interaction effect (Table 2.2) and include the BP angiogenesis (GO:0001525) and KEGG autoimmune thyroid disease and Epstein-Barr virus infection pathways (Table 2.5). Also enriched (Table 2.15) were the BP homeostatic (GO:0042592), MF ion binding (GO:0043167), and BP anatomical structure formation in morphogenesis (GO:0048646).

The GSEA enrichment results within the gene expression patterns of CON relative to MPA groups complemented the findings from DAVID. The most informative enriched categories are presented in Table 2.6, and the extended list of categories is presented in Table 2.16. Enriched clusters of genes over-expressed in CON relative to MPA detected by GSEA were the BP enrichment of microtubule bundle formation (GO:0001578) and cilium morphogenesis (GO:0060271).

Transcriptome Differences between Sexes Independent of Maternal Immune Activation

Overall, 150 genes were differentially expressed between males and females (FDR-adjusted $P < 0.05$). These genes exhibited a consistent differential expression between sexes, irrespective of the MIA group. The complete list of genes differentially expressed between sexes at FDR-adjusted $P < 0.1$ is available in Table 2.17, and the majority were over-expressed in males relative to females. Among the previous genes, excluding those that presented MIA-by-sex interaction effect, a selection of informative genes is listed in Table 2.7. Genes over-expressed in males relative to females included eukaryotic translation initiation factor 1A, Y-linked (EIF1AY), leptin receptor (LEPR), luteinizing hormone beta polypeptide (LHB), LIM homeobox 9 (LHX9), luteinizing hormone beta polypeptide (LHB), and immunoglobulin family member 1 (IGSF1).

Informative categories among the DAVID clusters of enriched categories for the genes differentially expressed between sexes are listed in Table 2.8 (a complete list is available in Table 2.18). The previous categories include BP gland development (GO:0048732), response to hormone (GO:0009725), and brain development (GO:0007420).

Weighted Gene Co-expression Network Analysis

The WGCNA study of the correlation between expression and experimental factors was based on the log-transformed TPM expression level of 16,175 genes. This study identified 62 modules of

expression correlated with MIA groups among males. The number of genes in each module ranges from 32 to 1381; Figure 2.3 depicts the relationship between gene modules using a dendrogram. The correlation (corr) between the eigengene expression profile and maternal treatment in males is depicted in Figure 2.4. A fairly even distribution of positive and negative correlation estimates was observed. The genes in the modules pale violet red (corr = -0.58, $P < 0.03$) and gray60 (corr = -0.59, $P < 0.06$) presented a strong negative correlation, indicating that low expression levels were associated with MPA.

The enrichment analysis of the genes in the WGCNA modules provided additional insights into the processes impacted by MIA. The extended list of enriched categories across modules is available in Table 2.19. Table 2.9 lists representative clusters of enriched categories in the gene modules that were highly correlated with MIA differences in males. Complementary categories that were enriched in modules encompassing gene patterns negatively correlated with MPA include the KEGG AD and oxidative phosphorylation pathways in the pale violet red3 and the gray60 modules, MF NADH dehydrogenase activity (GO:0003954) in the gray60 module, and the KEGG ribosomal pathway and associated GO processes in the light yellow module. Confirming the enrichment results from the previous differential expression analysis (Table 2.2, Table 2.12), categories enriched in modules encompassing gene patterns negatively correlated with MPA include the BP ion transport (also in Table 2.2, Table 2.18) in the pale violet red3 and gray60 modules, and BP oxidoreductase activity acting on a heme group of donors (GO:0016675) in the gray60 module (also in Table 2.18).

The WGCNA study identified 61 modules of expression correlated with sex among MPA pigs. The number of genes in each module range from 34 to 2082 and Figure 2.5 depicts the dendrogram

of modules. Positive correlation estimates that indicate higher expression in male than female were identified in the ivory (corr = 0.65, P < 0.03), and antique maroon (corr = 0.62, P < 0.04) modules, whereas negative correlations denoting lower expression in male were identified in sienna3 (corr = -0.65, P < 0.03) (Figure 2.6). Table 2.10 lists representative clusters of enriched functional categories in these modules. Within the ivory module of positively correlated gene patterns, the BP synapse (GO:0007416) and neural development (GO:0007399) were enriched.

2.5 Discussion

The present study uses a validated model of MIA triggered by a live viral (i.e., PRRSV) infection during a critical neurodevelopmental stage (Antonson et al., 2017) to gain innovative insights into sex-dependent molecular changes in the amygdala. The changes in gilt body weight and temperature within 2 weeks postinfection were consistent with the mode of action of the PRRSV and previous reports (Antonson et al., 2017). These results indicate that the PRRSV-infected gilts experienced extended activation of inflammatory pathways during gestation. The present study characterized the prolonged effect of the MIA, 60 days after exposure, on 3-week-old offspring.

Our study identified patterns of differential gene expression and prevalently dysregulated gene networks and processes, some of which have been reported in clinical and preclinical studies of AD, ASD, and SSD (Malkova et al., 2012; Xuan and Hampson, 2014; Aavani et al., 2015). These disorders have been associated with MIA and amygdala functions, yet the corresponding neurological and molecular changes have been studied mostly using pathogen mimetic challenges on rodents (Xuan and Hampson, 2014; Aavani et al., 2015). Moreover, our study identified sex-dependent molecular patterns that are consistent with the differential prevalence and symptoms of ASD, SSD, and MIA-related disorders between sexes reported in rodent and human studies

(Wischhof et al., 2015). For example ASD tends to be more prevalent in young males (Kirsten et al., 2010; Haida et al., 2019), while SSD tends to be more prevalent in females (Bale et al., 2010; Bale, 2011). Similarly, lower sociability and preference for social novelty were observed in 2-week-old pigs from gilts inoculated with PRRSV at gestation day 76 than from control gilts (Antonson et al., 2017). A discussion of the molecular mechanisms impacted by MIA can offer insights into therapies to ameliorate the lasting effects on physiology and behavior.

Sex-Dependent Transcriptome Changes Associated with Maternal Immune Activation

The evaluation of the 328 genes presenting a significant MIA-by-sex interaction effect augmented the understanding of the differential response of transcripts to MIA between sexes (Table 2.1, Table 2.11). The majority of the previous genes were under-expressed in MPA relative to CON males, and the profile in females was opposite or less extreme. Many genes presenting a significant MIA-by-sex effect code for neuropeptides and hormones, or participate in glutamatergic processes.

The lower NTS levels in the amygdala of male rats associated with lower conditioned place preference (Laszlo et al., 2010) is consistent with the lower level of NTS transcripts in MPA males observed in the present study (Table 2.1). The under-expression of neuropeptide gene POMC in MPA relative to CON males (Table 2.1) may be associated with the changes in POMC-related peptide transmission that has been reported in the brains of patients diagnosed with SSD (Jamali and Tramu, 1997). The under-expression of the neuropeptide gene PENK in MPA relative to CON males (Table 2.1) is in agreement with lower levels of PENK expression in the brains of mice models of SSD (Gottschalk et al., 2013). PENK was also differentially expressed in the amygdala of an ASD rat model using prenatal valproic acid exposure (Oguchi-Katayama et al., 2013). Valproic acid treatment during pregnancy was associated with a sevenfold increase in ASD

incidence, social difficulties, and reduced attention (Roullet et al., 2013). Also, CACNA2D3 was under-expressed in the amygdala of rats exposed prenatally to valproic acid and coincided with social behavior abnormalities including heightened anxiety (Barrett et al., 2017). In the present study, the interaction pattern of CACNA2D3 was characterized by under-expression in MPA relative to CON males (Table 2.1).

The over-expression of the neuropeptide receptor VIPR2 in the amygdala of MPA relative to CON females (Table 2.1) is consistent with reports that duplications in this gene confer a significant risk for SSD (Morris and Pratt, 2014). The differential expression of the VIP receptor is particularly important because GABAergic interneurons in the amygdala express the neuropeptide VIP that facilitates cell firing (Rhomberg et al., 2018) and maintains the balance of pro- and anti-inflammatory cytokines (Martinez et al., 2020). The under-expression of GPX3 in MPA relative to CON males (Table 2.1) is consistent with the association between GPX3 gene expression and SSD (Zhao et al., 2018).

The sex-dependent response to MIA of hormone receptor CRHR genes detected in our study (Table 2.1) has been also reported by others. The expression of CRHR1 in the amygdala of 10-week-old female pigs from sows exposed to a social stressor during mid-gestation was higher than in pigs from control gilts, whereas no stressor effects were observed in males nor in the expression of CRHR2 (Rutherford et al., 2014). Also, the expression of CRHR was associated with SSD (Mistry et al., 2013). The alignment between the profiles of the CRHR2 and neuropeptide GRP genes observed in our study (Table 2.1) is in agreement with reports of simultaneous release of CRH and GRP in the amygdala of rats elicited by the stress hormone corticosterone (Merali et al., 2008). The over-expression of the parathyroid hormone receptor PTH1R gene in response to MIA

(Table 2.1) is consistent with the over-expression of this gene in SSD and AD (Ibanez et al., 2014). The over-expression of the functionally related thyroid hormone responsive gene THRSP in MPA relative to CON females further supports the PTH1R pattern (Munshi and Rosenkranz, 2018).

Several genes in the glutamatergic and GABAergic pathways displayed sex-dependent MIA effects (Table 2.1). This shared pattern may stem from pro-inflammatory cytokines intensifying glutamatergic release by the amygdala in a sex-dependent manner. The glutamate receptor GRM4 was under-expressed in MPA relative to CON males, while a less extreme and opposite trend was detected in females (Table 2.11). Supporting our finding, the expression of glutamate receptor genes was lower in SSD brains (Meador-Woodruff and Healy, 2000). The pattern differences between sexes could be connected with differences in gene expression across sexes in multiple GRM genes including GRM4 in association with behavior disorders (Gray et al., 2015). The expression pattern of SLC17A6, a gene in the glutamatergic pathway, was consistent with that of GRM4 (Table 2.1). Moreover, NDNF and RELN (two genes in the GABAergic pathway) displayed similar expression patterns in our study in agreement with previous reports (Hou and Capogna, 2018). NDNF interneurons evoke inhibitory postsynaptic potentials mediated by GABA receptors. Also, the GABAergic gene RELN has been associated with ASD and SSD (Canitano and Pallagrosi, 2017) and is under-expressed in the prefrontal cortex of subjects diagnosed with SSD (Fatemi et al., 2005). Consistent with our results, genes that regulate neural migration of GABAergic interneurons were under-expressed in the brain of offspring from rats exposed to lipopolysaccharide (LPS)-induced MIA (Oskvig et al., 2012). The activity of GABA and glutamate on serotonergic neurons is modulated by chemokine ligands such as CXCL12 (Stuart and Baune, 2014), and consistent with this interaction, CXCL12 and CXCL13 were under-expressed in MPA relative to CON males (Table 2.1, Table 2.11). Our results are also consistent with findings that

LPS injection of adult mice dysregulated CXCL12, which in turn increased glutamatergic release in the amygdala, and anxiety-like behavior occurrence (Yang et al., 2016). EFHD1, a calcium binding protein associated with synaptic transmission and levels of gamma glutamyltransferase was over-expressed in MPA relative to CON females (Table 2.11). This gene was also over-expressed in the amygdala of patients diagnosed with SSD (Chang et al., 2017).

Among the 16,175 genes tested for differential expression in the present study, the profile of several proinflammatory and neuroinflammatory genes were consistent with those from a candidate gene study of the amygdala from 9-day-old mice exposed to MIA (Carlezon et al., 2019). Consistent with the patterns observed in mice exposed to viral mimetic Poly(I:C) MIA (Carlezon et al., 2019), an interaction between PRRSV-elicited MIA and sex was detected in pigs for the genes glial fibrillary acidic protein (GFAP), nitric oxide synthases 1 and 2 (NOS1 and NOS2, respectively), and translocator protein (TSPO)-associated protein ($0.006 < P < 0.02$). These patterns, albeit consistent, failed to surpass the FDR-adjusted $P < 0.05$ threshold. Also consistent with the MIA study of mice amygdala (Carlezon et al., 2019), the differences in expression between MPA and CON males for tumor necrosis factor alpha (TNF-α), and interleukin 1 beta (IL-1β) were not statistically significant. The expression levels for interleukin 6 (IL-6) and interleukin 1 beta (IL-1β) among MPA males were below the minimum threshold for testing, and therefore, the interaction effects for these genes are not reported. IL-6 and IL-1β were differentially expressed between MIA groups in female mice (Carlezon et al., 2019); however, the reported relative abundances for these genes suggests that MIA male mice, like MPA male pigs, presented the lowest levels of IL-6 and IL-1β abundance of all groups studied.

The pattern of several genes presenting a MIA-by-sex interaction effect was characterized by the same relative abundance between MIA groups, albeit sexes differed in magnitude (Table 2.1). Males presented a more extreme under-expression of CGA in MPA relative to CON than females (Table 2.1). This difference could be associated with the participation of CGA in multiple hormone processes that regulate female reproductive performance. The lower impact of MIA on the CGA levels in females may prevent the dysregulation of multiple downstream processes associated with reproductive function. Likewise, the under-expression of TTR in MPA relative to CON was more acute in males than in females (Table 2.1). Over-expression of TTR was noted in the amygdala of rats treated with MK-801, a N-methyl-D-aspartate antagonist that elicits SSD-like behavior (Matsuoka et al., 2008). The differential expression of HBB and GBP1 among MIA groups detected in our study are also observed in the amygdala of SSD cases (Chang et al., 2017).

Functional Analysis of Sex-Dependent Maternal Immune Activation Transcriptome

The study of over-represented functional categories among the genes presenting sex-dependent profiles between MPA and CON pigs (Tables 2.2, 2.3, 2.12 and 2.13) identified categories consistent with previous studies of MIA and amygdala inflammation. The enrichment of the KEGG pathways related to autoimmune disease and antigen processing and presentation via histocompatibility complex (MHC) (Table 2.2, Table 2.12) are in agreement with the reported association between autoimmune diseases, SSD, and variants in the MHC gene family (Anders and Kinney, 2015). Autoimmune reactions are capable of inducing psychiatric symptoms that are mediated by the amygdala such as those associated with SSD (Lennox et al., 2012). Genes annotated to MHC receptor activity are over-expressed in the amygdala of individuals that have SSD (Chang et al., 2017). The cytokine-mediated signaling pathway was also over-represented among the genes under-expressed in MPA relative to CON pigs (Table 2.3). Consistent with our

results, the expression of 28 genes annotated to immune stimulus had MIA-by-sex interaction effects in the microglia of gestation day 97 fetuses after gestation day 76 PRRSV injection (Antonson et al., 2019).

Multiple BPs associated with homeostasis and extracellular matrix assembly were enriched among the genes presenting a significant MIA-by-sex effect (Tables 2.2, 2.3, 2.12, and 2.13). This finding is in agreement with the deficit in perineuronal nets in the amygdala of patients diagnosed with SSD (Paylor et al., 2016). These nets are extracellular matrix structures that support the high metabolic demand of the interneurons, and contribute to ion homeostasis around them.

The enrichment of BP axon and brain development among the genes presenting an MIA-by-sex effect (Table 2.2, Table 2.12) is consistent with a report that LPS-elicited MIA is associated with under-expression of neurodevelopmental genes in the rat fetal brain, including genes linked to ASD (Oskvig et al., 2012). Furthermore, the amygdala of rats prenatally exposed to valproic acid, a stressor that leads to ASD, presented activation of neuron development pathways (Barrett et al., 2017). Similarly, the KEGG pathway of cell-adhesion molecules (CAMs), molecules that are fundamental for nervous system development and maintenance, was enriched among the genes presenting a sex-dependent MIA effect. This pathway was also enriched among genes under-expressed in the brain of rats exposed to LPS-triggered MIA and among genes under-expressed in the cortex of patients diagnosed with ASD (Lombardo et al., 2018).

The KEGG pathway neuroactive ligand receptor interaction was enriched among the genes presenting a significant interaction effect characterized by under-expression in the amygdala of CON relative to MPA males (Table 2.3). This pattern is aligned with findings that Poly(I:C)-elicited MIA augmented the synaptic strength of glutamatergic projections from the frontal cortex

into the amygdala of mice (Li et al., 2018a). The neuroactive ligand receptor pathway encompasses neuroreceptor genes such as dopamine, serotonin, GABA, and glutamate receptors.

The impact of sex-dependent MIA effects on neuropeptide and hormone genes (e.g., CGA, POMC, and SSTR1) expressed in the amygdala is evidenced by the enrichment of GnRH signaling pathway and hormone activity among the genes under-expressed in MPA relative to CON pigs (Table 2.2, Table 2.12). Our results suggest that the disruption of glucocorticoid hormone balance on the HPA axis initiated by MIA can have long-lasting effects because amygdala processes are regulated by glucocorticoid receptors and glucocorticoids repress GnRH secretion.

Impact of Maternal Immune Activation on Gene Networks within Sex

Further understanding of sex-dependent effects of MIA on the co-expression of gene sets was gained from the identification of WGCNA modules of genes that share relative expression profiles between the CON and MPA groups in males (Table 2.9) or that share relative expression profiles between sexes in MPA pigs (Table 2.10). The WGCNA gene modules profiling changes between MIA groups in males uncovered enrichment of genes annotated to AD (Table 2.9). This result is consistent with findings of common molecular mechanisms shared between SSD and AD (Prestia, 2011; Sumitomo et al., 2018). Likewise, the enrichment of ATP metabolic processes among the module of genes associated with MIA effects in males is in agreement with evidence that mitochondrial dysfunction associated with SSD (Prabakaran et al., 2004).

Insights into the distinct vulnerability to MIA between sexes on the interplay between critical genes was gained from the study of the network of genes that had a significant MIA-by-sex effect in the enriched neuroactive ligand receptor pathway. The comparison of Figures 2.1 and 2.2 highlights the distinct interaction between genes in response to PRRSV in males and females,

respectively. Notably, males present a strong and consistent over-expression (i.e., red color) of genes in CON relative to MPA, with the exception of SSTR1. On the other hand, females present a weaker expression differential with a slight majority of genes under-expressed (i.e. blue color) in CON relative to MPA pigs. These results suggest lower vulnerability to MIA effects on gene expression in females than in males at 3 weeks of age. An example of this pattern is the module of the neuropeptide receptors, angiotensin II receptor type 1 (AGTR1), and PTH1R. The co-expression of these two G-coupled receptors is consistent with the shared metabolic function (Regard et al., 2008). Distinct to the opposite patterns between sexes observed in the previous network cluster, the highly connected CGA and GH1 are over-expressed in CON relative to MPA in both sexes, albeit the differences are more extreme in males than in females. Correlated under-expression of GH1 and CGA was observed in the cerebellum and prefrontal cortex of rats that presented altered depressive-like behavior (Yamamoto et al., 2015).

Sex-Independent Associations between Maternal Immune Activation and Transcriptome Changes

The 161 differentially expressed genes between MPA and CON pigs (Table 2.4, Table 2.14) included genes supported by previous studies of MIA. Additionally, the differential expression of several genes in Table 2.4 has been linked to neurological disorders such as SSD, ASD, and AD. The over-expression of ANKRD24 in MPA relative to CON pigs (Table 2.4) is supported by the over-expression of an ankyrin repeat domain family member (ANKRD32) in rat fetal brains exposed to MIA elicited by LPS (Oskvig et al., 2012). IFITM3, IFITM1, and CTSC were over-expressed in the amygdala of MPA relative to CON pigs (Table 2.4). Similarly, these genes were over-expressed in the amygdala of individuals diagnosed with SSD (Takao et al., 2012; Chang et al., 2017). Consistent with our results, IFITM3 was over-expressed in the hippocampi of neonatal

mice treated with Poly(I:C) that resulted in developmental impairment of the central nervous system and lasting brain dysfunction. Conversely, *Ifitm3*$^{-/-}$ mice treated with Poly(I:C) exhibited normal neural development and did not present neural deficiencies (Ibi et al., 2013). CTSC was also over-expressed in the hippocampus of Shn-2 KO mice that exhibited SSD-like behaviors (Takao et al., 2012). MAP2K7 was over-expressed in MPA relative to CON pigs (Table 2.4), and this gene has been implicated in SSD incidence. MAP2K7 exclusively activates c-Jun N-terminal kinases (JNK) (Lisnock et al., 2000; Zeke et al., 2016), a mediator of the MIA response in the developing fetus that likely contributes to the neurological abnormalities in SSD (Openshaw et al., 2019).

HS3ST5 and SPP1 were over-expressed in the amygdala of MPA compared to CON pigs (Table 2.4), and both genes have been linked to ASD. Consistent with the patterns in our study, the expression of SPP1 in the temporal cortex of humans was higher in individuals diagnosed with ASD compared to controls (Garbett et al., 2008). Indeed, SPP1 participates in multiple immuno-related pathways in neural tissues (Carecchio and Comi, 2011; Brown, 2012). Genome-wide association studies identified a genetic variation near HS3ST5 that was significantly associated with ASD while a single-nucleotide polymorphism within this gene has been associated with SSD (Wang et al., 2009a; Wang et al., 2015).

TACC1, CRABP2, and ALDH1A1 participate in the retinoid signaling and metabolic pathways and were differentially expressed in MPA compared to CON pigs (Table 2.4, Table 2.14). Dysregulation of retinoid pathways may disrupt neural development leading to SSD (Goodman, 1996), and retinoid toxicity and deficiency are associated with central nervous system abnormalities (Maden, 1994). The differential expression of genes in the retinoid pathways is

consistent with the previously described changes in the expression of genes in the thyroid hormone cascades. Defective cross-talk between the retinoid and/or thyroid hormone processes have been associated with the development of SSD (Palha and Goodman, 2006). CRABP2 was under-expressed in MPA compared to CON pigs (Table 2.14) and mutations in this gene have been implicated in SSD (Goodman, 1995). Aldehyde dehydrogenase 1 family member A1 (ALDH1A1) was under-expressed in MPA compared to CON pigs (Table 2.4). ALDH1A1 was under-expressed in the amygdala of neonatal rats exposed to odor-shock conditioning, mimicking the effects of unpredictable early-life trauma and resulting in amygdala dysfunction (Sarro et al., 2014).

IGF2 was under-expressed in MPA compared to CON pigs (Table 2.4), and consistent with our results, the systemic administration of IGF2 reduces ASD phenotypes; promotes normal social interaction, cognition, and executive function; and reduces repetitive behavior (Steinmetz et al., 2018). TTR was over-expressed in the amygdala of MPA compared to CON pigs. Over-expression of TTR was noted in the amygdala of rats treated with MK-801, a N-methyl-D-aspartate antagonist that elicits SSD-like behavior (Matsuoka et al., 2008).

Functional Analysis of Sex-independent Maternal Immune Activation Transcriptome

The functional categories over-represented among the genes differentially expressed between MPA and CON pigs (Table 2.5, Table 2.15) were supported by previous studies of MIA and associated neurodevelopmental disorders. Among these categories was the BP anatomical structure formation involved in morphogenesis and angiogenesis (Table 2.5). This result is consistent with the under-expression of early growth response 1 (EGR1, a regulator of angiogenic factors) in the gestation day 97 fetal microglia of MPA relative to CON pigs of both sexes after gestation day 76 PRRSV challenge (Antonson et al., 2019). Angiogenesis was also enriched

among differentially expressed genes in the frontal cortex of rats that are exposed to valproic acid *in utero* (Hill et al., 2015) to model ASD (Favre et al., 2013). The observed enrichment of the BP angiogenesis was also reported among genes dysregulated in the hippocampal microglia of mice exposed to Poly(I:C) relative to control mice (Mattei et al., 2017a).

Several KEGG pathways associated with inflammation and infection, including allograft rejection, Epstein-Barr virus infection, and autoimmune thyroid disease, were enriched, among the genes differentially expressed between MPA and CON pigs (Table 2.5, Table 2.15). This finding is consistent with the significant effect of MIA from gestation day 76 PRRSV injection on expression of 12 genes in the amygdala of gestation day 97 fetuses from both sexes (Antonson et al., 2019). At this fetal stage, most of the genes differentially expressed between MPA and CON gilts were annotated to the BP immune response, including genes annotated to the BP cytokine-mediated signaling pathway, and to the toll-like receptor pathway (Antonson et al., 2019). This enrichment is in agreement with reports of amygdala inflammation and transcriptome changes in glial cells in response to MIA elicited by LPS administration in mice that persist into adulthood (O'Loughlin et al., 2017).

Many BPs that modulate neurodevelopment were enriched among genes under-expressed in MPA compared to CON pigs, including microtubule bundle formation, cilium morphogenesis, cilium organization, cilium movement, and axoneme assembly (Table 2.6, Table 2.16). Reduced neuronal primary cilia can reduce cellular communication during development, the number of dendrites (Goetz and Anderson, 2010; Guadiana et al., 2013), and can hinder neurogenesis in the adult brain (Amador-Arjona et al., 2011). Furthermore, primary cilia participate in the development of the circuitry of GABAergic interneurons, and disrupted cilia formation leads to dysregulated

excitatory/inhibitory signaling between neurons (Guo et al., 2017). This finding is consistent with the glutamatergic and GABAergic-associated genes that presented a significant MIA-by-sex interaction effect previously discussed (Table 2.1). Disruption of this circuitry underlies the neurological disorders associated with ASD and SSD (Bourgeron, 2009; Marin, 2012; Li et al., 2016), and olfactory neuronal precursors collected from SSD patients were found to have less primary cilia growth *in vitro* compared to controls (Munoz-Estrada et al., 2018).

Main Effect of Sex on Gene Expression and Functional Enrichment

The amygdala is a sexually dimorphic area of the brain that is highly responsive to signaling from gonadal steroid hormones (Hines et al., 1992; Cooke and Woolley, 2005). Supporting this, 150 genes were differentially expressed (Table 2.7, Table 2.17), and most were over-expressed in males compared to females. The activity of the amygdala has been related to cortisol response, immune responses, and hormonal physiology that differs between sexes (Goldstein et al., 2019). The amygdala is a brain region dense in sex steroid, glucocorticoid, and cytokine receptors that are key co-activators of the HPA axis. The amygdala of male mice has more excitatory synapses per neuron compared to female mice (Cooke and Woolley, 2005; Guneykaya et al., 2018).

The enriched KEGG pathway neuroactive ligand-receptor interaction and biological process response to hormone (Table 2.8, Table 2.18) are supported by the evidence indicating that the amygdala development is greatly influenced by sex hormones (Cooke and Woolley, 2005). LHX9 and LHB were strongly over-expressed, while IGSF1 was slightly over-expressed in males compared to females (Table 2.7). The importance of LHX9 in the sexual dimorphism of males and females is highlighted by evidence that *Lhx9*$^{-/-}$ mice fail to produce gonads, and male *Lhx9*$^{-/-}$

resemble females phenotypically (Birk et al., 2000). IGSF1-deficient males have later testosterone secretion than individuals with normal IGSF1 expression (Joustra et al., 2013).

Several developmental BP including gland, embryo, sensory organ, and brain development, along with the MF extracellular matrix structural constituent, were enriched among the genes differentially expressed between sexes (Table 2.8). Supporting these categories, EIF1AY was over-expressed in the amygdala of males compared to females (Table 2.7). Consistent with our results, EIF1AY was over-expressed in the male brain at early childhood, puberty, and adulthood and contributes to the structural sexual dimorphism of the amygdala (Shi et al., 2016).

2.6 Additional Considerations

The results of our study of long-lasting changes in the amygdala transcriptome profiles at approximately 60 days after exposure to PRRSV advanced the understanding of the impact of MIA on molecular pathways associated with neurodevelopmental processes, neurodegenerative diseases, and behavior disorders. Biological processes impacted at in the amygdala of postnatal day 22 pigs were also impacted at other developmental stages such as fetal gestation day 83, 96, or 111 (Antonson et al., 2018; Antonson et al., 2019) including antigen processing and presentation of peptide or polysaccharide antigen via MHC class II and immune response. Likewise, neurodevelopmental processes impacted in the present study were also reported in the amygdala of rats prenatally exposed to MIA by means of valproic acid (Barrett et al., 2017).

Notably, we identified sex-dependent vulnerability to the effects of MIA on gene expression in the amygdala of pigs at postnatal day 22. Sex-independent effects dominated in gestation day 96 fetuses (Antonson et al., 2019). This comparison supports the hypothesis that sex-dependent

effects of MIA in the amygdala become stronger as the animal develops. Additional understanding of MIA effects on the amygdala requires the evaluation of female and male pigs at older ages, in consideration that female pigs reach puberty at 5 months of age. Also, evaluation of the impact of MIA on other brain structures that interact with the amygdala will enable the determination of broader molecular profiles.

2.7 Conclusions

The present study advances the understanding of the prolonged effects of MIA in the molecular pathways of the amygdala, a brain structure key to social, feeding, and other behaviors. The RNA-Seq profiling of 3-week-old female and male pigs, 2 months after viral infection during gestation, offered insights into MIA-associated neurodevelopmental diseases in humans such as ASD and SSD and potential effects in livestock health. The prevalent and sex-dependent dysregulation of genes in immune pathways was detected, supporting established immunotherapies to alleviate the pathophysiology of SSD, ASD, and AD (Busche et al., 2015; Miller and Buckley, 2016).

Our study detected lesser explored molecular processes affected by MIA including the neuroactive ligand-receptor, glutamatergic, amyloid peptides, neuropeptide, retinoid, and ciliogenesis systems. The detection of the previous processes backs the integration of therapies based on immune modulation together with therapies that target neurochemical dysfunction in MIA-associated disorders. The effectiveness of these therapies may be further advanced by our innovative identification of frequently disrupted neuropeptide systems. Our functional and network analyses solidify the promise of multifactorial therapeutic strategies combining immune and neurochemical targets to ameliorate MIA-associated neurodevelopmental and neurodegenerative disorders.

2.8 References

Aavani T, Rana SA, Hawkes R, Pittman QJ. 2015. Maternal immune activation produces cerebellar hyperplasia and alterations in motor and social behaviors in male and female mice. Cerebellum. 14(5):491-505.

Alfarano C, Andrade CE, Anthony K, Bahroos N, Bajec M, Bantoft K, Betel D, Bobechko B, Boutilier K, Burgess E et al. 2005. The biomolecular interaction network database and related tools 2005 update. Nucleic Acids Res. 33(Database issue):D418-424.

Amador-Arjona A, Elliott J, Miller A, Ginbey A, Pazour GJ, Enikolopov G, Roberts AJ, Terskikh AV. 2011. Primary cilia regulate proliferation of amplifying progenitors in adult hippocampus: Implications for learning and memory. J Neurosci. 31(27):9933-9944.

Anders S, Kinney DK. 2015. Abnormal immune system development and function in schizophrenia helps reconcile diverse findings and suggests new treatment and prevention strategies. Brain Res. 1617:93-112.

Andrews S. 2010. Fastqc: A quality control tool for high throughput sequence data.

Antonson AM, Balakrishnan B, Radlowski EC, Petr G, Johnson RW. 2018. Altered hippocampal gene expression and morphology in fetal piglets following maternal respiratory viral infection. Dev Neurosci. 40(2):104-119.

Antonson AM, Lawson MA, Caputo MP, Matt SM, Leyshon BJ, Johnson RW. 2019. Maternal viral infection causes global alterations in porcine fetal microglia. Proc Natl Acad Sci U S A. 116(40):20190-20200.

Antonson AM, Radlowski EC, Lawson MA, Rytych JL, Johnson RW. 2017. Maternal viral infection during pregnancy elicits anti-social behavior in neonatal piglet offspring independent of postnatal microglial cell activation. Brain Behav Immun. 59:300-312.

Baird AD, Wilson SJ, Bladin PF, Saling MM, Reutens DC. 2007. Neurological control of human sexual behaviour: Insights from lesion studies. Journal of neurology, neurosurgery, and psychiatry. 78(10):1042-1049.

Bale TL. 2011. Sex differences in prenatal epigenetic programing of stress pathways. Stress-the International Journal on the Biology of Stress. 14(4):348-356.

Bale TL, Baram TZ, Brown AS, Goldstein JM, Insel TR, McCarthy MM, Nemeroff CB, Reyes TM, Simerly RB, Susser ES et al. 2010. Early life programming and neurodevelopmental disorders. Biol Psychiatry. 68(4):314-319.

Barrett CE, Hennessey TM, Gordon KM, Ryan SJ, McNair ML, Ressler KJ, Rainnie DG. 2017. Developmental disruption of amygdala transcriptome and socioemotional behavior in rats exposed to valproic acid prenatally. Mol Autism. 8.

Benjamini Y, Hochberg Y. 1995. Controlling the false discovery rate - a practical and powerful approach to multiple testing. Journal of the Royal Statistical Society Series B-Statistical Methodology. 57(1):289-300.

Birk OS, Casiano DE, Wassif CA, Cogliati T, Zhao LP, Zhao YG, Grinberg A, Huang SP, Kreidberg JA, Parker KL et al. 2000. The lim homeobox gene lhx9 is essential for mouse gonad formation. Nature. 403(6772):909-913.

Bourgeron T. 2009. A synaptic trek to autism. Curr Opin Neurobiol. 19(2):231-234.

Bray NL, Pimentel H, Melsted P, Pachter L. 2016. Near-optimal probabilistic rna-seq quantification (vol 34, pg 525, 2016). Nature Biotechnology. 34(8):888-888.

Brown A. 2012. Osteopontin: A key link between immunity, inflammation and the central nervous system. Transl Neurosci. 3(3):288-293.

Busche MA, Grienberger C, Keskin AD, Song B, Neumann U, Staufenbiel M, Förstl H, Konnerth A. 2015. Decreased amyloid-β and increased neuronal hyperactivity by immunotherapy in alzheimer's models. Nat Neurosci. 18(12):1725-1727.

Caetano-Anolles K, Mishra S, Rodriguez-Zas SL. 2015. Synergistic and antagonistic interplay between myostatin gene expression and physical activity levels on gene expression patterns in triceps brachii muscles of c57/bl6 mice. PloS one. 10(2):e0116828.

Caetano-Anollés K, Rhodes JS, Garland Jr T, Perez SD, Hernandez AG, Southey BR, Rodriguez-Zas SL. 2016. Cerebellum transcriptome of mice bred for high voluntary activity offers insights into locomotor control and reward-dependent behaviors. PloS one. 11(11):e0167095.

Canetta S, Bolkan S, Padilla-Coreano N, Song LJ, Sahn R, Harrison NL, Gordon JA, Brown A, Kellendonk C. 2016. Maternal immune activation leads to selective functional deficits in offspring parvalbumin interneurons. Mol Psychiatry. 21(7):956-968.

Canitano R, Pallagrosi M. 2017. Autism spectrum disorders and schizophrenia spectrum disorders: Excitation/inhibition imbalance and developmental trajectories. Frontiers in Psychiatry. 8.

Carecchio M, Comi C. 2011. The role of osteopontin in neurodegenerative diseases. Journal of Alzheimers Disease. 25(2):179-185.

Carlezon WA, Kim W, Missig G, Finger BC, Landino SM, Alexander AJ, Mokler EL, Robbins JO, Li Y, Bolshakov VY et al. 2019. Maternal and early postnatal immune activation produce sex-specific effects on autism-like behaviors and neuroimmune function in mice. Sci Rep. 9(1):16928.

Chang X, Liu Y, Hahn CG, Gur RE, Sleiman PMA, Hakonarson H. 2017. Rna-seq analysis of amygdala tissue reveals characteristic expression profiles in schizophrenia. Translational Psychiatry. 7.

Cooke BM, Woolley CS. 2005. Sexually dimorphic synaptic organization of the medial amygdala. J Neurosci. 25(46):10759-10767.

Delfino KR, Rodriguez-Zas SL. 2013. Transcription factor-microrna-target gene networks associated with ovarian cancer survival and recurrence. PloS one. 8(3):e58608.

Delfino KR, Serao NV, Southey BR, Rodriguez-Zas SL. 2011. Therapy-, gender- and race-specific microrna markers, target genes and networks related to glioblastoma recurrence and survival. Cancer genomics & proteomics. 8(4):173-183.

Fatemi SH, Stary JM, Earle JA, Araghi-Niknam A, Egan E. 2005. Gabaergic dysfunction in schizophrenia and mood disorders as reflected by decreased levels of glutamic acid decarboxylase 65 and 67 kda and reelin proteins in cerebellum (vol 72, pg 109, 2004). Schizophr Res. 74(2-3):287-287.

Favre MR, Barkat TR, LaMendola D, Khazen G, Markram H, Markram K. 2013. General developmental health in the vpa-rat model of autism. Front Behav Neurosci. 7.

Felix B, Leger ME, Albe-Fessard D. 1999. Stereotaxic atlas of the pig brain. Brain Res Bull. 49(1-2):1-+.

Fernandez-Irigoyen J, Zelaya MV, Santamaria E. 2014. Applying mass spectrometry-based qualitative proteomics to human amygdaloid complex. Frontiers in Cellular Neuroscience. 8.

Garbett K, Ebert PJ, Mitchell A, Lintas C, Manzi B, Mirnics K, Persico AM. 2008. Immune transcriptome alterations in the temporal cortex of subjects with autism. Neurobiol Dis. 30(3):303-311.

Goetz SC, Anderson KV. 2010. The primary cilium: A signalling centre during vertebrate development. Nat Rev Genet. 11(5):331-344.

Goldstein JM, Hale T, Foster SL, Tobet SA, Handa RJ. 2019. Sex differences in major depression and comorbidity of cardiometabolic disorders: Impact of prenatal stress and immune exposures. Neuropsychopharmacology. 44(1):59-70.

Gonzalez-Pena D, Nixon SE, O'Connor JC, Southey BR, Lawson MA, McCusker RH, Borras T, Machuca D, Hernandez AG, Dantzer R. 2016a. Microglia transcriptome changes in a model of depressive behavior after immune challenge. PloS one. 11(3):e0150858.

Gonzalez-Pena D, Nixon SE, Southey BR, Lawson MA, McCusker RH, Hernandez AG, Dantzer R, Kelley KW, Rodriguez-Zas SL. 2016b. Differential transcriptome networks between ido1-knockout and wild-type mice in brain microglia and macrophages. PLoS One. 11(6):e0157727.

Goodman AB. 1995. Chromosomal locations and modes of action of genes of the retinoid (vitamin-a) system support their involvement in the etiology of schizophrenia. Am J Med Genet. 60(4):335-348.

Goodman AB. 1996. Congenital anomalies in relatives of schizophrenic probands may indicate a retinoid pathology. Schizophr Res. 19(2-3):163-170.

Gottschalk MG, Sarnyai Z, Guest PC, Harris LW, Bahn S. 2013. Estudos traducionais de neuropsiquiatria e esquizofrenia: Modelos animais genéticos e de neurodesenvolvimento. Archives of Clinical Psychiatry (São Paulo). 40:41-50.

Gray AL, Hyde TM, Deep-Soboslay A, Kleinman JE, Sodhi MS. 2015. Sex differences in glutamate receptor gene expression in major depression and suicide (vol 20, pg 1057, 2015). Mol Psychiatry. 20(9):1139-1139.

Guadiana SM, Semple-Rowland S, Daroszewski D, Madorsky I, Breunig JJ, Mykytyn K, Sarkisian MR. 2013. Arborization of dendrites by developing neocortical neurons is dependent on primary cilia and type 3 adenylyl cyclase. J Neurosci. 33(6):2626-2638.

Guneykaya D, Ivanov A, Hernandez DP, Haage V, Wojtas B, Meyer N, Maricos M, Jordan P, Buonfiglioli A, Gielniewski B et al. 2018. Transcriptional and translational differences of microglia from male and female brains. Cell Reports. 24(10):2773-+.

Guo J, Otis JM, Higginbotham H, Monckton C, Cheng J, Asokan A, Mykytyn K, Caspary T, Stuber GD, Anton ES. 2017. Primary cilia signaling shapes the development of interneuronal connectivity. Dev Cell. 42(3):286-+.

Haida O, Al Sagheer T, Balbous A, Francheteau M, Matas E, Soria F, Fernagut PO, Jaber M. 2019. Sex-dependent behavioral deficits and neuropathology in a maternal immune activation model of autism. Translational Psychiatry. 9.

Hamann S. 2005. Sex differences in the responses of the human amygdala. Neuroscientist. 11(4):288-293.

Hill DS, Cabrera R, Schultz DW, Zhu HP, Lu W, Finnell RH, Wlodarczyk BJ. 2015. Autism-like behavior and epigenetic changes associated with autism as consequences of in utero exposure to environmental pollutants in a mouse model. Behav Neurol.

Hines M, Allen LS, Gorski RA. 1992. Sex differences in subregions of the medial nucleus of the amygdala and the bed nucleus of the stria terminalis of the rat. Brain Res. 579(2):321-326.

Hou WH, Capogna M. 2018. Dendritic inhibition in layer 1 cortex gates associative memory. Neuron. 100(3):516-519.

Huang DW, Sherman BT, Lempicki RA. 2009. Systematic and integrative analysis of large gene lists using david bioinformatics resources. Nature protocols. 4(1):44.

Ibanez K, Boullosa C, Tabares-Seisdedos R, Baudot A, Valencia A. 2014. Molecular evidence for the inverse comorbidity between central nervous system disorders and cancers detected by transcriptomic meta-analyses. PLoS Genet. 10(2).

Ibi D, Nagai T, Nakajima A, Mizoguchi H, Kawase T, Tsuboi D, Kano SI, Sato Y, Hayakawa M, Lange UC et al. 2013. Astroglial ifitm3 mediates neuronal impairments following neonatal immune challenge in mice. Glia. 61(5):679-693.

Jamali AK, Tramu G. 1997. Daily cycle of fos expression within hypothalamic pomc neurons of the male rat. Brain Res. 771(1):45-54.

Joustra SD, Schoenmakers N, Persani L, Campi I, Bonomi M, Radetti G, Beck-Peccoz P, Zhu H, Davis TME, Sun Y et al. 2013. The igsf1 deficiency syndrome: Characteristics of male and female patients. J Clin Endocrinol Metab. 98(12):4942-4952.

Kerrien S, Alam-Faruque Y, Aranda B, Bancarz I, Bridge A, Derow C, Dimmer E, Feuermann M, Friedrichsen A, Huntley R et al. 2007. Intact--open source resource for molecular interaction data. Nucleic Acids Res. 35(Database issue):D561-565.

Killgore WD, Yurgelun-Todd DA. 2001. Sex differences in amygdala activation during the perception of facial affect. Neuroreport. 12(11):2543-2547.

Kirsten TB, Taricano M, Florio JC, Palermo-Neto J, Bernardi MM. 2010. Prenatal lipopolysaccharide reduces motor activity after an immune challenge in adult male offspring. Behav Brain Res. 211(1):77-82.

Knuesel I, Chicha L, Britschgi M, Schobel SA, Bodmer M, Hellings JA, Toovey S, Prinssen EP. 2014. Maternal immune activation and abnormal brain development across cns disorders. Nature Reviews Neurology. 10(11):643-660.

Kroismayr R, Baranyi U, Stehlik C, Dorfleutner A, Binder BR, Lipp J. 2004. Herc5, a hect e3 ubiquitin ligase tightly regulated in lps activated endothelial cells. J Cell Sci. 117(20):4749-4756.

Langfelder P, Horvath S. 2008. Wgcna: An r package for weighted correlation network analysis. BMC Bioinformatics. 9.

Laszlo K, Toth K, Kertes E, Peczely L, Lenard L. 2010. The role of neurotensin in positive reinforcement in the rat central nucleus of amygdala. Behav Brain Res. 208(2):430-435.

Lennox BR, Coles AJ, Vincent A. 2012. Antibody-mediated encephalitis: A treatable cause of schizophrenia. Br J Psychiatry. 200(2):92-94.

Li Y, Missig G, Finger BC, Landino SM, Alexander AJ, Mokler EL, Robbins JO, Manasian Y, Kim W, Kim KS et al. 2018. Maternal and early postnatal immune activation produce dissociable effects on neurotransmission in mpfc-amygdala circuits. J Neurosci. 38(13):3358-3372.

Li YF, Sun H, Chen ZC, Xu HX, Bu GJ, Zheng H. 2016. Implications of gabaergic neurotransmission in alzheimer's disease. Front Aging Neurosci. 8.

Licata L, Briganti L, Peluso D, Perfetto L, Iannuccelli M, Galeota E, Sacco F, Palma A, Nardozza AP, Santonico E et al. 2012. Mint, the molecular interaction database: 2012 update. Nucleic Acids Res. 40(Database issue):D857-861.

Lisnock J, Griffin P, Calaycay J, Frantz B, Parsons J, O'Keefe SJ, LoGrasso P. 2000. Activation of jnk3 alpha 1 requires both mkk4 and mkk7: Kinetic characterization of in vitro phosphorylated jnk3 alpha 1. Biochemistry. 39(11):3141-3148.

Lombardo MV, Moon HM, Su J, Palmer TD, Courchesne E, Pramparo T. 2018. Maternal immune activation dysregulation of the fetal brain transcriptome and relevance to the pathophysiology of autism spectrum disorder. Mol Psychiatry. 23(4):1001-1013.

Maden M. 1994. Vitamin-a in embryonic-development. Nutr Rev. 52(2):3-12.

Malkova NV, Yu CZ, Hsiao EY, Moore MJ, Patterson PH. 2012. Maternal immune activation yields offspring displaying mouse versions of the three core symptoms of autism. Brain Behav Immun. 26(4):607-616.

Marin O. 2012. Interneuron dysfunction in psychiatric disorders. Nat Rev Neurosci. 13(2):107-120.

Martin A, Ochagavia M, Rabasa L, Miranda J, Fernandez-de-Cossio J, Bringas R. 2010. Bisogenet: A new tool for gene network building, visualization and analysis. Bmc Bioinformatics. 11(1):1-9.

Martinez C, Juarranz Y, Gutierrez-Canas I, Carrion M, Perez-Garcia S, Villanueva-Romero R, Castro D, Lamana A, Mellado M, Gonzalez-Alvaro I et al. 2020. A clinical approach for the use of vip axis in inflammatory and autoimmune diseases. International Journal of Molecular Sciences. 21(1).

Matsuoka T, Tsunoda M, Sumiyoshi T, Takasaki I, Tabuchi Y, Tanaka K, Uechara T, Itoh H, Suzuki M, Kurachi M. 2008. Effect of mk-801 on gene expressions in the amygdala of rats. Int J Neuropsychopharmacol. 11:265-265.

Mattei D, Ivanov A, Ferrai C, Jordan P, Guneykaya D, Buonfiglioli A, Schaafsma W, Przanowski P, Deuther-Conrad W, Brust P et al. 2017a. Maternal immune activation results in complex microglial transcriptome signature in the adult offspring that is reversed by minocycline treatment. Transl Psychiat. 7(5):e1120-e1120.

Mattei D, Ivanov A, Ferrai C, Jordan P, Guneykaya D, Buonfiglioli A, Schaafsma W, Przanowski P, Deuther-Conrad W, Brust P et al. 2017b. Maternal immune activation results in complex microglial transcriptome signature in the adult offspring that is reversed by minocycline treatment. Transl Psychiat. 7.

Meador-Woodruff JH, Healy DJ. 2000. Glutamate receptor expression in schizophrenic brain. Brain Res Rev. 31(2-3):288-294.

Merali Z, Anisman H, James JS, Kent P, Schulkin J. 2008. Effects of corticosterone on corticotrophin-releasing hormone and gastrin-releasing peptide release in response to an aversive stimulus in two regions of the forebrain (central nucleus of the amygdala and prefrontal cortex). Eur J Neurosci. 28(1):165-172.

Miller BJ, Buckley PF. 2016. The case for adjunctive monoclonal antibody immunotherapy in schizophrenia. Psychiatric Clinics. 39(2):187-198.

Mishra GR, Suresh M, Kumaran K, Kannabiran N, Suresh S, Bala P, Shivakumar K, Anuradha N, Reddy R, Raghavan TM et al. 2006. Human protein reference database--2006 update. Nucleic Acids Res. 34(Database issue):D411-414.

Mistry M, Gillis J, Pavlidis P. 2013. Genome-wide expression profiling of schizophrenia using a large combined cohort. Mol Psychiatry. 18(2):215-225.

Morris BJ, Pratt JA. 2014. Novel treatment strategies for schizophrenia from improved understanding of genetic risk. Clinical Genetics. 86(5):401-411.

Munoz-Estrada J, Lora-Castellanos A, Meza I, Elizalde SA, Benitez-King G. 2018. Primary cilia formation is diminished in schizophrenia and bipolar disorder: A possible marker for these psychiatric diseases. Schizophr Res. 195:412-420.

Munshi S, Rosenkranz JA. 2018. Effects of peripheral immune challenge on in vivo firing of basolateral amygdala neurons in adult male rats. Neuroscience. 390:174-186.

Murphy E, Nordquist RE, van der Staay FJ. 2014. A review of behavioural methods to study emotion and mood in pigs, sus scrofa. Appl Anim Behav Sci. 159:9-28.

O'Loughlin E, Pakan JMP, Yilmazer-Hanke D, McDermott KW. 2017. Acute in utero exposure to lipopolysaccharide induces inflammation in the pre- and postnatal brain and alters the glial cytoarchitecture in the developing amygdala. Journal of Neuroinflammation. 14.

Odorizzi PM, Feeney ME. 2016. Impact of in utero exposure to malaria on fetal t cell immunity. Trends in Molecular Medicine. 22(10):877-888.

Oguchi-Katayama A, Monma A, Sekino Y, Moriguchi T, Sato K. 2013. Comparative gene expression analysis of the amygdala in autistic rat models produced by pre- and post-natal exposures to valproic acid. Journal of Toxicological Sciences. 38(3):391-402.

Openshaw RL, Kwon J, McColl A, Penninger JM, Cavanagh J, Pratt JA, Morris BJ. 2019. Jnk signalling mediates aspects of maternal immune activation: Importance of maternal genotype in relation to schizophrenia risk. J Neuroinflammation. 16.

Oskvig DB, Elkahloun AG, Johnson KR, Phillips TM, Herkenham M. 2012. Maternal immune activation by lps selectively alters specific gene expression profiles of interneuron migration and oxidative stress in the fetus without triggering a fetal immune response. Brain Behav Immun. 26(4):623-634.

Palha JA, Goodman AB. 2006. Thyroid hormones and retinoids: A possible link between genes and environment in schizophrenia. Brain Res Rev. 51(1):61-71.

Paylor JW, Lins BR, Greba Q, Moen N, De Moraes RS, Howland JG, Winship IR. 2016. Developmental disruption of perineuronal nets in the medial prefrontal cortex after maternal immune activation. Sci Rep. 6.

Petrovich GD, Gallagher M. 2003. Amygdala subsystems and control of feeding behavior by learned cues. Amygdala in Brain Function: Bacic and Clinical Approaches. 985:251-262.

Pieczenik SR, Neustadt J. 2007. Mitochondrial dysfunction and molecular pathways of disease. Experimental and Molecular Pathology. 83(1):84-92.

Prabakaran S, Swatton JE, Ryan MM, Huffaker SJ, Huang JTJ, Griffin JL, Wayland M, Freeman T, Dudbridge F, Lilley KS et al. 2004. Mitochondrial dysfunction in schizophrenia: Evidence for compromised brain metabolism and oxidative stress. Mol Psychiatry. 9(7):684-697.

Prestia A. 2011. Alzheimer's disease and schizophrenia: Evidence of a specific, shared molecular background. Future Neurol. 6(1):17-21.

Prins JR, Eskandar S, Eggen BJL, Scherjon SA. 2018. Microglia, the missing link in maternal immune activation and fetal neurodevelopment; and a possible link in preeclampsia and disturbed neurodevelopment? Journal of Reproductive Immunology. 126:18-22.

Pruitt KD, Tatusova T, Maglott DR. 2007. Ncbi reference sequences (refseq): A curated non-redundant sequence database of genomes, transcripts and proteins. Nucleic Acids Res. 35:D61-D65.

Regard JB, Sato IT, Coughlin SR. 2008. Anatomical profiling of g protein-coupled receptor expression. Cell. 135(3):561-571.

Rhomberg T, Rovira-Esteban L, Vikor A, Paradiso E, Kremser C, Nagy-Pal P, Papp OI, Tasan R, Erdelyi F, Szabo G et al. 2018. Vasoactive intestinal polypeptide-immunoreactive interneurons within circuits of the mouse basolateral amygdala. J Neurosci. 38(31):6983-7003.

Ritchie ME, Phipson B, Wu D, Hu YF, Law CW, Shi W, Smyth GK. 2015. Limma powers differential expression analyses for rna-sequencing and microarray studies. NAR. 43(7).

Robinson MD, McCarthy DJ, Smyth GK. 2010. Edger: A bioconductor package for differential expression analysis of digital gene expression data. Bioinformatics. 26(1):139-140.

Roullet FI, Lai JKY, Foster JA. 2013. In utero exposure to valproic acid and autism - a current review of clinical and animal studies. Neurotoxicol Teratol. 36:47-56.

Rutherford KM, Piastowska-Ciesielska A, Donald RD, Robson SK, Ison SH, Jarvis S, Brunton PJ, Russell JA, Lawrence AB. 2014. Prenatal stress produces anxiety prone female offspring and impaired maternal behaviour in the domestic pig. Physiol Behav. 129:255-264.

Salwinski L, Miller CS, Smith AJ, Pettit FK, Bowie JU, Eisenberg D. 2004. The database of interacting proteins: 2004 update. Nucleic Acids Res. 32(Database issue):D449-451.

Sarro EC, Sullivan RM, Barr G. 2014. Unpredictable neonatal stress enhances adult anxiety and alters amygdala gene expression related to serotonin and gaba. Neuroscience. 258:147-161.

Schumann CM, Bauman MD, Amaral DG. 2011. Abnormal structure or function of the amygdala is a common component of neurodevelopmental disorders. Neuropsychologia. 49(4):745-759.

Serao NV, Delfino KR, Southey BR, Beever JE, Rodriguez-Zas SL. 2011. Cell cycle and aging, morphogenesis, and response to stimuli genes are individualized biomarkers of glioblastoma progression and survival. BMC medical genomics. 4:49-8794-8794-8749.

Shannon P, Markiel A, Ozier O, Baliga NS, Wang JT, Ramage D, Amin N, Schwikowski B, Ideker T. 2003. Cytoscape: A software environment for integrated models of biomolecular interaction networks. Genome research. 13(11):2498-2504.

Shi L, Zhang Z, Su B. 2016. Sex biased gene expression profiling of human brains at major developmental stages. Sci Rep-Uk. 6.

Sragovich S, Merenlender-Wagner A, Gozes I. 2017. Adnp plays a key role in autophagy: From autism to schizophrenia and alzheimer's disease. Bioessays. 39(11).

Stark C, Breitkreutz BJ, Reguly T, Boucher L, Breitkreutz A, Tyers M. 2006. Biogrid: A general repository for interaction datasets. Nucleic Acids Res. 34(Database issue):D535-539.

Steinmetz AB, Stern SA, Kohtz AS, Descalzi G, Alberini CM. 2018. Insulin-like growth factor ii targets the mtor pathway to reverse autism-like phenotypes in mice. J Neurosci. 38(4):1015-1029.

Stuart MJ, Baune BT. 2014. Chemokines and chemokine receptors in mood disorders, schizophrenia, and cognitive impairment: A systematic review of biomarker studies. Neurosci Biobehav Rev. 42:93-115.

Subramanian A, Kuehn H, Gould J, Tamayo P, Mesirov JP. 2007. Gsea-p: A desktop application for gene set enrichment analysis. Bioinformatics. 23(23):3251-3253.

Sumitomo A, Horike K, Hirai K, Butcher N, Boot E, Sakurai T, Nucifora FC, Jr., Bassett AS, Sawa A, Tomoda T. 2018. A mouse model of 22q11.2 deletions: Molecular and behavioral signatures of parkinson's disease and schizophrenia. Sci Adv. 4(8):eaar6637.

Takao K, Kobayashi K, Esaki K, Furuya S, Takagi T, Walton N, Hayashi N, Suzuki H, Matsumoto M, Ishii S et al. 2012. Deficiency of schnurri-2, an mhc enhancer binding protein, induces mild chronic inflammation in the brain and confers molecular, neuronal, and behavioral phenotypes related to schizophrenia. Int J Neuropsychopharmacol. 15:136-136.

Tian J, Dai HM, Deng YY, Zhang J, Li Y, Zhou J, Zhao MY, Zhao MW, Zhang C, Zhang YX et al. 2015. The effect of hmgb1 on sub-toxic chlorpyrifos exposure-induced neuroinflammation in amygdala of neonatal rats. Toxicology. 338:95-103.

Wang K, Zhang HT, Ma DQ, Bucan M, Glessner JT, Abrahams BS, Salyakina D, Imielinski M, Bradfield JP, Sleiman PMA et al. 2009. Common genetic variants on 5p14.1 associate with autism spectrum disorders. Nature. 459(7246):528-533.

Wang Q, Xiang B, Deng W, Wu J, Li M, Ma X. 2015. Genome-wide association analysis with gray matter volume as a quantitative phenotype in first-episode treatment-naive patients with schizophrenia (vol 8, e75083, 2013). PLoS ONE. 10(4).

Wischhof L, Irrsack E, Osorio C, Koch M. 2015. Prenatal lps-exposure - a neurodevelopmental rat model of schizophrenia - differentially affects cognitive functions, myelination and parvalbumin expression in male and female offspring. Prog Neuro-Psychopharmacol Biol Psychiatry. 57:17-30.

Xuan ICY, Hampson DR. 2014. Gender-dependent effects of maternal immune activation on the behavior of mouse offspring. PLoS ONE. 9(8).

Yamamoto Y, Ueyama T, Ito T, Tsuruo Y. 2015. Downregulation of growth hormone 1 gene in the cerebellum and prefrontal cortex of rats with depressive-like behavior. Physiol Genomics. 47(5):170-176.

Yang L, Wang M, Guo YY, Sun T, Li YJ, Yang Q, Zhang K, Liu SB, Zhao MG, Wu YM. 2016. Systemic inflammation induces anxiety disorder through cxcl12/cxcr4 pathway. Brain Behav Immun. 56:352-362.

Zeke A, Misheva M, Remenyi A, Bogoyevitch MA. 2016. Jnk signaling: Regulation and functions based on complex protein-protein partnerships. Microbiol Mol Biol Rev. 80(3):793-835.

Zhao Y, He AW, Zhu F, Ding M, Hao JC, Fan QR, Li P, Liu L, Du YN, Liang X et al. 2018. Integrating genome-wide association study and expression quantitative trait locus study identifies multiple genes and gene sets associated with schizophrenia. Prog Neuro-Psychopharmacol Biol Psychiatry. 81:50-54.

2.9 Tables

Table 2.1. Genes exhibiting significant (FDR-adjusted P-value < 0.1) maternal immune activation-by-sex interaction effect.

Gene Symbol	P-value	[a]CON Fe-CON Ma	MPA Fe-MPA Ma	CON Fe-MPA Fe	CON Ma-MPA Ma	CON Fe-MPA Ma	CON Ma-MPA Fe
RGS16	<5E-11	-3.25	2.24	-2.44	3.06	-0.19	0.81
CGA	<5E-11	-5.86	0.36	0.27	6.49	0.63	6.13
POMC	<5E-11	-2.79	0.33	0.06	3.19	0.39	2.86
GPX3	<5E-11	-1.19	0.99	-0.37	1.81	0.63	0.82
RELN	<5E-11	-0.17	0.66	-0.74	0.09	-0.08	-0.57
VIPR2	<5E-11	-1.17	1.04	-1.03	1.18	0.00	0.14
ANKRD34C	<5E-11	-0.77	0.87	-0.71	0.93	0.16	0.06
GBP1	<5E-11	0.92	-0.32	-0.75	-1.99	-1.07	-1.66
GRM4	<5E-11	-0.97	0.91	-0.70	1.17	0.20	0.27
CCDC136	5.3E-09	-0.39	0.43	-0.15	0.67	0.29	0.24
SLC17A6	1.1E-08	-0.40	0.54	-0.16	0.77	0.37	0.23
BTBD11	4.4E-08	-0.62	0.45	-0.40	0.67	0.05	0.22
TTR	5.0E-08	-0.47	0.24	0.29	1.00	0.53	0.76
CACNA2D3	4.8E-07	-0.50	0.44	-0.26	0.68	0.18	0.23
CRHR2	2.8E-06	-0.24	1.09	-0.36	0.97	0.74	-0.12
NDNF	2.8E-06	-0.09	0.88	-0.70	0.27	0.18	-0.61
CXCL12	6.2E-06	-0.41	-0.01	-0.10	0.29	-0.11	0.30
USP43	6.4E-06	-0.64	0.43	-0.34	0.72	0.09	0.29
CCDC17	7.1E-06	0.74	-0.30	0.26	-0.40	0.03	0.12
KCNIP4	7.2E-06	-0.01	0.35	0.11	0.47	0.46	0.11
CAMK2N2	9.6E-06	-0.24	0.16	-0.23	0.18	-0.07	0.01
ALDH1A2	1.4E-05	-1.35	0.50	0.48	2.32	0.98	1.83
GRP	1.5E-05	-0.89	0.73	-0.61	1.02	0.12	0.28
PENK	1.6E-05	-0.10	0.46	-0.04	0.51	0.42	0.06
SYT12	2.9E-05	-0.16	0.32	-0.11	0.37	0.21	0.05
PTH1R	3.7E-05	-0.33	0.52	-0.51	0.34	0.01	-0.18
HBB	6.7E-05	-0.48	0.10	0.12	0.70	0.22	0.60
ESYT1	8.5E-05	-0.47	0.29	-0.27	0.49	0.02	0.20
EFHD1	9.6E-05	-0.31	0.42	-0.37	0.36	0.05	-0.06
BHLHE22	1.0E-04	0.06	-0.59	0.05	-0.61	-0.55	-0.01
ZFP37	1.2E-04	0.60	0.60	-0.19	-0.18	0.41	-0.78
SLC2A2	1.5E-04	0.08	0.50	-0.04	0.38	0.46	-0.12
THRSP	3.1E-04	-0.72	0.51	-1.24	-0.01	-0.73	-0.52

Table 2.1 (cont.)

NR4A3	3.3E-04	-0.12	-0.01	-0.08	0.04	-0.08	0.04
LOC396781	4.4E-04	-0.75	1.36	-5.38	-3.27	-4.01	-4.63
C1QTNF1	4.5E-04	-0.37	0.32	-0.23	0.46	0.09	0.14
RAB27A	5.6E-04	-0.97	0.05	-0.25	0.77	-0.20	0.72
NTS	7.9E-04	-1.43	2.81	-1.78	2.47	1.03	-0.35
GVIN1	7.9E-04	0.80	-0.41	-1.01	-2.22	-1.42	-1.81
SSTR1	8.6E-04	0.11	-0.38	0.16	-0.33	-0.22	0.05
CCDC9B	8.8E-04	-0.24	0.35	-0.34	0.25	0.01	-0.10
CCDC33	1.4E-03	0.48	-0.39	0.49	-0.38	0.10	0.01
CCDC162P	1.4E-03	0.11	-0.48	0.36	-0.23	-0.12	0.25
PTH	1.4E-03	-0.03	0.29	-0.68	-0.36	-0.39	-0.65
SYNPO2L	1.5E-03	-0.28	0.59	-0.44	0.43	0.15	-0.16
CHGB	1.8E-03	-0.58	-0.16	0.37	0.79	0.21	0.96

[a]Log_2[fold change] between two maternal immune activation-sex groups: MPA = PRRSV-induced maternal immune activation; CON = control; Fe = females; Ma = males.

Table 2.2. Most enriched DAVID cluster and supporting functional categories (enrichment score ES > 1.3) among the genes presenting significant maternal immune activation-by-sex interaction effect.

[a]Category	Category Identifier and Name	P-value	[b]FDR P-value
Cluster 1	**ES=2.74**		
KEGG	ssc05320:Autoimmune thyroid disease	2.90E-06	4.50E-04
BP	GO:000250~Antigen processing and presentation of peptide or polysaccharide antigen via MHC class II	1.90E-03	3.40E-01
KEGG	ssc04514:Cell adhesion molecules (CAMs)	2.30E-03	3.20E-02
KEGG	ssc05323:Rheumatoid arthritis	4.80E-03	5.60E-02
KEGG	ssc05164:Influenza A	2.00E-02	1.70E-01
Cluster 2	**ES=1.9**		
BP	GO:0051050~Positive regulation of transport	4.40E-03	3.50E-01
BP	GO:0051049~Regulation of transport	4.50E-03	3.20E-01
BP	GO:0050801~Ion homeostasis	1.30E-02	3.60E-01
BP	GO:0048878~Chemical homeostasis	2.80E-02	4.80E-01
BP	GO:0030001~Metal ion transport	4.50E-02	5.70E-01
Cluster 3	**ES=1.75**		
BP	GO:0048871~Multicellular organismal homeostasis	2.00E-04	3.70E-01
Cluster 4	**ES=1.69**		
BP	GO:0061564~Axon development	6.40E-05	1.70E-01
BP	GO:0007420~Brain development	1.30E-03	3.10E-01

[a] BP: biological process; KEGG: KEGG pathway

[b] False Discovery Rate adjusted P-value.

Table 2.3. Enriched informative categories (NES > |1.3|) using GSEA among the genes based on the overall maternal immune activation-by-sex interaction.

[a]Category	Category Identifier and Name	[b]NES	P-value	[c]FDR P-value
KEGG	ssc04080:Neuroactive ligand receptor interaction	-1.84	< 1.0E-10	8.3E-02
KEGG	ssc04912:GnRH signaling pathway	-1.83	< 1.0E-10	9.9E-02
MF	GO:0005179~Hormone activity	-1.80	< 1.0E-10	2.2E-01
BP	GO:0006970~Response to osmotic stress	-1.79	< 1.0E-10	3.5E-01
BP	GO:0019221~Cytokine mediated signaling pathway	-1.33	9.1E-02	5.4E-01
BP	GO:1901385~Regulation of voltage gated calcium channel activity	-1.37	1.2E-01	5.4E-01
KEGG	ssc04020:Calcium signaling pathway	-1.34	1.2E-01	5.4E-01
BP	GO:0085029~Extracellular matrix assembly	-1.31	1.8E-01	5.5E-01

[a]MF: molecular function; KEGG: KEGG pathway; BP: biological process

[b] normalized enrichment score; negative values indicate genes under-expression in CON females relative to males but over-expression in MPA females relative to males.

[c] False Discovery Rate adjusted P-value.

Table 2.4. Representative genes differentially expressed (FDR-adjusted P-value < 0.1) between pigs from control (CON) relative to PRRSV-treated (MPA) gilts.

Gene symbol	Gene Name	[a]CON-MPA	P-value	[b]FDR P-value
IGHG	IgG heavy chain	-4.74	1.1E-31	<1.0E-10
IFITM3	interferon induced transmembrane prot 3	-1.27	7.6E-11	6.2E-08
IGF2	insulin-like growth factor 2	1.28	8.1E-07	2.7E-04
PAQR6	progestin and adipoQ receptor family member 6	-1.02	1.9E-06	5.6E-04
RGS8	regulator of G protein signaling 8	-0.88	8.6E-06	2.0E-03
NDNF	neuron derived neurotrophic factor	-1.27	1.5E-05	3.3E-03
HS3ST5	heparan sulfate-glucosamine 3-sulfotransferase 5	-1.24	3.5E-05	6.8E-03
CTSC	cathepsin C	-1.03	4.1E-05	7.7E-03
SPP1	secreted phosphoprotein 1	-0.89	4.1E-05	7.7E-03
TACC1	transforming acidic coiled-coil-containing protein 1	-1.55	5.5E-05	9.7E-03
IFITM1	interferon induced transmembrane prot 1	-1.15	7.4E-05	1.2E-02
ALDH1A1	aldehyde dehydrogenase 1 fam mem A1	0.79	9.7E-05	1.5E-02
PLEKHD1	pleckstrin homology coiled-coil domain containing D1	-0.99	5.6E-04	6.5E-02
HERC5	HECT and RLD domain contain E3 ubiquitin ligase 5	-1.05	5.7E-04	6.6E-02
IAPP	islet amyloid polypeptide	-1.36	7.0E-04	7.7E-02
ISLR	immunoglobulin superfamily contain leucine rich repeat	1.13	8.3E-04	8.5E-02
ANKRD24	ankyrin repeat domain 24	-0.73	8.7E-04	8.9E-02
MAP2K7	mitogen-activated protein kinase kinase 7	-0.64	9.9E-04	1.0E-01

[a] Log_2[fold change] between CON and MPA pigs.

[b] False Discovery Rate adjusted P-value.

Table 2.5. Clusters of enriched functional categories (enrichment score ES > 1.3) among the genes presenting significant maternal immune activation effect, and representative categories identified using DAVID.

[a]Category	Category Identifier and Name	P-value	[b]FDR P-value
Cluster 1	**ES=1.51**		
BP	GO:0048646~anatomic structure formation in morphogenesis	3.7E-03	9.7E-01
BP	GO:0001525~angiogenesis	8.4E-02	9.8E-01
Cluster 2	**ES=1.40**		
KEGG	ssc05330:Allograft rejection	1.7E-02	8.0E-01
KEGG	ssc05169:Epstein-Barr virus infection	2.3E-02	6.7E-01
KEGG	ssc05320:Autoimmune thyroid disease	3.0E-02	6.1E-01

[a] BP: biological process; KEGG: KEGG pathway.

[b] False Discovery Rate adjusted P-value.

Table 2.6. Enriched informative categories (NES > |1.3|) among the genes differentially expressed between pigs from the control relative to the maternal immune activation group using GSEA.

[a] Category	Category Identifier and Name	[b]NES	P-value	[c]FDR P-value
BP	GO:0001578~Microtubule bundle formation	2.03	<1.0E-10	<1.0E-08
BP	GO:0060271~Cilium morphogenesis	2.01	<1.0E-10	<1.0E-08
BP	GO:0044782~Cilium organization	1.97	<1.0E-10	<1.0E-08
BP	GO:0035082~Axoneme assembly	1.94	<1.0E-10	1.8E-04
BP	GO:0003341~Cilium movement	1.94	<1.0E-10	1.4E-04

[a]BP: biological process.

[b] normalized enrichment score, positive values refer to genes under-expressed in maternal immune activated relative to control pigs.

[b] False Discovery Rate adjusted P-value.

Table 2.7. Informative genes presenting significant differential expression between males (Ma) and females (Fe).

Gene symbol	Gene Name	[a]Ma-Fe	P-value	[b]FDR P-value
EIF1AY	eukaryotic translation initiation factor 1A, Y-linked	13.68	<1.0E-08	<1.0E-08
LHX9	LIM homeobox 9	3.38	<1.0E-08	<1.0E-08
LHB	luteinizing hormone beta polypeptide	3.92	<1.0E-08	<1.0E-08
TRPC3	transient receptor potential cation channel C3	1.83	1.7E-07	4.4E-05
WNT3	Wnt family member 3	1.72	9.0E-07	2.0E-04
IGSF1	immunoglobulin superfamily member 1	0.85	6.4E-06	1.3E-03
NPM2	nucleophosmin/nucleoplasmin 2	1.79	1.8E-05	2.8E-03
RORA	RAR related orphan receptor A	0.74	2.0E-04	2.4E-02
LEPR	leptin receptor	0.62	8.8E-04	8.4E-02

[a] Log_2[fold change] between male and female offspring.

[b] False Discovery Rate adjusted P-value.

Table 2.8. Clusters of informative enriched functional categories (enrichment score ES > 1.3) among the genes differentially expressed between sexes identified using DAVID.

[a]Category	Category Identifier and Name	P-value	[b]FDR P-value
Cluster 1	**ES=1.82**		
MF	GO:0005201~extracellular matrix structural constituent	3.0E-02	7.9E-01
Cluster 2	**ES=1.74**		
KEGG	ssc04080:Neuroactive ligand-receptor interaction	2.7E-06	2.4E-04
BP	GO:0009725~response to hormone	7.3E-04	9.4E-01
Cluster 3	**ES=1.74**		
BP	GO:0048732~gland development	1.7E-03	5.7E-01
Cluster 4	**ES=1.45**		
BP	GO:0007420~brain development	1.1E-01	7.9E-01
BP	GO:0030900~forebrain development	1.9E-01	8.7E-01
Cluster 5	**ES=1.41**		
MF	GO:0020037~heme binding	6.2E-02	9.1E-01
MF	GO:0005506~iron ion binding	9.3E-02	9.3E-01
Cluster 6	**ES=1.35**		
BP	GO:0009790~embryo development	5.8E-03	5.4E-01
BP	GO:0090596~sensory organ morphogenesis	8.9E-03	5.1E-01

[a] BP: biological process; MF: molecular function; KEGG: KEGG pathway.

[b] False Discovery Rate adjusted P-value.

Table 2.9. Clusters of enriched functional categories (enrichment score ES > 1.3) among the genes in modules presenting a significant correlation with maternal immune activation (MPA) relative to control within males using DAVID.

[a]Category	Category Identifier and Name	P-value	[b]FDR P-value
MODULE	**Grey60 (low expression in MPA)**		
Cluster 1	**ES=14.5**		
KEGG	Ssc05010:Alzheimer's disease	1.3E-18	9.1E-17
KEGG	Ssc05012:Parkinson's disease	9.8E-18	4.7E-16
Cluster 2	**ES=7.32**		
MF	GO:0016651~oxidoreductase activity, acting on NAD(P)H	3.6E-10	1.5E-07
MF	GO:0003954~NADH dehydrogenase activity	3.4E-09	6.8E-07
Cluster 3	**ES=6.41**		
BP	GO:0042775~mitochondrial ATP synthesis electron	4.0E-10	8.6E-07
BP	GO:0046034~ATP metabolic process	8.0E-10	8.7E-07
BP	GO:0009116~nucleoside metabolic process	7.8E-08	9.4E-06
MODULE	**Light yellow (low expression in MPA)**		
Cluster 1	**ES=4.18**		
KEGG	ssc03010:Ribosome	3.7E-06	5.9E-05
BP	GO:0006412~translation	9.5E-06	1.7E-02
Cluster 1	**ES=2.49**		
BP	GO:0007006~mitochondrial membrane organization	5.1E-04	7.8E-02
BP	GO:0007007~inner mitochondrial organization	1.1E-02	3.5E-01

[a] BP: biological process; MF: molecular function; KEGG: KEGG pathway.

[b] False Discovery Rate adjusted P-value.

Table 2.10. Clusters of enriched functional categories (enrichment score ES > 1.3) among the genes in modules presenting a significant correlation with sex within the maternal immune activation treatment using DAVID.

[a]Category	Category Identifier and Name	P-value	[b]FDR P-value
MODULE	**Sienna3 (low expression in males)**		
Cluster 1	**ES=1.58**		
BP	GO:0044255~cellular lipid metabolic process	1.1E-02	1.0E+00
BP	GO:0044283~small molecule biosynthetic process	3.3E-02	9.8E-01
MODULE	**Ivory (high expression in males)**		
Cluster 1	**ES=1.47**		
BP	GO:0007416~synapse assembly	8.1E-03	1.0E+00
BP	GO:0007399~nervous system development	2.7E-02	9.1E-01

[a] BP: biological process; MF: molecular function; KEGG: KEGG pathway.

[b] False Discovery Rate adjusted P-value.

2.10 Figures

Figure 2.1. Network of genes differentially expressed in the amygdala of males (Ma) from control (CON) relative to maternal immune activation (MPA) (contrast between CON_Ma and MPA_Ma). Framework square node color: red and blue denote framework genes over- and under-expressed in CON relative to MPA pigs, respectively; framework node size: -Log_{10}[P-value]; other genes connecting framework nodes were not differentially expressed in this study.

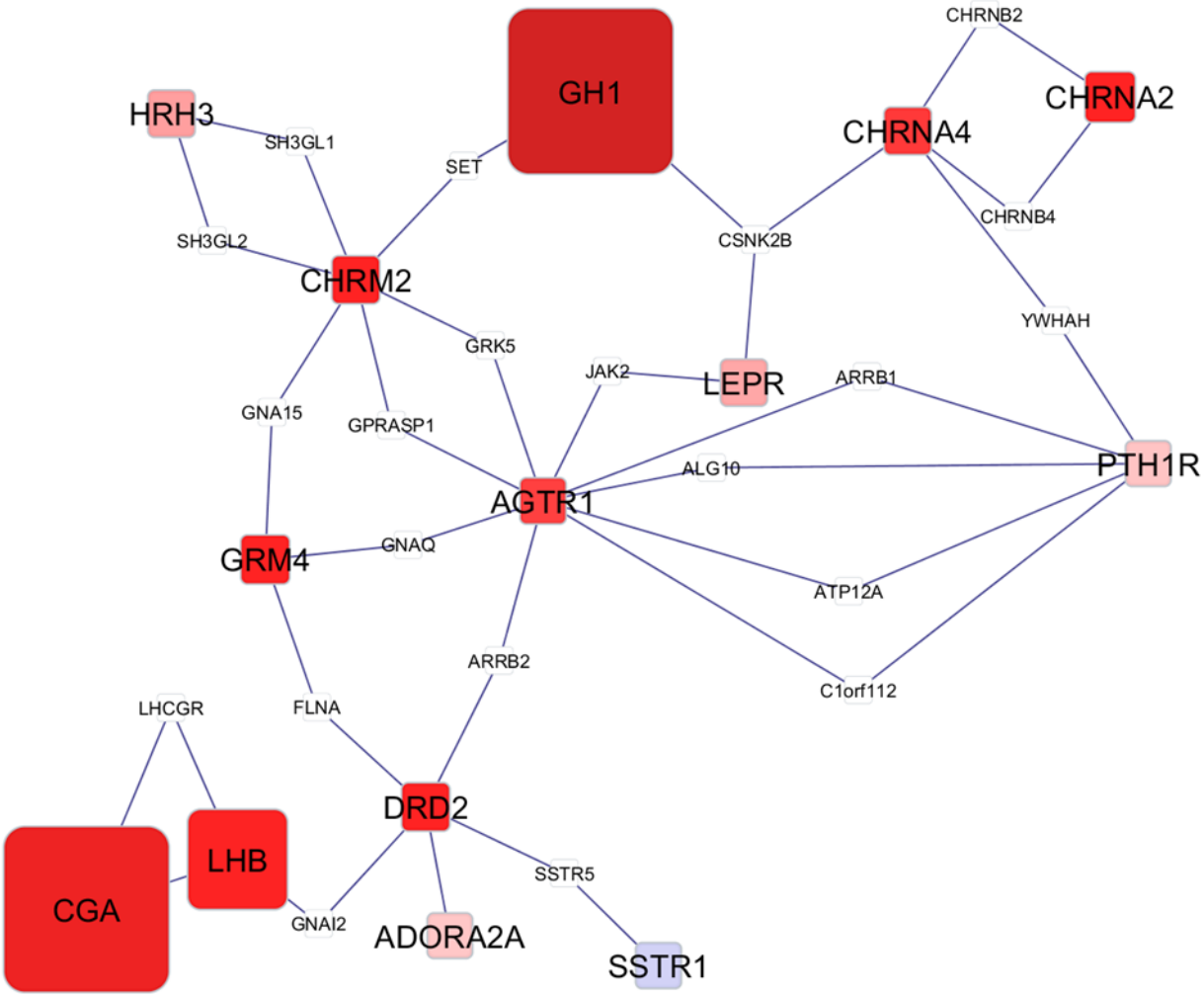

Figure 2.2. Network of genes differentially expressed in the amygdala of females (Fe) from control (CON) relative to maternal immune activation (MPA) (contrast between CON_Fe and MPA_Fe). Framework square node color: red and blue denote framework genes over- and under-expressed in CON relative to MPA pigs, respectively; framework node size: -Log$_{10}$[P-value]; other genes connecting framework nodes were not differentially expressed in this study.

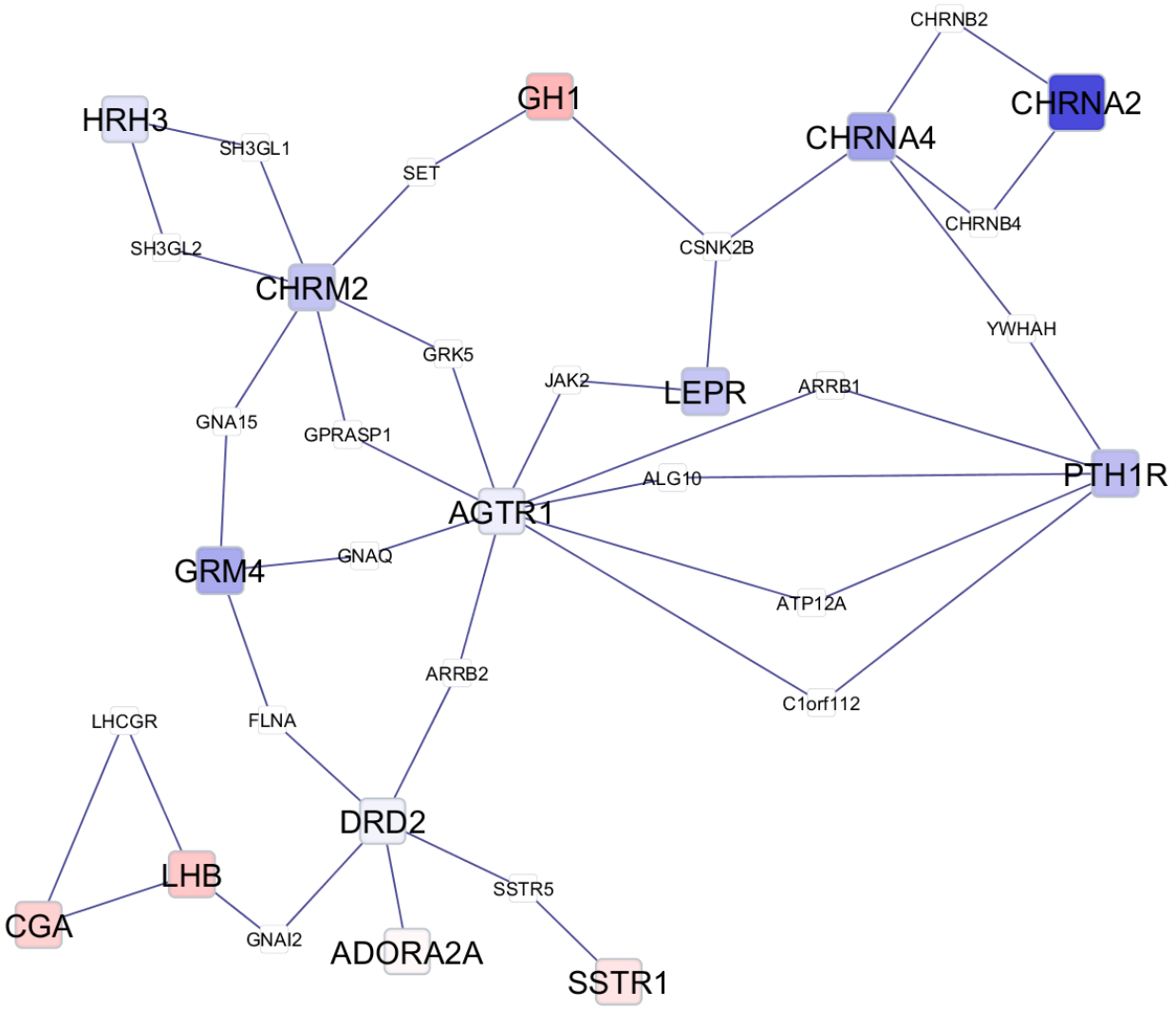

Chapter 3: Interacting impact of maternal inflammatory response and stress on the amygdala transcriptome of pigs[2]

3.1 Abstract

Changes at the molecular level capacitate the plasticity displayed by the brain in response to stress stimuli. Weaning stress can trigger molecular changes that influence the physiology of the offspring. Likewise, maternal immune activation (MIA) during gestation has been associated with behavior disorders and molecular changes in the amygdala of the offspring. This study advances the understanding of the effects of pre-and postnatal stressors in amygdala gene networks. The amygdala transcriptome was profiled on female and male pigs that were either exposed to viral-elicited MIA or not and were weaned or nursed. Overall, 111 genes presented interacting or independent effects of weaning, MIA or sex (FDR-adjusted P-value < 0.05). PIGY upstream reading frame (PYURF) and orthodenticle homeobox 2 (OTX2) are genes associated with MIA-related neurological disorders, and presented significant under-expression in weaned relative to nursed pigs exposed to MIA, with moderate pattern observed in non-MIA pigs. Enriched among the genes presenting highly over- or under-expression profiles were 24 KEGG pathways including inflammation, and neurological disorders. Our results indicate that MIA and sex can modulate the effect of weaning stress on the molecular mechanisms in the developing brain. Our findings can help identify molecular targets to ameliorate the effects of pre-and postnatal stressors on behaviors regulated by the amygdala such as aggression and feeding.

[2]Marissa R. Keever-Keigher, Pan Zhang, Courtni R. Bolt, Haley E. Rymut, Adrienne M. Antonson, Megan P. Corbett, Alexandra K. Houser, Alvaro G. Hernandez, Bruce R. Southey, Laurie A. Rund, Rodney W. Johnson, Sandra L. Rodriguez-Zas. G3: Genes| Genomes| Genetics (2021)

3.2 Introduction

Weaning encompasses social, physical, and environmental stresses (Campbell et al. 2013; Curley et al. 2009). The separation of the offspring from their mother and familiar littermates, the physical handling and transport, co-mingling of unfamiliar individuals, new surroundings, and new feeding strategies can all contribute to the stress experienced by weaned rodents and pigs (Campbell et al. 2013; Curley et al. 2009). This event is accompanied by hormonal and immunological changes (Gimsa et al. 2018; Pie et al. 2004). Marked increases in plasma lymphocytic trapping and cortisol level were detected in pigs one day after weaning (Kick et al. 2012). Decreases in the concentrations of T cells, B cells, and natural killer cells in response to a stressful event corresponding with lymphocytic trapping were also observed in mice (Kick et al. 2012). A review of stress effects on pigs (Gimsa et al. 2018) highlighted the association of weaning with lower glucocorticoid receptor (GR) binding in the hippocampus and amygdala of one-month-old pigs (Kanitz et al. 1998). Weaning together with isolation was associated with lower levels of the hydroxysteroid dehydrogenase enzyme that processes glucocorticoids, GR, and mineralocorticoid receptor (MR) in the prefrontal cortex of 2-3-week-old pigs (Poletto et al. 2006).

Infectious agents and environmental stressors can result in maternal immune activation (MIA) during gestation, and the ensuing changes in cytokine signaling can alter brain and nervous system development (Odorizzi and Feeney 2016; Prins et al. 2018). Using a viral model of MIA, we demonstrated the dysregulation of multiple genes and processes in the amygdalae of 3-week-old pigs, including immune response, neuroactive ligand-receptor, and glutamatergic pathways (Keever et al. 2020a; Keever et al. 2020b). This brain structure plays a central role in behaviors, including some that are sexually dimorphic or social in nature, and learning; thus, the plastic nature

of this structure and its response to insults in crucial. Additionally, the amygdala regulates responses to pathogen infection and environmental stressors (Tian et al. 2015).

The response to postnatal stressors can be affected by prenatal MIA. Studies of MIA-associated behavior disorders such as schizophrenia spectrum disorders (SSD), autism spectrum disorders (ASD) (Canetta et al. 2016; Knuesel et al. 2014; Mattei et al. 2017) using rodent and primate models offer evidence of the combined effects of MIA and a second immune challenge (Giovanoli et al. 2013; Imanaka et al. 2006; Maynard et al. 2001; Walker et al. 2009). The double-hit hypothesis proposes that exposure to MIA elicits long-term neural and immune disruptions that subsequently modify the offspring's response to a second immune challenge later in life (Bayer et al. 1999).

Offspring exposed to MIA can be more sensitive or more tolerant to a second stressor, and this response can modulate the incidence of behavioral disorders (Wang et al. 2007). Pigs exposed to MIA elicited by porcine reproductive and respiratory syndrome virus (PRRSV) during gestation and subsequently exposed to bacterial endotoxin lipopolysaccharide (LPS) at two weeks of age had higher circulating levels of pro-inflammatory cytokines and cortisol than pigs from PRRSV-infected gilts that did not receive the second challenge (Antonson et al. 2017).

Previous studies have reported molecular changes in the pig brain associated with weaning stress in the absence of MIA (Kanitz et al. 1998). Conversely, we focused on the study of MIA in absence of a second stressor and reported on the dysregulation of genes annotated to immune response pathways in the amygdalae of 3-week-old pigs exposed to MIA in the absence of weaning stress (Keever et al. 2020a). A study of the simultaneous effects of MIA and weaning stress on the amygdala pathways is necessary to assess possible interactions among both challenges.

The principal goal of this study is to advance the understanding of the effect of the double-hit paradigm on the amygdala gene networks of pigs. The combined effects on the molecular profiles 1) of MIA stress elicited by PRRSV, 2) of weaning stress, and 3) the interactions of these effects with sex were tested. A supporting objective is to reconstruct gene and transcription factor networks to augment the understanding of the effects of MIA and weaning stress on the interaction among genes and on gene regulatory elements. Molecular profiles of weaned pigs not exposed to MIA and of weaned pigs exposed to MIA were compared to existing profiles from pigs that did not experience weaning stress (Keever et al. 2020a). Conclusions drawn from these complementary approaches will aid in revealing the consequences of multiple stressors on the amygdala and may help in developing therapeutic strategies to mitigate these consequences.

3.3 Materials and Methods

Animal Experiments

Published protocols were used for all experimental procedures (Antonson et al. 2018; Antonson et al. 2017; Keever et al. 2020a). Illinois Institutional Animal Care and Use Committee (IACUC) at the University of Illinois approved the animal studies, and they are in compliance with the USDA Animal Welfare Act and the NIH Public Health Service Policy on the Humane Care and Use of Animals.

Similar to our focused study of the effect of MIA alone (Keever et al. 2020a), PIC 359 boar semen was used to inseminate 205-day-old, PRRSV-negative Camborough gilts, which were born and raised at the University of Illinois at Urbana-Champaign (Antonson et al. 2018; Antonson et al. 2017). At gestation day 69, the gilts were moved into disease containment chambers maintained

at 22°C and a 12-h light/dark cycle with lights on at 7:00AM, and they were fed daily 2.3 kg of a gestational diet with *ad libitum* water access. Following an acclimation period of one week, six gilts were inoculated intranasally with live PRRSV strain P129-BV (School of Veterinary Medicine at Purdue University, West Lafayette, IN, USA) using 5 mL of 1×10^5 median tissue culture infectious dose ($TCID_{50}$) diluted in sterile Dulbecco's modified Eagle medium (DMEM; 5 mL total volume), while five gilts in the Control group were intranasally inoculated with an 5 mL of sterile DMEM. The timing of the intranasal inoculation corresponded to the last third of gestation in both pigs and humans, which coincides with the initiation of rapid fetal brain growth (Antonson et al. 2018; Antonson et al. 2017; Keever et al. 2020a). Following inoculation, the PRRSV-challenged and control gilts were housed in separate containment chambers. PRRSV infection among PRRSV inoculated gilts and absence of infection among DMEM inoculated gilts was confirmed one week after exposure with a PCR-test. The significant increase in body temperature and decrease in feed intake of PRRSV-challenged relative to control gilts resolved within 14 days post injection.

Given that the average gestation lasting 114 days, an intramuscular injection of 10 mg of Lutalyse (dinoprost tromethamine, Pfizer, New York, NY, USA) was used to induce farrowing on gestation day 113 (Antonson et al. 2018; Antonson et al. 2017), with gilts contained in individual farrowing crates of standard dimensions (1.83 x 1.83 m). Following farrowing, the gilts were fed 5 kg of a nutritionally complete diet twice daily for the lactating period with water available *ad libitum*. Intramuscular injections of iron dextran (100 mg/pig, Butler Schein Animal Health, Dublin, OH, USA) and Excede for Swine (25 mg/pig; Zoetis, Parsippany, NJ, USA) to control for respiratory diseases were administered to pigs. The pigs remained with the dam in the farrowing crates until

weaning until 21 days of age, when approximately half of the pigs in each litter were weaned and the rest remained with the sow.

Weaned pigs were housed in groups of four, with *ad libitum* access to water and received a nutritionally complete diet for growing pigs. The nursing pigs that remained with the sow continued receiving the same feeding as before. The experiment concluded one day after weaning, a time point of high weaning stress. Reports confirm that pigs present heightened dysregulation of physiological stress indicators (e. g. blood neutrophil/ lymphocyte ratio, glucose level, cortisol) one day after weaning (Puppe et al. 1997; Turpin et al. 2017), yet no significant effect on body weight (Giroux et al. 2000a; Giroux et al. 2000b; Puppe et al. 1997; Turpin et al. 2017). Our analysis of body weight using a mixed effect model include the effects of weaning, MIA, sex, and interactions and random effects of gilt and replicate confirmed the absence of significant stressor effects. The experimental design encompassed 48 pigs distributed between all eight groups representing MIA, weaning stress, and sex classes. To study the effect of MIA, we compared pigs that experienced maternal PRRSV-elicited activation (MIA group of pigs) relative to non-pigs from control gilts (non-MIA group of pigs). To study the effect of postnatal stress we compared pigs that were weaned at day 21 of age (weaned group of pigs) relative to pigs that remained with the gilt nursing until day 22 of age (nursed group of pigs). The comparison of male and female pigs enabled the study of sex effects.

RNA Extraction and Sequencing

Pigs were anesthetized intramuscularly using a drug cocktail of telazol:ketamine:xylazine (50 mg of tiletamine; 50 mg of zolazepam) reconstituted with 2.5 mL ketamine (100 g/L) and 2.5 mL xylazine (100 g/L; Fort Dodge Animal Health, Fort Dodge, IA, USA) at a dose of 0.03 mL/kg

body weight, following protocols (Antonson et al. 2017) at 22 days of age. An intracardiac injection of sodium pentobarbital (86 mg/kg body weight, Fata Plus, Vortech Pharmaceuticals, Dearborn, MI, USA) was used to euthanize the pigs after anesthetization. After euthanasia, the pig brains were removed, and the stereotaxic atlas of the pig brain (Félix et al. 1999) was used to identify the amygdalae. Amygdalae were dissected out, flash frozen on dry ice, and stored at -80 ºC following published protocols (Antonson et al. 2019). EZNA isolation kit (Omega Biotek, Norcross, GA, USA) was used to isolate RNA per manufacturer's instructions. The RNA integrity numbers of the samples were above 7.3, indicating low RNA degradation. TruSeq Stranded mRNAseq Sample Prep kit' (Illumina Inc, San Diego, CA, USA) was used to prepare RNAseq libraries, and libraries were quantitated by qPCR and sequenced on one lane on a NovaSeq 6000 for 151 cycles from each end of the fragments using NovaSeq S4 reagent kit. The bcl2fastq v2.20 conversion software was used to produce and demultiplex FASTQ files.

RNA Sequence Mapping and Differential Expression Analysis

Assessment of read quality found a minimum Phred score of 35 across all read positions using FASTQC (Andrews 2010), and, therefore, no reads were trimmed based on quality. Paired-end reads were aligned to the *Sus scrofa* transcriptome (version Sscrofa 11.1(Pruitt et al. 2007)) and quantified using kallisto v. 0.43.0 (Bray et al. 2016) with default settings. The normalized (trimmed mean of M-values) gene expression values were described using a generalized linear model encompassing the effects of MIA group (MIA and non-MIA levels), weaning stress (weaned or nursed levels), sex (female or male levels), weaning stress-by-sex interaction, MIA-by-weaning stress interaction, and MIA-by-sex interaction. Few genes presented three-way interaction effects and, therefore, only two-way interactions and main effects were further considered. Genes

supported by > 5 transcripts per million (TPM) RNA molecules by each weaning-MIA-sex combination were analyzed for differential gene expression using edgeR (v. 3.14.0) in the R v. 3.3.1 environment (Robinson et al. 2010). A conservative cut-off for differential expression of FDR-adjusted P-value 5.0E-05 and $\log_2$(fold change between pig groups) > 2 was considered to highlight strong trends. A positive $\log_2$(fold change) denotes over-expression in the first pig group relative to the second pig group in the comparison. A negative $\log_2$(fold change) denotes under-expression in the first pig group relative to the second pig group in the comparison. The raw and normalized gene expression levels for the 16523 genes in the 48 samples are available in the National Center for Biotechnology Information (NCBI) Gene Expression Omnibus (GEO) database, series identifier GSE165059.

Functional Enrichment, Network Inference, and Transcription Factor Analysis

Identification of the over-represented Kyoto Encyclopedia of Genes and Genomes (KEGG) pathways (Kanehisa 2019; Kanehisa and Goto 2000) among all genes analyzed for the interaction and main effects of weaning stress, MIA, and sex was performed using the Gene Set Enrichment Analysis (GSEA) approach with the WebGESTALT software (Liao et al. 2019). The complete list The GSEA used the information from all genes analyzed, ranked from the most over-expressed to the most under-expressed to identify over-represented pathways within both profiles. The normalized enrichment score (NES) of the pathways was calculated using the maximum deviation of the cumulative sum based on the signed fold-change of the ranked genes divided by the average of the permutated enrichment scores. For the enrichment analysis, *Sus scrofa* was selected as the organism of interest, and a minimum of 5 genes and a maximum of 2000 genes per category were used. Statistical significance was determined by calculating the FDR-adjusted P-value from 1000

permutations. A conservative cut-off for differential expression of FDR-adjusted P-value 5.0E-05 and NES > 2 was considered to highlight highly enriched pathways.

The sign of the NES from GSEA offered insights into the predominance of the gene expression profile within the enriched categories for each effect tested. Pathways characterized with a NES > 0 are enriched among the genes over-expressed while the pathways characterized with a NES < 0 are enriched among the genes under-expressed. The consideration of the estimable functions and comparison against the pair-wise contrast of gene expression levels between pig groups enabled the characterization of the predominant profiles within positive (NES > 0) and negative (NES < 0) group. For the weaning-by-MIA interaction effect, NES > 0 denoted gene over-expression in non-MIA nursed relative to MIA weaned pigs and NES < 0 denoted gene under-expression in non-MIA nursed relative to MIA weaned pigs. For the weaning-by-sex interaction effect, NES > 0 denoted gene over-expression in nursed males relative to weaned females, and NES < 0 denoted gene under-expression in nursed males relative to weaned females. For the MIA-by-sex interaction effect, NES > 0 denoted gene over-expression in MIA females relative to MIA males, and NES < 0 denoted gene under-expression in MIA females relative to MIA males. For the weaning effect, NES > 0 denoted over-expression in weaned relative to nursed pigs, and NES < 0 denoted over-expression in nursed relative to weaned pigs. For the MIA effect, NES > 0 denoted gene over-expression in non-MIA relative to MIA pigs, and NES < 0 denoted gene over-expression in MIA relative to non-MIA pigs. For the sex effect, NES > 0 denoted gene over-expression in males relative of females, and NES < 0 gene denoted over-expression in females relative of males. Positive fold change and NES values from GSEA for the main effects of MIA, weaning stress, and sex indicated over-expression in weaned relative to nursed pigs, non-MIA relative to MIA pigs, and male relative of female pigs.

The genes that showed significant MIA-by-weaning stress effect and differential expression between nursed and weaned pigs in the MIA and non-MIA groups (FDR-adjusted P-value < 0.1) were further studied. First, the genes presenting weaning effects within MIA group were used to build the framework of gene networks that could help uncover distinct gene interaction patterns between weaning groups. A preliminary identification of interacting proteins coded by the differentially expressed genes in our study was generated using STRING v. 11.0 (Szklarczyk et al. 2019). The relationships between genes depicted in STRING are based on known data contained in manually-curated databases, such as BioCyc (Karp et al. 2019), Gene Ontology (Ashburner et al. 2000; Carbon et al. 2019), and KEGG (Kanehisa 2019; Kanehisa and Goto 2000), and predicted protein-protein interactions mined from high throughput experiments and primary literature. To understand the potential changes in the relationship between genes elicited by MIA in either weaning group, the STRING networks were subsequently enhanced in Cytoscape v. 3.8.1 (Shannon et al. 2003) by including the gene expression profiles measured in the present study. In the reconstructed networks, the color of the gene reflects the sign of the fold change where red denotes over-expression in weaned relative to nursed pigs and blue denotes the opposite pattern,

The set of genes presenting MIA interaction effects was also studied with the goal of identifying shared transcription regulators. The identification of potential transcription factors and motifs over-represented among the target genes was carried out using the iRegulon application (Janky et al. 2014) in Cytoscape v. 3.8.1 (Shannon et al. 2003). Default settings of receiver operator curve estimation of the area under the curve threshold equal to 0.03 and motif similarity of FDR-adjusted P-value < 0.001 were used to rank motifs based on position weight matrices, and transcription factors capable of regulating differentially expressed target genes were deemed enriched when supported by > 15% of the input genes and NES ≥ 3 (Janky et al. 2014).

3.4 Results

Maternal Immune Activation and Sequencing Metrics

The sequencing produced 6.59E+09 reads across all 48 libraries. The median number of reads per pig group is 1.35E+08 for weaned pigs, 1.22E+08 for nursed pigs, 1.35E+08 for non-MIA pigs, 1.31E+08 for MIA pigs, 1.34E+08 for females, and 1.35E+08 for males. The median number of reads mapped by the kallisto software per group is 6.77E+07 for weaned pigs, 6.62E+07 for nursed pigs, 6.81E+07 for non-MIA pigs, 6.54E+07 for MIA pigs, 7.03E+07 for females, and 6.54E+07 for males. The analysis of 16,529 genes that had > 5 mapped read counts per pig group enabled testing the factors of weaning, MIA, sex, and interaction on the gene expression profiles.

Effects of Weaning Stress, Maternal Immune Activation, and Sex on the Amygdala Pathways

Table 3.1 presents a summary of the KEGG pathways enriched in at least one tested interaction or main effect at FDR-adjusted P-value < 0.05 and NES > |2|. Table 3.3 presents an extended list of the 115 KEGG pathways enriched in at least one effect at P-value < 0.05. Weaning stress showed significant effects, interacting with other factors or alone, on the gene expression profiles in the amygdala of pigs. The GSEA of the genes ranked from highly over-expressed to highly under-expressed identified 21 KEGG pathways enriched (Table 3.1) among the genes presenting MIA-by-weaning interaction effect, and 13 KEGG pathways enriched among genes presenting weaning stress effect. An extended list of pathways at P-value < 0.05 is included in Table 3.3.

Among the enriched KEGG pathways in Table 3.1 there is a predominance of immune- and neurologically-related functional categories. Based on the NES values in Table 3.1, there is a prevalence of GSEA enrichment among genes under-expressed in weaned relative to nursed pigs,

under-expressed in MIA relative to non-MIA pigs. The more significant enrichments of KEGG pathways were identified among genes presenting weaning-by-MIA, MIA-by-sex, weaning, and MIA effects.

Effects of Weaning Stress, Maternal Immune Activation, and Sex on the Gene Expression Profiles in the Amygdala

Overall, 111 genes had significant (FDR-adjusted P-value < 0.05) effects of weaning stress, MIA, and sex interacting or acting independently. At P-value < 0.005, a total of 254 genes exhibited significant changes in the profile associated with the previous effects. Table 3.2 summarizes the genes that presented one or more significant main or interaction effects at $|\log_2(\text{fold change between pig groups})| > 2$ and P-value < 5.0E-05 (approximately FDR-adjusted P-value < 0.05), and Figure 3.1 provides the corresponding expression profiles characterized by the $\log_2$(fold change between pig groups. Table 3.4 includes an extended list of 71 genes that presented at least one significant effect at FDR-adjusted P-value < 0.1.

Overall, 54 genes presented significant (FDR-adjusted P-value < 0.05) interaction effects and 68 genes presented significant main effects. The majority of the genes presenting significant main effect included a significant interaction of this effect with the remaining effects (Table 3.2 and Figure 3.1, Table 3.4). Among the 71 genes that presented one or more significant effects at FDR-adjusted P-value < 0.1 (Table 3.4), 87% were over-expressed in non-MIA pigs, 86% were over-expressed in males, and 70% were over-expressed in weaned pigs, relative to the alternative factor levels.

Among the genes that presented at least one significant effect at FDR-adjusted P-value < 0.05 and $|\log_2(\text{fold change})| > 2$, (Figure 3.1), the majority were under-expressed in female relative to male nursed pigs under-expressed in female relative to male non-MIA pigs, over-expressed in nursed relative to weaned males, and over-expressed in non-MIA relative to MIA males.

Effects of Weaning Stress and Maternal Immune Activation on Gene Networks and Regulatory Mechanisms in the Amygdala

The simultaneous study of the profile and interconnection between the genes that presented MIA-by-weaning stress interaction offered insights into the potential impact of the first and second stressors on the relationship between the genes.

Figures 3.2A and 3.2B depict two modules of genes that presented a MIA-by-weaning interaction effect where the yellow and green denote genes under- and over-expressed in weaned relative to nursed pigs exposed to MIA. Figures 3.2C and 3.2D depict two modules of genes that presented a MIA-by-weaning interaction effect where the yellow and green denote genes under- and over-expressed in non-MIA weaned relative to nursed pigs. Higher color intensities denote higher fold changes that are reported in Table 3.2, Figure 3.1, and Table 3.4. The depicted genes included nexilin F-actin binding protein (NEXN), forhead box B1 (FOXB1), LIM homeobox 9 (LHX9), orthodenticle homeobox 2 (OTX2), SIX homeobox 1 (SIX1), Zic family member 1(ZIC1), transcription factor 7 like 2 (TCF7L2), vasoactive intestinal peptide receptor 2 (VIPR2), luteinizing hormone subunit beta (LHB), glycoprotein hormones, alpha polypeptide (CGA), growth hormone 1 (GH1), proopiomelanocortin (POMC), neurotensin (NTS), and calbindin 1 (CALB1).

The comparison of expression patterns in consideration of the relationships between gene nodes highlights the profile change between MIA (Figure 3.2A) and non-MIA (Figure 3.2C) pigs in response to weaning stress in the module of the interacting OTX2, ZIC1, and TCFL2. The changes between MIA groups in the neuropeptide hormone gene module is the attenuation in the weaning effect on the profiles of VIPR2, POMC, and LHB that MIA exerted. This attenuation is visualized by the lower color intensity of the nodes in Figure 3.2B relative to Figure 3.2D.

The study of the enrichment of transcription factors among the genes that presented MIA-by-weaning stress interaction advanced the understanding of the impact of the first and second stressors on the co-expression profile of these genes. Transcription factors RAD21 and SUZ12 were enriched. Among the potential targets of RAD21 are three genes that shared the same differential expression between weaned and nursed in the MIA (Figures 3.2A and 3.2B) and non-MIA groups (Figures 3.2C and 3.2D). RAD21 targets POMC and GH1 and the differential expression of these genes between nursed and weaned pigs was consistent across MIA groups. RAD21 was over-expressed in weaned relative to nursed pigs and over-expressed in MIA relative to non-MIA groups.

The detected enrichment of the transcription factor SUZ12 among genes presenting MIA-by-weaning effect can be related to the over-expression of this gene in the MIA relative to non-MIA group. Targets of SUZ12 include FOXB1, a gene that was over-expressed in MIA pigs relative to non-MIA pigs. OTX2 and ZIC1 are also targets of SUZ12 and presented different profiles in response to weaning across MIA groups.

3.5 Discussion

Studies in rodents and humans surmise that prenatal immune challenge can augment (i.e., sensitization) or reduce (i.e., tolerance) the vulnerability of the brain and ensuing behavior disruption to subsequent challenges (Eklind et al. 2005; Eklind et al. 2001; Wang et al. 2007). Our results offer evidence that the double-hit hypothesis postulated in studies of behavior disorders associated with amygdala functions, including ASD and SSD in humans (Feigenson et al. 2014) and comparable behaviors in rodents (Wang et al. 2007), is germane to molecular pathways in the amygdala of weaned pigs exposed to viral infection during gestation. Moreover, we uncovered sex-dependent effects of pre and post-natal stressors in pigs.

The present study evaluated the effects of MIA and the postnatal stress of weaning on the amygdala transcriptome of female and male pigs. The mapped reads averaged 67% per sample and pig group, and is consistent with the mapping by kallisto software in other pig RNA-seq studies (Tan et al. 2017). The experimental design enabled the simultaneous testing of the impact of MIA and weaning within sex, in addition to detecting the independent effects of each stressor. The GSEA of the genes analyzed yielded 24 KEGG pathways enriched in at least one tested effect at FDR-adjusted P-value < 0.05 (Table 3.1) and the expression profiles of 118 genes presented MIA, weaning, sex, effects at FDR-adjusted P-value < 0.5. Pathways associated with immune and neurological processes dominated the enriched categories (Tables 3.1 and 3.2).

Effect of Weaning-by-Maternal Immune Activation Interaction on Amygdala Pathways

The majority of the KEGG pathways enriched among the genes presenting weaning-by-MIA interaction effects were characterized by pigs in the MIA weaned group presenting decreased expression levels that were comparable to the non-MIA nursed group, relative to MIA nursed and

non-MIA weaned groups. This blunting effect of the double hit indicates a prolonged effect of MIA dampening the immune response or related pathways, following the second stress of weaning. For certain processes, the decreased gene expression profiles in the MIA weaned pigs may sensitize the amygdala, making this brain structure more vulnerable to the second stressor. In contrast, for other processes, the decreased gene expression profiles in the MIA weaned pigs may afford tolerance, lowering the amygdala response to the postnatal stressor. This duality can be observed in molecular mechanisms associated with immune functions that include genes acting in feedforward and feedback manner, such as those detected in the present study.

The infection- and inflammation-associated pathways enriched among the genes presenting decreased expression in MIA weaned pigs included the Epstein-Barr virus infection (ssc05169) and influenza A (ssc05164) pathways (Table 3.1, Table 3.3). Weaning can trigger inflammatory processes and rats that have undergone maternal separation presented over-expression of inflammation-related genes in the microglia within the dorsal striatum and nucleus accumbens, and sustained hippocampal inflammation (Banqueri et al. 2019). Also, the pro-inflammatory cytokine TNF-α was over-expressed in the hippocampi of piglets exposed to MIA via PRRSV (Antonson et al. 2018). These reports illustrate responses to a single stressor, whereas a growing number of studies report that a first stressor may confer resilience to future insults (Ashby et al. 2010; Goh et al. 2020; Yee et al. 2011a). Consistent with our findings a study of mice exposed to MIA triggered by polyinosinic:polycytidylic acid (Poly(I:C)) or social isolation reported higher cytokine expression in either condition whereas cytokine levels were lower in the brains of mice that experienced a double-hit, MIA, and social isolation (Yee et al. 2011b).

Enriched among the genes exhibiting a significant MIA-by-weaning interaction effect were several pathways associated with autoimmune diseases, such as autoimmune thyroid disease (ssc05320) and rheumatoid arthritis (ssc05323, Table 3.1). The detected pathways, characterized genes under-expressed in MIA weaned pigs, are consistent with reports of a link between dysregulation of autoimmune pathways and SSD-related behaviors (Eaton et al. 1992). In agreement with our results, autoimmune diseases associated with the thyroid have an increased prevalence among parents of patients with SSD compared to parents of control subjects (Eaton et al. 2006). Additionally, both LPS-induced MIA and early weaning have been shown to increase the susceptibility of mice and rats, respectively, to experimental autoimmune encephalomyelitis (Laban et al. 1995; Zager et al. 2015). Similarly, pathways associated with cells involved in the pathogenesis of autoimmune disease, including Th1 and Th2 cell differentiation (ssc04658) and Th17 cell differentiation (ssc04659), were also enriched among the genes presenting a significant MIA-by-weaning interaction and under-expressed in MIA weaned pigs.

The cell adhesion molecules (CAMs) pathway (ssc04514) was enriched among genes exhibiting MIA-by-weaning interaction effects (Table 3.1). The over-representation of the CAMs pathway among genes under-expressed in MIA weaned pigs is also supported by the enrichment of this pathway in genes under-expressed in the cortex of ASD patients, with similar results found in the brains of rats subject to LPS-induced MIA (Lombardo et al. 2018). Our characterization of the double hit impact offered evidence that MIA can disrupt the immune response to weaning stress.

Effects of Weaning and Maternal Immune Activation on Gene Interactions and Regulation

The reconstruction of gene networks in consideration of the differential expression patterns between nursed and weaned pigs and contrast between MIA and non-MIA groups advanced the

recognition of the interplay between expression profiles in response to gestation and postnatal stressors. The comparison of networks underscored the diminished effect of weaning stress on the expression of neuropeptide hormone-related genes, including VIPR2, POMC, and LHB, among MIA relative to non-MIA pigs. The long-lasting impact of stressors during gestation on the POMC regulation and permanent effects on the hypothalamic-pituitary-adrenal axis function have been noted (Amath et al. 2012). Also, the expression level of LHB was altered in the peripheral blood of subjects with ASD (Kuwano et al. 2011), and polymorphisms and copy number variants in VIPR2 have been associated with ASD and SSD (Firouzabadi et al. 2017).

The weakened effect of weaning on the expression of multiple genes that have signaling roles suggests an antagonistic relationship between immune activation during gestation and weaning stress. This result aligns with the double-hit hypothesis (Giovanoli et al. 2013; Imanaka et al. 2006; Maynard et al. 2001; Walker et al. 2009) that gestational immune challenge can elicit long-term molecular disruptions that alter the offspring's response to another stressor later in life.

The expression patterns in Figure 3.1 suggest that some targets of the transcription factor ZBTB4 are less affected by MIA (e.g., SIX1), whereas targets that have a more moderate differential expression in response weaning are affected by MIA (e.g. TCF7L2, ZIC1, FOXB1). The exception was OTX2 that was over-expressed in MIA pigs relative to non-MIA pigs. The epigenetic action of ZBTB4 has been associated with the MIA-related condition of ASD (Smith et al. 2010).

The profiles of the transcription factors RAD21 and SUZ12 were associated with multiple genes exhibiting MIA-by-weaning effect and were over-expressed in MIA relative to non-MIA pigs, albeit at lower statistical significance than the target genes. RAD21 was negatively associated with the expression of neuropeptide gene GH1 and positively associated with the expression of POMC

and NTS. A key role of RAD21 in brain development has been proposed (Benitez-Burraco and Uriagereka 2016), and RAD21 has been associated with ASD (Persico et al. 2020). SUZ12 is considered a risk gene for ASD (Crawley et al. 2016) and could target FOXB1, OTX2, and ZIC1. The effect of SUZ12 is evident in the different impact of weaning across MIA groups on the target genes.

Sex-dependent Effects of Weaning and Maternal Immune Activation on Amygdala Pathways

Notably, the most enriched pathways among the genes that presented weaning-by-sex interaction effects were characterized by gene under-expression in weaned males and nursed female relative to weaned female and nursed male groups (Table 3.1). This pattern suggests that weaning stress depresses gene expression in males while heightening the level in females. Pathways involved in neurodegenerative diseases, including AD and Parkinson's disease, were enriched among genes with a profile of over-expression in weaned females (Table 3.1**)**.

The stress triggered by maternal separation has been associated with long-term modifications in midbrain dopaminergic neurons, primarily in females (Chocyk et al. 2011). This pattern is consistent with the over-expression of genes such as OTX2 that modulates midbrain GABA, dopamine, and serotonin-releasing neurons in weaned females. The enrichment of the oxidative phosphorylation pathway (ssc00190, Table 3.1) is consistent with findings that short-term treatment of neurons with corticosterone, a mediator of the stress response, increases mitochondrial oxidation potential within neurons, exerting a neuroprotective effect against stress (Du et al. 2009).

The enrichment of the neuroactive ligand-receptor interaction pathway (ssc04080) among the genes under-expressed in weaned males and nursed females (Table 3.1**)** is consistent with a similar enrichment among genes dysregulated in the amygdalae of mice exposed to psychological and physical stress (Sun et al. 2019). The neuroactive ligand-receptor interaction pathway was enriched among genes over-expressed in the amygdalae of mice that are resilient to chronic unpredictable mild stress (Shen et al. 2019). The retrograde endocannabinoid signaling pathway (ssc04723, Table 3.3) was also enriched among genes exhibiting a profile of under-expression in weaned males and nursed females. Increased endocannabinoid signaling is associated with a dampened stress response (Hillard 2014). The neuroactive ligand-receptor and the retrogragde endocannabinoid signaling pathways support the hypothesis that females could curb the effects of MIA on behavioral or neurological mechanisms regulated by the amygdala.

Effects of Weaning Stress, Maternal Immune Activation and Sex on Genes Profiles

Multiple genes presenting significant differential expression in the amygdala of pigs across weaning, MIA, and sex groups (Table 3.2 and Figure 3.1, Table 3.4) have been associated with stress effects. Genes associated with neural pathways and neurological disorders and immune-related functions presented significant weaning-by-MIA interaction effect, including OTX2, cholinergic receptor nicotinic alpha 2 subunit (CHRNA2), acid phosphatase 7, immunoglobulin heavy variable 3-23 (VHZ), and a gene annotated to the ribosome pathway PIGY upstream reading frame (PYURF) (Tables 3.1 and 3.2). For these genes, the double hit mode of action was characterized by reversal of the weaned effect between the non-MIA and MIA groups with the exception of MAGED4, which had a weakened weaning effect in MIA relative to non-MIA pigs.

The expression patterns of OTX2 in response to weaning and MIA effects is in agreement with reports of under-expression in the amygdala of rats exposed to neonatal stress and displaying anxiety as adults (Sarro et al. 2014). OTX2 modulates midbrain GABA, dopamine, and serotonin-releasing neurons and binding of OTX2 to perineuronal nets (biomarkers for SSD) grants neuroplasticity (Sarro et al. 2014). Postnatal stress was also associated with the under-expression of OTX2 in the ventral tegmental area in mice (Pena et al. 2017). MAGED4 has been linked to ASD (Kanduc and Polito 2018), and CHRNA2 was differentially methylated in a study of the effects of maternal psychosocial stress (Schroeder et al. 2012).

The significant weaning and MIA effects detected for PYURF are consistent with reports that this gene was under-expressed in the amygdala of low-novelty responder rats modeling anxiety-like behaviors relative to high novelty responders (Cohen 2017). Similarly, PYURF was under-expressed in weaned relative to nursed MIA pigs, while the expression was not affected in non-MIA pigs. Weaned MIA pigs showed a PYURF profile akin to anxiety-responsive rats.

Several genes presented significant simultaneous interactions of sex with weaning and sex with MIA (Table 3.2), including genes annotated to immune and neurological functions such as CGA, GH1, SIX1. GH1 and CGA were under-expressed in weaned relative to nursed MIA pigs and reversed and greater differences were detected among non-MIA pigs. Consistent with this finding, CGA and GH1 were under-expressed in the prefrontal cortex and cerebellum of rats that exhibited disrupted depressive-like behavior (Yamamoto et al. 2015).

The expression profile of SIX1 suggests that MIA reduced the effect of weaning, while this gene is substantially over-expressed in MIA weaned relative to nursed pigs. The transcription factor

SIX1 was annotated to a cluster of over-expressed genes in high-anxiety mice exposed to lipopolysaccharide immune challenge (Li et al. 2014).

Many genes that presented significant MIA effects, alone or interacting with sex (Table 3.2) such as NTS, CALB1, Purkinje cell protein 4 (PCP4), and LHX9 also have neurological functions. These genes shared the pattern of under-expression in MIA relative to non-MIA pigs with some genes presenting significant interactions between MIA and sex. NTS presented opposite profiles across sexes characterized by lower NTS levels in MIA relative to non-MIA males. This profile is consistent with the lower level of NTS in the amygdala of male rats that showed lower conditioned place preference consistent with MIA-associated behaviors (Laszlo et al. 2010). CALB1 has been associated with regulation of synaptic plasticity and ASD (Carter 2019). PCP4-null mice presented disruptions in cerebellar synaptic plasticity and impaired locomotor learning (Wei et al. 2011). LHX9 presented a highly significant MIA-by-sex interaction effect that could be linked to the role of LHX9 in the sexual dimorphism such that $LHX9^{-/-}$ mice do not produce gonads, and males display females phenotypes (Birk et al. 2000). Our results highlight the insights gained from studying the effect at the molecular level of postnatal stress conditional on prenatal stress and sex.

3.6 Conclusions

The study of the expression pattern of more than 17,000 genes in the amygdalae of 22 day old pigs uncovered evidence of disrupted immune pathways suggesting that pigs exposed to MIA are primed to be more sensitive to weaning. Also dysregulated were genes annotated to pathways with known connections to neurological disorders, including SSD and AD. The visualization of expression profiles in gene networks and study of the potential role of transcription factors such as SIX1 and ZBTB4 as possible mediators of stress within the amygdala. Additionally, the

functional enrichment of pathways associated with the sex-dependent response to weaning offered a potential means by which females may be more tolerant to the adverse effects of weaning stress.

The enriched pathways and transcription factors offer possible targets for therapies that may reduce the cumulative effects of both stressors. Furthermore, identifying potentially protective pathways in females exposed to weaning stress may help develop strategies to mitigate the more adverse effects of weaning on the amygdala molecular pathways of males.

3.7 References

Amath A, Foster JA, Sidor MM. 2012. Developmental alterations in cns stress-related gene expression following postnatal immune activation. Neuroscience. 220:90-99.

Andrews S. 2010. Fastqc: A quality control tool for high throughput sequence data. [Online] Available online at: https://www.bioinformatics.babraham.ac.uk/projects/fastqc/.

Antonson AM, Balakrishnan B, Radlowski EC, Petr G, Johnson RW. 2018. Altered hippocampal gene expression and morphology in fetal piglets following maternal respiratory viral infection. Dev Neurosci. 40(2):104-119.

Antonson AM, Lawson MA, Caputo MP, Matt SM, Leyshon BJ, Johnson RW. 2019. Maternal viral infection causes global alterations in porcine fetal microglia. Proc Natl Acad Sci U S A. 116(40):20190-20200.

Antonson AM, Radlowski EC, Lawson MA, Rytych JL, Johnson RW. 2017. Maternal viral infection during pregnancy elicits anti-social behavior in neonatal piglet offspring independent of postnatal microglial cell activation. Brain Behav Immun. 59:300-312.

Ashburner M, Ball CA, Blake JA, Botstein D, Butler H, Cherry JM, Davis AP, Dolinski K, Dwight SS, Eppig JT et al. 2000. Gene ontology: Tool for the unification of biology. Nat Genet. 25(1):25-29.

Ashby DM, Habib D, Dringenberg HC, Reynolds JN, Beninger RJ. 2010. Subchronic mk-801 treatment and post-weaning social isolation in rats: Differential effects on locomotor activity and hippocampal long-term potentiation. Behavioural Brain Research. 212(1):64-70.

Banqueri M, Mendez M, Gomez-Lazaro E, Arias JL. 2019. Early life stress by repeated maternal separation induces long-term neuroinflammatory response in glial cells of male rats. Stress-the International Journal on the Biology of Stress. 22(5):563-570.

Bayer TA, Falkai P, Maier W. 1999. Genetic and non-genetic vulnerability factors in schizophrenia: The basis of the "two hit hypothesis.". Journal of Psychiatric Research. 33(6):543-548.

Benitez-Burraco A, Uriagereka J. 2016. The immune syntax revisited: Opening new windows on language evolution. Frontiers in Molecular Neuroscience. 8:84.

Birk OS, Casiano DE, Wassif CA, Cogliati T, Zhao LP, Zhao YG, Grinberg A, Huang SP, Kreidberg JA, Parker KL et al. 2000. The lim homeobox gene lhx9 is essential for mouse gonad formation. Nature. 403(6772):909-913.

Bray NL, Pimentel H, Melsted P, Pachter L. 2016. Near-optimal probabilistic rna-seq quantification. Nat Biotechnol. 34(5):525-527.

Campbell JM, Crenshaw JD, Polo J. 2013. The biological stress of early weaned piglets. J Anim Sci Biotechno. 4(1):19.

Canetta S, Bolkan S, Padilla-Coreano N, Song LJ, Sahn R, Harrison NL, Gordon JA, Brown A, Kellendonk C. 2016. Maternal immune activation leads to selective functional deficits in offspring parvalbumin interneurons. Mol Psychiatry. 21(7):956-968.

Carbon S, Douglass E, Dunn N, Good B, Harris NL, Lewis SE, Mungall CJ, Basu S, Chisholm RL, Dodson RJ et al. 2019. The gene ontology resource: 20 years and still going strong. Nucleic Acids Research. 47(D1):D330-D338.

Carter CJ. 2019. Autism genes and the leukocyte transcriptome in autistic toddlers relate to pathogen interactomes, infection and the immune system. A role for excess neurotrophic sapp alpha and reduced antimicrobial a beta. Neurochem Int. 126:36-58.

Chocyk A, Przyborowska A, Dudys D, Majcher I, Mackowiak M, Wedzony K. 2011. The impact of maternal separation on the number of tyrosine hydroxylase-expressing midbrain neurons during different stages of ontogenesis. Neuroscience. 182:43-61.

Cohen JL, Jackson NL, Ballestas ME, Webb WM, Lubin FD, Clinton SM. 2017. Amygdalar expression of the microRNA miR-101a and its target Ezh2 contribute to rodent anxiety-like behaviour. Eur J Neurosci. 46(7):2241-2252. Crawley JN, Heyer WD, LaSalle JM. 2016. Autism and cancer share risk genes, pathways, and drug targets. Trends Genet. 32(3):139-146.

Curley JP, Jordan ER, Swaney WT, Izraelit A, Kammel S, Champagne FA. 2009. The meaning of weaning: Influence of the weaning period on behavioral development in mice. Developmental Neuroscience. 31(4):318-331.

Du J, Wang Y, Hunter R, Wei YL, Blumenthal R, Falke C, Khairova R, Zhou RL, Yuan PX, Machado-Vieira R et al. 2009. Dynamic regulation of mitochondrial function by glucocorticoids. Proceedings of the National Academy of Sciences of the United States of America. 106(9):3543-3548.

Eaton WW, Byrne M, Ewald H, Mors O, Chen CY, Agerbo E, Mortensen PB. 2006. Association of schizophrenia and autoimmune diseases: Linkage of danish national registers. Am J Psychiat. 163(3):521-528.

Eaton WW, Hayward C, Ram R. 1992. Schizophrenia and rheumatoid-arthritis - a review. Schizophrenia Research. 6(3):181-192.

Eklind S, Mallard C, Arvidsson P, Hagberg H. 2005. Lipopolysaccharide induces both a primary and a secondary phase of sensitization in the developing rat brain. Pediatric research. 58(1):112-116.

Eklind S, Mallard C, Leverin AL, Gilland E, Blomgren K, Mattsby-Baltzer I, Hagberg H. 2001. Bacterial endotoxin sensitizes the immature brain to hypoxic--ischaemic injury. Eur J Neurosci. 13(6):1101-1106.

Feigenson KA, Kusnecov AW, Silverstein SM. 2014. Inflammation and the two-hit hypothesis of schizophrenia. Neuroscience and Biobehavioral Reviews. 38:72-93.

Félix B, Léger M-E, Albe-Fessard D, Marcilloux JC, Rampin O, Laplace JP, Duclos A, Fort F, Gougis S, Costa M et al. 1999. Stereotaxic atlas of the pig brain. Brain Res Bull. 49(1):1-137.

Firouzabadi SG, Kariminejad R, Vameghi R, Darvish H, Ghaedi H, Banihashemi S, Moghaddam MF, Jamali P, Tehrani HFM, Dehghani H et al. 2017. Copy number variants in patients with autism and additional clinical features: Report of vipr2 duplication and a novel microduplication syndrome. Mol Neurobiol. 54(9):7019-7027.

Gimsa U, Tuchscherer M, Kanitz E. 2018. Psychosocial stress and immunity-what can we learn from pig studies? Front Behav Neurosci. 12:64.

Giovanoli S, Engler H, Engler A, Richetto J, Voget M, Willi R, Winter C, Riva MA, Mortensen PB, Feldon J et al. 2013. Stress in puberty unmasks latent neuropathological consequences of prenatal immune activation in mice. Science. 339(6123):1095-1099.

Giroux S, Martineau GP, Robert S. 2000a. Relationships between individual behavioural traits and post-weaning growth in segregated early-weaned piglets. Appl Anim Behav Sci. 70(1):41-48.

Giroux S, Robert S, Martineau GP. 2000b. The effects of cross-fostering on growth rate and post-weaning behavior of segregated early-weaned piglets. Can J Anim Sci. 80(4):533-538.

Goh J-Y, O'Sullivan SE, Shortall SE, Zordan N, Piccinini AM, Potter HG, Fone KCF, King MV. 2020. Gestational poly(i:C) attenuates, not exacerbates, the behavioral, cytokine and mtor changes caused by isolation rearing in a rat 'dual-hit' model for neurodevelopmental disorders. Brain, Behavior, and Immunity. 89:100-117.

Hillard CJ. 2014. Stress regulates endocannabinoid-cb1 receptor signaling. Semin Immunol. 26(5):380-388.

Imanaka A, Morinobu S, Toki S, Yamawaki S. 2006. Importance of early environment in the development of post-traumatic stress disorder-like behaviors. Behavioural Brain Research. 173(1):129-137.

Janky R, Verfaillie A, Imrichova H, Van de Sande B, Standaert L, Christiaens V, Hulselmans G, Herten K, Sanchez MN, Potier D et al. 2014. Iregulon: From a gene list to a gene regulatory network using large motif and track collections. Plos Comput Biol. 10(7):e1003731.

Kanduc D, Polito A. 2018. From viral infections to autistic neurodevelopmental disorders via cross-reactivity. Journal of Psychiatry and Brain Science. 3(6):14.

Kanehisa M. 2019. Toward understanding the origin and evolution of cellular organisms. Protein Sci. 28(11):1947-1951.

Kanehisa M, Goto S. 2000. Kegg: Kyoto encyclopedia of genes and genomes. Nucleic Acids Research. 28(1):27-30.

Kanitz E, Manteuffel G, Otten W. 1998. Effects of weaning and restraint stress on glucocorticoid receptor binding capacity in limbic areas of domestic pigs. Brain Research. 804(2):311-315.

Karp PD, Billington R, Caspi R, Fulcher CA, Latendresse M, Kothari A, Keseler IM, Krummenacker M, Midford PE, Ong Q et al. 2019. The biocyc collection of microbial genomes and metabolic pathways. Brief Bioinform. 20(4):1085-1093.

Keever MR, Zhang P, Bolt CR, Antonson AM, Rymut HE, Caputo MP, Houser AK, Hernandez AG, Southey BR, Rund LA et al. 2020a. Lasting and sex-dependent impact of maternal immune activation on molecular pathways of the amygdala. Frontiers in Neuroscience. 14:774.

Keever MR, Zhang P, Bolt CR, Rymut HE, Antonson AM, Corbett MP, Houser AK, Southy BR, Rund LA, Johnson RW. 2020b. Psviii-1 a transcriptomic study of the effect of prrsv infection during gestation on the piglet amygdala. Journal of Animal Science. 98(Supplement_4):255-256.

Kick AR, Tompkins MB, Flowers WL, Whisnant CS, Almond GW. 2012. Effects of stress associated with weaning on the adaptive immune system in pigs. Journal of Animal Science. 90(2):649-656.

Knuesel I, Chicha L, Britschgi M, Schobel SA, Bodmer M, Hellings JA, Toovey S, Prinssen EP. 2014. Maternal immune activation and abnormal brain development across cns disorders. Nat Rev Neurol. 10(11):643-660.

Kuwano Y, Kamio Y, Kawai T, Katsuura S, Inada N, Takaki A, Rokutan K. 2011. Autism-associated gene expression in peripheral leucocytes commonly observed between subjects with autism and healthy women having autistic children. Plos One. 6(9):e24723.

Laban O, Markovic BM, Dimitrijevic M, Jankovic BD. 1995. Maternal-deprivation and early weaning modulate experimental allergic encephalomyelitis in the rat. Brain Behavior and Immunity. 9(1):9-19.

Laszlo K, Toth K, Kertes E, Peczely L, Ollmann T, Lenard L. 2010. Effects of neurotensin in amygdaloid spatial learning mechanisms. Behav Brain Res. 210(2):280-283.

Li ZL, Ma L, Kulesskaya N, Voikar V, Tian L. 2014. Microglia are polarized to m1 type in high-anxiety inbred mice in response to lipopolysaccharide challenge. Journal of Neuroimmunology. 275(1-2):183-184.

Liao Y, Wang J, Jaehnig EJ, Shi Z, Zhang B. 2019. Webgestalt 2019: Gene set analysis toolkit with revamped uis and apis. Nucleic Acids Research. 47(W1):W199-W205.

Lombardo MV, Moon HM, Su J, Palmer TD, Courchesne E, Pramparo T. 2018. Maternal immune activation dysregulation of the fetal brain transcriptome and relevance to the pathophysiology of autism spectrum disorder. Molecular Psychiatry. 23(4):1001-1013.

Mattei D, Ivanov A, Ferrai C, Jordan P, Guneykaya D, Buonfiglioli A, Schaafsma W, Przanowski P, Deuther-Conrad W, Brust P et al. 2017. Maternal immune activation results in complex microglial transcriptome signature in the adult offspring that is reversed by minocycline treatment. Translational Psychiatry. 7(5):e1120-e1120.

Maynard TM, Sikich L, Lieberman JA, LaMantia A-S. 2001. Neural development, cell-cell signaling, and the “two-hit” hypothesis of schizophrenia. Schizophrenia Bulletin. 27(3):457-476.

Odorizzi PM, Feeney ME. 2016. Impact of in utero exposure to malaria on fetal t cell immunity. Trends Mol Med. 22(10):877-888.

Pena CJ, Kronman HG, Walker DM, Cates HM, Bagot RC, Purushothaman I, Issler O, Loh YHE, Leong T, Kiraly DD et al. 2017. Early life stress confers lifelong stress susceptibility in mice via ventral tegmental area otx2. Science. 356(6343):1185-1188.

Persico AM, Cucinotta F, Ricciardello A, Turriziani L. 2020. Chapter 3 - autisms. In: Rubenstein J, Rakic P, Chen B, Kwan KY, editors. Neurodevelopmental disorders. Academic Press. p. 35-77.

Pie S, Lalles JP, Blazy F, Laffitte J, Seve B, Oswald IP. 2004. Weaning is associated with an upregulation of expression of inflammatory cytokines in the intestine of piglets. J Nutr. 134(3):641-647.

Poletto R, Steibel JP, Siegford JM, Zanella AJ. 2006. Effects of early weaning and social isolation on the expression of glucocorticoid and mineralocorticoid receptor and 11 beta-hydroxysteroid dehydrogenase 1 and 2 mrnas in the frontal cortex and hippocampus of piglets. Brain Research. 1067(1):36-42.

Prins JR, Eskandar S, Eggen BJL, Scherjon SA. 2018. Microglia, the missing link in maternal immune activation and fetal neurodevelopment; and a possible link in preeclampsia and disturbed neurodevelopment? Journal of Reproductive Immunology. 126:18-22.

Pruitt KD, Tatusova T, Maglott DR. 2007. Ncbi reference sequences (refseq): A curated non-redundant sequence database of genomes, transcripts and proteins. Nucleic Acids Research. 35:D61-D65.

Puppe B, Tuchscherer M, Tuchscherer A. 1997. The effect of housing conditions and social environment immediately after weaning on the agonistic behaviour, neutrophil/lymphocyte ratio, and plasma glucose level in pigs. Livest Prod Sci. 48(2):157-164.

Robinson MD, McCarthy DJ, Smyth GK. 2010. Edger: A bioconductor package for differential expression analysis of digital gene expression data. Bioinformatics. 26(1):139-140.

Sarro EC, Sullivan RM, Barr G. 2014. Unpredictable neonatal stress enhances adult anxiety and alters amygdala gene expression related to serotonin and gaba. Neuroscience. 258:147-161.

Schroeder JW, Smith AK, Brennan PA, Conneely KN, Kilaru V, Knight BT, Newport DJ, Cubells JF, Stowe ZN. 2012. DNA methylation in neonates born to women receiving psychiatric care. Epigenetics-Us. 7(4):409-414.

Shannon P, Markiel A, Ozier O, Baliga NS, Wang JT, Ramage D, Amin N, Schwikowski B, Ideker T. 2003. Cytoscape: A software environment for integrated models of biomolecular interaction networks. Genome Research. 13(11):2498-2504.

Shen MM, Song ZH, Wang JH. 2019. Microrna and mrna profiles in the amygdala are associated with stress-induced depression and resilience in juvenile mice. Psychopharmacology. 236(7):2119-2142.

Smith CL, Bolton A, Nguyen G. 2010. Genomic and epigenomic instability, fragile sites, schizophrenia and autism. Curr Genomics. 11(6):447-469.

Sun Y, Lu W, Du KX, Wang JH. 2019. Microrna and mrna profiles in the amygdala are relevant to fear memory induced by physical or psychological stress. Journal of Neurophysiology. 122(3):1002-1022.

Szklarczyk D, Gable AL, Lyon D, Junge A, Wyder S, Huerta-Cepas J, Simonovic M, Doncheva NT, Morris JH, Bork P et al. 2019. String v11: Protein-protein association networks with increased coverage, supporting functional discovery in genome-wide experimental datasets. Nucleic Acids Research. 47(D1):D607-D613.

Tan Z, Wang Y, Yang T, Xing K, Ao H, Chen S, Zhang F, Zhao X, Liu J, Wang C. 2017. Differentially expressed genes in the caecal and colonic mucosa of landrace finishing pigs with high and low food conversion ratios. Scientific Reports. 7(1):14886.

Tian J, Dai HM, Deng YY, Zhang J, Li Y, Zhou J, Zhao MY, Zhao MW, Zhang C, Zhang YX et al. 2015. The effect of hmgb1 on sub-toxic chlorpyrifos exposure-induced neuroinflammation in amygdala of neonatal rats. Toxicology. 338:95-103.

Turpin DL, Langendijk P, Plush K, Pluske JR. 2017. Intermittent suckling with or without co-mingling of non-littermate piglets before weaning improves piglet performance in the immediate post-weaning period when compared with conventional weaning. J Anim Sci Biotechno. 8:14.

Walker AK, Nakamura T, Byrne RJ, Naicker S, Tynan RJ, Hunter M, Hodgson DM. 2009. Neonatal lipopolysaccharide and adult stress exposure predisposes rats to anxiety-like behaviour and blunted corticosterone responses: Implications for the double-hit hypothesis. Psychoneuroendocrinology. 34(10):1515-1525.

Wang X, Hagberg H, Nie C, Zhu C, Ikeda T, Mallard C. 2007. Dual role of intrauterine immune challenge on neonatal and adult brain vulnerability to hypoxia-ischemia. Journal of Neuropathology & Experimental Neurology. 66(6):552-561.

Wei P, Blundon JA, Rong YQ, Zakharenko SS, Morgan JI. 2011. Impaired locomotor learning and altered cerebellar synaptic plasticity in pep-19/pcp4-null mice. Molecular and Cellular Biology. 31(14):2838-2844.

Yamamoto Y, Ueyama T, Ito T, Tsuruo Y. 2015. Downregulation of growth hormone 1 gene in the cerebellum and prefrontal cortex of rats with depressive-like behavior. Physiological Genomics. 47(5):170-176.

Yee N, Ribic A, de Roo CC, Fuchs E. 2011a. Differential effects of maternal immune activation and juvenile stress on anxiety-like behaviour and physiology in adult rats: No evidence for the "double-hit hypothesis". Behavioural Brain Research. 224(1):180-188.

Yee N, Ribic A, de Roo CC, Fuchs E. 2011b. Differential effects of maternal immune activation and juvenile stress on anxiety-like behaviour and physiology in adult rats: No evidence for the “double-hit hypothesis”. Behavioural Brain Research. 224(1):180-188.

Zager A, Peron JP, Mennecier G, Rodrigues SC, Aloia TP, Palermo-Neto J. 2015. Maternal immune activation in late gestation increases neuroinflammation and aggravates experimental autoimmune encephalomyelitis in the offspring. Brain Behavior and Immunity. 43:159-171.

3.8 Tables

Table 3.1. Pathways enriched in at least one effect including interaction or main effect of weaning (Wea), maternal immune activation (MIA), and sex at P-value < 5.0E-05, and normalized enrichment score |NES| > 2.

	Wea*MIA[b]		Wea*Sex		Wea		MIA*Sex		MIA		Sex	
KEGG Pathway	N[a]	P	N	P	N	P	N	P	N	P	N	P
ssc04080:Neuroactive ligand-receptor	-1.5	6.E-03	-2.0	1.E-05	1.5	1.E-02	-2.0	1.E-05	-1.4	5.E-02		
ssc05010:Alzheimer disease	-1.3	5.E-02	-1.9	1.E-03			-2.0	1.E-05				
ssc04514:Cell adhesion molecules	1.9	1.E-05			-1.5	6.E-03	1.4	3.E-02	-1.8	2.E-03		
ssc04932:Non-alcoholic fatty liver disease	-1.6	6.E-03	-2.0	1.E-05			-2.1	1.E-05	-1.8	5.E-03	1.5	6.E-02
ssc05012:Parkinson disease	-1.5	4.E-02	-2.0	1.E-05			-2.1	1.E-05	-1.4	4.E-02	1.6	5.E-02
ssc04659:Th17 cell differentiation	2.0	1.E-05			-1.5	1.E-02	1.7	8.E-03	-1.5	4.E-02		
ssc04623:Cytosolic DNA-sensing pathway	2.1	1.E-05			-1.6	2.E-02	1.4	7.E-02				
ssc04145:Phagosome	2.2	1.E-05			-1.4	2.E-02	1.6	1.E-05	-1.9	1.E-03		
ssc05164:Influenza A	2.1	1.E-05			-1.7	1.E-05	2.0	1.E-05	-1.7	3.E-03		
ssc04658:Th1 & Th2 cell differentiation	2.1	1.E-05			-1.6	1.E-02	1.7	1.E-05	-1.5	4.E-02		
ssc05169:Epstein-Barr virus infection	2.1	1.E-05			-1.8	1.E-05	1.6	1.E-05	-1.9	1.E-05		

Table 3.1 (cont.)

ssc05323:Rheumatoid arthritis	2.2	1.E-05					1.6	1.E-02	-1.6	1.E-02		
ssc05168:Herpes simplex infection	2.2	1.E-05			-1.7	2.E-03	2.0	1.E-05	-1.7	9.E-03		
ssc00190:Oxidative phosphorylation	-1.3	9.E-02	-1.9	3.E-03			-2.3	1.E-05	-1.3	7.E-02	1.5	7.E-02
ssc03010:Ribosome			-2.2	1.E-05	2.2	1.E-05	-2.5	1.E-05	-1.9	2.E-03	1.4	1.E-01
ssc04612:Antigen processing, presentation	2.6	1.E-05			-2.2	1.E-05	2.5	1.E-05	-1.6	2.E-02	-1.7	6.E-03
ssc04940:Type I diabetes mellitus	2.4	1.E-05			-2.1	1.E-05	2.4	1.E-05	-1.7	1.E-02	-1.7	5.E-03
ssc05320:Autoimmune thyroid disease	2.4	1.E-05	-1.5	5.E-02	-2.1	1.E-05	1.6	2.E-02	-1.9	2.E-03	1.4	1.E-01
ssc05322:Systemic lupus erythematosus	2.4	1.E-05			-1.7	6.E-03	1.9	1.E-05	-1.5	3.E-02		
ssc05332:Graft-versus-host disease	2.4	1.E-05			-2.2	1.E-05	2.3	1.E-05	-1.7	9.E-03	-1.7	2.E-02

[a] N=NES;

[b] P = P-value < 5.0E-05 corresponds to a False Discovery Rate P-value < 5.0E-02.

[c] Wea*MIA = weaning-by-MIA interaction effect where NES > 0 denotes gene over-expression in non-MIA nursed relative to MIA weaned pigs, and NES < 0 denotes gene under-expression in non-MIA nursed relative to MIA weaned pigs;

Wean*Sex = weaning-by-sex interaction effect where NES > 0 denotes gene over-expression in nursed males relative to weaned females, and NES < 0 denotes gene under-expression in nursed males relative to weaned females;

MIA*Sex = MIA-by-sex interaction effect where NES > 0 denotes gene over-expression in MIA females relative to MIA males, and NES < 0 denotes gene under-expression in MIA females relative to MIA males;

Table 3.1 (cont.)

Wea = weaning effect where NES > 0 denotes gene over-expression in weaned relative to nursed pigs, and NES < 0 denotes gene over-expression in nursed relative to weaned pigs;

MIA = maternal immune activation effect where NES > 0 denotes gene over-expression in non-MIA relative to MIA pigs, and NES- denotes gene over-expression in MIA relative to non-MIA pigs; and

Sex effect where NES > 0 denotes gene over-expression in males relative of females, and NES < 0 denotes gene over-expression in females relative of male

Table 3.2. P-value (P) and False discovery rate adjusted P-value (FDR) of genes that presented at least one significant interaction or main effect of weaning, maternal immune activation at P-value < 5.0E-05 and $|\log_2(\text{fold change between pig groups})| > 2.0$.

Gene Symbol	MIA[a] P	MIA FDR	MIA*S P	MIA*S FDR	W*MIA P	W*MIA FDR	Sex P	Sex FDR	W*Sex P	W*Sex FDR	Wea P	Wea FDR
PYURF	4.E-25	7.E-21	4.E-15	2.E-11	2.E-17	2.E-13	2.E-20	3.E-17	2.E-36	4.E-32	2.E-20	4.E-16
EIF1AY	9.E-03	1.E+00	1.E-02	1.E+00	1.E-01	1.E+00	6.E-34	5.E-30	2.E-01	1.E+00	2.E-01	1.E+00
EIF2S3Y	6.E-02	1.E+00	9.E-02	1.E+00	8.E-01	1.E+00	2.E-32	8.E-29	5.E-01	1.E+00	4.E-01	1.E+00
GH1	8.E-01	1.E+00	2.E-19	3.E-15	8.E-01	1.E+00	2.E-32	8.E-29	7.E-22	5.E-18	4.E-01	1.E+00
DDX3Y	1.E-01	1.E+00	1.E-01	1.E+00	4.E-01	1.E+00	9.E-32	3.E-28	3.E-01	1.E+00	3.E-01	1.E+00
VHZ	8.E-20	7.E-16	1.E-05	8.E-03	2.E-06	5.E-03	8.E-04	3.E-01	2.E-02	1.E+00	4.E-04	9.E-01
CGA	9.E-01	1.E+00	2.E-13	5.E-10	5.E-01	1.E+00	3.E-19	4.E-16	1.E-14	8.E-11	4.E-01	1.E+00
OTX2	9.E-10	4.E-06	6.E-17	3.E-13	3.E-08	1.E-04	2.E-09	2.E-06	5.E-06	1.E-02	2.E-01	1.E+00
SIX1	5.E-01	1.E+00	3.E-08	3.E-05	2.E-01	1.E+00	1.E-13	1.E-10	9.E-09	4.E-05	2.E-04	5.E-01
RGS16	7.E-07	1.E-03	1.E-13	4.E-10	1.E-04	2.E-01	3.E-09	3.E-06	1.E-05	2.E-02	9.E-01	1.E+00
IGHG	9.E-11	5.E-07	5.E-02	1.E+00	3.E-01	1.E+00	3.E-01	1.E+00	9.E-01	1.E+00	5.E-01	1.E+00
CHRNA2	2.E-07	4.E-04	1.E-10	3.E-07	1.E-04	2.E-01	3.E-05	1.E-02	1.E-03	1.E+00	7.E-01	1.E+00
NTS	4.E-05	4.E-02	1.E-09	2.E-06	2.E-02	1.E+00	2.E-04	8.E-02	5.E-03	1.E+00	3.E-01	1.E+00

Table 3.2 (cont.)

AHNAK2	8.E-05	7.E-02	1.E-09	2.E-06	8.E-03	1.E+00	5.E-05	3.E-02	2.E-02	1.E+00	2.E-01	1.E+00
CALB1	1.E-04	8.E-02	1.E-09	2.E-06	2.E-02	1.E+00	2.E-06	1.E-03	1.E-03	8.E-01	4.E-01	1.E+00
PCP4	4.E-04	2.E-01	2.E-09	2.E-06	8.E-03	1.E+00	1.E-05	7.E-03	1.E-03	8.E-01	1.E+00	1.E+00
FOXB1	2.E-05	2.E-02	2.E-09	2.E-06	7.E-02	1.E+00	6.E-05	3.E-02	2.E-02	1.E+00	6.E-01	1.E+00
DLK1	6.E-03	1.E+00	2.E-09	3.E-06	5.E-01	1.E+00	2.E-06	2.E-03	3.E-03	1.E+00	1.E+00	1.E+00
KRT8	1.E-02	1.E+00	7.E-05	3.E-02	3.E-01	1.E+00	3.E-09	3.E-06	2.E-04	2.E-01	1.E-05	5.E-02
NEXN	1.E-04	9.E-02	7.E-09	8.E-06	1.E-03	1.E+00	5.E-06	3.E-03	6.E-04	6.E-01	6.E-01	1.E+00
LHB	3.E-01	1.E+00	1.E-04	6.E-02	5.E-01	1.E+00	1.E-08	1.E-05	8.E-05	1.E-01	6.E-01	1.E+00
ZFY	1.E+00	1.E+00	8.E-01	1.E+00	8.E-01	1.E+00	2.E-08	1.E-05	1.E+00	1.E+00	7.E-01	1.E+00
CD5L	3.E-08	8.E-05	1.E-02	1.E+00	4.E-01	1.E+00	4.E-03	1.E+00	2.E-01	1.E+00	6.E-01	1.E+00
LHX9	8.E-04	5.E-01	3.E-08	3.E-05	1.E-02	1.E+00	6.E-07	4.E-04	1.E-03	8.E-01	5.E-01	1.E+00
POMC	9.E-01	1.E+00	7.E-06	4.E-03	8.E-01	1.E+00	4.E-08	3.E-05	2.E-05	3.E-02	8.E-01	1.E+00
ACP7	2.E-07	4.E-04	5.E-07	4.E-04	4.E-08	1.E-04	3.E-04	1.E-01	1.E-05	2.E-02	1.E-02	1.E+00
ISM1	2.E-03	1.E+00	2.E-07	1.E-04	8.E-03	1.E+00	7.E-06	4.E-03	4.E-04	4.E-01	6.E-01	1.E+00
FAM83B	2.E-02	1.E+00	2.E-07	2.E-04	9.E-04	1.E+00	6.E-07	5.E-04	8.E-06	2.E-02	1.E-03	1.E+00
POU1F1	8.E-01	1.E+00	8.E-04	3.E-01	7.E-01	1.E+00	2.E-07	2.E-04	5.E-05	7.E-02	6.E-01	1.E+00
NTNG1	2.E-03	8.E-01	4.E-07	3.E-04	1.E-02	1.E+00	1.E-04	5.E-02	7.E-03	1.E+00	5.E-01	1.E+00

Table 3.2 (cont.)

[a] MIA = maternal immune activation effect; MIA*S = maternal immune activation-by-sex interaction effect; W*MIA = weaning-by-maternal immune activation interaction effect; Sex = sex effect; W*Sex = weaning-by-sex interaction effect; Wea = weaning effect; P-value < 5.0E-05 corresponds to approximate False Discovery Rate-adjusted P-value < 5.0E-02.

3.9 Figures

Figure 3.1. Heatmap listing the differential expression (log_2(fold change between pig groups)) of genes that presented at least one significant interaction or main effect of weaning, maternal immune activation at P-value < 5.0E-05 and |log_2(fold change between pig groups)| > 2.0 .

	Gene	Weaning*MIA[b]				Weaning*Sex				MIA*Sex			
F	Symbol	CN-CW[c]	CN-PN	CW-PW	PN-PW	NF-NM	NF-WF	NM-WM	WF-WM	CF-CM	CF-PF	CM-PM	PF-PM
N[a]	PYURF	-0.06[d]	-2.35	-0.24	2.05	-0.46	0.09	9.74	9.19	-0.15	-2.03	-1.07	0.82
I	EIF1AY	-0.15	-0.07	0.03	-0.05	-11.49	0.29	-0.11	-11.89	-13.01	-1.95	0.09	-10.96
	EIF2S3Y	-0.13	-0.14	-0.02	-0.02	-10.85	0.54	-0.08	-11.47	-12.35	-1.83	0.04	-10.48
N	GH1	8.09	9.21	-1.04	-1.34	-10.02	-0.44	7.79	-1.8	-9.61	0.4	7.79	-2.22
N	DDX3Y	-0.2	-0.19	-0.04	-0.05	-11.16	0.49	-0.13	-11.78	-12.84	-2.08	0.01	-10.76
I	VHZ	-1.69	-6.1	-3.43	0.99	1.72	2	-0.78	-1.06	-1.45	-5.85	-3.61	0.79
I	CGA	5.77	6.12	0.49	0.13	-6.1	-0.24	6.39	0.52	-5.86	0.27	6.49	0.36
N	OTX2	2.42	-0.12	0.98	3.52	-0.08	2.84	2.94	0.02	-2.91	-2.88	3.47	3.44
N	SIX1	2.07	4.32	0.9	-1.35	-4.57	-2.03	2.59	0.06	-3.13	0.45	3.79	0.21
N	RGS16	3.21	0.68	-0.07	2.45	-0.89	2.54	3.13	-0.3	-3.25	-2.44	3.06	2.24
I	IGHG	-0.51	-3.86	-4.66	-1.3	0.85	-1.5	-1.09	1.26	-0.75	-5.38	-3.27	1.36
N	CHRNA2	1.78	-0.72	-0.14	2.36	0.52	2.3	1.81	0.03	-1.88	-2.52	1.79	2.44
N	NTS	1.06	-0.18	0.05	1.29	0.2	0.88	1.58	0.9	-1.43	-1.78	2.47	2.81
	AHNAK2	2.28	0.11	0.05	2.23	-0.12	2.37	2.17	-0.32	-2.13	-1.98	2.38	2.23
N	CALB1	1.66	0.55	-0.26	0.86	-0.69	0.92	1.61	0.01	-2.17	-1.66	2.02	1.52
N	PCP4	2.05	0.54	0.21	1.72	-0.54	1.49	2.32	0.29	-2.03	-1.51	2.61	2.09
N	FOXB1	1.2	-0.15	-0.41	0.94	0.08	0.88	1.24	0.44	-1.87	-2.17	2.04	2.34
I	DLK1	2.05	1.32	-0.4	0.33	-1.22	0.38	2.14	0.54	-2.42	-1.53	2.92	2.03
I	KRT8	-0.11	4.87	1.53	-3.45	-3.68	-3.05	0.39	-0.25	-1.88	0.7	3.47	0.89
N	NEXN	1.85	0.39	0.28	1.75	-0.56	1.51	2.08	0.02	-2.05	-1.54	2.2	1.69
N	LHB	3.13	3.35	0.16	-0.05	-3.22	0.13	3.24	-0.12	-3.16	0.32	3.36	-0.12
	ZFY	-0.31	-0.41	0.05	0.16	-4.02	-0.12	-0.08	-3.98	-3.91	0.11	-0.09	-4.1
I	CD5L	0.55	-2.65	-2.69	0.5	-0.12	0.18	0.7	0.4	-1.41	-3.71	-1.86	0.44
N	LHX9	1.79	0.94	0.4	1.26	-1.19	0.91	2.1	0.01	-2.37	-1.29	2.48	1.4
N	POMC	2.76	2.93	0.17	-0.01	-2.8	0.02	3.02	0.21	-2.79	0.06	3.19	0.33
N	ACP7	0.58	-1.2	-0.28	1.51	0.6	1.53	0.65	-0.29	-0.65	-1.63	-0.01	0.97
I	ISM1	1.86	0.82	0.44	1.48	-0.95	1.05	2.31	0.31	-1.97	-1.06	2.36	1.45
	FAM83B	0.65	1.58	1.32	0.39	-1.66	-0.71	1.59	0.64	-1.34	0.27	2.58	0.98
I	POU1F1	2.37	2.49	0.29	0.18	-2.7	-0.11	2.65	0.06	-2.49	0.33	2.55	-0.27
N	NTNG1	1.16	0.41	0.53	1.29	-0.47	0.91	1.52	0.13	-1.6	-1.11	2.09	1.6

Footnote:

[a] Functional annotation of the gene; N: neuro-associated or I = immune-associated function.

[b] Weaning*MIA: log_2(fold change between pig groups) characterizing the weaning-by-maternal immune activation effect; Weaning*Sex: log_2(fold change between pig groups) characterizing the weaning-by-sex effect; MIA*Sex: log_2(fold change between pig groups) characterizing the maternal immune activation-by-sex effect.

Figure 3.1 (cont.)

[c]Log_2(fold change of pig group X relative to group Y) = $log_2(X/Y) = log_2(X) – log_2(Y)$. The pig groups compared included: non-MIA or control nursed pigs (CN), non-MIA weaned pigs (CW), PRRSV-elicited MIA nursed pigs (PN), MIA weaned pigs (PW), nursed females (NF), nursed males (NM), weaned females (WF), weaned males (PM), non-MIA females (CF), non-MIA males (CM), PRRSV-elicited MIA females (PF), MIA males (PM).

[d] Red (green) denotes under(over)-expression in the X or first pig group relative to the Y or second pig group.

Figure 3.2. Gene network submodules of the gene orthodenticle homeobox 2 (A and C) and the gene vasoactive intestinal peptide receptor 2 (B and D). Modules A and B depict under- (yellow) and over- (green) expression between MIA weaned and nursed pigs while modules C and D depict under- (yellow) and over- (green) expression between non-MIA weaned and nursed pigs.

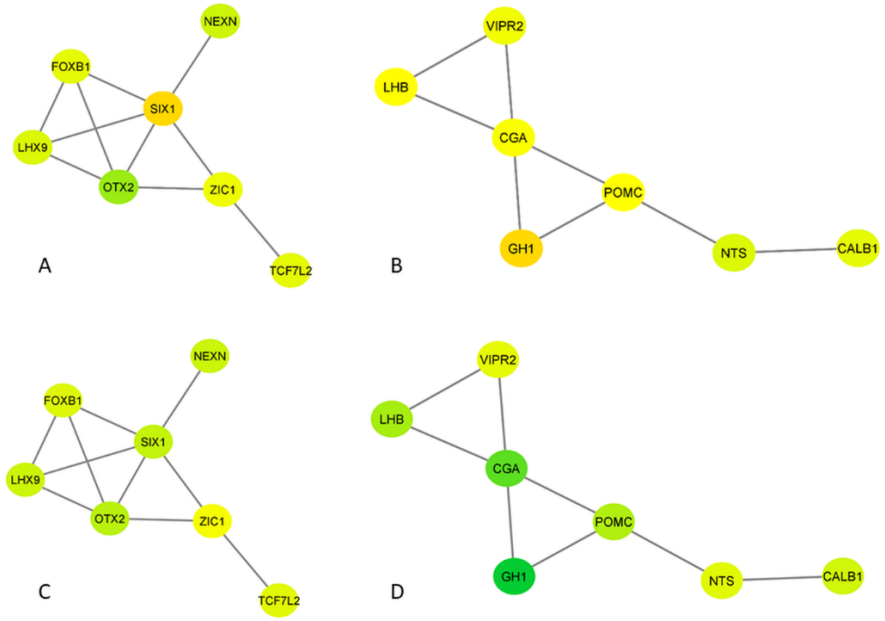

Chapter 4: Disruption of alternative splicing in the amygdala of pigs exposed to immune activation

4.1 Abstract

The intrauterine environment during pregnancy greatly impacts the developmental trajectory of the fetal brain, and evidence shows that maternal immune activation (MIA) during pregnancy leads to lasting structural and functional changes in the amygdalae of offspring, a region whose dysregulation has been linked to neurodevelopmental, neurodegenerative, and behavioral disorders. Brain tissues have some of the largest number of alternatively spliced genes, and aberrant splicing has been observed in the same neurological disorders associated with MIA. This study enhances our understanding of the effects of MIA on alternative splicing in the amygdala. Differential alternative splicing was profiled between pigs exposed to viral-elicited MIA and controls within female and male pigs. Overall, 132 loci and 176 loci were found to be differentially alternatively spliced between MIA and control pigs within females and males, respectively. The genes identified as being significantly differentially alternatively spliced have been previously associated with neurodevelopmental, neurodegenerative, and mood disorders. In females, enriched pathways were associated with Alzheimer's disease and synaptic integrity. The differentially alternatively spliced genes observed in males have been linked to dendritic spine density and neuronal excitability, and enriched pathways among genes showing significant alternative splicing have been implicated in homeostasis and reward pathways within the brain.

4.2 Introduction

The intrauterine environment during pregnancy greatly impacts the developmental trajectory of the fetal brain. Insults that elicit an immune response in the mother during pregnancy, also known as maternal immune activation (MIA) can have adverse and lasting effects on offspring. These effects have been increasingly associated with neurodevelopmental, neurodegenerative, and behavioral disorders (Patterson, 2002; Brown, 2006; Brown and Patterson, 2011). Many of these disorders have been linked to dysregulation and abnormal structure of the amygdala (Schumann et al., 2011; Fernandez-Irigoyen et al., 2014). This brain structure influences many neurological pathways associated with learning, cognition, sexually dimorphic behaviors, and neuroendocrine responses and modulates the response of these processes to stressors (Ressler, 2010).

Evidence supports that MIA leads to lasting altered amygdala function and structure. Using a model of MIA elicited by a live virus in pigs, we showed evidence of disrupted excitatory/inhibitory and immune pathways within the amygdala of 3-week-old pigs (Keever et al., 2020), as well as an alterations in the response of the amygdala to stress following MIA (Keever-Keigher et al., 2021). Similarly, lipopolysaccharide (LPS)-elicited MIA in mice led to dysregulation in astrocytes and microglia in the amygdalae of both fetal and young adult offspring, resulting in an increase of pro-inflammatory markers (O'Loughlin et al., 2017). Also, MIA elicited by polyinosinic:polycytidylic acid (Poly(I:C)) in mice increased the synaptic strength of glutamatergic projections from the prefrontal cortex to the amygdala (Li et al., 2018a). Structural changes have also been noted, with in rats subject to Poly(I:C)-elicited MIA having reduced amygdalar volume (Crum et al., 2017).

Alternative splicing of pre-mRNA allows for functionally distinct proteins to be produced from the same gene and plays a critical role in neuronal growth development (Li et al., 2007; Zheng and Black, 2013). The brain has among the largest number of alternatively spliced genes compared to other tissues (Yeo et al., 2004), underlining the importance of the alternative splicing process in neurological development. Aberrant alternative splicing has been observed in the same neurological disorders associated with MIA. Analysis of brain tissue of patients diagnosed with autism spectrum disorder (ASD) identified hundreds of alternatively spliced targets neuronal specific splicing factor ataxin 2-binding protein 1 (A2BP1) associated with the ASD phenotype (Voineagu et al., 2011). Dysregulated alternative splicing contributes to the pathophysiology of schizophrenia spectrum disorders (SSD) (Morikawa and Manabe, 2010). Recent evidence has confirmed that interfering with the transcription of the long non-coding RNA (lncRNA) Gomafu interferes with splicing factors and results in the aberrant alternative splicing patterns typically observed in individuals with SSD (Barry et al., 2014). The non-coding RNA 17A has also been shown to exert effects that lead to pathological neurodegeneration through alternative splicing of G protein-coupled receptor (GPR51), increasing the production of a non-canonical GABA B isoform and, thus, leading to impaired neural inhibition and increased amyloid β secretion (Massone et al., 2011).

The primary objective of this study is to enhance our knowledge of the effects of MIA on alternative splicing within the amygdala, a brain region critical to behavior and cognition. Characterization of the effects that MIA has on transcript isoform abundance will augment our understanding of the effects that MIA has on the molecular mechanisms within the amygdala and complement our previous research. The evaluation of potential differences in splicing events associated with MIA between sexes was of particular interest. The supporting objective of this

study aimed at determining the pathways enriched among genes with dysregulated alternative splicing. Detection of aberrant alternative splicing and associated pathways in the amygdalae of individuals exposed to MIA will aid in understanding the antagonistic effects of MIA within the brain and help identify potential targets for treatment.

4.3 Materials and Methods

Animal Experiments

The experimental procedures in this study were described in details in published protocols (Keever et al., 2020; Keever-Keigher et al., 2021). We highlight animal and molecular methods that can influence the results from the alternative splicing analysis. The animal studies were approved by the Illinois Institutional Animal Care and Use Committee (IACUC) at the University of Illinois and are in compliance with the USDA Animal Welfare Act and the NIH Public Health Service Policy on the Humane Care and Use of Animals.

At 205 days of age, PRRS-negative Camborough gilts that were born and raised at the University of Illinois at Urbana-Champaign, were inseminated with PIC 359 boar semen (Keever et al., 2020; Keever-Keigher et al., 2021). The gilts were moved into disease containment chambers maintained at 22°C with a 12-h light/dark cycle with lights on at 7:00AM at gestation day 69 and were fed daily 2.3 kg of a gestational diet with *ad libitum* water access. The gilts were allowed to acclimate to their environment for one week, and on gestation day 76, four gilts were inoculated intranasally with live PRRSV strain P129-BV (School of Veterinary Medicine at Purdue University, West Lafayette, IN) using 5 mL of 1×10^5 median tissue culture infectious dose ($TCID_{50}$) diluted in sterile Dulbecco's modified Eagle medium (DMEM; 5 mL total volume). Similarly, four gilts in

the control group were inoculated intranasally with a 5 mL of sterile DMEM. The PRRSV-inoculated and Control groups were housed in separate containment chambers to prevent contamination. Timing of the PRRSV inoculation is consistent with initiation of rapid brain development and corresponds to the last third of gestation in pigs and humans (Keever et al., 2020; Keever-Keigher et al., 2021). Body temperature and feed intake were recorded post-inoculation, and significant increase in body temperature and decrease in feed intake of PRRSV-challenged relative to control gilts resolved within 14 days post inoculation.

With 114 days being the average duration of gestation in pigs, farrowing was induced on gestation day 113 with an intramuscular injection of 10 mg of Lutalyse (dinoprost tromethamine, Pfizer, New York, NY) (Keever et al., 2020; Keever-Keigher et al., 2021), with gilts confined to farrowing crates of standard dimensions (1.83 x 1.83 m). Gilts were fed 5 kg of a nutritionally complete diet for the lactating period with *ad libitum* water following farrowing, and intramuscular injections of iron dextran (100 mg/pig, Butler Schein Animal Health, Dublin, OH) and Excede for Swine (25 mg/pig; Zoetis, Parsippany, NJ) were administered to newborn pigs to control for respiratory diseases. The pigs remained with their mothers until postnatal day 22, and body weight of pigs was measured daily. Analysis of body weight using a mixed effect model include the effects of MIA, sex, interactions, random effects of gilt, and replicate confirmed the absence of significant stressor effects.

RNA Extraction and Sequencing

On postnatal day 22, pigs were anesthetized intramuscularly using a telazol:ketamine:xylazine drug cocktail (50 mg of tiletamine; 50 mg of zolazepam) reconstituted with 2.5 mL ketamine (100 g/L) and 2.5 mL xylazine (100 g/L; Fort Dodge Animal Health, Fort Dodge, IA) at a dose of 0.03

mL/kg body weight, following protocols (ME), and euthanized using an intracardiac injection of sodium pentobarbital (86 mg/kg body weight, Fata Plus, Vortech Pharmaceuticals, Dearborn, MI). Immediately following euthanasia, pig brains were extracted, amygdalae were recognized using the stereotaxic atlas of the pig brain (Felix et al., 1999), dissected out, flash frozen on dry ice, and stored at -80 ºC following published protocols (Antonson et al., 2019). The EZNA isolation kit (Omega Biotek, Norcross, GA) was used to isolate RNA from amygdalae samples per the manufacturer's instructions. All samples had RNA integrity numbers above 7.5, indicating low RNA degradation, and preparation of RNA-Seq libraries were was carried out with TruSeq Stranded mRNAseq Sample Prep kit' (Illumina Inc, San Diego, CA). Libraries were quantitated by qPCR and sequenced on one lane on a NovaSeq 6000 for 151 cycles from each end of the fragments using NovaSeq S4 reagent kit. Paired-end reads (150nt long) were obtained, and the FASTQ produced and demultiplexed using bcl2fastq v2.20 conversion software. FASTQ files are available in the National Center for Biotechnology Information Gene Expression Omnibus (GEO) database (experiment accession number GSE149695).

RNA Sequence Mapping and Differential Expression Analysis

Read quality assessment with FastQC (Andrews, 2010) found a minimum Phred quality score of 35 across all read positions, thus, no reads were trimmed. Paired-end reads from the individual samples were aligned to the *Sus scrofa* genome (version Sscrofa 11.1(Pruitt et al., 2007)) using STAR v2.7.8a (Dobin et al., 2013) in "twopassMode". Junction information was extracted from alignment files using RegTools (Feng et al., 2018), and junctions with unmapped locations were removed. Differential alternative splicing analysis was performed using LeafCutter (Li et al., 2018b) to evaluate the effects of MIA within sex, yielding the percent spliced in (ΔPSI), a

proportion of the difference in splice site usage between groups. The Benjamini-Hochberg False Discovery Rate (FDR) approach (Benjamini and Hochberg, 1995) was used to adjust P-values to account for multiple testing. LeafCutter was used to visualize the isoform percentages across treatments within sex for individual genes.

Functional Enrichment

The identification of over-represented functional categories among differentially alternatively spliced genes (FDR < 0.1) between MIA and Control groups within females and males relied on the Database for Annotation, Visualization and Integrated Discovery (DAVID 6.8) (Huang et al., 2009). The enrichment of KEGG pathways between treatments within males and females was assessed using the *Sus scrofa* genome as the background. The enrichment was calculated using a one-tailed jackknifed Fisher hypergeometric exact test on the Expression Analysis Systematic Explorer (EASE) score.

4.4 Results

Sequencing and Alignment Metrics

Sequencing produced 6.6 billion reads across the 24 RNA, with approximately 69 million paired-end reads per sample, and the number of reads was consistent across MIA and sex groups (coefficient of variation < 0.1). The median alignment rate of reads per sample was 84.14%, and the median number of splice junctions detected per sample was 36,894,791.

Differential Alternative Splicing Associated with Maternal Immune Activation

A total of 132 loci were significantly differentially alternatively spliced between MIA and control females (FDR < 0.1). The genes presenting most significant differential splicing genes (FDR-adjusted P-value < 0.001) are listed in Table 4.1, along with the most extreme positive and negative ΔPSI, and the unadjusted and adjusted P-value. The genes with the most significant differential splicing included, ubiquitin carboxyl-terminal hydrolase 30 (USP30), protein kinase CAMP-dependent type I regulatory subunit beta (PRKAR1B), and NSFL1 cofactor p47 (NSFL1C).

Overall, 176 loci were found to be differentially alternatively spliced between MIA and control males (FDR-adjusted P-value < 0.1). The genes presenting most significant differential splicing genes are listed in Table 4.2 and included septin 7 (SEPT7), zinc finger protein 672 (ZNF672), and potassium voltage-gated channel subfamily A member 6 (KCNA6).

Figures 4.1 and 4.2 depict relative isoform abundance within genes between MIA and control females and males, respectively. Bluer lines indicate relatively less abundant isoforms, while redder lines indicate more abundant isoforms.

Functional Enrichment of Genes that Exhibit Differential Alternative Splicing Associated with Maternal Immune Activation

Genes found to be significantly differentially alternatively spliced between MIA and control pigs (FDR-adjusted P-value < 0.1) were analyzed for functional enrichment in DAVID. Table 4.3 presents the KEGG pathways with the highest enrichment among the differentially alternatively spliced genes between MIA and control in females and males.

Enriched pathways among alternatively spliced genes in females were associated with non-alcoholic fatty liver disease and endocytosis, whereas pathways in males were associated with signaling, and dopaminergic synapse (Table 4.3).

4.5 Discussion

The present study of differential alternative splicing associated with MIA in the amygdala offered novel insights into the underlying transcriptional mechanisms that could explain the impact of gestational inflammatory signals on postnatal physiology and behavior. The analysis of changes in the relative abundance of transcript isoforms enabled us to uncover novel associations between genes expression profiles and MIA and also to further the understanding to known associations. Moreover, the sex-dependent alternative splicing events detected by our analysis advance the knowledge about the differential effect of MIA in neurodevelopmental disorders resulting in differences in postnatal inflammatory response and behavior between females and males.

Alternative splicing associated with maternal immune association in females

Several genes that presented changes in alternative splicing in the present study, have been previously associated with MIA. Myelin-associated glycoprotein (MAG) was differentially alternatively spliced between MIA and control females and included one extreme transcript isoforms that was 2% under-expressed and another that was 1% over-expressed in MIA relative to control females.

The more extreme MAG isoform under-expression in MIA females is in agreement with the under-expression of long-form of MAG in the amygdala of MIA mice exposed to Poly(I:C) during gestation (Zhang et al., 2020). Also, MAG was under-expressed in the prefrontal cortex of MIA

rats exposed to Poly(I:C) during gestation (Farrelly et al., 2015), in the prefrontal cortex and nucleus accumbens of MIA mice exposed to Poly(I:C) during development (Richetto et al., 2017), and the cerebellum of mice exposed to influenza-elicited MIA (Fatemi et al., 2009). The less extreme isoform over-expression of MAG in MIA females is consistent with the over-expression of MAG in the hippocampus of MIA offspring of rhesus macaques subject to Poly(I:C) (Page et al., 2020). Isoform bias in MAG has been proposed as an important factor in the development of SSD. While both short- and long-forms of MAG were under-expressed in the frontal cortex of SSD patients, long-form MAG was under-expressed to a greater extent altering the ratio of short-form MAG to long-form MAG in SSD patients compared to controls (Aberg et al., 2006).

The TATA-box binding protein associated factor (TAF1D), also among differentially alternatively spliced genes between MIA and control females. The most extreme under- and over-expressed TAF1D isoform in MIA females were 3.7% and 2.8%, respectively. Although there are no reports of the association of TAF1D and MIA at the isoform level, TAF1D was over-expressed in the prefrontal cortex of MIA offspring from Poly(I:C)-treated mice (Richetto et al., 2017).

Many genes presenting differential alternative splicing between MIA and control females have been associated with neurodevelopmental disorders including neuronal pentraxin receptor (NPTXR), regulating synaptic membrane exocytosis 1 (RIMS1), protein kinase CAMP-dependent type I regulatory subunit beta (PRKAR1B), solute carrier family 25 member 11 (SLC25A11), and zinc finger protein 513 (ZNF513).

A similar level of relative expression between the most extreme over- and under-expressed isoforms was identified for NPTXR, RIMS1, SLC25A11, and ZNF513. The most extreme under- and over-expressed NPTXR isoforms presented similar relative differential abundance (2.4% to

3.1%) between MIA and control groups. NPTXR was over-expressed in the caudate gray matter of SSD patients compared to controls (Cohen et al., 2012). Additionally, a NPTXR knockout mice line displayed behavioral deficits (Pelkey et al., 2016). A similar pattern was observed in RIMS1 that presented similar levels of under- and over-expressed isoforms (2.5% to 3.0%) between MIA and control females. Single-nucleotide polymorphisms in RIMS1 were associated with SSD (Ripke et al., 2014), and RIMS1 polymorphisms were associated with vulnerability to ASD (Ronemus et al., 2014). The most extreme over- and under-expressed isoforms in SLC25A11 in MIA relative to control females had comparable relative differential expression (|1.8%|). At the gene level, SLC25A11 was under-expressed in the cingulate cortex of SSD patients compared to controls (Focking et al., 2015) and over-expressed in the hippocampus in rats exposed to chronic mild stress, which is a model for MDD (Han et al., 2015). The expression of genes in the SLC25 family in the brain was associated with chronic social defeat stress in mice and potentially related to neurological and psychiatric disorders (Babenko et al., 2018). Last among the genes presenting similar extreme levels of over- and under-expression of isoforms, polymorphisms in ZNF513 were associated with altered brainstem volume in patients diagnosed with a variety of mental disorders (Campbell et al., 2021).

The most extreme differentially abundant isoforms of PRKAR1B were 5.3% under-expressed and 9.6% over-expressed in MIA relative to control females. In agreement with our findings, the expression of PRKAR1B has been associated with ASD. Moreover, PRKAR1B was differentially methylated in the brains of ASD patients compared to controls and identified as an important hub gene in the gene network analysis (Nardone et al., 2017). Also, a mutation in PRKAR1B has been associated with a rare neurodegenerative disorder (Wong et al., 2015).

Other genes that were differentially alternatively spliced between MIA and control females have roles in brain development and function pathways. In females, pyruvate dehydrogenase kinase 2 (PDK2), NSFL1 cofactor p47 (NSFL1C), and ubiquitin carboxyl-terminal hydrolase 30 (USP30) were among these genes found to be differentially alternatively spliced between MIA and control. The most differential under- and over-expression in MIA of isoforms was detected in USP30 (14.7% and 10.2%, respectively), and NSFL1C (11.6% and 2.1%, respectively, Table 4.1). Figure 4.1 depicts the detection of an isoform in NSFLC1C that spans the middle and the most 3' exon in control females yet this isoform was not detected in MIA females. Figure 4.1) and this is consistent with the most extreme over-expressed isoform in MIA (4.1%, Table 4.1).

The distribution of the differential isoform expression detected in this study, indicates that an NSFL1C transcript is substantially under-expressed in MIA (11.6%) relative to control females and this pattern is consistent with previous reports on the function of this gene. NSFL1C encodes a cofactor that is critical to the formation of dendritic spines (Shih and Hsueh, 2016) and is necessary for PTEN-induced kinase 1 (PINK1), an inhibitor of synapse degeneration (Wang et al., 2018). Expression of this gene was decreased in the brain proteome of a mouse strain used as a model of anxiety (Szego et al., 2010). Similarly, PDK2 participates in pathways associated with synaptic strength in depression and spatial memory (Strutz-Seebohm et al., 2005). Also, the product of this gene participates in mTOR signaling, whose dysregulation likely contributes to impaired synaptic plasticity and neurological disorders (Hoeffer and Klann, 2010; Gipson and Johnston, 2012).

Also, with roles in brain signaling, USP30 presented the most extreme over- and under-expression of isoforms in MIA and control females. This gene inhibits mitophagy, a process by which

damaged mitochondria are broken down (Bingol et al., 2014), and mitochondrial deficits have been shown to disrupt neurological function and are associated with Parkinson's disease (PD) (Abou-Sleiman et al., 2006).

Alternative splicing associated with maternal immune association in males

Among the alternatively spliced genes detected in males, 2',3'-Cyclic Nucleotide 3' Phosphodiesterase (CNP), glial fibrillary acidic protein (GFAP), and myelin transcription factor 1 like (MYT1L) have been associated with maternal immune activation. The level of relative differential expression for the most extreme over- and under-expressed isoforms were similar for CNP (2.4% to 3.1%) and MYT1L (1.7% to 1.2%). The similar levels of over- and under-expressed isoforms observed in the present study are consistent with the opposite MIA association patterns reported for CNP. CNP was over-expressed in the hippocampus of MIA offspring of rhesus macaques exposed to Poly(I:C) (Page et al., 2020). On the other hand, CNP was under-expressed in the prefrontal cortex of MIA mice exposed to Poly(I:C) during gestation (Richetto et al., 2017).

In agreement with the detection of differential CNP splicing in males, a significant MIA-by-sex interaction largely driven by under-expression of CNP in the white matter of MIA males was reported in mice exposed to lipopolysaccharide (LPS) during development (Makinson et al., 2017). Also, under-expression of CNP was detected in the amygdala of patients with major depressive disorder (MDD) and mice exposed to chronic physical and psychological stress (Sibille et al., 2009; Sun et al., 2019). Myt1l, a gene implicated in ASD (Garbett et al., 2008), SSD (Vrijenhoek et al., 2008), and MDD (Wang et al., 2010) was over-expressed in the hippocampus of MIA mice exposed to influenza during gestation (Farrelly et al., 2015).

A substantial difference in the levels of over- and under-expressed isoforms was detected for GFAP (3.7% to 2.8%). Consistent with our findings, bias in the expression of GFAP transcripts has been found in a mouse model of autism-like behavior. The shorter isoform was three times over-expressed in the cortex of PTEN mutant mice that present autism-like behavior compared to wild-type controls (Thacker et al., 2020). GFAP was over-expressed in the frontal cortex (de Souza et al., 2015) and hippocampus (Hao et al., 2010) of MIA rat exposed to LPS, and the hippocampus of MIA mice exposed to the pro-inflammatory cytokine interleukin-6 (IL-6) during gestation (Samuelsson et al., 2006). Additionally, higher abundance of the GFAP product was observed in the amygdala of MIA mice exposed to LPS (O'Loughlin et al., 2017).

Many genes presenting differential alternative splicing between MIA and control males, have been connected to behavioral disorders stemming from neurodevelopmental conditions including septin 7 (SEPT7), zinc finger protein 672 (ZNF672), zinc finger protein 74 (ZNF74), DiGeorge syndrome critical region gene 2 (DGCR2), and GC-rich promoter binding protein 1 (GPBP1). In all these cases, the level of the most extreme under- and under-expressed isoforms in MIA relative to control males were comparable, with SEPT7 exhibiting the highest differential relative expression (|31%|, Table 4.2).

The gene presenting most extreme isoform patterns, SEPT7, has expression patterns correlated with dendritic spine density in neurons and is under- expressed in the prefrontal cortex of SSD patients compared to control (Ide and Lewis, 2010). Although there are no reports of ZNF672 associations with behavioral disorders at the isoform level, this gene appears to contribute to the progression of SSD (Yazdani et al., 2020) and was over-expressed in blood of SSD patients compared to controls (Gardiner et al., 2013). Similarly, the identification of alternative splicing

associated with co-located genes ZNF74 and DGCR2 can be related to reports of the association between copy number variation in both genes and higher vulnerability to SSD and ASD (Birnbaum et al., 2014). Moreover, polymorphisms within ZNF74 and DGCR2 may contribute to age-of-onset of SSD (Takase et al., 2001) and to the overall risk of developing SSD (Horowitz et al., 2005; Shifman et al., 2006).In the present study, one isoform was over-expressed in MIA relative to control males (1.9%) and the remaining two isoforms were under-expressed (with the most extreme isoform under-expressed in MIA by 1.5%). The relative pattern of the GBP1 isoforms is depicted in Figure 4.2. Gpbp1 was over-expressed in the forebrain of rats given clomipramine to disrupt sleep, a model for depression and mood disorders (Lagus et al., 2010). Among the alternatively spliced genes associated with MIA and participating in molecular pathways in the brain was potassium voltage-gated channel subfamily A member 6. The expression of KCNA6 is developmentally regulated and reduces neuronal excitability (Okaty et al., 2009), and polymorphisms in KCNA6 are associated with SSD (Lee et al., 2013).

Functional analysis of alternatively spliced genes associated with maternal immune activation in females and males

The investigation of categories enriched among alternatively spliced genes between MIA and control female pigs yielded pathways associated with neurological and behavioral deficits, as well as neuron development. The most significantly enriched pathway among alternatively spliced genes in females, Non-alcoholic fatty liver disease (NAFLD; ssc04932; Table 4.3), has been associated with cognitive impairment (Seo et al., 2016), lower cerebral volume, and possibly accelerated brain aging in adults (Weinstein et al., 2018). This pathway was enriched among the proteomic profiles in the hippocampus of mice models of Alzheimer's disease (AD) (He et al.,

2019). Similarly, another significantly enriched pathway from the analysis of alternatively spliced genes among females, Fc gamma R-mediated phagocytosis (ssc04666) has also been associated with neurological disorders. This pathway was enriched among genes perturbed in the brains of mice injected with LPS (Gao et al., 2019) and among differentially expressed genes found between patients with AD and controls (Kong et al., 2015).

The endocytosis pathway (ssc04144) was also among the enriched pathways between MIA and control females. Endosomes are not only important for the role they play in signal transduction between neurons, they are also crucial for many facets of neuron development, including dendritic arborization and axon growth and guidance (Cosker and Segal, 2014).

Several of the pathways enriched among differentially alternatively spliced genes between MIA and control male pigs have been previously linked to MIA and MIA-associated disorders, including cGMP-PKG signaling pathway (ssc04022), dopaminergic synapse (ssc04728), amphetamine addiction (ssc05031), ribosome (ssc03010), and calcium signaling pathway (ssc04020) (Table 4.3). Members of the cGMP-PKG signaling pathways have been implicated in previous studies. Phodiesterase-9 (PDE9) inhibition, which is hypothesized to increase cGMP levels thereby increasing synaptic plasticity, attenuating the behavioral deficits observed in offspring mice exposed to Poly(I:C)-elicited MIA (Richetto et al., 2019). Additionally, increased phosphorylation of targets of PKG has been observed in the anterior cingulate cortex of patients with SSD compared to controls (McGuire et al., 2014), and PKG may play a role in ASD, enhancing the activity of serotonin transporter (SERT) (Blakely et al., 2005), a gene located in a region with high linkage to ASD in males (Muller et al., 2016).

Similar to our finding of enrichment of the KEGG pathway dopaminergic synapse among alternatively spliced genes between MIA and control males, this pathway was also enriched within a network of differentially expressed genes between rats exposed to LPS-induced MIA and controls (Straley et al., 2017). Likewise, altered dopaminergic pathways have been noted in rats exposed to Poly(I:C)-elicited MIA, including a reduction in spontaneous firing of dopaminergic neurons in the ventral tegmental area and an increase in the levels of extracellular dopamine in the nucleus accumbens (Luchicchi et al., 2016). The amphetamine addiction pathway is related to the dopamine synapse pathway, as amphetamine is a dopamine agonist that acts by increasing extracellular dopamine levels (Fleckenstein et al., 2007). The enrichment of the amphetamine pathway is in agreement with evidence of altered amphetamine response in rats subject to LPS-induced MIA compared to controls (Straley et al., 2017).

The enrichment of KEGG pathway calcium signaling pathway among alternatively spliced genes between MIA and control males is supported by evidence that this pathway is dysregulated in patients diagnosed with ASD. Functional analysis of ASD-associated genes from yielded calcium signaling as one of the most dysregulated pathways among ASD-related genes (Wen et al., 2016), and analysis of the concentration of calcium ions in the neocortex of post-mortem samples taken from people with ASD and controls, showed increased calcium levels, indicating altered calcium-ion homeostasis (Palmieri et al., 2010).

In agreement with previous research, we found the ribosome pathway to be enriched among alternatively spliced gene between MIA and control males. Decreased expression of ribosomal subunits and genes essential to protein synthesis have been observed in the fetal brains of mice offspring subject to Poly(I:C)-MIA compared to controls (Kalish et al., 2021).

4.6 Conclusions

The present investigation of differential alternative splicing between MIA and control pigs within sex uncovered several genes and pathways that have been previously associated with neurodevelopmental, neurodegenerative, and mood disorders. Genes showing dysregulated alternative splicing in females have been linked to mitochondrial dysfunction and reduced synaptic plasticity. Enriched pathways among significantly alternatively spliced genes in females have been associated with Alzheimer's disease and synaptic integrity. The differentially alternatively spliced genes observed in males have been linked to dendritic spine density and neuronal excitability, and enriched pathways among genes showing significant alternative splicing have been implicated in homeostasis and reward pathways within the brain.

This study advances our understanding of the complex molecular mechanisms impacted by MIA during fetal brain development. Furthermore, it supports investigation into alternative splicing as a potential target for therapies aiming to ameliorate the behavioral and cognitive deficits associated with MIA.

4.7 References

Aberg K, Saetre P, Jareborg N, Jazin E. 2006. Human qki, a potential regulator of mrna expression of human oligodendrocyte-related genes involved in schizophrenia. P Natl Acad Sci USA. 103(19):7482-7487.

Abou-Sleiman PM, Muqit MMK, Wood NW. 2006. Expanding insights of mitochondrial dysfunction in parkinson's disease. Nat Rev Neurosci. 7(3):207-219.

Andrews S. 2010. Fastqc: A quality control tool for high throughput sequence data.

Antonson AM, Lawson MA, Caputo MP, Matt SM, Leyshon BJ, Johnson RW. 2019. Maternal viral infection causes global alterations in porcine fetal microglia. Proc Natl Acad Sci U S A. 116(40):20190-20200.

Babenko VN, Smagin DA, Galyamina AG, Kovalenko IL, Kudryavtseva NN. 2018. Altered slc25 family gene expression as markers of mitochondrial dysfunction in brain regions under experimental mixed anxiety/depression-like disorder. Bmc Neurosci. 19.

Barry G, Briggs JA, Vanichkina DP, Poth EM, Beveridge NJ, Ratnu VS, Nayler SP, Nones K, Hu J, Bredy TW et al. 2014. The long non-coding rna gomafu is acutely regulated in response to neuronal activation and involved in schizophrenia-associated alternative splicing. Mol Psychiatr. 19(4):486-494.

Benjamini Y, Hochberg Y. 1995. Controlling the false discovery rate - a practical and powerful approach to multiple testing. Journal of the Royal Statistical Society Series B-Statistical Methodology. 57(1):289-300.

Bingol B, Tea JS, Phu L, Reichelt M, Bakalarski CE, Song QH, Foreman O, Kirkpatrick DS, Sheng MG. 2014. The mitochondrial deubiquitinase usp30 opposes parkin-mediated mitophagy. Nature. 510(7505):370-+.

Birnbaum R, Jaffe AE, Hyde TM, Kleinman JE, Weinberger DR. 2014. Prenatal expression patterns of genes associated with neuropsychiatric disorders. Am J Psychiat. 171(7):758-767.

Blakely RD, DeFelice LJ, Galli A. 2005. Biogenic amine neurotransmitter transporters: Just when you thought you knew them. Physiology. 20:225-231.

Brown AS. 2006. Prenatal infection as a risk factor for schizophrenia. Schizophrenia Bull. 32(2):200-202.

Brown AS, Patterson PH. 2011. Maternal infection and schizophrenia: Implications for prevention. Schizophrenia Bull. 37(2):284-290.

Campbell M, Jahanshad N, Mufford M, Choi KW, Lee P, Ramesar R, Smoller JW, Thompson P, Stein DJ, Dalvie S. 2021. Overlap in genetic risk for cross-disorder vulnerability to mental disorders and genetic risk for altered subcortical brain volumes. J Affect Disorders. 282:740-756.

Cohen OS, Mccoy SY, Middleton FA, Bialosuknia S, Zhang-James Y, Liu L, Tsuang MT, Faraone SV, Glatt SJ. 2012. Transcriptomic analysis of postmortem brain identifies dysregulated splicing events in novel candidate genes for schizophrenia. Schizophr Res. 142(1-3):188-199.

Cosker KE, Segal RA. 2014. Neuronal signaling through endocytosis. Csh Perspect Biol. 6(2).

Crum WR, Sawiak SJ, Chege W, Cooper JD, Williams SCR, Vernon AC. 2017. Evolution of structural abnormalities in the rat brain following in utero exposure to maternal immune activation: A longitudinal in vivo mri study. Brain Behav Immun. 63:50-59.

de Souza DF, Wartchow KM, Lunardi PS, Brolese G, Tortorelli LS, Batassini C, Biasibetti R, Goncalves CA. 2015. Changes in astroglial markers in a maternal immune activation model of schizophrenia in wistar rats are dependent on sex. Front Cell Neurosci. 9.

Dobin A, Davis CA, Schlesinger F, Drenkow J, Zaleski C, Jha S, Batut P, Chaisson M, Gingeras TR. 2013. Star: Ultrafast universal rna-seq aligner. Bioinformatics. 29(1):15-21.

Farrelly L, Focking M, Piontkewitz Y, Dicker P, English J, Wynne K, Cannon M, Cagney G, Cotter DR. 2015. Maternal immune activation induces changes in myelin and metabolic proteins, some of which can be prevented with risperidone in adolescence. Dev Neurosci-Basel. 37(1):43-55.

Fatemi SH, Folsom TD, Reutiman TJ, Abu-Odeh D, Mori S, Huang H, Oishi K. 2009. Abnormal expression of myelination genes and alterations in white matter fractional anisotropy following prenatal viral influenza infection at e16 in mice. Schizophr Res. 112(1-3):46-53.

Felix B, Leger ME, Albe-Fessard D. 1999. Stereotaxic atlas of the pig brain. Brain Res Bull. 49(1-2):1-+.

Feng YY, Ramu A, Skidmore ZL, Kunisaki J, Cotto KC, Griffith OL, Griffith M. 2018. Regtools: Integrated analysis of genomic and transcriptomic data for discovery of mutations associated with aberrant splicing in cancer. Cancer Res. 78(13).

Fernandez-Irigoyen J, Zelaya MV, Santamaria E. 2014. Applying mass spectrometry-based qualitative proteomics to human amygdaloid complex. Front Cell Neurosci. 8.

Fleckenstein AE, Volz TJ, Riddle EL, Gibb JW, Hanson GR. 2007. New insights into the mechanism of action of amphetamines. Annu Rev Pharmacol. 47:681-698.

Focking M, Lopez LM, English JA, Dicker P, Wolff A, Brindley E, Wynne K, Cagney G, Cotter DR. 2015. Proteomic and genomic evidence implicates the postsynaptic density in schizophrenia. Mol Psychiatr. 20(4):424-432.

Gao Y, Liang X, Ren Z, Li Y, Yang X. 2019. Systematic search for schizophrenia pathways sensitive to perturbation by immune activation. bioRxiv.730655.

Garbett K, Ebert PJ, Mitchell A, Lintas C, Manzi B, Mirnics K, Persico AM. 2008. Immune transcriptome alterations in the temporal cortex of subjects with autism. Neurobiol Dis. 30(3):303-311.

Gardiner EJ, Cairns MJ, Liu B, Beveridge NJ, Carr V, Kelly B, Scott RJ, Tooney PA, Bank ASR. 2013. Gene expression analysis reveals schizophrenia-associated dysregulation of immune pathways in peripheral blood mononuclear cells. J Psychiatr Res. 47(4):425-437.

Gipson TT, Johnston MV. 2012. Plasticity and mtor: Towards restoration of impaired synaptic plasticity in mtor-related neurogenetic disorders. Neural Plast. 2012.

Han X, Shao W, Liu Z, Fan S, Yu J, Chen J, Qiao R, Zhou J, Xie P. 2015. Itraq-based quantitative analysis of hippocampal postsynaptic density-associated proteins in a rat chronic mild stress model of depression. Neuroscience. 298:220-292.

Hao LY, Hao XQ, Li SH, Li XH. 2010. Prenatal exposure to lipopolysaccharide results in cognitive deficits in age-increasing offspring rats. Neuroscience. 166(3):763-770.

He KW, Nie LL, Zhou Q, Rahman SU, Liu JJ, Yang XF, Li SP. 2019. Proteomic profiles of the early mitochondrial changes in app/ps1 and apoe4 transgenic mice models of alzheimer's disease. J Proteome Res. 18(6):2632-2642.

Hoeffer CA, Klann E. 2010. Mtor signaling: At the crossroads of plasticity, memory and disease. Trends Neurosci. 33(2):67-75.

Horowitz A, Shifman S, Rivlin N, Pisante A, Darvasi A. 2005. A survey of the 22q11 microdeletion in a large cohort of schizophrenia patients. Schizophr Res. 73(2-3):263-267.

Huang DW, Sherman BT, Lempicki RA. 2009. Systematic and integrative analysis of large gene lists using david bioinformatics resources. Nature protocols. 4(1):44.

Ide M, Lewis DA. 2010. Altered cortical cdc42 signaling pathways in schizophrenia: Implications for dendritic spine deficits. Biological Psychiatry. 68(1):25-32.

Kalish BT, Kim E, Finander B, Duffy EE, Kim H, Gilman CK, Yim YS, Tong LL, Kaufman RJ, Griffith EC et al. 2021. Maternal immune activation in mice disrupts proteostasis in the fetal brain. Nat Neurosci. 24(2):204-+.

Keever-Keigher MR, Zhang P, Bolt CR, Rymut HE, Antonson AM, Corbett MP, Houser AK, Hernandez AG, Southey BR, Rund LA et al. 2021. Interacting impact of maternal inflammatory response and stress on the amygdala transcriptome of pigs. G3 (Bethesda).

Keever MR, Zhang P, Bolt CR, Antonson AM, Rymut HE, Caputo MP, Houser AK, Hernandez AG, Southey BR, Rund LA et al. 2020. Lasting and sex-dependent impact of maternal immune activation on molecular pathways of the amygdala. Front Neurosci-Switz. 14.

Kong W, Mou X, Zhang N, Zeng W, Li S, Yang Y. 2015. The construction of common and specific significance subnetworks of alzheimer's disease from multiple brain regions. Biomed Res Int. 2015:394260.

Lagus M, Gass N, Saharinen J, Saarela J, Porkka-Heiskanen T, Paunio T. 2010. Gene expression patterns in a rodent model for depression. Eur J Neurosci. 31(8):1465-1473.

Lee YH, Kim JH, Song GG. 2013. Pathway analysis of a genome-wide association study in schizophrenia. Gene. 525(1):107-115.

Li Q, Lee JA, Black DL. 2007. Neuronal regulation of alternative pre-mrna splicing. Nat Rev Neurosci. 8(11):819-831.

Li Y, Missig G, Finger BC, Landino SM, Alexander AJ, Mokler EL, Robbins JO, Manasian Y, Kim W, Kim KS et al. 2018a. Maternal and early postnatal immune activation produce dissociable effects on neurotransmission in mpfc-amygdala circuits. J Neurosci. 38(13):3358-3372.

Li YI, Knowles DA, Humphrey J, Barbeira AN, Dickinson SP, Im HK, Pritchard JK. 2018b. Annotation-free quantification of rna splicing using leafcutter. Nat Genet. 50(1):151-+.

Luchicchi A, Lecca S, Melis M, De Felice M, Cadeddu F, Frau R, Muntoni AL, Fadda P, Devoto P, Pistis M. 2016. Maternal immune activation disrupts dopamine system in the offspring. Int J Neuropsychoph. 19(7).

Makinson R, Lloyd K, Rayasam A, McKee S, Brown A, Barila G, Grissom N, George R, Marini M, Fabry Z et al. 2017. Intrauterine inflammation induces sex-specific effects on neuroinflammation, white matter, and behavior. Brain Behav Immun. 66:277-288.

Massone S, Vassallo I, Fiorino G, Castelnuovo M, Barbieri F, Borghi R, Tabaton M, Robello M, Gatta E, Russo C et al. 2011. 17a, a novel non-coding rna, regulates gaba b alternative splicing and signaling in response to inflammatory stimuli and in alzheimer disease. Neurobiol Dis. 41(2):308-317.

McGuire JL, Hammond JH, Yates SD, Chen DQ, Haroutunian V, Meador-Woodruff JH, McCullumsmith RE. 2014. Altered serine/threonine kinase activity in schizophrenia. Brain Res. 1568:42-54.

Morikawa T, Manabe T. 2010. Aberrant regulation of alternative pre-mrna splicing in schizophrenia. Neurochem Int. 57(7):691-704.

Muller CL, Anacker J, Veenstra-Vanderweele J. 2016. The serotonin system in autism spectrum disorder: From biomarker to animal models. Neuroscience. 321:24-41.

Nardone S, Sams DS, Zito A, Reuveni E, Elliott E. 2017. Dysregulation of cortical neuron DNA methylation profile in autism spectrum disorder. Cereb Cortex. 27(12):5739-5754.

O'Loughlin E, Pakan JMP, Yilmazer-Hanke D, McDermott KW. 2017. Acute in utero exposure to lipopolysaccharide induces inflammation in the pre- and postnatal brain and alters the glial cytoarchitecture in the developing amygdala. J Neuroinflamm. 14.

Okaty BW, Miller MN, Sugino K, Hempel CM, Nelson SB. 2009. Transcriptional and electrophysiological maturation of neocortical fast-spiking gabaergic interneurons. J Neurosci. 29(21):7040-7052.

Page NF, Gandal M, Estes M, Cameron S, Buth J, Parhami S, Ramaswami G, Murray K, Amaral DG, Van de Water JA et al. 2020. Alterations in retrotransposition, synaptic connectivity, and myelination implicated by transcriptomic changes following maternal immune activation in non-human primates. Biological Psychiatry. 89(9):896-910.

Palmieri L, Papaleo V, Porcelli V, Scarcia P, Gaita L, Sacco R, Hager J, Rousseau F, Curatolo P, Manzi B et al. 2010. Altered calcium homeostasis in autism-spectrum disorders: Evidence from biochemical and genetic studies of the mitochondrial aspartate/glutamate carrier agc1. Mol Psychiatr. 15(1):38-52.

Patterson PH. 2002. Maternal infection: Window on neuroimmune interactions in fetal brain development and mental illness. Curr Opin Neurobiol. 12(1):115-118.

Pelkey KA, Barksdale E, Craig MT, Yuan XQ, Sukumaran M, Vargish GA, Mitchell RM, Wyeth MS, Petralia RS, Chittajallu R et al. 2016. Pentraxins coordinate excitatory

synapse maturation and circuit integration of parvalbumin interneurons (vol 85, pg 1257, 2015). Neuron. 90(3):661-661.

Pruitt KD, Tatusova T, Maglott DR. 2007. Ncbi reference sequences (refseq): A curated non-redundant sequence database of genomes, transcripts and proteins. NAR. 35:D61-D65.

Ressler KJ. 2010. Amygdala activity, fear, and anxiety: Modulation by stress. Biological Psychiatry. 67(12):1117-1119.

Richetto J, Chesters R, Cattaneo A, Labouesse MA, Gutierrez AMC, Wood TC, Luoni A, Meyer U, Vernon A, Riva MA. 2017. Genome-wide transcriptional profiling and structural magnetic resonance imaging in the maternal immune activation model of neurodevelopmental disorders. Cereb Cortex. 27(6):3397-3413.

Richetto J, Scarborough J, Arban R, Dorner-Ciossek C, Rosenbrock H, Meyer U. 2019. The phosphodiesterase-9 inhibitor bi 409306 attenuates social interaction and dopaminergic deficits in adult offspring of poly(i:C)-based maternal immune activation neurodevelopmental mouse model. Schizophrenia Bull. 45:S262-S262.

Ripke S, Neale BM, Corvin A, Walters JTR, Farh KH, Holmans PA, Lee P, Bulik-Sullivan B, Collier DA, Huang HL et al. 2014. Biological insights from 108 schizophrenia-associated genetic loci. Nature. 511(7510):421-+.

Ronemus M, Iossifov I, Levy D, Wigler M. 2014. The role of de novo mutations in the genetics of autism spectrum disorders. Nat Rev Genet. 15(2):133-141.

Samuelsson AM, Jennische E, Hansson HA, Holmang A. 2006. Prenatal exposure to interleukin-6 results in inflammatory neurodegeneration in hippocampus with nmda/gabaa dysregulation and impaired spatial learning. American Journal of Physiology-Regulatory, Integrative and Comparative Physiology. 290(5):R1345-R1356.

Schumann CM, Bauman MD, Amaral DG. 2011. Abnormal structure or function of the amygdala is a common component of neurodevelopmental disorders. Neuropsychologia. 49(4):745-759.

Seo SW, Gottesman RF, Clark JM, Hernaez R, Chang Y, Kim C, Ha KH, Guallar E, Lazo M. 2016. Nonalcoholic fatty liver disease is associated with cognitive function in adults. Neurology. 86(12):1136-1142.

Shifman S, Levit A, Chen ML, Chen CH, Bronstein M, Weizman A, Yakir B, Navon R, Darvasi A. 2006. A complete genetic association scan of the 22q11 deletion region and functional evidence reveal an association between dgcr2 and schizophrenia. Hum Genet. 120(2):160-170.

Shih YT, Hsueh YP. 2016. Vcp and atl1 regulate endoplasmic reticulum and protein synthesis for dendritic spine formation. Nat Commun. 7.

Sibille E, Wang YJ, Joeyen-Waldorf J, Gaiteri C, Surget A, Oh S, Belzung C, Tseng GC, Lewis DA. 2009. A molecular signature of depression in the amygdala. Am J Psychiat. 166(9):1011-1024.

Straley ME, Van Oeffelen W, Theze S, Sullivan AM, O'Mahony SM, Cryan JF, O'Keeffe GW. 2017. Distinct alterations in motor & reward seeking behavior are dependent on the gestational age of exposure to lps-induced maternal immune activation. Brain Behav Immun. 63:21-34.

Strutz-Seebohm N, Seebohm G, Mack AF, Wagner HJ, Just L, Skutella T, Lang UE, Henke G, Striegel M, Hollmann M et al. 2005. Regulation of glur1 abundance in murine hippocampal neurones by serum- and glucocorticoid-inducible kinase 3. J Physiol. 565(Pt 2):381-390.

Sun Y, Lu W, Du KX, Wang JH. 2019. Microrna and mrna profiles in the amygdala are relevant to fear memory induced by physical or psychological stress. J Neurophysiol. 122(3):1002-1022.

Szego EM, Janaky T, Szabo Z, Csorba A, Kompagne H, Wuller G, Levay G, Simor A, Juhasz G, Kekesi KA. 2010. A mouse model of anxiety molecularly characterized by altered protein networks in the brain proteome. Eur Neuropsychopharm. 20(2):96-111.

Takase K, Ohtsuki T, Migita O, Toru M, Inada T, Yamakawa-Kobayashi K, Arinami T. 2001. Association of znf74 gene genotypes with age-at-onset of schizophrenia. Schizophr Res. 52(3):161-165.

Thacker S, Sefyi M, Eng C. 2020. Alternative splicing landscape of the neural transcriptome in a cytoplasmic-predominant pten expression murine model of autism-like behavior. Transl Psychiat. 10(1).

Voineagu I, Wang XC, Johnston P, Lowe JK, Tian Y, Horvath S, Mill J, Cantor RM, Blencowe BJ, Geschwind DH. 2011. Transcriptomic analysis of autistic brain reveals convergent molecular pathology. Nature. 474(7351):380-+.

Vrijenhoek T, Buizer-Voskamp JE, van der Stelt I, Strengman E, Sabatti C, van Kessel AG, Brunner HG, Ophoff RA, Veltman JA, Grp GROP. 2008. Recurrent cnvs disrupt three candidate genes in schizophrenia patients. Am J Hum Genet. 83(4):504-510.

Wang KZQ, Steer E, Otero PA, Bateman NW, Cheng MH, Scott AL, Wu C, Bahar I, Shih YT, Hsueh YP et al. 2018. Pink1 interacts with vcp/p97 and activates pka to promote nsfl1c/p47 phosphorylation and dendritic arborization in neurons. Eneuro. 5(6).

Wang T, Zeng Z, Li T, Liu J, Li JY, Li Y, Zhao QA, Wei ZY, Wang Y, Li BJ et al. 2010. Common snps in myelin transcription factor 1-like (myt1l): Association with major depressive disorder in the chinese han population. Plos One. 5(10).

Weinstein G, Zelber-Sagi S, Preis SR, Beiser AS, DeCarli C, Speliotes EK, Satizabal CL, Vasan RS, Seshadri S. 2018. Association of nonalcoholic fatty liver disease with lower brain volume in healthy middle-aged adults in the framingham study. Jama Neurol. 75(1):97-104.

Wen Y, Alshikho MJ, Herbert MR. 2016. Pathway network analyses for autism reveal multisystem involvement, major overlaps with other diseases and convergence upon mapk and calcium signaling. Plos One. 11(4).

Wong TH, Chiu WZ, Breedveld GJ, Li KW, Verkerk AJMH, Hondius D, Hukema RK, Seelaar H, Frick P, Severijnen LA et al. 2015. Prkar1b mutation associated with a new neurodegenerative disorder with unique pathology (vol 137, pg 1361, 2014). Brain. 138:E331-E331.

Yazdani A, Mendez-Giraldez R, Yazdani A, Kosorok MR, Roussos P. 2020. Differential gene regulatory pattern in the human brain from schizophrenia using transcriptomic-causal network. Bmc Bioinformatics. 21(1).

Yeo G, Holste D, Kreiman G, Burge CB. 2004. Variation in alternative splicing across human tissues. Genome Biol. 5(10).

Zhang XF, Chen T, Yan AF, Xiao J, Xie YL, Yuan J, Chen P, Wong AOL, Zhang Y, Wong NK. 2020. Poly(i:C) challenge alters brain expression of oligodendroglia-related genes of adult progeny in a mouse model of maternal immune activation. Front Mol Neurosci. 13.

Zheng S, Black DL. 2013. Alternative pre-mrna splicing in neurons: Growing up and extending its reach. Trends Genet. 29(8):442-448.

4.8 Tables

Table 4.1. Genes presenting differential alternative splicing (False Discovery Rate-adjusted P-value < 0.001) in the amygdala between female pigs exposed to maternal immune activation (MIA) and controls.

Gene Symbol	Extreme negative[1] ΔPSI	Extreme positive ΔPSI	Isoform Number	P-value	FDR P-value
NSFL1C	-0.116	0.021	9	3.02E-15	1.02E-10
PDK2	-0.036	0.041	7	1.94E-14	3.27E-10
USP30	-0.147	0.102	6	2.09E-10	2.35E-06
MAG	-0.019	0.010	4	4.48E-08	2.15E-04
NPTXR	-0.024	0.031	3	1.14E-07	4.78E-04
TAF1D	-0.037	0.028	18	1.68E-07	6.27E-04
SLC25A11	-0.018	0.018	3	2.14E-07	6.91E-04
ZNF513	-0.017	0.012	4	2.26E-07	6.91E-04
RIMS1	-0.025	0.030	17	3.31E-07	9.27E-04
PRKAR1B	-0.053	0.096	3	3.71E-07	9.60E-04

[1]The positive □PSI column identifies the most extreme over-expressed isoform in MIA relative to control female pigs expressed in proportions. The negative ΔPSI column identifies the most extreme under-expressed isoform in MIA relative to control female pigs. The most extreme positive and negative ΔPSI among all the isoforms in the intron cluster of the gene are reported. Isoform number identifies the number of isoforms in the intron clusters of the gene presenting alternative splicing.

Table 4.2. Genes presenting differential alternative splicing (False Discovery Rate-adjusted P-value < 0.001) in the amygdala between male pigs exposed to maternal immune activation (MIA) and controls.

Gene Symbol	Extreme negative[1] ΔPSI	Extreme positive ΔPSI	Isoform Number	P-value	FDR P-value
KCNA6	-0.052	0.068	11	1.34E-11	4.65E-07
GPBP1	-0.015	0.019	3	4.18E-10	7.24E-06
SEPT7	-0.315	0.305	3	1.22E-09	1.41E-05
ZNF672	-0.114	0.067	12	1.78E-09	1.54E-05
CNP	-0.005	0.005	6	1.18E-08	7.30E-05
GFAP	-0.008	0.017	6	1.26E-08	7.30E-05
ZNF74,DGCR2	-0.019	0.016	12	5.79E-08	2.87E-04
MYT1L	-0.027	0.053	11	1.62E-07	7.01E-04

[1]The positive □PSI column identifies the most extreme over-expressed isoform in MIA relative to control male pigs expressed in proportions. The negative ΔPSI column identifies the most extreme under-expressed isoform in MIA relative to control male pigs. The most extreme positive and negative ΔPSI among all the isoforms in the intron cluster of the gene are reported. Isoform number identifies the number of isoforms in the intron clusters of the gene presenting alternative splicing.

Table 4.3. Enriched KEGG pathways among genes presenting alternative splicing (False Discovery Rate-adjusted P-value < 0.1) between pigs exposed to maternal immune activation (MIA) and controls by sex tested using the hypergeometric test in DAVID.

KEGG Path	Description	Size[1]	Enr. Score	FDR P-Value
Females				
ssc04932	Non-alcoholic fatty liver disease (NAFLD)	4	3.48	0.039
ssc04666	Fc gamma R-mediated phagocytosis	3	2.61	0.056
ssc04144	Endocytosis	4	3.48	0.097
Males				
ssc04022	cGMP-PKG signaling pathway	6	3.90	0.006
ssc04728	Dopaminergic synapse	5	3.25	0.011
ssc05031	Amphetamine addiction	4	2.59	0.012
ssc03010	Ribosome	5	3.25	0.021
ssc04020	Calcium signaling pathway	5	3.24	0.042

[1]Size = number of distinct genes in the pathway; Enr. score = enrichment score.

4.9 Figures

Figure 4.1. Genes presenting alternative splicing (False Discovery Rate-adjusted P-value < 0.001) between female pigs exposed to maternal immune activation (P or PRRSV-elicited MIA) and controls (C). The semicircles indicate the clusters of introns corresponding to transcript isoforms. The thickness and color scheme of the isoforms indicate the number or count of isoform reads with thinker blue isoforms denoting lower counts and thicker red isoforms denoting higher counts.

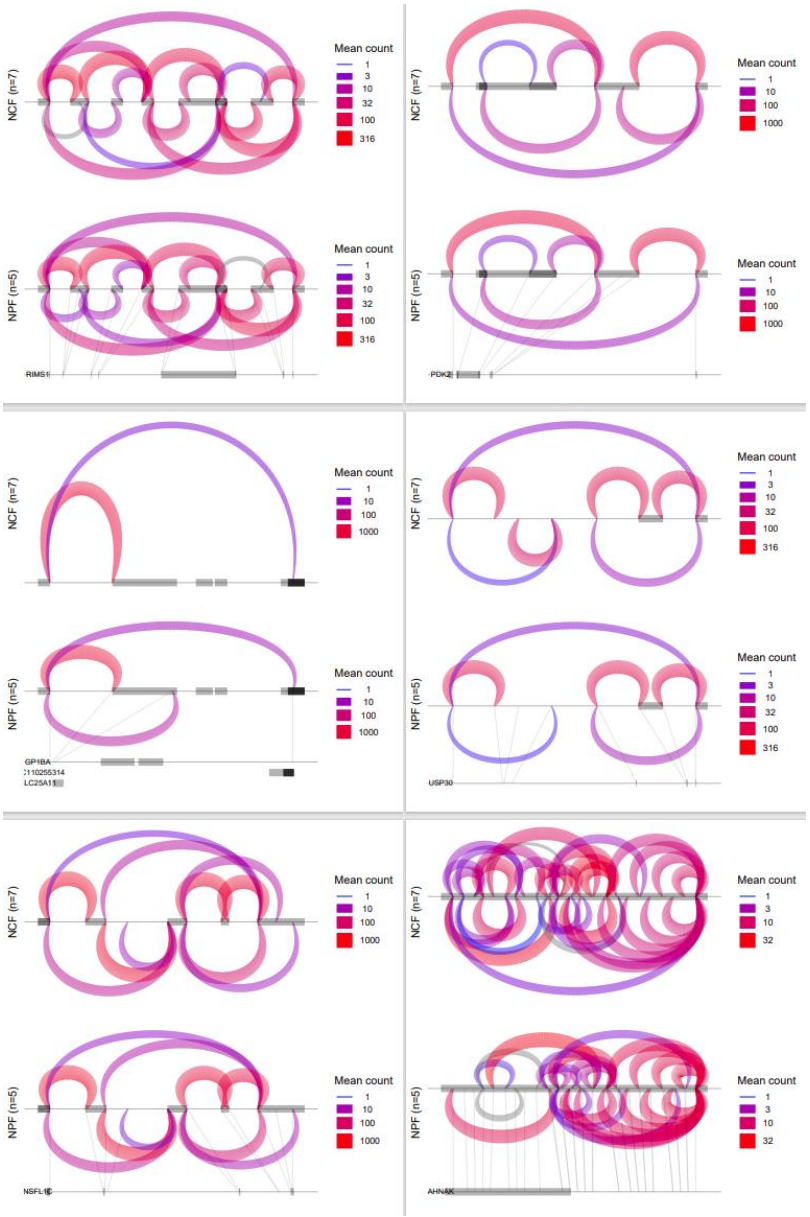

Figure 4.2. Genes presenting alternative splicing (False Discovery Rate-adjusted P-value < 0.001) between male pigs exposed to maternal immune activation (P or PRRSV-elicited MIA) and controls (C). The semicircles indicate the clusters of introns corresponding to transcript isoforms. The thickness and color scheme of the isoforms indicate the number or count of isoform reads with thinker blue isoforms denoting lower counts and thicker red isoforms denoting higher counts.

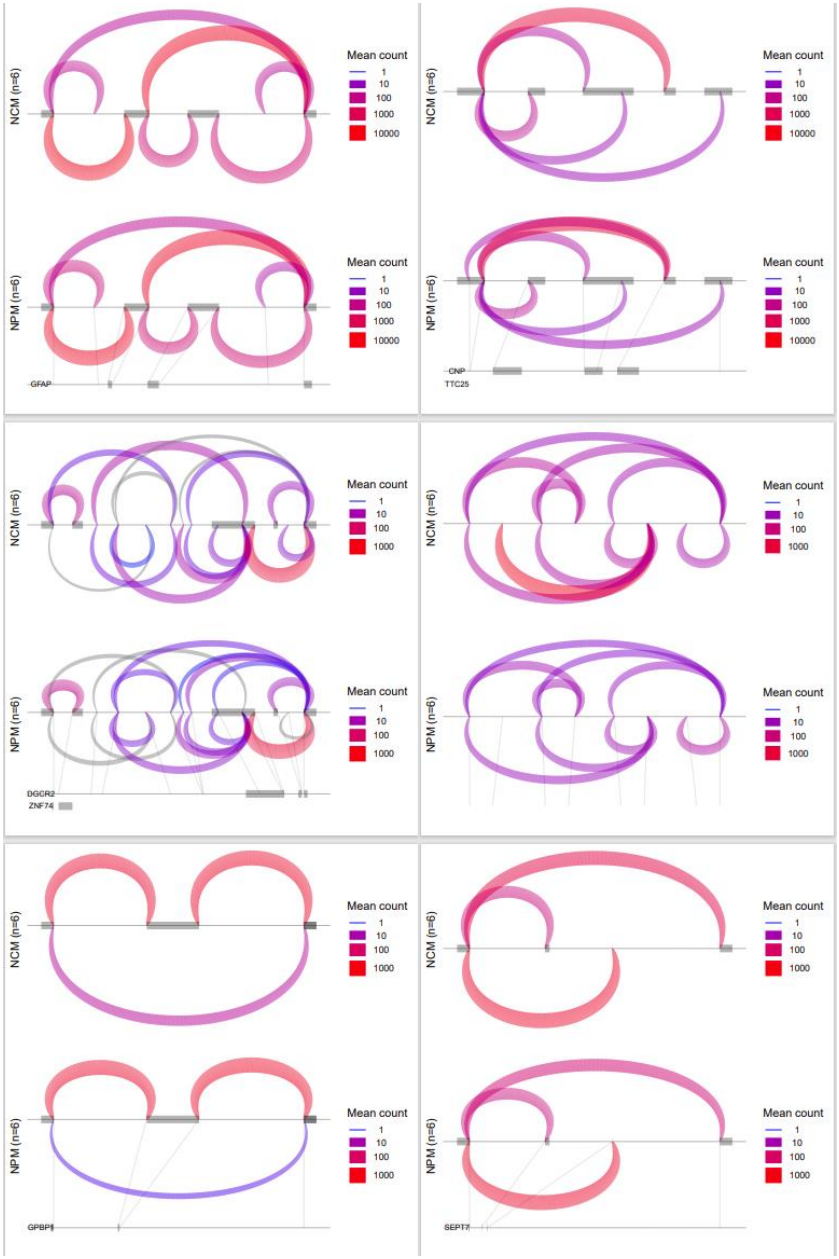

Table 2.11. Extended list of genes exhibiting treatment-by-sex interaction effect (FDR-adjusted P-value < 0.1).

ge.	P-value	FDR P-value	log 2(Fold change)					
			CON Fe-CON Ma	MPA Fe-MPA Ma	CON Fe-MPA Fe	CON Ma-MPA Ma	CON Fe-MPA Ma	CON Ma-MPA Fe
RGS16	1.4E-127	2.2E-123	-3.25	2.24	-2.44	3.06	-0.19	0.81
CGA	8.7E-115	7.1E-111	-5.86	0.36	0.27	6.49	0.63	6.13
GH1	5.2E-113	2.8E-109	-9.61	-2.22	0.40	7.79	-1.82	10.02
PCP4	9.4E-80	3.8E-76	-2.03	2.09	-1.51	2.61	0.58	0.52
NTNG1	3.1E-58	1.0E-54	-1.60	1.60	-1.11	2.09	0.49	0.49
NEXN	3.6E-53	9.8E-50	-2.05	1.69	-1.54	2.20	0.14	0.51
POMC	1.1E-50	2.5E-47	-2.79	0.33	0.06	3.19	0.39	2.86
AHNAK2	3.5E-48	7.2E-45	-2.13	2.23	-1.98	2.38	0.25	0.15
PYURF	1.9E-45	3.5E-42	-0.15	0.82	-2.03	-1.07	-1.22	-1.88
LOC110255204	4.4E-37	7.2E-34	5.15	4.81	1.45	1.10	6.26	-3.70
LHB	2.5E-35	3.6E-32	-3.16	-0.12	0.32	3.36	0.20	3.48
NTS	5.7E-35	7.7E-32	-1.43	2.81	-1.78	2.47	1.03	-0.35
PLXDC1	1.8E-34	2.3E-31	-0.99	1.68	-0.95	1.71	0.73	0.04
TCF7L2	8.8E-32	1.0E-28	-1.29	0.86	-1.01	1.14	-0.14	0.28
CHRNA2	9.3E-30	1.0E-26	-1.88	2.44	-2.52	1.79	-0.08	-0.65
AKAP12	5.9E-28	6.0E-25	-1.13	0.88	-1.07	0.94	-0.19	0.06
ISM1	1.4E-25	1.4E-22	-1.97	1.45	-1.06	2.36	0.39	0.92
DLK1	4.0E-24	3.6E-21	-2.42	2.03	-1.53	2.92	0.50	0.89
CALB1	3.7E-23	3.2E-20	-2.17	1.52	-1.66	2.02	-0.15	0.50
GRID2IP	4.6E-22	3.7E-19	-2.00	1.22	-1.62	1.60	-0.40	0.38
LHX9	7.0E-22	5.4E-19	-2.37	1.40	-1.29	2.48	0.10	1.08
E2F7	8.8E-20	6.5E-17	-2.20	0.95	-1.21	1.94	-0.27	0.99
GPX3	5.9E-19	4.1E-16	-1.19	0.99	-0.37	1.81	0.63	0.82
LOC110260685	2.3E-17	1.5E-14	2.37	3.22	0.88	1.72	4.10	-1.50
CPNE9	2.6E-17	1.7E-14	-1.75	0.96	-0.78	1.93	0.18	0.96

Table 2.11 (cont.)

SYNDIG1L	1.3E-16	8.1E-14	-1.13	1.13	-0.91	1.35	0.22	0.22
SPTSSB	4.1E-16	2.4E-13	-0.88	1.05	-0.84	1.09	0.21	0.04
ZIC1	4.8E-16	2.8E-13	-1.01	0.92	-0.78	1.15	0.13	0.23
FAM163A	1.3E-15	7.1E-13	-0.91	1.44	-0.79	1.56	0.65	0.12
PTPN3	1.3E-15	7.3E-13	-0.86	0.55	-0.64	0.77	-0.09	0.22
CEACAM16	4.6E-15	2.4E-12	-1.68	1.43	-0.84	2.27	0.59	0.83
FNDC5	9.7E-15	4.9E-12	-0.52	0.71	-0.50	0.73	0.21	0.02
CD74	1.1E-14	5.2E-12	0.55	-0.79	-0.97	-2.31	-1.76	-1.52
TP53INP2	6.7E-14	3.2E-11	-0.59	0.93	-0.89	0.63	0.05	-0.30
MBP	7.8E-14	3.6E-11	-0.78	1.05	-1.10	0.73	-0.04	-0.32
LOC110261683	5.3E-13	2.4E-10	-0.03	1.41	-1.30	0.14	0.11	-1.27
VAMP1	4.5E-12	1.9E-09	-0.64	0.49	-0.58	0.56	-0.08	0.07
BCAS1	5.4E-12	2.3E-09	-0.56	1.04	-0.95	0.65	0.10	-0.39
EPGN	7.4E-12	2.9E-09	-1.35	1.10	-1.04	1.41	0.06	0.31
PRKCH	7.4E-12	2.9E-09	-1.06	0.58	-0.89	0.76	-0.31	0.18
SCRT1	7.2E-12	2.9E-09	-0.50	0.56	-0.57	0.50	0.00	-0.07
SLA-DRA	1.2E-11	4.7E-09	0.43	-1.25	-1.72	-3.39	-2.96	-2.14
MOBP	1.7E-11	6.4E-09	-0.73	0.92	-0.98	0.67	-0.06	-0.25
RELN	1.8E-11	6.5E-09	-0.17	0.66	-0.74	0.09	-0.08	-0.57
IGSF5	2.0E-11	7.0E-09	-0.33	1.65	-0.87	1.11	0.78	-0.54
VIPR2	2.0E-11	7.0E-09	-1.17	1.04	-1.03	1.18	0.00	0.14
IRS4	2.1E-11	7.3E-09	-1.31	1.05	-0.43	1.92	0.61	0.87
ANKRD34C	3.3E-11	1.1E-08	-0.77	0.87	-0.71	0.93	0.16	0.06
APLNR	4.8E-11	1.6E-08	0.18	1.17	-0.93	0.06	0.24	-1.11
TRPC3	7.5E-11	2.4E-08	-1.00	0.82	-0.91	0.90	-0.09	0.09
KIAA1324	1.1E-10	3.6E-08	-1.57	0.04	0.06	1.67	0.10	1.63
SEMA7A	1.7E-10	5.3E-08	-0.54	0.44	-0.52	0.46	-0.07	0.02
TNNT1	1.7E-10	5.3E-08	-1.23	0.89	-0.64	1.48	0.25	0.59
GPR153	3.8E-10	1.1E-07	-0.64	0.51	-0.41	0.74	0.10	0.23
GBP1	8.0E-10	2.3E-07	0.92	-0.32	-0.75	-1.99	-1.07	-1.66

Table 2.11 (cont.)

CDR2L	9.6E-10	2.8E-07	-0.53	0.58	-0.67	0.43	-0.09	-0.14
RGS8	1.2E-09	3.3E-07	-0.52	0.32	-0.43	0.41	-0.12	0.09
GRM4	1.8E-09	4.9E-07	-0.97	0.91	-0.70	1.17	0.20	0.27
TF	2.2E-09	6.1E-07	-0.51	0.79	-0.92	0.39	-0.12	-0.41
TUBA8	2.4E-09	6.5E-07	-1.51	0.47	-0.65	1.33	-0.18	0.86
POU1F1	2.6E-09	6.9E-07	-2.49	-0.27	0.33	2.55	0.06	2.82
KIF1C	2.9E-09	7.6E-07	-0.46	0.76	-0.79	0.43	-0.03	-0.33
LOC100525692	3.1E-09	7.9E-07	0.51	3.03	-0.39	2.13	2.64	-0.90
CHRNA4	3.4E-09	8.7E-07	-0.97	0.74	-0.79	0.92	-0.05	0.18
IRX3	4.0E-09	1.0E-06	-1.15	0.88	-1.19	0.83	-0.32	-0.05
ANKRD24	4.1E-09	1.0E-06	-0.50	0.59	-0.35	0.73	0.23	0.15
HRH3	4.9E-09	1.2E-06	-0.18	0.54	-0.20	0.52	0.34	-0.02
PAQR6	4.9E-09	1.2E-06	-0.42	0.76	-0.65	0.53	0.11	-0.22
CCDC136	5.3E-09	1.2E-06	-0.39	0.43	-0.15	0.67	0.29	0.24
SAMD4A	6.9E-09	1.6E-06	-0.48	0.79	-0.89	0.37	-0.11	-0.42
SLITRK6	7.0E-09	1.6E-06	-1.00	0.71	-0.43	1.29	0.28	0.57
LEPR	9.5E-09	2.1E-06	-0.13	0.78	-0.43	0.49	0.35	-0.30
SLC17A6	1.1E-08	2.5E-06	-0.40	0.54	-0.16	0.77	0.37	0.23
PAIP2B	1.3E-08	2.9E-06	-0.44	0.57	-0.75	0.27	-0.17	-0.31
ATP8B4	2.7E-08	5.9E-06	0.63	-0.55	0.15	-1.04	-0.40	-0.48
EPCAM	2.8E-08	6.1E-06	-1.67	0.03	-0.26	1.44	-0.23	1.41
OLFM3	3.0E-08	6.4E-06	-0.13	0.53	-0.02	0.64	0.51	0.11
ACBD7	4.3E-08	9.0E-06	-0.90	0.64	-0.91	0.63	-0.28	-0.01
BTBD11	4.4E-08	9.0E-06	-0.62	0.45	-0.40	0.67	0.05	0.22
LOC110255964	4.9E-08	9.8E-06	-0.64	0.79	-0.39	1.05	0.41	0.26
TTR	5.0E-08	9.9E-06	-0.47	0.24	0.29	1.00	0.53	0.76
CLEC2L	5.5E-08	1.1E-05	0.04	0.66	-0.27	0.34	0.38	-0.32
ZDHHC22	5.5E-08	1.1E-05	-0.09	0.49	0.05	0.63	0.54	0.15
HAPLN2	8.2E-08	1.6E-05	-0.57	0.77	-0.86	0.47	-0.10	-0.29
AQP3	9.8E-08	1.9E-05	-0.96	0.59	-1.07	0.48	-0.48	-0.11

Table 2.11 (cont.)

UCMA	1.0E-07	1.9E-05	-0.61	0.76	-0.81	0.57	-0.05	-0.20
VAV3	1.1E-07	2.0E-05	-0.75	0.51	-0.71	0.55	-0.20	0.04
TRAK2	1.3E-07	2.5E-05	-0.39	0.65	-0.63	0.41	0.02	-0.24
GRP	1.8E-07	3.3E-05	-0.89	0.73	-0.61	1.02	0.12	0.28
LOC110257661	1.8E-07	3.3E-05	1.28	-0.65	0.62	-1.30	-0.03	-0.65
LOC110261685	2.0E-07	3.6E-05	-0.19	0.16	-0.61	-0.27	-0.46	-0.42
SLA-DRB1	2.1E-07	3.7E-05	0.27	-1.67	-0.66	-2.60	-2.33	-0.93
TMIE	2.8E-07	4.8E-05	-0.87	0.71	-0.50	1.07	0.20	0.37
RSAD2	3.4E-07	5.9E-05	0.98	-0.83	-1.45	-3.26	-2.28	-2.44
SLA-DQA1	3.5E-07	6.0E-05	-0.13	-1.40	-1.64	-2.91	-3.04	-1.52
MSX1	3.6E-07	6.0E-05	-1.37	0.11	0.35	1.83	0.46	1.72
HS3ST5	3.9E-07	6.6E-05	-0.67	0.61	-0.80	0.49	-0.19	-0.12
MAB21L1	4.0E-07	6.6E-05	-0.75	1.06	-1.31	0.50	-0.25	-0.56
CASQ2	4.4E-07	7.2E-05	-1.01	0.50	-0.69	0.83	-0.18	0.32
CACNA2D3	4.8E-07	7.8E-05	-0.50	0.44	-0.26	0.68	0.18	0.23
ADORA2A	6.7E-07	1.1E-04	-0.67	-0.38	0.04	0.33	-0.34	0.71
SHISAL1	6.8E-07	1.1E-04	-0.26	0.39	-0.23	0.43	0.16	0.04
SYT9	8.8E-07	1.4E-04	-0.57	0.54	-0.43	0.68	0.11	0.14
WNT3	8.8E-07	1.4E-04	-1.11	0.43	-0.45	1.08	-0.02	0.65
DRD2	1.1E-06	1.7E-04	-1.09	0.30	-0.08	1.31	0.22	1.01
LDB3	1.1E-06	1.7E-04	-1.07	0.64	-0.79	0.92	-0.15	0.28
COL25A1	1.2E-06	1.8E-04	-0.44	0.30	-0.41	0.32	-0.11	0.02
ISOC1	1.2E-06	1.8E-04	-0.47	0.42	-0.09	0.80	0.33	0.38
SCN4B	1.5E-06	2.2E-04	-0.49	0.70	-0.17	1.01	0.53	0.31
EPN3	1.5E-06	2.2E-04	-0.69	0.65	-0.72	0.63	-0.06	-0.02
LOC110257359	1.5E-06	2.2E-04	-0.07	0.72	-0.39	0.40	0.33	-0.32
CA5B	1.6E-06	2.3E-04	-0.31	0.51	-0.39	0.43	0.11	-0.08
CHRM2	1.6E-06	2.3E-04	-0.56	0.98	-0.45	1.09	0.53	0.11
NEFH	1.8E-06	2.6E-04	-0.43	0.44	-0.26	0.61	0.18	0.17
SCNN1B	2.1E-06	2.9E-04	-0.92	0.74	-0.41	1.25	0.32	0.51

Table 2.11 (cont.)

TMEM41A	2.1E-06	3.0E-04	-0.58	0.39	-0.32	0.65	0.07	0.26
PCP4L1	2.6E-06	3.6E-04	-0.24	0.43	-0.29	0.37	0.13	-0.06
CRHR2	2.8E-06	3.8E-04	-0.24	1.09	-0.36	0.97	0.74	-0.12
NDNF	2.8E-06	3.8E-04	-0.09	0.88	-0.70	0.27	0.18	-0.61
SLA-DQB1	2.9E-06	3.9E-04	0.24	-0.83	-0.98	-2.05	-1.81	-1.22
PHACTR2	3.1E-06	4.1E-04	-0.31	0.19	-0.29	0.21	-0.10	0.02
KCNH2	3.5E-06	4.6E-04	-0.33	0.40	-0.21	0.52	0.19	0.12
LRRC39	3.7E-06	4.8E-04	-0.70	0.48	-0.27	0.91	0.21	0.43
NELL1	4.8E-06	6.3E-04	-0.59	0.28	-0.48	0.39	-0.20	0.11
KLK6	5.7E-06	7.3E-04	-0.96	0.67	-1.31	0.33	-0.63	-0.35
ANLN	6.2E-06	7.9E-04	-0.47	0.47	-0.62	0.32	-0.15	-0.15
CXCL12	6.2E-06	7.9E-04	-0.41	-0.01	-0.10	0.29	-0.11	0.30
USP43	6.4E-06	8.1E-04	-0.64	0.43	-0.34	0.72	0.09	0.29
PAPPA	6.7E-06	8.3E-04	-1.13	0.60	-0.89	0.84	-0.29	0.24
IGSF1	7.0E-06	8.6E-04	-0.57	0.19	-0.13	0.63	0.06	0.44
IRF6	7.0E-06	8.6E-04	-0.78	0.32	-0.48	0.62	-0.16	0.30
CCDC17	7.1E-06	8.7E-04	0.74	-0.91	-0.10	-1.75	-1.01	-0.84
KCNIP4	7.2E-06	8.8E-04	-0.01	0.35	0.11	0.47	0.46	0.11
IRX1	7.7E-06	9.3E-04	-1.00	0.52	-0.99	0.52	-0.47	0.01
CAMK2N2	9.6E-06	1.1E-03	-0.24	0.16	-0.23	0.18	-0.07	0.01
MAP2K7	9.7E-06	1.2E-03	-0.23	0.55	-0.41	0.38	0.14	-0.17
CTSC	9.7E-06	1.2E-03	-0.57	0.39	-0.69	0.26	-0.31	-0.13
SPP1	1.1E-05	1.3E-03	-0.51	0.35	-0.51	0.35	-0.16	0.00
AR	1.2E-05	1.4E-03	-0.48	0.78	-0.84	0.43	-0.06	-0.36
LOC110260298	1.3E-05	1.5E-03	0.00	0.51	-0.17	0.34	0.34	-0.18
CYP4F55	1.4E-05	1.6E-03	-0.55	0.92	-0.58	0.89	0.34	-0.03
ALDH1A2	1.4E-05	1.6E-03	-1.35	0.50	0.48	2.32	0.98	1.83
GJB1	1.5E-05	1.7E-03	-0.31	0.73	-0.62	0.42	0.10	-0.31
PENK	1.6E-05	1.8E-03	-0.10	0.46	-0.04	0.51	0.42	0.06
NPM2	1.6E-05	1.8E-03	-1.01	0.41	-0.66	0.76	-0.25	0.36

Table 2.11 (cont.)

MPPED1	1.6E-05	1.8E-03	0.62	-0.66	0.59	-0.68	-0.06	-0.02
LOC100524773	1.7E-05	1.9E-03	0.22	-0.29	0.18	-0.33	-0.12	-0.04
RELL2	1.7E-05	1.9E-03	-0.23	0.41	-0.21	0.43	0.19	0.02
KCNG4	1.9E-05	2.1E-03	-0.11	0.54	0.01	0.66	0.55	0.12
LOC110259891	2.1E-05	2.2E-03	-0.23	0.60	-0.40	0.42	0.20	-0.17
CXCL10	2.1E-05	2.3E-03	0.55	-0.15	-2.12	-2.82	-2.27	-2.67
PLEKHD1	2.3E-05	2.4E-03	-0.55	0.37	-0.52	0.40	-0.15	0.03
PLCB4	2.6E-05	2.7E-03	-0.27	0.38	-0.27	0.38	0.10	0.00
PVALB	2.6E-05	2.8E-03	0.22	1.04	-0.10	0.72	0.94	-0.32
CDH1	2.7E-05	2.8E-03	-0.97	0.23	0.22	1.41	0.44	1.19
CRTAC1	2.7E-05	2.8E-03	-0.08	0.36	-0.01	0.42	0.34	0.06
PRSS12	2.8E-05	2.9E-03	-0.04	-0.33	-0.12	-0.41	-0.45	-0.08
SYT12	2.9E-05	3.0E-03	-0.16	0.32	-0.11	0.37	0.21	0.05
LOC102158399	3.0E-05	3.0E-03	-0.23	0.52	-0.58	0.17	-0.07	-0.35
OAZ3	3.2E-05	3.2E-03	0.56	-0.79	0.81	-0.54	0.02	0.25
FOXP2	3.3E-05	3.3E-03	-0.66	0.63	-0.21	1.08	0.42	0.45
KCNJ16	3.5E-05	3.5E-03	-0.28	0.30	-0.36	0.22	-0.05	-0.08
LOC100513119	3.5E-05	3.5E-03	0.81	-0.31	0.65	-0.48	0.33	-0.17
RORA	3.6E-05	3.6E-03	-0.40	0.11	-0.21	0.31	-0.09	0.19
PTH1R	3.7E-05	3.6E-03	-0.33	0.52	-0.51	0.34	0.01	-0.18
LOC110261244	3.9E-05	3.8E-03	-0.42	0.90	-0.98	0.34	-0.08	-0.56
ISG15	4.2E-05	4.1E-03	0.35	-0.34	-0.42	-1.12	-0.76	-0.77
LOC100523789	4.4E-05	4.2E-03	0.75	-0.74	1.06	-0.44	0.31	0.30
LOC106505010	4.5E-05	4.3E-03	0.32	-1.08	0.93	-0.46	-0.15	0.61
C1QL3	4.5E-05	4.3E-03	-0.30	-0.18	-0.36	-0.24	-0.54	-0.06
LOC100155195	5.0E-05	4.7E-03	0.73	-0.23	-0.82	-1.78	-1.05	-1.54
ZFHX3	5.7E-05	5.4E-03	-0.51	0.31	-0.59	0.24	-0.27	-0.08
RFLNB	6.0E-05	5.6E-03	-0.23	0.51	-0.61	0.14	-0.10	-0.38
LOC102158585	6.2E-05	5.8E-03	-0.09	0.87	-0.16	0.80	0.71	-0.07
HYDIN	6.6E-05	6.1E-03	0.26	-0.47	0.43	-0.30	-0.04	0.16

Table 2.11 (cont.)

HBB	6.7E-05	6.2E-03	-0.48	0.10	0.12	0.70	0.22	0.60
ZNF804A	6.9E-05	6.3E-03	-0.57	0.16	-0.23	0.50	-0.06	0.34
CBX3	7.2E-05	6.6E-03	0.13	-0.41	0.94	0.40	0.53	0.80
LOC102164141	7.3E-05	6.6E-03	0.74	-1.32	0.60	-1.46	-0.73	-0.14
TH	7.7E-05	6.9E-03	0.04	1.40	-0.32	1.04	1.08	-0.36
LOC100737600	7.9E-05	7.0E-03	-0.36	0.38	-0.41	0.34	-0.02	-0.04
APOD	8.1E-05	7.2E-03	-0.26	0.52	-0.50	0.27	0.01	-0.24
SKAP1	8.1E-05	7.2E-03	-0.56	0.58	-0.42	0.72	0.16	0.14
ESYT1	8.5E-05	7.3E-03	-0.47	0.29	-0.27	0.49	0.02	0.20
EVI2A	8.5E-05	7.3E-03	-0.17	0.58	-0.46	0.29	0.11	-0.29
GSG1	8.5E-05	7.3E-03	1.39	1.61	0.32	0.54	1.93	-1.06
JCAD	8.5E-05	7.3E-03	-0.27	0.49	-0.56	0.21	-0.07	-0.28
PLEKHB1	8.4E-05	7.3E-03	-0.30	0.63	-0.41	0.52	0.22	-0.10
MRVI1	8.6E-05	7.4E-03	-0.17	0.50	-0.25	0.43	0.26	-0.07
TMSB15A	9.1E-05	7.7E-03	-0.28	0.39	-0.32	0.36	0.08	-0.03
SPATA18	9.2E-05	7.8E-03	0.33	-0.36	0.47	-0.23	0.11	0.14
KCNC2	9.5E-05	8.0E-03	-0.24	0.24	-0.19	0.28	0.04	0.05
EFHD1	9.6E-05	8.0E-03	-0.31	0.42	-0.37	0.36	0.05	-0.06
WFDC1	9.8E-05	8.1E-03	-0.32	0.44	-0.29	0.46	0.14	0.03
CCNI2	9.9E-05	8.2E-03	1.09	-0.93	0.96	-1.06	0.03	-0.13
CACNA1G	9.9E-05	8.2E-03	-0.51	0.25	-0.37	0.40	-0.11	0.15
BHLHE22	1.0E-04	8.3E-03	0.06	-0.59	0.05	-0.61	-0.55	-0.01
RCAN2	1.0E-04	8.4E-03	-0.10	0.36	-0.02	0.44	0.34	0.08
LOC102157546	1.2E-04	9.6E-03	0.72	-0.12	0.75	-0.09	0.63	0.04
EPS8L2	1.2E-04	9.9E-03	-0.26	0.64	0.34	1.24	0.98	0.60
ZFP37	1.2E-04	9.9E-03	0.60	0.60	-0.19	-0.18	0.41	-0.78
RASD1	1.2E-04	9.9E-03	-0.52	0.48	-0.14	0.86	0.34	0.38
EGFL7	1.3E-04	1.0E-02	-0.05	0.49	-0.08	0.46	0.41	-0.04
MGP	1.3E-04	1.0E-02	-0.51	0.51	-0.20	0.83	0.31	0.32
EMILIN2	1.4E-04	1.1E-02	-0.54	0.54	-0.81	0.27	-0.27	-0.27

Table 2.11 (cont.)

DNAH12	1.5E-04	1.2E-02	0.49	-0.53	0.77	-0.25	0.24	0.28
SLC2A2	1.5E-04	1.2E-02	0.08	0.50	-0.04	0.38	0.46	-0.12
LOC100737768	1.5E-04	1.2E-02	-0.31	-0.04	0.15	0.42	0.11	0.46
IFI27	1.6E-04	1.2E-02	0.13	-0.16	-0.95	-1.24	-1.11	-1.08
LOC100515788	1.6E-04	1.3E-02	-0.50	0.22	0.06	0.78	0.28	0.56
PDP1	1.7E-04	1.3E-02	-0.29	0.16	-0.14	0.30	0.02	0.15
LOC102166944	1.7E-04	1.3E-02	-0.06	1.08	-0.57	0.57	0.51	-0.51
IGFBP2	1.7E-04	1.3E-02	-0.45	0.25	-0.18	0.51	0.07	0.27
ADAMTS9	1.8E-04	1.3E-02	-0.14	0.59	-0.90	-0.18	-0.32	-0.77
ADGRV1	1.8E-04	1.4E-02	0.09	-0.48	0.26	-0.31	-0.22	0.17
VWDE	1.9E-04	1.5E-02	-0.76	0.21	-0.68	0.29	-0.47	0.08
SLC24A3	2.0E-04	1.5E-02	-0.47	0.23	-0.41	0.30	-0.17	0.07
SRXN1	2.0E-04	1.5E-02	-0.30	0.34	-0.29	0.34	0.04	0.00
NEUROD2	2.1E-04	1.5E-02	0.30	-0.36	0.24	-0.41	-0.11	-0.05
OPALIN	2.1E-04	1.5E-02	-0.48	0.53	-0.57	0.45	-0.04	-0.08
FOXJ1	2.2E-04	1.6E-02	0.28	-0.19	0.39	-0.08	0.20	0.11
PADI2	2.2E-04	1.6E-02	-0.18	0.50	-0.37	0.30	0.12	-0.20
MYH11	2.3E-04	1.7E-02	-0.54	0.48	-0.45	0.56	0.03	0.08
LOC100155249	2.6E-04	1.9E-02	-0.41	-0.24	0.08	0.25	-0.16	0.49
GPR88	2.7E-04	1.9E-02	-0.18	0.05	0.01	0.24	0.06	0.19
LOC110257282	2.7E-04	1.9E-02	0.40	-0.54	0.36	-0.57	-0.18	-0.03
UBD	2.7E-04	1.9E-02	0.62	-0.20	-2.06	-2.89	-2.26	-2.69
UPP1	2.9E-04	2.0E-02	-0.98	0.10	-0.52	0.56	-0.42	0.47
LOC106506288	2.9E-04	2.0E-02	-0.08	0.42	-0.24	0.25	0.18	-0.16
SCN1B	2.9E-04	2.0E-02	0.08	0.38	0.11	0.42	0.49	0.03
DNAH2	3.0E-04	2.1E-02	0.14	-0.31	0.25	-0.20	-0.06	0.11
THRSP	3.1E-04	2.2E-02	-0.72	0.51	-1.24	-0.01	-0.73	-0.52
SLA-2	3.2E-04	2.2E-02	0.38	-0.24	-0.98	-1.60	-1.22	-1.36
NR4A3	3.3E-04	2.2E-02	-0.12	-0.01	-0.08	0.04	-0.08	0.04
LGALS3BP	3.3E-04	2.3E-02	0.16	-0.33	-0.68	-1.17	-1.01	-0.84

Table 2.11 (cont.)

PIP4K2A	3.4E-04	2.3E-02	-0.30	0.25	-0.37	0.18	-0.12	-0.06
EIF5A2	3.7E-04	2.5E-02	-0.33	0.28	-0.36	0.25	-0.09	-0.03
GGTA1P	4.0E-04	2.7E-02	-0.37	0.18	-0.40	0.14	-0.23	-0.03
CPLX1	4.1E-04	2.8E-02	-0.18	0.24	-0.18	0.24	0.06	0.00
ZIC2	4.3E-04	2.9E-02	-0.54	0.18	-0.40	0.32	-0.22	0.14
LOC396781	4.4E-04	2.9E-02	-0.75	1.36	-5.38	-3.27	-4.01	-4.63
C1QTNF1	4.5E-04	3.0E-02	-0.37	0.32	-0.23	0.46	0.09	0.14
COL8A2	4.7E-04	3.1E-02	0.08	-0.48	0.04	-0.51	-0.44	-0.03
CD247	4.7E-04	3.1E-02	-0.20	0.26	0.03	0.49	0.29	0.23
MYH2	4.7E-04	3.1E-02	-0.71	0.42	-0.82	0.31	-0.40	-0.11
ST8SIA6	5.0E-04	3.3E-02	-0.33	0.92	-0.70	0.56	0.23	-0.37
LOC106505355	5.0E-04	3.3E-02	-0.03	-2.30	3.12	0.85	0.82	3.15
QPCT	5.2E-04	3.4E-02	-0.32	0.27	-0.10	0.49	0.17	0.21
KLHDC8A	5.4E-04	3.5E-02	-0.15	0.53	0.10	0.77	0.62	0.24
RAB27A	5.6E-04	3.6E-02	-0.97	0.05	-0.25	0.77	-0.20	0.72
C16H5orf49	5.7E-04	3.7E-02	-0.03	0.51	-0.06	0.49	0.46	-0.02
MAP4	5.8E-04	3.7E-02	-0.32	0.36	-0.48	0.21	-0.11	-0.15
CTGF	5.9E-04	3.8E-02	0.02	-0.16	0.37	0.20	0.22	0.36
SLC10A4	6.3E-04	4.0E-02	-1.25	-0.11	-0.04	1.10	-0.15	1.21
CBLN2	6.4E-04	4.1E-02	-0.42	-0.06	0.06	0.43	0.00	0.49
CDR2	6.4E-04	4.1E-02	-0.53	0.26	-0.27	0.52	-0.01	0.26
FRZB	6.6E-04	4.2E-02	-0.55	0.08	-0.21	0.41	-0.14	0.34
LOC102164266	7.2E-04	4.5E-02	0.00	1.25	0.34	1.58	1.58	0.33
MAP3K19	7.3E-04	4.6E-02	0.28	-0.23	0.35	-0.17	0.12	0.06
CALN1	7.4E-04	4.6E-02	0.18	-0.35	0.16	-0.36	-0.19	-0.02
LOC110258846	7.7E-04	4.8E-02	0.16	-0.99	0.83	-0.31	-0.15	0.68
INSM2	7.9E-04	4.8E-02	-0.03	0.40	-0.40	0.03	0.00	-0.36
LCN2	7.8E-04	4.8E-02	-0.64	0.42	0.23	1.29	0.65	0.87
NTSR2	7.9E-04	4.8E-02	-0.20	0.40	-0.14	0.45	0.26	0.05
GVIN1	7.9E-04	4.8E-02	0.80	-0.41	-1.01	-2.22	-1.42	-1.81

Table 2.11 (cont.)

DTHD1	8.3E-04	5.0E-02	0.28	-0.37	0.22	-0.44	-0.15	-0.07
PHLDA3	8.6E-04	5.2E-02	-0.21	0.49	-0.28	0.41	0.21	-0.07
SSTR1	8.6E-04	5.2E-02	0.11	-0.38	0.16	-0.33	-0.22	0.05
LOC100158003	8.7E-04	5.3E-02	0.25	-0.40	0.57	-0.09	0.17	0.32
CCDC9B	8.8E-04	5.3E-02	-0.24	0.35	-0.34	0.25	0.01	-0.10
PKP4	8.9E-04	5.3E-02	-0.21	0.48	-0.50	0.18	-0.02	-0.29
TMPRSS3	9.0E-04	5.3E-02	-0.51	0.76	-0.57	0.70	0.19	-0.06
LOC110260237	9.0E-04	5.3E-02	1.55	-0.96	1.35	-1.17	0.38	-0.21
FAM216B	9.3E-04	5.5E-02	0.18	-0.18	0.20	-0.16	0.03	0.02
HES3	9.5E-04	5.6E-02	0.12	0.97	-0.11	0.74	0.86	-0.22
PWWP2B	9.6E-04	5.6E-02	-0.51	0.40	-0.27	0.63	0.12	0.24
SLC9A3R2	9.9E-04	5.8E-02	-0.12	0.41	-0.16	0.37	0.25	-0.04
WNT5B	1.0E-03	5.9E-02	-0.58	0.50	-0.16	0.91	0.33	0.41
GDA	1.0E-03	6.0E-02	0.16	-0.38	0.06	-0.48	-0.32	-0.10
LDHD	1.1E-03	6.1E-02	-0.26	0.49	-0.22	0.53	0.27	0.04
PPP1R14A	1.1E-03	6.3E-02	-0.28	0.54	-0.48	0.33	0.06	-0.20
CROCC2	1.1E-03	6.3E-02	0.23	-0.46	0.47	-0.22	0.01	0.24
HCN2	1.1E-03	6.4E-02	-0.23	0.25	-0.34	0.14	-0.09	-0.11
STRIP2	1.1E-03	6.4E-02	-0.19	0.18	-0.20	0.18	-0.01	-0.01
ARC	1.2E-03	6.6E-02	0.24	-0.16	0.52	0.12	0.36	0.28
AGTR1	1.2E-03	6.7E-02	-0.97	0.04	-0.12	0.90	-0.07	0.86
SLA-5	1.2E-03	6.7E-02	0.63	-0.04	-0.96	-1.63	-1.00	-1.59
PLXNA4	1.2E-03	6.7E-02	0.21	-0.28	0.20	-0.29	-0.08	-0.01
RLBP1	1.2E-03	6.9E-02	-0.12	0.24	0.01	0.37	0.25	0.13
AK9	1.3E-03	7.1E-02	0.39	-0.48	0.64	-0.23	0.16	0.25
GPRIN2	1.3E-03	7.3E-02	-0.62	0.54	-0.42	0.74	0.12	0.20
WDR78	1.3E-03	7.4E-02	0.46	-0.39	0.52	-0.33	0.13	0.06
SLC2A13	1.3E-03	7.4E-02	0.20	-0.27	0.36	-0.11	0.09	0.16
ACYP2	1.4E-03	7.5E-02	-0.21	0.33	-0.23	0.31	0.10	-0.02
CCDC162P	1.4E-03	7.5E-02	0.11	-0.48	0.36	-0.23	-0.12	0.25

Table 2.11 (cont.)

CCDC33	1.4E-03	7.5E-02	0.48	-0.39	0.49	-0.38	0.10	0.01
MID1IP1	1.4E-03	7.5E-02	-0.11	0.44	-0.28	0.26	0.15	-0.18
KRT5	1.4E-03	7.6E-02	0.56	-0.23	0.48	-0.31	0.25	-0.08
CYS1	1.4E-03	7.6E-02	-0.09	0.35	0.07	0.51	0.42	0.16
LOC106506286	1.4E-03	7.6E-02	0.07	-0.37	0.29	-0.15	-0.08	0.22
LRTM2	1.4E-03	7.6E-02	-0.06	0.39	0.05	0.50	0.44	0.11
OC90	1.4E-03	7.6E-02	0.35	0.82	-0.05	0.43	0.78	-0.40
PTH	1.4E-03	7.6E-02	-0.03	0.29	-0.68	-0.36	-0.39	-0.65
S100A1	1.4E-03	7.6E-02	-0.02	0.60	-0.17	0.45	0.43	-0.15
SCGN	1.4E-03	7.7E-02	-2.09	0.04	-0.89	1.23	-0.85	1.20
SYNPO2L	1.5E-03	7.9E-02	-0.28	0.59	-0.44	0.43	0.15	-0.16
KITLG	1.5E-03	7.9E-02	-0.22	0.17	0.12	0.51	0.29	0.34
MYADML2	1.5E-03	7.9E-02	-0.44	0.67	-0.35	0.76	0.32	0.09
FRMPD2	1.5E-03	8.0E-02	0.25	-0.50	0.54	-0.20	0.05	0.30
COL2A1	1.5E-03	8.1E-02	-1.16	0.04	-0.52	0.67	-0.49	0.64
LOC110257059	1.6E-03	8.1E-02	-0.10	-0.76	0.27	-0.40	-0.50	0.37
PKIB	1.6E-03	8.3E-02	-0.21	0.23	-0.06	0.38	0.17	0.15
DOK7	1.6E-03	8.3E-02	-0.17	0.91	-0.34	0.73	0.56	-0.18
SLCO1A2	1.6E-03	8.3E-02	-0.25	0.31	-0.38	0.18	-0.07	-0.13
TMEM30B	1.6E-03	8.3E-02	-1.12	0.02	0.01	1.14	0.02	1.13
RASGRF2	1.6E-03	8.3E-02	0.35	-0.42	0.59	-0.18	0.17	0.24
DNAH11	1.6E-03	8.3E-02	0.23	-0.59	0.62	-0.21	0.03	0.38
AIF1	1.6E-03	8.4E-02	-0.28	0.26	-0.44	0.10	-0.18	-0.16
LOC110261076	1.7E-03	8.4E-02	-0.07	0.75	-0.22	0.60	0.53	-0.14
LGALS1	1.7E-03	8.6E-02	-0.21	0.46	0.01	0.68	0.47	0.22
CD320	1.8E-03	8.9E-02	-0.12	0.46	-0.18	0.40	0.28	-0.07
CHGB	1.8E-03	9.2E-02	-0.58	-0.16	0.37	0.79	0.21	0.96
C1R	1.8E-03	9.2E-02	0.22	-0.28	-0.14	-0.64	-0.42	-0.36
KCNH5	1.8E-03	9.2E-02	-0.13	0.39	-0.03	0.49	0.36	0.11
LOC110256808	1.9E-03	9.4E-02	-0.15	0.35	-0.30	0.21	0.05	-0.15

Table 2.11 (cont.)

PPP1R1B	1.9E-03	9.6E-02	0.01	0.15	0.11	0.25	0.26	0.10
CFAP46	2.0E-03	9.7E-02	0.17	-0.09	0.27	0.00	0.17	0.09
LOC100513133	2.0E-03	1.0E-01	-0.16	0.49	-0.43	0.21	0.05	-0.27

Table 2.12. Extended list of enriched clusters and supporting functional categories among the genes presenting significant treatment-by-sex interaction effect, and representative categories identified using DAVID.

[a]Category	GO Identifier	GO name	[b]Count	P-value	[c]FDR P-value
Cluster 1 (ES: 2.74)					
KEGG	ssc05320	Autoimmune thyroid disease	8	2.9E-06	4.5E-04
KEGG	ssc05330	Allograft rejection	7	6.4E-06	5.0E-04
KEGG	ssc04612	Antigen processing and presentation	8	1.9E-05	7.5E-04
KEGG	ssc05332	Graft-versus-host disease	6	6.5E-05	2.0E-03
BP	GO:0019882	antigen processing and presentation	8	7.2E-05	9.8E-02
KEGG	ssc05416	Viral myocarditis	7	1.3E-04	3.4E-03
KEGG	ssc04940	Type I diabetes mellitus	6	1.6E-04	3.6E-03
KEGG	ssc05310	Asthma	5	1.9E-04	3.6E-03
KEGG	ssc04672	Intestinal immune network for IgA production	6	2.1E-04	3.5E-03
KEGG	ssc04145	Phagosome	9	4.7E-04	7.3E-03
BP	GO:0002504	antigen processing and presentation of peptide or polysaccharide antigen via MHC class II	4	1.9E-03	3.4E-01
KEGG	ssc04514	Cell adhesion molecules (CAMs)	8	2.3E-03	3.2E-02
KEGG	ssc05150	Staphylococcus aureus infection	5	2.8E-03	3.5E-02
KEGG	ssc05323	Rheumatoid arthritis	6	4.8E-03	5.6E-02
KEGG	ssc05140	Leishmaniasis	5	8.1E-03	8.6E-02
KEGG	ssc05164	Influenza A	7	2.0E-02	1.7E-01
KEGG	ssc05168	Herpes simplex infection	7	2.9E-02	2.3E-01
KEGG	ssc05322	Systemic lupus erythematosus	5	3.6E-02	2.5E-01
KEGG	ssc05166	HTLV-I infection	8	4.0E-02	2.6E-01
KEGG	ssc05321	Inflammatory bowel disease (IBD)	4	4.3E-02	2.7E-01
KEGG	ssc05152	Tuberculosis	6	7.3E-02	4.0E-01
BP	GO:0048002	antigen processing and presentation of peptide antigen	3	8.6E-02	7.0E-01
KEGG	ssc05145	Toxoplasmosis	4	1.5E-01	5.5E-01
KEGG	ssc05169	Epstein-Barr virus infection	4	1.8E-01	6.1E-01
Cluster 2 (ES: 1.90)					

Table 2.12 (cont.)

BP	GO:0051050	positive regulation of transport	16	4.4E-03	3.5E-01
BP	GO:0051049	regulation of transport	25	4.5E-03	3.2E-01
BP	GO:0050801	ion homeostasis	13	1.3E-02	3.6E-01
BP	GO:0048878	chemical homeostasis	16	2.8E-02	4.8E-01
BP	GO:0030001	metal ion transport	11	4.5E-02	5.7E-01
Cluster 3 (ES: 1.76)					
BP	GO:0048871	multicellular organismal homeostasis	11	2.1E-04	1.8E-01
BP	GO:0001503	ossification	10	3.0E-03	3.7E-01
BP	GO:0001894	tissue homeostasis	7	8.7E-03	3.4E-01
BP	GO:0060249	anatomical structure homeostasis	8	2.6E-02	4.6E-01
BP	GO:0031214	biomineral tissue development	5	2.9E-02	4.8E-01
BP	GO:0045453	bone resorption	3	7.3E-02	6.7E-01
BP	GO:0046849	bone remodeling	3	1.7E-01	8.5E-01
BP	GO:0048771	tissue remodeling	4	1.8E-01	8.6E-01
Cluster 4 (ES: 1.69)					
BP	GO:0061564	axon development	14	6.4E-05	1.7E-01
BP	GO:0048468	cell development	33	3.0E-04	1.9E-01
BP	GO:0060322	head development	15	7.9E-04	2.8E-01
BP	GO:0007417	central nervous system development	17	8.8E-04	2.7E-01
BP	GO:0007420	brain development	14	1.3E-03	3.1E-01
BP	GO:0051240	positive regulation of multicellular organismal process	24	1.7E-03	3.6E-01
BP	GO:0007399	nervous system development	30	1.8E-03	3.5E-01
BP	GO:0007409	axonogenesis	11	2.1E-03	3.5E-01
BP	GO:0045597	positive regulation of cell differentiation	16	2.9E-03	3.7E-01
BP	GO:2000026	regulation of multicellular organismal development	26	3.2E-03	3.6E-01
BP	GO:0000904	cell morphogenesis involved in differentiation	15	4.2E-03	3.5E-01
BP	GO:0051094	positive regulation of developmental process	19	4.5E-03	3.1E-01
BP	GO:0031175	neuron projection development	15	4.7E-03	3.0E-01
BP	GO:0051962	positive regulation of nervous system development	10	5.4E-03	2.9E-01

Table 2.12 (cont.)

BP	GO:0048667	cell morphogenesis involved in neuron differentiation	11	7.4E-03	3.2E-01
BP	GO:0030900	forebrain development	9	7.8E-03	3.2E-01
BP	GO:0045595	regulation of cell differentiation	23	8.2E-03	3.3E-01
BP	GO:0021537	telencephalon development	7	1.1E-02	3.5E-01
BP	GO:0048812	neuron projection morphogenesis	11	1.3E-02	3.6E-01
BP	GO:0051960	regulation of nervous system development	13	1.8E-02	4.2E-01
BP	GO:0048666	neuron development	15	2.2E-02	4.5E-01
BP	GO:0048699	generation of neurons	19	2.5E-02	4.6E-01
BP	GO:0022008	neurogenesis	20	2.8E-02	4.8E-01
BP	GO:0032989	cellular component morphogenesis	19	3.3E-02	5.1E-01
BP	GO:0007411	axon guidance	6	3.7E-02	5.3E-01
BP	GO:0097485	neuron projection guidance	6	3.8E-02	5.4E-01
BP	GO:0030182	neuron differentiation	17	3.8E-02	5.4E-01
BP	GO:0060284	regulation of cell development	13	4.3E-02	5.6E-01
BP	GO:0006928	movement of cell or subcellular component	22	4.4E-02	5.6E-01
BP	GO:0040012	regulation of locomotion	12	4.7E-02	5.7E-01
BP	GO:0030030	cell projection organization	17	5.2E-02	6.0E-01
BP	GO:0050769	positive regulation of neurogenesis	7	5.3E-02	6.0E-01
BP	GO:0051270	regulation of cellular component movement	12	5.5E-02	6.1E-01
BP	GO:0006935	chemotaxis	10	5.7E-02	6.2E-01
BP	GO:0042330	taxis	10	5.8E-02	6.2E-01
BP	GO:0000902	cell morphogenesis	17	6.4E-02	6.5E-01
BP	GO:0048858	cell projection morphogenesis	12	6.9E-02	6.6E-01
BP	GO:0010720	positive regulation of cell development	8	7.2E-02	6.7E-01
BP	GO:0050767	regulation of neurogenesis	10	7.8E-02	6.8E-01
BP	GO:0040011	locomotion	19	8.0E-02	6.9E-01
BP	GO:0032990	cell part morphogenesis	12	8.0E-02	6.9E-01
BP	GO:0010770	positive regulation of cell morphogenesis involved in differentiation	4	1.1E-01	7.6E-01
BP	GO:0045666	positive regulation of neuron differentiation	5	1.4E-01	8.2E-01

Table 2.12 (cont.)

BP	GO:0010976	positive regulation of neuron projection development	4	1.5E-01	8.4E-01
BP	GO:0045664	regulation of neuron differentiation	7	2.4E-01	9.1E-01
BP	GO:0010769	regulation of cell morphogenesis involved in differentiation	5	2.7E-01	9.2E-01
BP	GO:0031346	positive regulation of cell projection organization	4	3.1E-01	9.4E-01
BP	GO:0010975	regulation of neuron projection development	5	3.4E-01	9.5E-01
BP	GO:0022604	regulation of cell morphogenesis	6	4.6E-01	9.8E-01
BP	GO:0031344	regulation of cell projection organization	5	5.7E-01	9.9E-01
Cluster 5 (ES: 1.60)					
BP	GO:0040008	regulation of growth	13	3.1E-03	3.6E-01
BP	GO:0040007	growth	17	4.0E-03	3.5E-01
BP	GO:0048638	regulation of developmental growth	8	1.6E-02	3.9E-01
BP	GO:0048589	developmental growth	11	3.2E-02	5.0E-01
BP	GO:0035264	multicellular organism growth	5	4.0E-02	5.5E-01
BP	GO:0045927	positive regulation of growth	6	4.3E-02	5.6E-01
BP	GO:0040018	positive regulation of multicellular organism growth	3	4.6E-02	5.7E-01
BP	GO:0048639	positive regulation of developmental growth	5	4.9E-02	5.9E-01
BP	GO:0040014	regulation of multicellular organism growth	3	1.6E-01	8.4E-01
Cluster 6 (ES: 1.56)					
MF	GO:0005509	calcium ion binding	16	2.2E-03	2.7E-01
MF	GO:0046872	metal ion binding	41	5.7E-02	8.5E-01
MF	GO:0043169	cation binding	41	6.5E-02	8.4E-01
MF	GO:0043167	ion binding	42	7.5E-02	8.4E-01
Cluster 7 (ES: 1.50)					
BP	GO:0006874	cellular calcium ion homeostasis	10	3.7E-03	3.5E-01
BP	GO:0055074	calcium ion homeostasis	10	4.6E-03	3.1E-01
BP	GO:0051480	regulation of cytosolic calcium ion concentration	8	5.3E-03	2.9E-01
BP	GO:0072503	cellular divalent inorganic cation homeostasis	10	5.7E-03	2.9E-01
BP	GO:0006875	cellular metal ion homeostasis	11	6.9E-03	3.1E-01

Table 2.12 (cont.)

BP	GO:0072507	divalent inorganic cation homeostasis	10	7.8E-03	3.3E-01
BP	GO:0050801	ion homeostasis	13	1.3E-02	3.6E-01
BP	GO:0055065	metal ion homeostasis	11	1.5E-02	3.9E-01
BP	GO:0030003	cellular cation homeostasis	11	1.8E-02	4.2E-01
BP	GO:0042592	homeostatic process	23	1.8E-02	4.2E-01
BP	GO:0006873	cellular ion homeostasis	11	2.1E-02	4.4E-01
BP	GO:2000021	regulation of ion homeostasis	6	2.2E-02	4.5E-01
BP	GO:0055082	cellular chemical homeostasis	12	2.5E-02	4.6E-01
BP	GO:0048878	chemical homeostasis	16	2.8E-02	4.8E-01
BP	GO:0055080	cation homeostasis	11	3.8E-02	5.4E-01
BP	GO:0010959	regulation of metal ion transport	7	4.2E-02	5.6E-01
BP	GO:0007204	positive regulation of cytosolic calcium ion concentration	6	4.3E-02	5.6E-01
BP	GO:0098771	inorganic ion homeostasis	11	4.4E-02	5.6E-01
BP	GO:0019725	cellular homeostasis	12	6.9E-02	6.6E-01
BP	GO:0070838	divalent metal ion transport	6	1.6E-01	8.5E-01
BP	GO:0072511	divalent inorganic cation transport	6	1.6E-01	8.5E-01
BP	GO:0051924	regulation of calcium ion transport	4	2.0E-01	8.8E-01
BP	GO:0006816	calcium ion transport	5	2.5E-01	9.1E-01
BP	GO:0010035	response to inorganic substance	4	4.2E-01	9.7E-01
BP	GO:0010038	response to metal ion	3	4.3E-01	9.7E-01
Cluster 8 (ES: 1.48)					
BP	GO:0046879	hormone secretion	8	4.4E-03	3.2E-01
BP	GO:0060986	endocrine hormone secretion	3	5.3E-02	6.0E-01
BP	GO:0050886	endocrine process	3	1.6E-01	8.4E-01
Cluster 9 (ES: 1.44)					
BP	GO:0009914	hormone transport	9	1.3E-03	3.4E-01
BP	GO:0007267	cell-cell signaling	21	2.8E-03	3.8E-01
BP	GO:0032940	secretion by cell	16	3.4E-03	3.4E-01
BP	GO:0046879	hormone secretion	8	4.4E-03	3.2E-01

Table 2.12 (cont.)

BP	GO:0046903	secretion	17	5.5E-03	2.9E-01
BP	GO:0023061	signal release	9	1.1E-02	3.5E-01
BP	GO:0010817	regulation of hormone levels	9	1.4E-02	3.8E-01
BP	GO:0046883	regulation of hormone secretion	6	2.6E-02	4.6E-01
BP	GO:0042886	amide transport	6	4.1E-02	5.5E-01
BP	GO:1903530	regulation of secretion by cell	10	5.7E-02	6.2E-01
BP	GO:0030072	peptide hormone secretion	5	7.4E-02	6.7E-01
BP	GO:0002790	peptide secretion	5	8.4E-02	6.9E-01
BP	GO:0051046	regulation of secretion	10	8.5E-02	7.0E-01
BP	GO:0015833	peptide transport	5	1.0E-01	7.4E-01
BP	GO:0090276	regulation of peptide hormone secretion	4	1.3E-01	8.0E-01
BP	GO:0002791	regulation of peptide secretion	4	1.4E-01	8.1E-01
BP	GO:0090087	regulation of peptide transport	4	1.4E-01	8.2E-01
BP	GO:0071705	nitrogen compound transport	8	2.0E-01	8.8E-01
BP	GO:0009306	protein secretion	5	4.6E-01	9.8E-01
BP	GO:0050708	regulation of protein secretion	4	5.6E-01	9.9E-01
Cluster 10 (ES: 1.42)					
BP	GO:0001975	response to amphetamine	3	5.8E-03	2.9E-01
BP	GO:0014075	response to amine	3	5.8E-03	2.9E-01
KEGG	ssc04024	cAMP signaling pathway	6	1.1E-01	4.7E-01
KEGG	ssc05034	Alcoholism	3	5.4E-01	9.3E-01
Cluster 11 (ES: 1.42)					
BP	GO:0007268	chemical synaptic transmission	11	1.1E-02	3.4E-01
BP	GO:0098916	anterograde trans-synaptic signaling	11	1.1E-02	3.4E-01
BP	GO:0099536	synaptic signaling	11	1.1E-02	3.4E-01
BP	GO:0099537	trans-synaptic signaling	11	1.1E-02	3.4E-01
BP	GO:0050806	positive regulation of synaptic transmission	4	2.6E-02	4.6E-01
BP	GO:0017156	calcium ion regulated exocytosis	4	7.8E-02	6.8E-01
BP	GO:0099531	presynaptic process involved in chemical synaptic transmission	4	9.0E-02	7.1E-01

Table 2.12 (cont.)

BP	GO:0050804	modulation of synaptic transmission	5	9.3E-02	7.2E-01
BP	GO:0006836	neurotransmitter transport	4	1.5E-01	8.3E-01
BP	GO:0001505	regulation of neurotransmitter levels	4	2.0E-01	8.7E-01
Cluster 12 (ES: 1.36)					
BP	GO:0006955	immune response	23	6.8E-04	2.8E-01
BP	GO:0022407	regulation of cell-cell adhesion	10	3.3E-03	3.5E-01
BP	GO:0030155	regulation of cell adhesion	13	4.4E-03	3.3E-01
BP	GO:0007155	cell adhesion	22	4.4E-03	3.3E-01
BP	GO:0016337	single organismal cell-cell adhesion	15	4.8E-03	3.0E-01
BP	GO:0022610	biological adhesion	22	4.8E-03	2.9E-01
BP	GO:0002684	positive regulation of immune system process	15	4.9E-03	2.9E-01
BP	GO:0098602	single organism cell adhesion	15	9.0E-03	3.5E-01
BP	GO:0098609	cell-cell adhesion	16	9.9E-03	3.4E-01
BP	GO:0002682	regulation of immune system process	19	1.1E-02	3.5E-01
BP	GO:1903037	regulation of leukocyte cell-cell adhesion	8	1.1E-02	3.4E-01
BP	GO:0007159	leukocyte cell-cell adhesion	11	1.6E-02	3.9E-01
BP	GO:0070486	leukocyte aggregation	10	2.3E-02	4.5E-01
BP	GO:0045785	positive regulation of cell adhesion	8	3.0E-02	4.9E-01
BP	GO:0001775	cell activation	14	3.5E-02	5.2E-01
BP	GO:0042110	T cell activation	9	5.1E-02	5.9E-01
BP	GO:0070489	T cell aggregation	9	5.1E-02	5.9E-01
BP	GO:0071593	lymphocyte aggregation	9	5.1E-02	5.9E-01
BP	GO:0045321	leukocyte activation	12	5.5E-02	6.1E-01
BP	GO:1903039	positive regulation of leukocyte cell-cell adhesion	5	7.6E-02	6.8E-01
BP	GO:0050863	regulation of T cell activation	6	7.7E-02	6.8E-01
BP	GO:0050865	regulation of cell activation	8	8.3E-02	7.0E-01
BP	GO:0046649	lymphocyte activation	10	1.0E-01	7.4E-01
BP	GO:0022409	positive regulation of cell-cell adhesion	5	1.1E-01	7.6E-01
BP	GO:0002694	regulation of leukocyte activation	7	1.4E-01	8.1E-01
BP	GO:0030097	hemopoiesis	11	1.7E-01	8.6E-01

Table 2.12 (cont.)

BP	GO:0002696	positive regulation of leukocyte activation	5	1.8E-01	8.6E-01
BP	GO:0051249	regulation of lymphocyte activation	6	1.8E-01	8.6E-01
BP	GO:0050867	positive regulation of cell activation	5	2.0E-01	8.7E-01
BP	GO:0050870	positive regulation of T cell activation	4	2.0E-01	8.8E-01
BP	GO:0030098	lymphocyte differentiation	6	2.2E-01	9.0E-01
BP	GO:0048534	hematopoietic or lymphoid organ development	11	2.2E-01	9.0E-01
BP	GO:0002520	immune system development	11	2.7E-01	9.2E-01
BP	GO:0030217	T cell differentiation	4	2.8E-01	9.3E-01
BP	GO:0051251	positive regulation of lymphocyte activation	4	3.2E-01	9.4E-01
BP	GO:0002521	leukocyte differentiation	7	3.2E-01	9.4E-01
BP	GO:0042113	B cell activation	3	6.7E-01	1.0E+00
Cluster 13 (ES: 1.27)					
BP	GO:0021537	telencephalon development	7	1.1E-02	3.5E-01
BP	GO:0044708	single-organism behavior	8	4.0E-02	5.4E-01
BP	GO:0021543	pallium development	3	3.5E-01	9.5E-01
Cluster 14 (ES: 1.26)					
BP	GO:0050803	regulation of synapse structure or activity	7	6.6E-03	3.0E-01
BP	GO:0050806	positive regulation of synaptic transmission	4	2.6E-02	4.6E-01
BP	GO:0050804	modulation of synaptic transmission	5	9.3E-02	7.2E-01
BP	GO:0007270	neuron-neuron synaptic transmission	3	1.4E-01	8.2E-01
BP	GO:0048167	regulation of synaptic plasticity	3	2.1E-01	8.9E-01
Cluster 15 (ES: 1.18)					
BP	GO:0048732	gland development	9	1.8E-02	4.2E-01
BP	GO:0061180	mammary gland epithelium development	4	2.0E-02	4.3E-01
BP	GO:0030879	mammary gland development	4	8.4E-02	7.0E-01
BP	GO:0048729	tissue morphogenesis	6	6.3E-01	9.9E-01
Cluster 16 (ES: 1.17)					
MF	GO:0005344	oxygen transporter activity	3	6.4E-03	3.7E-01
MF	GO:0019825	oxygen binding	3	1.1E-02	5.0E-01
MF	GO:0005506	iron ion binding	5	9.6E-02	8.6E-01

Table 2.12 (cont.)

MF	GO:0020037	heme binding	3	4.3E-01	9.8E-01
MF	GO:0046906	tetrapyrrole binding	3	4.5E-01	9.8E-01
Cluster 17 (ES: 1.16)					
BP	GO:0048660	regulation of smooth muscle cell proliferation	4	1.6E-02	4.0E-01
BP	GO:0048659	smooth muscle cell proliferation	3	8.6E-02	7.0E-01
BP	GO:0033002	muscle cell proliferation	3	2.3E-01	9.0E-01
Cluster 18 (ES: 1.13)					
BP	GO:0044057	regulation of system process	11	2.2E-03	3.4E-01
BP	GO:0032844	regulation of homeostatic process	11	5.0E-03	2.9E-01
BP	GO:0051480	regulation of cytosolic calcium ion concentration	8	5.3E-03	2.9E-01
BP	GO:0002027	regulation of heart rate	5	6.0E-03	2.9E-01
BP	GO:1903522	regulation of blood circulation	7	9.4E-03	3.5E-01
BP	GO:0034765	regulation of ion transmembrane transport	8	9.7E-03	3.5E-01
BP	GO:0008016	regulation of heart contraction	6	1.1E-02	3.5E-01
BP	GO:0032846	positive regulation of homeostatic process	7	1.1E-02	3.4E-01
BP	GO:0034220	ion transmembrane transport	13	1.1E-02	3.4E-01
BP	GO:0034762	regulation of transmembrane transport	8	1.4E-02	3.7E-01
BP	GO:2000021	regulation of ion homeostasis	6	2.2E-02	4.5E-01
BP	GO:0043269	regulation of ion transport	9	2.2E-02	4.4E-01
BP	GO:0060306	regulation of membrane repolarization	3	2.3E-02	4.5E-01
MF	GO:0005261	cation channel activity	8	2.6E-02	7.1E-01
BP	GO:0048878	chemical homeostasis	16	2.8E-02	4.8E-01
BP	GO:1904062	regulation of cation transmembrane transport	6	3.1E-02	4.9E-01
BP	GO:0086091	regulation of heart rate by cardiac conduction	3	3.5E-02	5.2E-01
BP	GO:0006811	ion transport	17	3.5E-02	5.2E-01
MF	GO:0005272	sodium channel activity	3	4.0E-02	8.2E-01
BP	GO:0010959	regulation of metal ion transport	7	4.2E-02	5.6E-01
BP	GO:0007204	positive regulation of cytosolic calcium ion concentration	6	4.3E-02	5.6E-01
BP	GO:0030001	metal ion transport	11	4.5E-02	5.7E-01

Table 2.12 (cont.)

MF	GO:0046873	metal ion transmembrane transporter activity	9	4.8E-02	8.3E-01
BP	GO:0008015	blood circulation	8	4.9E-02	5.8E-01
BP	GO:0003013	circulatory system process	8	5.3E-02	6.0E-01
BP	GO:0032412	regulation of ion transmembrane transporter activity	5	5.4E-02	6.0E-01
BP	GO:0043270	positive regulation of ion transport	5	5.4E-02	6.0E-01
BP	GO:0060047	heart contraction	5	5.7E-02	6.2E-01
BP	GO:0022898	regulation of transmembrane transporter activity	5	6.1E-02	6.3E-01
BP	GO:0003015	heart process	5	6.1E-02	6.3E-01
BP	GO:0055085	transmembrane transport	14	6.2E-02	6.3E-01
MF	GO:0022838	substrate-specific channel activity	9	6.2E-02	8.6E-01
BP	GO:0003012	muscle system process	7	6.6E-02	6.5E-01
BP	GO:0042391	regulation of membrane potential	7	6.6E-02	6.5E-01
BP	GO:0098655	cation transmembrane transport	9	6.8E-02	6.5E-01
BP	GO:0006812	cation transport	12	7.2E-02	6.7E-01
BP	GO:0061337	cardiac conduction	3	7.3E-02	6.7E-01
BP	GO:0032409	regulation of transporter activity	5	7.6E-02	6.8E-01
MF	GO:0022803	passive transmembrane transporter activity	9	7.7E-02	8.2E-01
MF	GO:0015267	channel activity	9	7.7E-02	8.2E-01
MF	GO:0022836	gated channel activity	7	8.4E-02	8.3E-01
BP	GO:0006936	muscle contraction	6	8.7E-02	7.0E-01
MF	GO:0022832	voltage-gated channel activity	5	1.0E-01	8.6E-01
MF	GO:0005244	voltage-gated ion channel activity	5	1.0E-01	8.6E-01
BP	GO:0006941	striated muscle contraction	4	1.0E-01	7.5E-01
MF	GO:0005216	ion channel activity	8	1.2E-01	8.8E-01
BP	GO:0002028	regulation of sodium ion transport	3	1.2E-01	7.8E-01
MF	GO:0022890	inorganic cation transmembrane transporter activity	9	1.2E-01	8.8E-01
BP	GO:0043266	regulation of potassium ion transport	3	1.2E-01	7.9E-01
MF	GO:0015081	sodium ion transmembrane transporter activity	4	1.4E-01	8.6E-01
MF	GO:0008324	cation transmembrane transporter activity	10	1.4E-01	8.7E-01

Table 2.12 (cont.)

BP	GO:0006813	potassium ion transport	4	1.5E-01	8.3E-01
BP	GO:0015672	monovalent inorganic cation transport	6	1.6E-01	8.5E-01
BP	GO:0070838	divalent metal ion transport	6	1.6E-01	8.5E-01
BP	GO:0072511	divalent inorganic cation transport	6	1.6E-01	8.5E-01
BP	GO:0060048	cardiac muscle contraction	3	1.8E-01	8.6E-01
BP	GO:0010522	regulation of calcium ion transport into cytosol	3	1.9E-01	8.7E-01
BP	GO:0098662	inorganic cation transmembrane transport	7	1.9E-01	8.7E-01
BP	GO:0090257	regulation of muscle system process	4	1.9E-01	8.7E-01
BP	GO:0051924	regulation of calcium ion transport	4	2.0E-01	8.8E-01
BP	GO:0001508	action potential	3	2.1E-01	8.9E-01
BP	GO:1903169	regulation of calcium ion transmembrane transport	3	2.4E-01	9.0E-01
BP	GO:0035637	multicellular organismal signaling	3	2.4E-01	9.1E-01
BP	GO:0006816	calcium ion transport	5	2.5E-01	9.1E-01
BP	GO:0098660	inorganic ion transmembrane transport	7	2.6E-01	9.1E-01
MF	GO:0015077	monovalent inorganic cation transmembrane transporter activity	6	2.6E-01	9.5E-01
MF	GO:0016247	channel regulator activity	3	2.7E-01	9.5E-01
BP	GO:0060401	cytosolic calcium ion transport	3	2.9E-01	9.3E-01
BP	GO:0060402	calcium ion transport into cytosol	3	2.9E-01	9.3E-01
BP	GO:0071805	potassium ion transmembrane transport	3	3.0E-01	9.4E-01
BP	GO:0071804	cellular potassium ion transport	3	3.0E-01	9.4E-01
BP	GO:0006937	regulation of muscle contraction	3	3.4E-01	9.5E-01
MF	GO:0022834	ligand-gated channel activity	3	3.8E-01	9.8E-01
MF	GO:0015276	ligand-gated ion channel activity	3	3.8E-01	9.8E-01
BP	GO:0070509	calcium ion import	3	3.8E-01	9.6E-01
MF	GO:0022843	voltage-gated cation channel activity	3	4.1E-01	9.8E-01
BP	GO:0070588	calcium ion transmembrane transport	3	4.4E-01	9.7E-01
Cluster 19 (ES: 1.12)					
BP	GO:0050803	regulation of synapse structure or activity	7	6.6E-03	3.0E-01
BP	GO:0050807	regulation of synapse organization	5	1.4E-02	3.7E-01

Table 2.12 (cont.)

BP	GO:0051965	positive regulation of synapse assembly	3	1.1E-01	7.6E-01
BP	GO:0044089	positive regulation of cellular component biogenesis	7	1.6E-01	8.4E-01
BP	GO:0051963	regulation of synapse assembly	3	1.6E-01	8.4E-01
BP	GO:0050808	synapse organization	4	2.4E-01	9.1E-01
BP	GO:0007416	synapse assembly	3	2.4E-01	9.1E-01
Cluster 20 (ES: 1.08)					
BP	GO:0022408	negative regulation of cell-cell adhesion	5	1.9E-02	4.3E-01
BP	GO:0007162	negative regulation of cell adhesion	6	2.1E-02	4.4E-01
BP	GO:1903038	negative regulation of leukocyte cell-cell adhesion	3	1.7E-01	8.5E-01
BP	GO:0002683	negative regulation of immune system process	6	1.8E-01	8.6E-01
BP	GO:0050866	negative regulation of cell activation	3	3.0E-01	9.4E-01
Cluster 21 (ES: 1.08)					
BP	GO:2000401	regulation of lymphocyte migration	5	6.4E-04	3.1E-01
BP	GO:2000404	regulation of T cell migration	4	1.9E-03	3.4E-01
BP	GO:0072678	T cell migration	4	5.2E-03	2.9E-01
BP	GO:0072676	lymphocyte migration	5	5.6E-03	2.8E-01
BP	GO:0032102	negative regulation of response to external stimulus	8	7.7E-03	3.3E-01
BP	GO:2000406	positive regulation of T cell migration	3	1.8E-02	4.2E-01
BP	GO:0090026	positive regulation of monocyte chemotaxis	3	2.0E-02	4.4E-01
BP	GO:0090025	regulation of monocyte chemotaxis	3	2.9E-02	4.9E-01
BP	GO:2000403	positive regulation of lymphocyte migration	3	2.9E-02	4.9E-01
BP	GO:0032101	regulation of response to external stimulus	13	3.0E-02	4.9E-01
BP	GO:0050920	regulation of chemotaxis	6	3.3E-02	5.0E-01
BP	GO:0006928	movement of cell or subcellular component	22	4.4E-02	5.6E-01
BP	GO:0040012	regulation of locomotion	12	4.7E-02	5.7E-01
BP	GO:0030030	cell projection organization	17	5.2E-02	6.0E-01
BP	GO:0002686	negative regulation of leukocyte migration	3	5.3E-02	6.0E-01
BP	GO:0051270	regulation of cellular component movement	12	5.5E-02	6.1E-01
BP	GO:0030334	regulation of cell migration	11	5.7E-02	6.2E-01

Table 2.12 (cont.)

BP	GO:0006935	chemotaxis	10	5.7E-02	6.2E-01
BP	GO:0042330	taxis	10	5.8E-02	6.2E-01
BP	GO:0002685	regulation of leukocyte migration	5	6.2E-02	6.4E-01
BP	GO:0051271	negative regulation of cellular component movement	6	6.7E-02	6.5E-01
BP	GO:0040013	negative regulation of locomotion	6	6.7E-02	6.5E-01
BP	GO:2000145	regulation of cell motility	11	7.2E-02	6.7E-01
BP	GO:0040011	locomotion	19	8.0E-02	6.9E-01
BP	GO:0002688	regulation of leukocyte chemotaxis	4	8.4E-02	7.0E-01
BP	GO:0009605	response to external stimulus	24	8.4E-02	7.0E-01
BP	GO:0030336	negative regulation of cell migration	5	1.0E-01	7.5E-01
BP	GO:0050922	negative regulation of chemotaxis	3	1.1E-01	7.5E-01
BP	GO:2000146	negative regulation of cell motility	5	1.1E-01	7.7E-01
BP	GO:0002548	monocyte chemotaxis	3	1.1E-01	7.7E-01
BP	GO:0070098	chemokine-mediated signaling pathway	3	1.2E-01	7.9E-01
BP	GO:0048870	cell motility	16	1.3E-01	8.1E-01
BP	GO:0051674	localization of cell	16	1.3E-01	8.1E-01
BP	GO:0050900	leukocyte migration	6	1.4E-01	8.1E-01
BP	GO:0034097	response to cytokine	9	1.7E-01	8.5E-01
BP	GO:0016477	cell migration	14	1.8E-01	8.6E-01
BP	GO:0002683	negative regulation of immune system process	6	1.8E-01	8.6E-01
BP	GO:0002690	positive regulation of leukocyte chemotaxis	3	2.1E-01	8.9E-01
BP	GO:0060326	cell chemotaxis	5	2.4E-01	9.0E-01
BP	GO:0030595	leukocyte chemotaxis	4	2.7E-01	9.2E-01
BP	GO:0002687	positive regulation of leukocyte migration	3	2.8E-01	9.3E-01
BP	GO:0050921	positive regulation of chemotaxis	3	3.2E-01	9.4E-01
BP	GO:0006954	inflammatory response	7	3.8E-01	9.6E-01
BP	GO:0032103	positive regulation of response to external stimulus	4	3.9E-01	9.7E-01
BP	GO:0030335	positive regulation of cell migration	5	3.9E-01	9.7E-01
BP	GO:2000147	positive regulation of cell motility	5	4.2E-01	9.7E-01

Table 2.12 (cont.)

BP	GO:0051272	positive regulation of cellular component movement	5	4.3E-01	9.7E-01
BP	GO:0040017	positive regulation of locomotion	5	4.4E-01	9.8E-01
BP	GO:0097529	myeloid leukocyte migration	3	4.5E-01	9.8E-01
BP	GO:0071345	cellular response to cytokine stimulus	5	7.0E-01	1.0E+00
BP	GO:0019221	cytokine-mediated signaling pathway	4	7.1E-01	1.0E+00
KEGG	ssc04060	Cytokine-cytokine receptor interaction	3	7.4E-01	9.8E-01
Cluster 22 (ES: 1.05)					
BP	GO:0051130	positive regulation of cellular component organization	18	1.2E-02	3.4E-01
BP	GO:0044089	positive regulation of cellular component biogenesis	7	1.6E-01	8.4E-01
BP	GO:0010638	positive regulation of organelle organization	7	3.9E-01	9.7E-01
Cluster 23 (ES: 1.04)					
BP	GO:0001503	ossification	10	3.0E-03	3.7E-01
BP	GO:0051216	cartilage development	7	6.3E-03	2.9E-01
BP	GO:0061448	connective tissue development	7	1.8E-02	4.2E-01
BP	GO:0001501	skeletal system development	9	6.6E-02	6.5E-01
BP	GO:0061035	regulation of cartilage development	3	1.1E-01	7.7E-01
BP	GO:0060348	bone development	4	2.1E-01	8.9E-01
BP	GO:0002062	chondrocyte differentiation	3	2.2E-01	8.9E-01
BP	GO:0048705	skeletal system morphogenesis	4	3.8E-01	9.6E-01
BP	GO:0070848	response to growth factor	4	8.3E-01	1.0E+00
BP	GO:0071363	cellular response to growth factor stimulus	3	9.4E-01	1.0E+00
Cluster 24 (ES: 1.01)					
BP	GO:0009719	response to endogenous stimulus	21	2.4E-03	3.5E-01
BP	GO:0010033	response to organic substance	33	3.4E-03	3.5E-01
BP	GO:0010243	response to organonitrogen compound	11	9.7E-03	3.5E-01
BP	GO:0009725	response to hormone	11	2.2E-02	4.5E-01
BP	GO:1901698	response to nitrogen compound	12	2.4E-02	4.5E-01
BP	GO:0032870	cellular response to hormone stimulus	9	4.7E-02	5.7E-01

Table 2.12 (cont.)

BP	GO:0043434	response to peptide hormone	5	1.3E-01	8.1E-01
BP	GO:0071495	cellular response to endogenous stimulus	13	1.4E-01	8.2E-01
BP	GO:1901652	response to peptide	5	1.8E-01	8.6E-01
BP	GO:1901700	response to oxygen-containing compound	13	1.9E-01	8.7E-01
BP	GO:0071375	cellular response to peptide hormone stimulus	4	2.2E-01	8.9E-01
BP	GO:0019216	regulation of lipid metabolic process	5	2.2E-01	9.0E-01
BP	GO:1901653	cellular response to peptide	4	2.3E-01	9.0E-01
BP	GO:1901699	cellular response to nitrogen compound	6	2.8E-01	9.3E-01
BP	GO:0071417	cellular response to organonitrogen compound	5	3.3E-01	9.4E-01
BP	GO:0070887	cellular response to chemical stimulus	22	4.0E-01	9.7E-01
BP	GO:0071310	cellular response to organic substance	18	4.1E-01	9.7E-01
BP	GO:0032868	response to insulin	3	4.8E-01	9.8E-01
BP	GO:1901701	cellular response to oxygen-containing compound	7	5.6E-01	9.9E-01

[a]BP: biological process; MF: molecular function; KEGG: KEGG pathway.

[b]Number of genes in the category.

[c]False Discovery Rate adjusted P-value.

Table 2.13. Extended list of genes differentially expressed (FDR-adjusted P-value < 0.1) between pigs from control (CON) relative to PRRSV-treated (MPA) gilts.

Gene	description	[a]CON-MPA	P-value	[b]FDR P-value
PYURF	PIGY upstream reading frame	-9.83	3.5E-82	5.6E-78
RGS16	regulator of G protein signaling 16	-3.39	1.2E-57	9.8E-54
LOC396781	IgG heavy chain	-4.74	1.1E-31	6.0E-28
PCP4	Purkinje cell protein 4	-2.35	6.6E-29	2.7E-25
LOC110255204	melanoma-associated antigen D4-like	-4.14	2.9E-25	9.4E-22
NEXN	nexilin F-actin binding protein	-2.57	1.3E-24	3.5E-21
NTNG1	netrin G1	-2.07	1.7E-23	3.8E-20
AHNAK2	AHNAK nucleoprotein 2	-2.62	2.9E-21	5.8E-18
CHRNA2	cholinergic receptor nicotinic alpha 2 subunit	-3.60	4.4E-20	8.0E-17
NTS	neurotensin	-2.76	6.0E-17	9.7E-14
PLXDC1	plexin domain containing 1	-1.91	1.5E-16	2.2E-13
TCF7L2	transcription factor 7 like 2	-1.60	4.4E-16	5.9E-13
AKAP12	A-kinase anchoring protein 12	-1.72	8.1E-16	1.0E-12
RELN	reelin	-1.40	9.6E-13	1.1E-09
LOC110261683	uncharacterized LOC110261683	-2.48	1.4E-12	1.5E-09
LOC102163738	uncharacterized LOC102163738	-2.19	1.4E-11	1.4E-08
GRID2IP	Grid2 interacting protein	-2.10	1.6E-11	1.5E-08
LOC110261685	chromobox protein homolog 3	-1.31	2.0E-11	1.8E-08
APLNR	apelin receptor	-1.35	3.2E-11	2.7E-08
IFITM3	interferon induced transmembrane protein 3	-1.27	7.6E-11	6.2E-08
CALB1	calbindin 1	-2.61	2.7E-10	2.1E-07
LOC106505355	uncharacterized LOC106505355	3.05	5.7E-10	4.1E-07
TP53INP2	tumor protein p53 inducible nuclear protein 2	-1.37	5.8E-10	4.1E-07
MBP	myelin basic protein	-1.43	9.1E-10	6.1E-07
ISM1	isthmin 1	-2.01	1.5E-09	9.7E-07
SLA-1	MHC class I antigen 1	-1.20	1.6E-09	9.7E-07
SPTSSB	serine palmitoyltransferase small subunit B	-1.68	2.6E-09	1.6E-06

Table 2.13 (cont.)

LHX9	LIM homeobox 9	-2.23	8.0E-09	4.6E-06
BCAS1	breast carcinoma amplified sequence 1	-1.31	9.9E-09	5.5E-06
CTGF	Connective tissue growth factor	1.16	1.1E-08	6.2E-06
FAM163A	family with sequence similarity 163 member A	-2.13	1.6E-08	8.4E-06
PTPN3	protein tyrosine phosphatase, non-receptor type 3	-1.20	2.0E-08	1.0E-05
SAMD4A	sterile alpha motif domain containing 4A	-1.19	2.6E-08	1.3E-05
MOBP	myelin-associated oligodendrocytic basic protein	-1.27	3.7E-08	1.8E-05
ATP5PD	ATP synthase peripheral stalk subunit d	1.45	4.3E-08	2.0E-05
ZIC1	Zic family member 1	-1.53	4.5E-08	2.0E-05
SCRT1	scratch family transcriptional repressor 1	-1.07	4.9E-08	2.1E-05
IGSF5	immunoglobulin superfamily, member 5	-1.73	9.5E-08	4.0E-05
LOC102167506	uncharacterized LOC102167506	-1.78	9.8E-08	4.1E-05
E2F7	E2F transcription factor 7	-1.83	1.3E-07	5.3E-05
SLC22A2	solute carrier family 22 member 2	2.37	1.3E-07	5.3E-05
TF	transferrin	-1.16	1.6E-07	6.3E-05
PAIP2B	poly(A) binding protein interacting protein 2B	-1.02	1.7E-07	6.4E-05
KIF1C	kinesin family member 1C	-1.14	2.5E-07	9.0E-05
FNDC5	fibronectin type III domain containing 5	-1.10	3.6E-07	1.3E-04
CBX3	chromobox 3	1.01	6.1E-07	2.1E-04
LOX	lysyl oxidase	-1.94	6.1E-07	2.1E-04
HAPLN2	hyaluronan and proteoglycan link protein 2	-1.36	7.8E-07	2.6E-04
IGF2	insulin like growth factor 2	1.28	8.1E-07	2.7E-04
SYNDIG1L	synapse differentiation inducing 1 like	-1.50	9.0E-07	2.9E-04
SLC13A4	solute carrier family 13 member 4	1.52	1.1E-06	3.5E-04
ANKRD34C	ankyrin repeat domain 34C	-1.41	1.6E-06	4.9E-04
CDR2L	cerebellar degeneration related protein 2 like	-0.93	1.7E-06	5.2E-04
TRPC3	transient receptor potential cation channel subfamily C member 3	-1.73	1.7E-06	5.2E-04
MPZL2	myelin protein zero-like 2	2.09	2.0E-06	5.6E-04
PAQR6	progestin and adipoQ receptor family member 6	-1.02	1.9E-06	5.6E-04

Table 2.13 (cont.)

SEMA7A	semaphorin 7A (John Milton Hagen blood group)	-0.94	2.0E-06	5.6E-04
VAMP1	vesicle associated membrane protein 1	-0.94	2.1E-06	6.0E-04
DLK1	delta like non-canonical Notch ligand 1	-1.87	3.1E-06	8.6E-04
KLK6	kallikrein related peptidase 6	-1.90	5.1E-06	1.4E-03
CRABP2	cellular retinoic acid binding protein 2	1.97	5.6E-06	1.5E-03
IRX3	iroquois homeobox 3	-1.86	5.8E-06	1.5E-03
EPGN	epithelial mitogen	-1.77	6.0E-06	1.6E-03
ADAMTS9	ADAM metallopeptidase with thrombospondin type 1 motif 9	-1.38	6.9E-06	1.7E-03
TRAK2	trafficking kinesin protein 2	-0.97	6.9E-06	1.7E-03
ARC	activity regulated cytoskeleton associated protein	1.02	7.2E-06	1.7E-03
LOC102157546	uncharacterized LOC102157546	1.48	7.2E-06	1.7E-03
LOC100155249	keratin, type II cytoskeletal 3-like	1.93	7.5E-06	1.8E-03
MAB21L1	mab-21 like 1	-1.87	8.3E-06	1.9E-03
VIPR2	vasoactive intestinal peptide receptor 2	-1.77	8.3E-06	1.9E-03
RGS8	regulator of G protein signaling 8	-0.88	8.6E-06	2.0E-03
LEPR	leptin receptor	-0.86	9.2E-06	2.1E-03
LOC110261244	uncharacterized LOC110261244	-1.54	9.5E-06	2.1E-03
LOC110256276	uncharacterized LOC110256276	-1.46	1.0E-05	2.2E-03
KRT19	keratin 19	1.79	1.5E-05	3.2E-03
NDNF	neuron derived neurotrophic factor	-1.27	1.5E-05	3.3E-03
OAS1	2'-5'-oligoadenylate synthetase 1	-1.19	1.6E-05	3.5E-03
GPR153	G protein-coupled receptor 153	-1.14	1.9E-05	3.8E-03
PRKCH	protein kinase C eta	-1.16	2.0E-05	4.1E-03
LOC102158399	translation initiation factor IF-2-like	-0.91	2.8E-05	5.6E-03
LOC106505010	quinone oxidoreductase-like protein 2	1.67	2.8E-05	5.6E-03
CPNE9	copine family member 9	-1.34	3.4E-05	6.7E-03
HS3ST5	heparan sulfate-glucosamine 3-sulfotransferase 5	-1.24	3.5E-05	6.8E-03
SLC5A5	solute carrier family 5 member 5	1.69	3.8E-05	7.3E-03
CTSC	cathepsin C	-1.03	4.1E-05	7.7E-03

Table 2.13 (cont.)

SPP1	secreted phosphoprotein 1	-0.89	4.1E-05	7.7E-03
CEMIP	cell migration inducing hyaluronidase 1	1.08	4.3E-05	8.0E-03
LOC100518848	40S ribosomal protein S21	-1.07	4.9E-05	9.0E-03
LOC106506226	transforming acidic coiled-coil-containing protein 1	-1.55	5.5E-05	9.7E-03
ST6GALNAC1	ST6 N-acetylgalactosaminide alpha-2,6-sialyltransferase 1	-1.65	5.4E-05	9.7E-03
THRSP	thyroid hormone responsive	-1.70	5.4E-05	9.7E-03
CEACAM16	carcinoembryonic antigen related cell adhesion molecule 16	-1.57	5.6E-05	9.9E-03
EVI2A	ecotropic viral integration site 2A	-0.83	5.7E-05	9.9E-03
LOC110257359	uncharacterized LOC110257359	-0.79	5.7E-05	9.9E-03
PKD2L1	polycystin 2 like 1, transient receptor potential cation channel	1.54	6.1E-05	1.0E-02
LOC100513119	cyclin-dependent kinase 20-like	1.84	7.2E-05	1.2E-02
IFITM1	interferon induced transmembrane protein 1	-1.15	7.4E-05	1.2E-02
SLC22A8	solute carrier family 22 member 8	1.73	7.5E-05	1.2E-02
VAV3	vav guanine nucleotide exchange factor 3	-1.15	8.1E-05	1.3E-02
KCNJ16	potassium voltage-gated channel subfamily J member 16	-0.95	8.5E-05	1.4E-02
ACBD7	acyl-CoA binding domain containing 7	-1.36	8.8E-05	1.4E-02
OSR1	odd-skipped related transcription factor 1	1.60	9.5E-05	1.5E-02
ALDH1A1	aldehyde dehydrogenase 1 family member A1	0.79	9.7E-05	1.5E-02
TNMD	tenomodulin	1.66	1.0E-04	1.6E-02
RSAD2	radical S-adenosyl methionine domain containing 2	-1.17	1.1E-04	1.7E-02
UCMA	upper zone of growth plate and cartilage matrix associated	-1.40	1.2E-04	1.8E-02
ZFP37	zinc finger protein 37	-1.07	1.2E-04	1.9E-02
FOXJ1	forkhead box J1	0.77	1.3E-04	2.0E-02
AEBP1	AE binding protein 1	0.91	1.7E-04	2.4E-02
ANLN	anillin actin binding protein	-0.82	1.7E-04	2.4E-02
COL25A1	collagen type XXV alpha 1 chain	-0.75	1.7E-04	2.4E-02
GJB1	gap junction protein beta 1	-1.09	1.6E-04	2.4E-02
LOC100513133	uncharacterized LOC100513133	-0.75	1.9E-04	2.7E-02
CHRNA4	cholinergic receptor nicotinic alpha 4 subunit	-1.13	2.0E-04	2.9E-02

Table 2.13 (cont.)

IFI6	interferon alpha inducible protein 6	-0.81	2.0E-04	2.9E-02
LOC110257661	uncharacterized LOC110257661	1.65	2.1E-04	2.9E-02
IFI44L	interferon-induced protein 44-like	-0.83	2.2E-04	3.0E-02
PHACTR2	phosphatase and actin regulator 2	-0.74	2.2E-04	3.0E-02
FIBCD1	fibrinogen C domain containing 1	1.33	2.3E-04	3.1E-02
C14H10orf105	chromosome 14 C10orf105 homolog	0.95	2.4E-04	3.1E-02
EMILIN2	elastin microfibril interfacer 2	-1.41	2.4E-04	3.1E-02
XAF1	XIAP associated factor 1	-1.13	2.3E-04	3.1E-02
GRM4	glutamate metabotropic receptor 4	-1.13	2.5E-04	3.2E-02
SPATA18	spermatogenesis associated 18	0.81	2.9E-04	3.8E-02
CD2	CD2 molecule	-1.53	3.1E-04	3.9E-02
TTR	transthyretin	-0.79	3.1E-04	3.9E-02
PKP4	plakophilin 4	-0.81	3.2E-04	4.1E-02
AR	androgen receptor	-1.36	3.3E-04	4.1E-02
LOC110259891	uncharacterized LOC110259891	-0.88	3.5E-04	4.4E-02
ZFHX3	zinc finger homeobox 3	-0.93	4.3E-04	5.4E-02
CLEC2L	C-type lectin domain family 2 member L	-0.72	4.6E-04	5.6E-02
DNAH12	dynein axonemal heavy chain 12	1.13	4.6E-04	5.7E-02
IRX1	iroquois homeobox 1	-1.31	5.0E-04	6.1E-02
LOC110258846	ankyrin repeat domain-containing protein 26-like	1.40	5.0E-04	6.1E-02
JCAD	junctional cadherin 5 associated	-0.73	5.2E-04	6.3E-02
VWDE	von Willebrand factor D and EGF domains	-1.43	5.5E-04	6.5E-02
PLEKHD1	pleckstrin homology and coiled-coil domain containing D1	-0.99	5.5E-04	6.5E-02
AQP3	aquaporin 3	-1.12	5.6E-04	6.6E-02
KCTD14	potassium channel tetramerization domain containing 14	1.26	5.6E-04	6.6E-02
HERC5	HECT and RLD domain containing E3 ubiquitin protein ligase 5	-1.05	5.7E-04	6.6E-02
LOC110255964	uncharacterized LOC110255964	-1.18	5.8E-04	6.7E-02
CA5B	carbonic anhydrase 5B	-0.79	6.1E-04	7.0E-02
EMB	embigin	-1.11	6.7E-04	7.6E-02

Table 2.13 (cont.)

CENPE	centromere protein E	-1.17	7.0E-04	7.7E-02
IAPP	islet amyloid polypeptide	-1.36	7.0E-04	7.7E-02
LDB3	LIM domain binding 3	-1.33	6.9E-04	7.7E-02
LOC100739561	glycerophosphodiester phosphodiesterase domain-containing protein 1	-0.79	6.8E-04	7.7E-02
SLITRK6	SLIT and NTRK like family member 6	-1.13	7.0E-04	7.7E-02
TNNT1	troponin T1, slow skeletal type	-1.14	7.1E-04	7.7E-02
SHISAL1	shisa like 1	-0.71	7.3E-04	7.9E-02
NEUROD6	neuronal differentiation 6	0.74	7.5E-04	8.0E-02
SLA-3	MHC class I antigen 3	-0.66	7.5E-04	8.0E-02
OAS2	2'-5'-oligoadenylate synthetase 2	-0.71	7.7E-04	8.2E-02
FAM81B	family with sequence similarity 81 member B	1.42	7.9E-04	8.3E-02
LOC100737600	DBIRD complex subunit ZNF326	-0.66	8.1E-04	8.4E-02
EPN3	epsin 3	-1.12	8.2E-04	8.5E-02
ISLR	immunoglobulin superfamily containing leucine rich repeat	1.13	8.3E-04	8.5E-02
CFB	complement factor B	0.90	8.4E-04	8.6E-02
ANKRD24	ankyrin repeat domain 24	-0.73	8.7E-04	8.9E-02
APOD	apolipoprotein D	-0.73	9.0E-04	9.1E-02
MAP2K7	mitogen-activated protein kinase kinase 7	-0.64	9.9E-04	1.0E-01

[a]Log2(fold change) between CON and MPA pigs.

[b]False Discovery rate adjusted P-value.

Table 2.14. Extended list of enriched clusters and supporting functional categories among the genes presenting significant maternal immune activation effect, and representative categories identified using DAVID.

[a]Category	GO Identifier	GO name	[b]Count	P-value	[c]FDR P-value
Cluster 1 (ES: 1.51)					
BP	GO:0048646	anatomical structure formation involved in morphogenesis	13	3.7E-03	9.7E-01
BP	GO:0001568	blood vessel development	8	1.1E-02	9.5E-01
BP	GO:0001944	vasculature development	8	1.5E-02	9.5E-01
BP	GO:0072358	cardiovascular system development	10	1.7E-02	9.3E-01
BP	GO:0072359	circulatory system development	10	1.7E-02	9.3E-01
BP	GO:0001525	angiogenesis	5	8.4E-02	9.8E-01
BP	GO:0048514	blood vessel morphogenesis	5	1.4E-01	9.8E-01
BP	GO:0007507	heart development	4	3.7E-01	9.9E-01
Cluster 2 (ES: 1.40)					
KEGG	ssc05330	Allograft rejection	3	1.7E-02	8.0E-01
KEGG	ssc05169	Epstein-Barr virus infection	4	2.3E-02	6.7E-01
KEGG	ssc05320	Autoimmune thyroid disease	3	3.0E-02	6.1E-01
KEGG	ssc05416	Viral myocarditis	3	4.4E-02	5.7E-01
KEGG	ssc04145	Phagosome	3	1.8E-01	8.4E-01
Cluster 3 (ES: 1.38)					
BP	GO:0048871	multicellular organismal homeostasis	6	7.7E-03	9.8E-01
BP	GO:0060249	anatomical structure homeostasis	5	5.3E-02	9.7E-01
BP	GO:0001894	tissue homeostasis	4	5.7E-02	9.7E-01
BP	GO:0042592	homeostatic process	11	1.3E-01	9.8E-01
Cluster 4 (ES: 1.27)					
MF	GO:0043167	ion binding	23	3.3E-02	9.5E-01
MF	GO:0046872	metal ion binding	22	3.6E-02	8.7E-01
MF	GO:0043169	cation binding	22	4.0E-02	8.5E-01
MF	GO:0046914	transition metal ion binding	11	8.3E-02	8.8E-01
MF	GO:0008270	zinc ion binding	9	1.2E-01	9.0E-01
Cluster 5 (ES: 1.13)					
BP	GO:0001656	metanephros development	4	8.7E-03	9.7E-01
BP	GO:0060993	kidney morphogenesis	4	1.0E-02	9.7E-01
BP	GO:0072009	nephron epithelium development	4	1.5E-02	9.6E-01
BP	GO:0072006	nephron development	4	2.1E-02	9.4E-01
BP	GO:0072073	kidney epithelium development	4	3.2E-02	9.7E-01
BP	GO:0001655	urogenital system development	5	5.2E-02	9.7E-01
BP	GO:0009887	organ morphogenesis	9	5.6E-02	9.7E-01
BP	GO:0035295	tube development	7	5.8E-02	9.7E-01

Table 2.14 (cont.)

BP	GO:0072080	nephron tubule development	3	7.3E-02	9.8E-01
BP	GO:0060429	epithelium development	9	7.4E-02	9.8E-01
BP	GO:0061326	renal tubule development	3	7.8E-02	9.8E-01
BP	GO:0001657	ureteric bud development	3	8.4E-02	9.8E-01
BP	GO:0072163	mesonephric epithelium development	3	8.6E-02	9.8E-01
BP	GO:0072164	mesonephric tubule development	3	8.6E-02	9.8E-01
BP	GO:0001823	mesonephros development	3	9.5E-02	9.8E-01
BP	GO:0001822	kidney development	4	1.0E-01	9.8E-01
BP	GO:0072001	renal system development	4	1.2E-01	9.8E-01
BP	GO:0007389	pattern specification process	5	1.3E-01	9.8E-01
BP	GO:0051241	negative regulation of multicellular organismal process	7	2.1E-01	9.8E-01
BP	GO:0003002	regionalization	4	2.2E-01	9.8E-01
BP	GO:0051093	negative regulation of developmental process	4	5.8E-01	1.0E+00
BP	GO:0045596	negative regulation of cell differentiation	3	7.3E-01	1.0E+00
Cluster 6 (ES: 1.13)					
BP	GO:0030855	epithelial cell differentiation	7	2.6E-02	9.5E-01
BP	GO:0002064	epithelial cell development	4	7.4E-02	9.8E-01
BP	GO:0060429	epithelium development	9	7.4E-02	9.8E-01
BP	GO:0008285	negative regulation of cell proliferation	5	2.1E-01	9.8E-01

[a]BP: biological process; MF: molecular function; KEGG: KEGG pathway.

[b]Number of genes in the category.

[c]False Discovery Rate adjusted P-value.

Table 2.15. Extended list of enriched categories among the genes differentially expressed between pigs from the control relative to the maternal immune activation group GSEA.

[a]Expression/ [b]Category	GO Identifier	GO name	[c]NES	P-value	[d]FDR P-value
Over					
BP	GO:0001578	Microtubule bundle formation	2.03	0.0E+00	0.0E+00
BP	GO:0060271	Cilium morphogenesis	2.01	0.0E+00	0.0E+00
BP	GO:0044782	Cilium organization	1.97	0.0E+00	0.0E+00
BP	GO:0035082	Axoneme assembly	1.94	0.0E+00	1.8E-04
BP	GO:0003341	Cilium movement	1.94	0.0E+00	1.4E-04
MF	GO:0043539	Protein serine threonine kinase activator activity	1.73	0.0E+00	1.7E-01
BP	GO:0015893	Drug transport	1.72	0.0E+00	1.7E-01
BP	GO:0070286	Axonemal dynein complex assembly	1.71	2.4E-03	1.7E-01
BP	GO:1900078	Positive regulation of cellular response to insulin stimulus	1.69	2.4E-03	2.4E-01
BP	GO:0003351	Epithelial cilium movement	1.69	4.9E-03	2.1E-01
BP	GO:0032881	Regulation of polysaccharide metabolic process	1.68	1.1E-02	2.4E-01
BP	GO:0070873	Regulation of glycogen metabolic process	1.68	7.8E-03	2.4E-01

[a]Expression: Over- and under-expressed in CON vs MPA pigs.

[b]BP: biological process; MF: molecular function.

[c]normalized enrichment score.

[d]False Discovery Rate adjusted P-value.

Table 2.16. Extended list of genes differentially expressed (FDR-adjusted P-value < 0.1) between male (Ma) and female (Fe) pigs.

Gene	description	[a]Ma-Fe	P-value	[b]FDR P-value
LOC110257905	thymosin beta-4-like	13.17	9.2E-288	1.5E-283
GH1	growth hormone 1	10.93	7.1E-255	5.8E-251
LOC100624149	eukaryotic translation initiation factor 2 subunit 3	11.98	3.6E-202	2.0E-198
CGA	glycoprotein hormones, alpha polypeptide	7.13	2.9E-176	1.2E-172
LOC100625207	probable ubiquitin carboxyl-terminal hydrolase FAF-X	9.94	2.8E-169	9.2E-166
EIF1AY	eukaryotic translation initiation factor 1A, Y-linked	13.68	1.6E-162	4.4E-159
LOC100624590	ATP-dependent RNA helicase DDX3X	12.35	7.1E-149	1.6E-145
RGS16	regulator of G protein signaling 16	4.12	3.2E-83	6.4E-80
LHB	luteinizing hormone beta polypeptide	3.92	1.5E-78	2.7E-75
POMC	proopiomelanocortin	3.76	2.3E-76	3.8E-73
LOC110255257	oral-facial-digital syndrome 1 protein-like	9.89	1.8E-68	2.6E-65
PYURF	PIGY upstream reading frame	8.40	1.7E-62	2.2E-59
LOC110257883	lysine-specific demethylase 5D-like	10.97	5.5E-58	6.9E-55
LOC110255320	lysine-specific demethylase 6A-like	10.26	9.4E-47	1.1E-43
PCP4	Purkinje cell protein 4	2.86	7.6E-43	8.2E-40
LOC110257894	gamma-taxilin-like	5.64	2.7E-42	2.8E-39
LOC100624329	zinc finger X-chromosomal protein	3.89	4.1E-40	3.9E-37
NTNG1	netrin G1	2.50	1.1E-34	1.0E-31
NEXN	nexilin F-actin binding protein	3.01	7.7E-34	6.6E-31
LOC110257896	uncharacterized LOC110257896	5.73	3.4E-31	2.7E-28
AHNAK2	AHNAK nucleoprotein 2	2.63	1.5E-22	1.1E-19
TCF7L2	transcription factor 7 like 2	1.85	4.1E-22	3.0E-19
KIAA1324	KIAA1324 ortholog	2.31	4.0E-21	2.8E-18
POU1F1	POU class 1 homeobox 1	3.52	8.7E-21	5.9E-18
ISM1	isthmin 1	2.96	2.7E-19	1.8E-16
LHX9	LIM homeobox 9	3.38	2.1E-18	1.3E-15
LOC100624648	F-box-like/WD repeat-containing protein TBL1X	-2.07	4.1E-18	2.4E-15
E2F7	E2F transcription factor 7	2.87	8.1E-17	4.7E-14
GPX3	glutathione peroxidase 3	1.86	9.5E-17	5.3E-14

Table 2.16 (cont.)

AKAP12	A-kinase anchoring protein 12	1.71	1.0E-16	5.6E-14
GRID2IP	Grid2 interacting protein	2.51	2.4E-16	1.3E-13
DLK1	delta like non-canonical Notch ligand 1	3.24	4.2E-16	2.1E-13
CALB1	calbindin 1	3.21	3.8E-15	1.9E-12
PLXDC1	plexin domain containing 1	1.74	5.5E-15	2.6E-12
EPCAM	epithelial cell adhesion molecule	2.65	8.5E-15	3.9E-12
CPNE9	copine family member 9	2.46	1.2E-14	5.4E-12
NTS	neurotensin	2.42	2.8E-14	1.2E-11
CHRNA2	cholinergic receptor nicotinic alpha 2 subunit	2.78	1.3E-13	5.4E-11
TTR	transthyretin	1.52	6.9E-13	2.8E-10
MSX1	msh homeobox	2.57	7.0E-12	2.8E-09
LOC110260685	uncharacterized LOC110260685	-1.84	9.0E-12	3.5E-09
PTPN3	protein tyrosine phosphatase, non-receptor type 3	1.41	1.1E-11	4.2E-09
TUBA8	tubulin alpha 8	2.25	2.7E-11	1.0E-08
LOC100513601	patr class I histocompatibility antigen, A-126 alpha chain-like	1.24	4.0E-11	1.5E-08
IRS4	insulin receptor substrate 4	2.11	2.5E-10	9.0E-08
SYNDIG1L	synapse differentiation inducing 1 like	1.87	2.7E-10	9.5E-08
LOC110261685	chromobox protein homolog 3	1.18	3.7E-10	1.3E-07
CEACAM16	carcinoembryonic antigen related cell adhesion molecule 16	2.37	4.9E-10	1.6E-07
ALDH1A2	aldehyde dehydrogenase 1 family member A2	2.24	5.7E-10	1.9E-07
SPTSSB	serine palmitoyltransferase small subunit B	1.64	1.8E-09	5.7E-07
FAM163A	family with sequence similarity 163 member A	2.16	3.5E-09	1.1E-06
ZIC1	Zic family member 1	1.56	6.7E-09	2.1E-06
PRKCH	protein kinase C eta	1.52	7.0E-09	2.1E-06
CHGB	chromogranin B	1.27	7.7E-09	2.3E-06
SCGN	secretagogin, EF-hand calcium binding protein	2.09	1.4E-08	4.1E-06
TNNT1	troponin T1, slow skeletal type	1.79	4.0E-08	1.2E-05
GBP1	guanylate binding protein 1	-1.28	5.0E-08	1.4E-05
CDH1	cadherin 1	1.81	7.6E-08	2.1E-05
SLITRK6	SLIT and NTRK like family member 6	1.74	8.3E-08	2.3E-05

Table 2.16 (cont.)

VAMP1	vesicle associated membrane protein 1	1.02	8.6E-08	2.3E-05
VIPR2	vasoactive intestinal peptide receptor 2	2.05	9.3E-08	2.5E-05
EPGN	epithelial mitogen	2.02	9.5E-08	2.5E-05
TCTE1	t-complex-associated-testis-expressed 1	-1.37	1.3E-07	3.2E-05
CHRNA4	cholinergic receptor nicotinic alpha 4 subunit	1.53	1.8E-07	4.4E-05
TRPC3	transient receptor potential cation channel subfamily C member 3	1.83	1.7E-07	4.4E-05
LOC100623862	extracellular matrix protein 2	-1.93	3.9E-07	9.6E-05
TMEM30B	transmembrane protein 30B	1.79	5.1E-07	1.2E-04
RGS8	regulator of G protein signaling 8	0.95	6.7E-07	1.6E-04
ANKRD34C	ankyrin repeat domain 34C	1.40	7.8E-07	1.8E-04
FNDC5	fibronectin type III domain containing 5	1.02	7.9E-07	1.8E-04
WNT3	Wnt family member 3	1.72	9.0E-07	2.0E-04
SLC10A4	solute carrier family 10 member 4	1.79	1.2E-06	2.6E-04
GPR153	G protein-coupled receptor 153	1.24	1.3E-06	2.8E-04
DRD2	dopamine receptor D2	1.71	1.4E-06	3.1E-04
RAB27A	RAB27A, member RAS oncogene family	1.52	1.6E-06	3.6E-04
KRT19	keratin 19	1.73	1.8E-06	3.8E-04
SLC17A6	solute carrier family 17 member 6	0.90	2.0E-06	4.3E-04
SCRT1	scratch family transcriptional repressor 1	0.89	2.3E-06	4.8E-04
ADORA2A	adenosine A2a receptor	1.34	2.4E-06	4.8E-04
TMIE	transmembrane inner ear	1.34	4.0E-06	8.2E-04
LOC110257661	uncharacterized LOC110257661	-1.94	5.0E-06	1.0E-03
IGSF1	immunoglobulin superfamily member 1	0.85	6.4E-06	1.3E-03
ISOC1	isochorismatase domain containing 1	0.84	6.6E-06	1.3E-03
TBL1X	transducin beta like 1 X-linked	0.85	6.8E-06	1.3E-03
LCN2	lipocalin 2	1.62	7.0E-06	1.3E-03
CCDC136	coiled-coil domain containing 136	0.86	9.5E-06	1.8E-03
GSG1	germ cell associated 1	-1.16	1.1E-05	2.0E-03
SEMA7A	semaphorin 7A (John Milton Hagen blood group)	0.83	1.1E-05	2.1E-03

Table 2.16 (cont.)

TMEM41A	transmembrane protein 41A	1.11	1.1E-05	2.1E-03
LOC110256276	uncharacterized LOC110256276	-1.45	1.2E-05	2.1E-03
CASQ2	calsequestrin 2	1.56	1.2E-05	2.2E-03
CCDC17	coiled-coil domain containing 17	-1.79	1.3E-05	2.2E-03
LOC100624940	uncharacterized LOC100624940	1.27	1.3E-05	2.2E-03
IRX3	iroquois homeobox 3	1.72	1.3E-05	2.3E-03
AQP3	aquaporin 3	1.36	1.4E-05	2.4E-03
GRP	gastrin releasing peptide	1.51	1.5E-05	2.6E-03
BTBD11	BTB domain containing 11	1.02	1.5E-05	2.6E-03
UPP1	uridine phosphorylase 1	1.59	1.6E-05	2.6E-03
CXCL12	C-X-C motif chemokine ligand 12	0.81	1.6E-05	2.7E-03
NPM2	nucleophosmin/nucleoplasmin 2	1.79	1.7E-05	2.8E-03
VAV3	vav guanine nucleotide exchange factor 3	1.20	1.8E-05	2.8E-03
SCUBE3	signal peptide, CUB domain and EGF like domain containing 3	1.55	1.8E-05	2.9E-03
CACNA2D3	calcium voltage-gated channel auxiliary subunit alpha2delta 3	0.93	1.9E-05	3.0E-03
LOC110255964	uncharacterized LOC110255964	1.40	2.2E-05	3.4E-03
GRM4	glutamate metabotropic receptor 4	1.25	2.3E-05	3.5E-03
LLGL2	LLGL scribble cell polarity complex component 2	1.56	2.3E-05	3.5E-03
IRF6	interferon regulatory factor 6	1.30	2.9E-05	4.4E-03
LOC102157546	uncharacterized LOC102157546	-1.28	3.0E-05	4.4E-03
ACBD7	acyl-CoA binding domain containing 7	1.39	3.4E-05	4.9E-03
CBLN2	cerebellin 2 precursor	0.90	3.4E-05	4.9E-03
COL25A1	collagen type XXV alpha 1 chain	0.80	3.4E-05	4.9E-03
HBB	hemoglobin subunit beta	0.91	3.3E-05	4.9E-03
ZNF804A	zinc finger protein 804A	1.11	3.5E-05	5.0E-03
NELL1	neural EGFL like 1	1.04	3.6E-05	5.1E-03
FBN2	fibrillin 2	1.32	3.7E-05	5.2E-03
LRRC39	leucine rich repeat containing 39	1.53	4.4E-05	6.1E-03
GNRHR	gonadotropin releasing hormone receptor	1.39	4.6E-05	6.3E-03
LDB3	LIM domain binding 3	1.53	5.4E-05	7.4E-03

Table 2.16 (cont.)

ANKRD24	ankyrin repeat domain 24	0.84	5.6E-05	7.7E-03
SCNN1B	sodium channel epithelial 1 beta subunit	1.47	6.0E-05	8.1E-03
TP53INP2	tumor protein p53 inducible nuclear protein 2	0.84	6.5E-05	8.7E-03
PHACTR2	phosphatase and actin regulator 2	0.76	7.2E-05	9.6E-03
LOC100737768	hemoglobin subunit alpha-like	0.86	7.8E-05	1.0E-02
OLFM3	olfactomedin 3	0.75	9.3E-05	1.2E-02
AGTR1	angiotensin II receptor type 1	1.49	9.7E-05	1.3E-02
FRZB	frizzled related protein	0.96	1.3E-04	1.7E-02
ZDHHC22	zinc finger DHHC-type containing 22	0.71	1.5E-04	1.9E-02
NUCB2	nucleobindin 2	0.84	1.7E-04	2.1E-02
MBP	myelin basic protein	0.84	1.7E-04	2.2E-02
PAPPA	pappalysin 1	1.33	1.7E-04	2.2E-02
USP43	ubiquitin specific peptidase 43	1.28	1.8E-04	2.3E-02
NEFH	neurofilament heavy	0.71	1.9E-04	2.3E-02
LOC100515788	hemoglobin subunit beta-like	1.02	2.0E-04	2.4E-02
RORA	RAR related orphan receptor A	0.74	2.0E-04	2.4E-02
CRSP-2	calcitonin receptor-stimulating peptide-2	-0.71	2.1E-04	2.5E-02
LOC106506628	uncharacterized LOC106506628	1.38	2.1E-04	2.5E-02
PDP1	pyruvate dehyrogenase phosphatase catalytic subunit 1	0.69	2.2E-04	2.6E-02
FOXJ1	forkhead box J1	-0.69	2.5E-04	3.0E-02
LOC110255657	uncharacterized LOC110255657	-0.90	2.8E-04	3.3E-02
SP8	Sp8 transcription factor	1.43	2.9E-04	3.4E-02
SPINT2	serine peptidase inhibitor, Kunitz type 2	0.89	3.0E-04	3.5E-02
EPN3	epsin 3	1.16	3.2E-04	3.6E-02
IRX1	iroquois homeobox 1	1.30	3.3E-04	3.8E-02
PAPSS2	3'-phosphoadenosine 5'-phosphosulfate synthase 2	1.21	3.4E-04	3.8E-02
CBLN4	cerebellin 4 precursor protein	1.03	3.5E-04	3.9E-02
LOC100513317	coiled-coil-helix-coiled-coil-helix domain-containing protein 2 pseudogene	1.36	3.7E-04	4.1E-02
HRH3	histamine receptor H3	0.66	4.1E-04	4.5E-02

Table 2.16 (cont.)

DNAH12	dynein axonemal heavy chain 12	-1.07	4.1E-04	4.5E-02
LOC100513119	cyclin-dependent kinase 20-like	-1.49	4.5E-04	4.9E-02
SYT9	synaptotagmin 9	0.91	4.5E-04	4.9E-02
CACNA1G	calcium voltage-gated channel subunit alpha1 G	0.65	4.8E-04	5.1E-02
CDR2L	cerebellar degeneration related protein 2 like	0.65	4.8E-04	5.1E-02
HS3ST5	heparan sulfate-glucosamine 3-sulfotransferase 5	1.00	4.8E-04	5.1E-02
KITLG	KIT ligand	0.69	4.8E-04	5.1E-02
MGP	matrix Gla protein	1.09	5.1E-04	5.3E-02
PAQR6	progestin and adipoQ receptor family member 6	0.71	5.2E-04	5.4E-02
MAP3K19	mitogen-activated protein kinase kinase kinase 19	-0.78	5.4E-04	5.6E-02
VWDE	von Willebrand factor D and EGF domains	1.38	5.5E-04	5.6E-02
HYDIN	HYDIN, axonemal central pair apparatus protein	-0.73	5.7E-04	5.7E-02
MOBP	myelin-associated oligodendrocytic basic protein	0.76	5.7E-04	5.7E-02
SLC24A3	solute carrier family 24 member 3	0.70	6.6E-04	6.7E-02
COL2A1	collagen type II alpha 1 chain	1.37	6.9E-04	6.9E-02
CBX3	chromobox 3	-0.64	7.0E-04	7.0E-02
QPCT	glutaminyl-peptide cyclotransferase	0.84	7.4E-04	7.3E-02
ESYT1	extended synaptotagmin 1	0.81	7.4E-04	7.3E-02
ALPL	alkaline phosphatase, biomineralization associated	0.63	7.5E-04	7.3E-02
WFDC1	WAP four-disulfide core domain 1	0.78	7.7E-04	7.4E-02
APOLD1	apolipoprotein L domain containing 1	0.71	8.0E-04	7.7E-02
IFITM5	interferon induced transmembrane protein 5	-0.63	8.7E-04	8.3E-02
LEPR	leptin receptor	0.62	8.8E-04	8.4E-02
SPATA18	spermatogenesis associated 18	-0.70	9.1E-04	8.6E-02
LOC100523789	NKG2-A/NKG2-B type II integral membrane protein	-1.43	9.2E-04	8.6E-02
CYP2A19	cytochrome P450 2A19	-1.12	9.4E-04	8.8E-02
RASD1	ras related dexamethasone induced 1	0.91	9.9E-04	9.2E-02
CAMK2N2	calcium/calmodulin dependent protein kinase II inhibitor 2	0.63	1.0E-03	9.6E-02

[a]Log2(fold change) between Ma and Fe pigs.

[b]False Discovery rate adjusted P-value.

Table 2.17. Extended list of enriched clusters and supporting functional categories among genes differentially expressed between sexes, and representative categories identified using DAVID.

[a]Category	GO Identifier	GO name	[b]Count	P-value	[c]FDR P-value
Cluster 1 (ES: 1.82)					
BP	GO:0001503	ossification	7	4.6E-03	5.7E-01
BP	GO:0001501	skeletal system development	7	2.4E-02	6.3E-01
MF	GO:0005201	extracellular matrix structural constituent	3	3.0E-02	7.9E-01
Cluster 2 (ES: 1.74)					
KEGG	ssc04080	Neuroactive ligand-receptor interaction	11	2.7E-06	2.4E-04
BP	GO:0009719	response to endogenous stimulus	17	5.2E-05	9.9E-02
BP	GO:0010243	response to organonitrogen compound	9	1.5E-03	6.4E-01
BP	GO:0010033	response to organic substance	21	2.2E-03	4.3E-01
BP	GO:0009725	response to hormone	9	3.4E-03	5.0E-01
BP	GO:1901698	response to nitrogen compound	9	8.2E-03	5.3E-01
BP	GO:0071495	cellular response to endogenous stimulus	11	1.2E-02	5.4E-01
BP	GO:0032870	cellular response to hormone stimulus	7	1.8E-02	5.5E-01
BP	GO:0071375	cellular response to peptide hormone stimulus	4	5.2E-02	7.4E-01
BP	GO:1901653	cellular response to peptide	4	5.4E-02	7.5E-01
BP	GO:0071310	cellular response to organic substance	14	6.3E-02	7.5E-01
BP	GO:0071417	cellular response to organonitrogen compound	5	6.3E-02	7.5E-01
BP	GO:0043434	response to peptide hormone	4	8.2E-02	7.7E-01
BP	GO:1901652	response to peptide	4	1.1E-01	7.9E-01
BP	GO:1901699	cellular response to nitrogen compound	5	1.1E-01	7.9E-01
BP	GO:1901700	response to oxygen-containing compound	8	1.9E-01	8.7E-01
BP	GO:0070887	cellular response to chemical stimulus	14	2.2E-01	8.9E-01
BP	GO:1901701	cellular response to oxygen-containing compound	4	6.1E-01	9.9E-01
BP	GO:0007186	G-protein coupled receptor signaling pathway	6	9.2E-01	1.0E+00
Cluster 3 (ES: 1.74)					
BP	GO:0048732	gland development	8	1.7E-03	5.7E-01
BP	GO:0061180	mammary gland epithelium development	3	3.7E-02	6.7E-01

Table 2.17 (cont.)

BP	GO:0030879	mammary gland development	3	1.0E-01	7.9E-01
Cluster 4 (ES: 1.45)					
BP	GO:0040008	regulation of growth	9	3.4E-03	5.0E-01
BP	GO:0048639	positive regulation of developmental growth	5	5.7E-03	5.6E-01
BP	GO:0040007	growth	11	6.1E-03	5.4E-01
BP	GO:0048638	regulation of developmental growth	6	1.2E-02	5.4E-01
BP	GO:0040018	positive regulation of multicellular organism growth	3	1.4E-02	5.3E-01
BP	GO:0048589	developmental growth	8	1.7E-02	5.6E-01
BP	GO:0045927	positive regulation of growth	5	1.8E-02	5.6E-01
BP	GO:0035264	multicellular organism growth	4	2.9E-02	6.3E-01
BP	GO:0040014	regulation of multicellular organism growth	3	5.2E-02	7.5E-01
BP	GO:0060322	head development	7	5.6E-02	7.4E-01
BP	GO:0007420	brain development	6	1.1E-01	7.9E-01
BP	GO:0030900	forebrain development	4	1.9E-01	8.7E-01
BP	GO:0051174	regulation of phosphorus metabolic process	7	7.7E-01	1.0E+00
BP	GO:0019220	regulation of phosphate metabolic process	7	7.7E-01	1.0E+00
Cluster 5 (ES: 1.41)					
MF	GO:0005344	oxygen transporter activity	3	2.5E-03	2.2E-01
MF	GO:0019825	oxygen binding	3	4.5E-03	2.9E-01
MF	GO:0020037	heme binding	4	6.2E-02	9.1E-01
MF	GO:0046906	tetrapyrrole binding	4	6.9E-02	8.8E-01
MF	GO:0005506	iron ion binding	4	9.3E-02	9.3E-01
MF	GO:0046914	transition metal ion binding	8	7.4E-01	1.0E+00
Cluster 6 (ES: 1.35)					
BP	GO:0048568	embryonic organ development	8	5.0E-03	5.4E-01
BP	GO:0009790	embryo development	12	5.8E-03	5.4E-01
BP	GO:0048598	embryonic morphogenesis	9	7.2E-03	5.5E-01
BP	GO:0035107	appendage morphogenesis	5	7.9E-03	5.5E-01
BP	GO:0035108	limb morphogenesis	5	7.9E-03	5.5E-01
BP	GO:0090596	sensory organ morphogenesis	6	8.9E-03	5.1E-01

Table 2.17 (cont.)

BP	GO:0009887	organ morphogenesis	11	1.3E-02	5.4E-01
BP	GO:0060173	limb development	5	1.3E-02	5.3E-01
BP	GO:0048736	appendage development	5	1.3E-02	5.3E-01
BP	GO:0001501	skeletal system development	7	2.4E-02	6.3E-01
BP	GO:0042471	ear morphogenesis	4	2.5E-02	6.2E-01
BP	GO:0030326	embryonic limb morphogenesis	4	2.8E-02	6.4E-01
BP	GO:0035113	embryonic appendage morphogenesis	4	2.8E-02	6.4E-01
BP	GO:0060348	bone development	4	5.1E-02	7.5E-01
BP	GO:0051216	cartilage development	4	5.5E-02	7.5E-01
BP	GO:0007389	pattern specification process	6	5.7E-02	7.4E-01
BP	GO:0048562	embryonic organ morphogenesis	5	6.5E-02	7.5E-01
BP	GO:0060349	bone morphogenesis	3	6.6E-02	7.5E-01
BP	GO:0043583	ear development	4	8.6E-02	7.8E-01
BP	GO:0007423	sensory organ development	6	8.7E-02	7.7E-01
BP	GO:0042472	inner ear morphogenesis	3	8.8E-02	7.8E-01
BP	GO:0003002	regionalization	5	9.1E-02	7.8E-01
BP	GO:0061448	connective tissue development	4	9.5E-02	7.9E-01
BP	GO:0048705	skeletal system morphogenesis	4	1.1E-01	7.9E-01
BP	GO:0048839	inner ear development	3	2.2E-01	8.9E-01
BP	GO:0043010	camera-type eye development	3	3.5E-01	9.5E-01
BP	GO:0001654	eye development	3	4.2E-01	9.7E-01
BP	GO:0071363	cellular response to growth factor stimulus	3	6.7E-01	1.0E+00
BP	GO:0070848	response to growth factor	3	6.8E-01	1.0E+00
Cluster 7 (ES: 1.09)					
BP	GO:0048646	anatomical structure formation involved in morphogenesis	14	2.1E-03	4.6E-01
BP	GO:0048568	embryonic organ development	8	5.0E-03	5.4E-01
BP	GO:0009790	embryo development	12	5.8E-03	5.4E-01
BP	GO:0060706	cell differentiation involved in embryonic placenta development	3	9.4E-03	5.0E-01
BP	GO:0022414	reproductive process	12	1.4E-02	5.3E-01

Table 2.17 (cont.)

BP	GO:0000003	reproduction	12	1.5E-02	5.3E-01
BP	GO:0044702	single organism reproductive process	10	5.3E-02	7.5E-01
BP	GO:0001892	embryonic placenta development	3	7.7E-02	7.6E-01
BP	GO:0003006	developmental process involved in reproduction	7	8.5E-02	7.8E-01
BP	GO:0048608	reproductive structure development	5	1.2E-01	8.0E-01
BP	GO:0061458	reproductive system development	5	1.2E-01	8.0E-01
BP	GO:0001890	placenta development	3	1.6E-01	8.4E-01
BP	GO:0001701	in utero embryonic development	4	2.5E-01	9.1E-01
BP	GO:0019953	sexual reproduction	5	3.2E-01	9.4E-01
BP	GO:0043009	chordate embryonic development	5	3.5E-01	9.5E-01
BP	GO:0009792	embryo development ending in birth or egg hatching	5	3.5E-01	9.5E-01
BP	GO:0044703	multi-organism reproductive process	5	4.1E-01	9.7E-01
BP	GO:0007276	gamete generation	3	6.6E-01	1.0E+00
BP	GO:0048609	multicellular organismal reproductive process	3	7.5E-01	1.0E+00
BP	GO:0032504	multicellular organism reproduction	3	7.5E-01	1.0E+00
Cluster 8 (ES: 1.09)					
BP	GO:0001822	kidney development	5	3.2E-02	6.4E-01
BP	GO:0072073	kidney epithelium development	4	3.7E-02	6.7E-01
BP	GO:0072001	renal system development	5	4.0E-02	6.8E-01
BP	GO:0001655	urogenital system development	5	6.2E-02	7.5E-01
BP	GO:0001656	metanephros development	3	7.5E-02	7.6E-01
BP	GO:0060993	kidney morphogenesis	3	8.4E-02	7.8E-01
BP	GO:0001657	ureteric bud development	3	9.3E-02	7.9E-01
BP	GO:0072163	mesonephric epithelium development	3	9.6E-02	7.9E-01
BP	GO:0072164	mesonephric tubule development	3	9.6E-02	7.9E-01
BP	GO:0072009	nephron epithelium development	3	1.0E-01	7.9E-01
BP	GO:0001823	mesonephros development	3	1.1E-01	7.9E-01
BP	GO:0072006	nephron development	3	1.3E-01	8.2E-01
BP	GO:0035295	tube development	5	3.4E-01	9.5E-01
Cluster 9 (ES: 1.06)					

Table 2.17 (cont.)

BP	GO:0048468	cell development	22	1.3E-04	1.2E-01
BP	GO:0007399	nervous system development	19	1.8E-03	5.2E-01
BP	GO:0048639	positive regulation of developmental growth	5	5.7E-03	5.6E-01
BP	GO:0051962	positive regulation of nervous system development	7	6.9E-03	5.6E-01
BP	GO:0051094	positive regulation of developmental process	12	7.7E-03	5.6E-01
BP	GO:0045597	positive regulation of cell differentiation	10	8.0E-03	5.3E-01
BP	GO:0061564	axon development	7	1.1E-02	5.4E-01
BP	GO:0032989	cellular component morphogenesis	13	1.4E-02	5.3E-01
BP	GO:0000904	cell morphogenesis involved in differentiation	9	1.6E-02	5.5E-01
BP	GO:0045927	positive regulation of growth	5	1.8E-02	5.6E-01
BP	GO:0051240	positive regulation of multicellular organismal process	13	2.0E-02	5.9E-01
BP	GO:2000026	regulation of multicellular organismal development	14	2.9E-02	6.4E-01
BP	GO:0007409	axonogenesis	6	3.1E-02	6.4E-01
BP	GO:0051960	regulation of nervous system development	8	3.8E-02	6.7E-01
BP	GO:0010720	positive regulation of cell development	6	4.1E-02	6.8E-01
BP	GO:0050769	positive regulation of neurogenesis	5	5.1E-02	7.5E-01
BP	GO:0060322	head development	7	5.6E-02	7.4E-01
BP	GO:0048667	cell morphogenesis involved in neuron differentiation	6	6.0E-02	7.5E-01
BP	GO:0045595	regulation of cell differentiation	12	6.6E-02	7.5E-01
BP	GO:0060284	regulation of cell development	8	6.7E-02	7.5E-01
BP	GO:0048812	neuron projection morphogenesis	6	8.0E-02	7.7E-01
BP	GO:0000902	cell morphogenesis	10	9.9E-02	7.9E-01
BP	GO:0040012	regulation of locomotion	7	1.0E-01	7.9E-01
BP	GO:0051271	negative regulation of cellular component movement	4	1.0E-01	7.9E-01
BP	GO:0040013	negative regulation of locomotion	4	1.0E-01	7.9E-01
BP	GO:0051270	regulation of cellular component movement	7	1.1E-01	7.9E-01
BP	GO:0031175	neuron projection development	7	1.1E-01	7.9E-01
BP	GO:0048699	generation of neurons	10	1.2E-01	7.9E-01
BP	GO:0048858	cell projection morphogenesis	7	1.3E-01	8.2E-01

Table 2.17 (cont.)

BP	GO:0050767	regulation of neurogenesis	6	1.4E-01	8.2E-01
BP	GO:0032990	cell part morphogenesis	7	1.4E-01	8.3E-01
BP	GO:0022008	neurogenesis	10	1.6E-01	8.4E-01
BP	GO:2000145	regulation of cell motility	6	1.9E-01	8.7E-01
BP	GO:0002683	negative regulation of immune system process	4	2.1E-01	8.8E-01
BP	GO:0048666	neuron development	7	2.1E-01	8.9E-01
BP	GO:0050803	regulation of synapse structure or activity	3	2.2E-01	8.9E-01
BP	GO:2000146	negative regulation of cell motility	3	2.5E-01	9.1E-01
BP	GO:0032101	regulation of response to external stimulus	6	2.5E-01	9.1E-01
BP	GO:0030182	neuron differentiation	8	2.6E-01	9.1E-01
BP	GO:0045666	positive regulation of neuron differentiation	3	2.8E-01	9.3E-01
BP	GO:0030030	cell projection organization	8	2.9E-01	9.3E-01
BP	GO:0006928	movement of cell or subcellular component	10	3.2E-01	9.4E-01
BP	GO:0040011	locomotion	9	3.4E-01	9.5E-01
BP	GO:0030334	regulation of cell migration	5	3.4E-01	9.5E-01
BP	GO:0051674	localization of cell	8	3.5E-01	9.5E-01
BP	GO:0048870	cell motility	8	3.5E-01	9.5E-01
BP	GO:0009605	response to external stimulus	11	4.0E-01	9.6E-01
BP	GO:0002682	regulation of immune system process	7	4.2E-01	9.7E-01
BP	GO:0002684	positive regulation of immune system process	5	4.3E-01	9.7E-01
BP	GO:0050776	regulation of immune response	4	4.6E-01	9.7E-01
BP	GO:0006955	immune response	7	4.6E-01	9.7E-01
BP	GO:0016477	cell migration	6	5.8E-01	9.9E-01
BP	GO:0045664	regulation of neuron differentiation	3	6.4E-01	9.9E-01
BP	GO:0001817	regulation of cytokine production	3	6.9E-01	1.0E+00
BP	GO:0001816	cytokine production	3	7.3E-01	1.0E+00
Cluster 10 (ES: 1.05)					
BP	GO:0007267	cell-cell signaling	12	1.6E-02	5.6E-01
BP	GO:0099536	synaptic signaling	6	7.2E-02	7.6E-01
BP	GO:0099537	trans-synaptic signaling	6	7.2E-02	7.6E-01

Table 2.17 (cont.)

BP	GO:0098916	anterograde trans-synaptic signaling	6	7.2E-02	7.6E-01
BP	GO:0007268	chemical synaptic transmission	6	7.2E-02	7.6E-01
BP	GO:0050804	modulation of synaptic transmission	3	2.2E-01	8.9E-01
BP	GO:0006812	cation transport	5	4.6E-01	9.7E-01
Cluster 11 (ES: 1.01)					
BP	GO:0010243	response to organonitrogen compound	9	1.5E-03	6.4E-01
BP	GO:0051480	regulation of cytosolic calcium ion concentration	6	4.9E-03	5.6E-01
BP	GO:1901698	response to nitrogen compound	9	8.2E-03	5.3E-01
BP	GO:0044057	regulation of system process	7	8.6E-03	5.3E-01
BP	GO:0006874	cellular calcium ion homeostasis	6	2.2E-02	6.0E-01
BP	GO:0055074	calcium ion homeostasis	6	2.5E-02	6.2E-01
BP	GO:0072503	cellular divalent inorganic cation homeostasis	6	2.8E-02	6.4E-01
BP	GO:0072507	divalent inorganic cation homeostasis	6	3.4E-02	6.6E-01
BP	GO:0043279	response to alkaloid	3	3.5E-02	6.6E-01
BP	GO:0048878	chemical homeostasis	10	3.7E-02	6.7E-01
BP	GO:2000021	regulation of ion homeostasis	4	5.1E-02	7.5E-01
BP	GO:0014070	response to organic cyclic compound	7	5.3E-02	7.4E-01
BP	GO:0002027	regulation of heart rate	3	5.6E-02	7.4E-01
BP	GO:0006875	cellular metal ion homeostasis	6	5.7E-02	7.4E-01
BP	GO:1903522	regulation of blood circulation	4	6.8E-02	7.5E-01
BP	GO:0055082	cellular chemical homeostasis	7	7.2E-02	7.5E-01
BP	GO:0007204	positive regulation of cytosolic calcium ion concentration	4	7.8E-02	7.6E-01
BP	GO:0050801	ion homeostasis	7	8.0E-02	7.6E-01
BP	GO:0055065	metal ion homeostasis	6	8.6E-02	7.8E-01
BP	GO:0030003	cellular cation homeostasis	6	9.4E-02	7.8E-01
BP	GO:0042592	homeostatic process	12	9.9E-02	7.9E-01
BP	GO:0006873	cellular ion homeostasis	6	1.0E-01	7.9E-01
BP	GO:0019725	cellular homeostasis	7	1.3E-01	8.2E-01
BP	GO:0032844	regulation of homeostatic process	5	1.4E-01	8.2E-01

Table 2.17 (cont.)

BP	GO:0055080	cation homeostasis	6	1.4E-01	8.2E-01
BP	GO:0006816	calcium ion transport	4	1.5E-01	8.3E-01
BP	GO:0098771	inorganic ion homeostasis	6	1.5E-01	8.3E-01
BP	GO:0008016	regulation of heart contraction	3	1.5E-01	8.3E-01
BP	GO:0034220	ion transmembrane transport	6	1.7E-01	8.6E-01
BP	GO:0060047	heart contraction	3	1.7E-01	8.6E-01
BP	GO:0003015	heart process	3	1.8E-01	8.6E-01
BP	GO:0090257	regulation of muscle system process	3	1.9E-01	8.7E-01
BP	GO:0003012	muscle system process	4	1.9E-01	8.7E-01
BP	GO:0070838	divalent metal ion transport	4	1.9E-01	8.7E-01
BP	GO:0072511	divalent inorganic cation transport	4	1.9E-01	8.7E-01
BP	GO:0051924	regulation of calcium ion transport	3	1.9E-01	8.7E-01
BP	GO:0003008	system process	13	2.0E-01	8.8E-01
BP	GO:0008015	blood circulation	4	2.5E-01	9.1E-01
BP	GO:0032846	positive regulation of homeostatic process	3	2.5E-01	9.1E-01
BP	GO:0003013	circulatory system process	4	2.6E-01	9.1E-01
BP	GO:0006936	muscle contraction	3	3.5E-01	9.5E-01
BP	GO:0010959	regulation of metal ion transport	3	3.8E-01	9.6E-01
BP	GO:0006811	ion transport	7	4.0E-01	9.6E-01
BP	GO:0055085	transmembrane transport	6	4.1E-01	9.7E-01
BP	GO:0006812	cation transport	5	4.6E-01	9.7E-01
BP	GO:0043269	regulation of ion transport	3	5.4E-01	9.9E-01
BP	GO:0030001	metal ion transport	4	5.4E-01	9.9E-01
BP	GO:0098655	cation transmembrane transport	3	6.6E-01	1.0E+00

[a]BP: biological process; MF: molecular function; KEGG: KEGG pathway.

[b]Number of genes in the category.

[c]False Discovery Rate adjusted P-value.

Table 2.18. Extended list of enriched clusters and supporting functional categories among the genes in modules presenting a significant correlation with maternal immune activation (MPA) relative to control within males using DAVID.

[a]Category	GO Identifier	GO name	[b]Count	P-value	[c]FDR P-value
MODULE	**Grey60 (low expression in MPA)**				
Cluster 1 (ES: 14.5)					
KEGG	ssc00190	Oxidative phosphorylation	25	1.9E-21	2.6E-19
KEGG	ssc05010	Alzheimer's disease	25	1.3E-18	9.1E-17
KEGG	ssc05012	Parkinson's disease	23	9.8E-18	4.7E-16
KEGG	ssc04932	Non-alcoholic fatty liver disease (NAFLD)	22	6.1E-16	2.4E-14
KEGG	ssc05016	Huntington's disease	23	4.9E-15	1.4E-13
KEGG	ssc01100	Metabolic pathways	42	2.2E-10	5.2E-09
MF	GO:0015078	hydrogen ion transmembrane transporter activity	10	2.0E-07	1.6E-05
Cluster 2 (ES: 7.32)					
MF	GO:0016651	oxidoreductase activity, acting on NAD(P)H	12	3.6E-10	1.5E-07
MF	GO:0003954	NADH dehydrogenase activity	9	3.4E-09	6.8E-07
MF	GO:0016655	oxidoreductase activity, acting on NAD(P)H, quinone or similar compound as acceptor	8	1.4E-07	1.4E-05
MF	GO:0050136	NADH dehydrogenase (quinone) activity	7	1.2E-06	7.8E-05
MF	GO:0008137	NADH dehydrogenase (ubiquinone) activity	7	1.2E-06	7.8E-05
Cluster 3 (ES: 6.41)					
BP	GO:0042775	mitochondrial ATP synthesis coupled electron transport	10	4.0E-10	8.6E-07
BP	GO:0046034	ATP metabolic process	15	8.0E-10	8.7E-07
BP	GO:0042773	ATP synthesis coupled electron transport	10	1.1E-09	8.0E-07
BP	GO:0009205	purine ribonucleoside triphosphate metabolic process	15	4.0E-09	2.2E-06
BP	GO:0006119	oxidative phosphorylation	10	4.2E-09	1.8E-06
BP	GO:0009199	ribonucleoside triphosphate metabolic process	15	4.8E-09	1.7E-06
BP	GO:0009167	purine ribonucleoside monophosphate metabolic process	15	6.8E-09	2.1E-06
BP	GO:0009126	purine nucleoside monophosphate metabolic process	15	7.4E-09	2.0E-06

Table 2.18 (cont.)

BP	GO:0009144	purine nucleoside triphosphate metabolic process	15	7.4E-09	2.0E-06
MODULE	**Light yellow (low expression in MPA)**				
Cluster 1 (ES: 4.18)					
MF	GO:0003735	structural constituent of ribosome	12	1.9E-06	5.4E-04
KEGG	ssc03010	Ribosome	11	3.7E-06	5.9E-05
BP	GO:0006412	translation	18	9.5E-06	1.7E-02
BP	GO:0043043	peptide biosynthetic process	18	1.4E-05	1.2E-02
MF	GO:0005198	structural molecule activity	16	1.5E-05	2.1E-03
BP	GO:0043604	amide biosynthetic process	18	5.1E-05	2.9E-02
BP	GO:1901566	organonitrogen compound biosynthetic process	24	1.1E-04	4.5E-02
BP	GO:0006518	peptide metabolic process	18	1.2E-04	4.1E-02
BP	GO:0043603	cellular amide metabolic process	18	8.5E-04	1.0E-01
BP	GO:0034645	cellular macromolecule biosynthetic process	37	2.4E-01	9.7E-01
Cluster 2 (ES: 2.49)					
BP	GO:0007006	mitochondrial membrane organization	6	5.1E-04	7.8E-02
BP	GO:0042407	cristae formation	3	6.3E-03	2.8E-01
BP	GO:0007007	inner mitochondrial membrane organization	3	1.1E-02	3.5E-01
Cluster 3 (ES: 1.96)					
BP	GO:0022618	ribonucleoprotein complex assembly	10	1.2E-04	3.5E-02
BP	GO:0034622	cellular macromolecular complex assembly	19	1.4E-04	3.5E-02
BP	GO:0071826	ribonucleoprotein complex subunit organization	10	1.6E-04	3.5E-02
BP	GO:0022613	ribonucleoprotein complex biogenesis	12	1.3E-03	1.0E-01
BP	GO:0042255	ribosome assembly	5	2.4E-03	1.7E-01
BP	GO:0043933	macromolecular complex subunit organization	27	2.6E-03	1.7E-01
BP	GO:0033108	mitochondrial respiratory chain complex assembly	4	3.4E-03	1.8E-01

[a]BP: biological process; MF: molecular function; KEGG: KEGG pathway.

[b]Number of genes in the category.

[c]False Discovery Rate adjusted P-value.

Table 2.19. Extended list of enriched clusters and supporting functional categories among the genes in modules presenting a significant correlation with sex within the maternal immune activation treatments using DAVID.

[a]Category	GO Identifier	GO name	[b]Count	P-value	[c]FDR P-value
MODULE	**Sienna3 (low expression in Ma)**				
Cluster 1 (ES: 1.58)					
BP	GO:0044255	cellular lipid metabolic process	8	1.1E-02	1.0E+00
BP	GO:0008610	lipid biosynthetic process	6	1.3E-02	9.9E-01
BP	GO:0044283	small molecule biosynthetic process	5	3.3E-02	9.8E-01
BP	GO:0006629	lipid metabolic process	8	4.3E-02	9.6E-01
KEGG	ssc01100	Metabolic pathways	11	6.3E-02	7.3E-01
MODULE	**Ivory (high expression in Ma)**				
Cluster 1 (ES: 1.47)					
BP	GO:0007416	synapse assembly	3	8.1E-03	1.0E+00
BP	GO:0050808	synapse organization	3	2.5E-02	9.5E-01
BP	GO:0007399	nervous system development	7	2.7E-02	9.1E-01
BP	GO:0022607	cellular component assembly	7	7.1E-02	8.7E-01
BP	GO:0044085	cellular component biogenesis	7	1.1E-01	9.0E-01

[a]BP: biological process; MF: molecular function; KEGG: KEGG pathway.

[b]Number of genes in the category.

[c]False Discovery Rate adjusted P-value.

Figure 2.3. Clustering dendrogram of the gene modules identified by color for CON_Ma vs MPA_Ma.

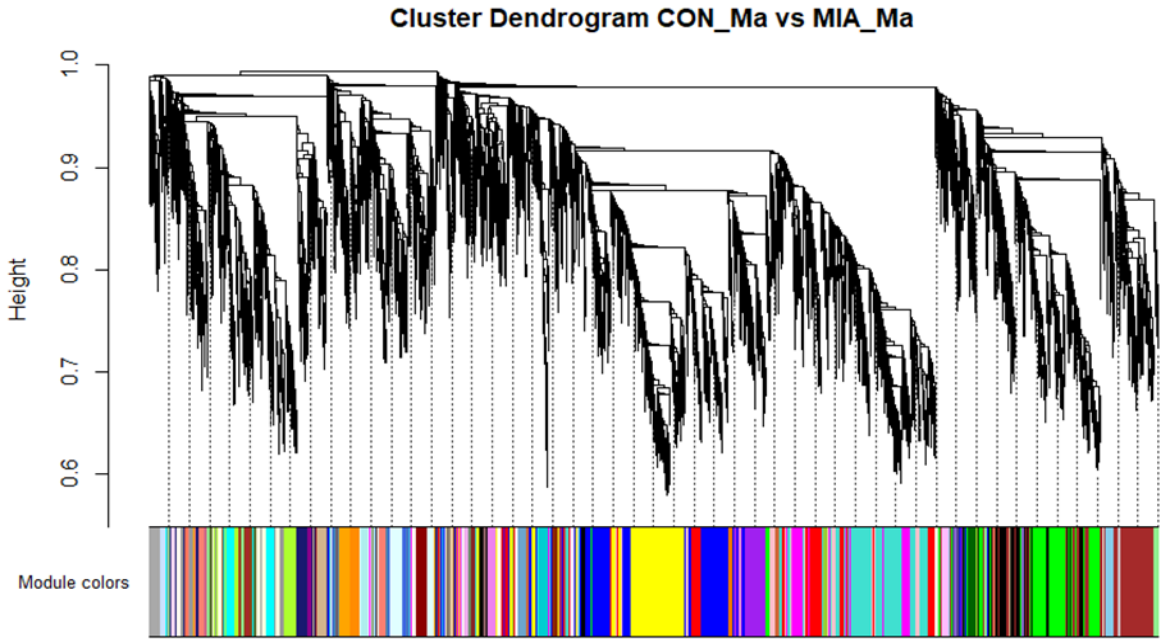

Figure 2.4. Heatmap of treatment correlations (upper cell value) and P-values (lower cell value) between traits (columns) and module eigenvalues (rows) for CON_Ma vs MPA_Ma (P-value < |0.1|). The color scale denotes the sign and strength of the correlation estimate from –1 (blue) to 1 (red).

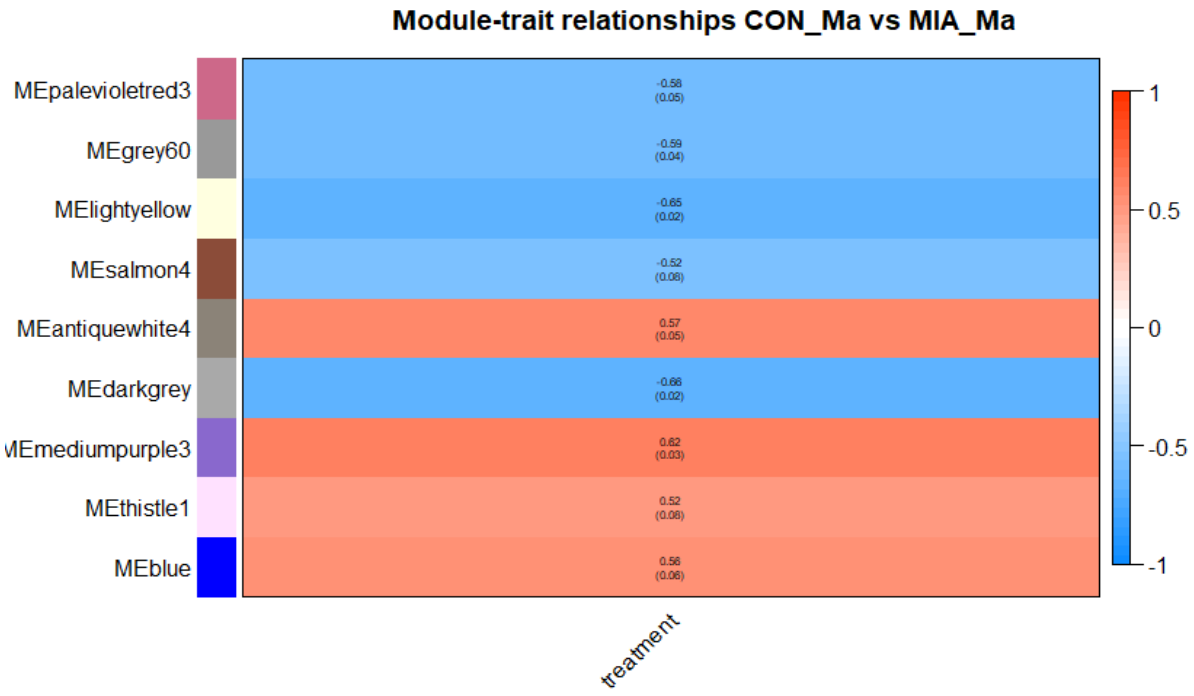

Figure 2.5. Clustering dendrogram of the gene modules identified by color for MPA_Fe vs MPA_Ma.

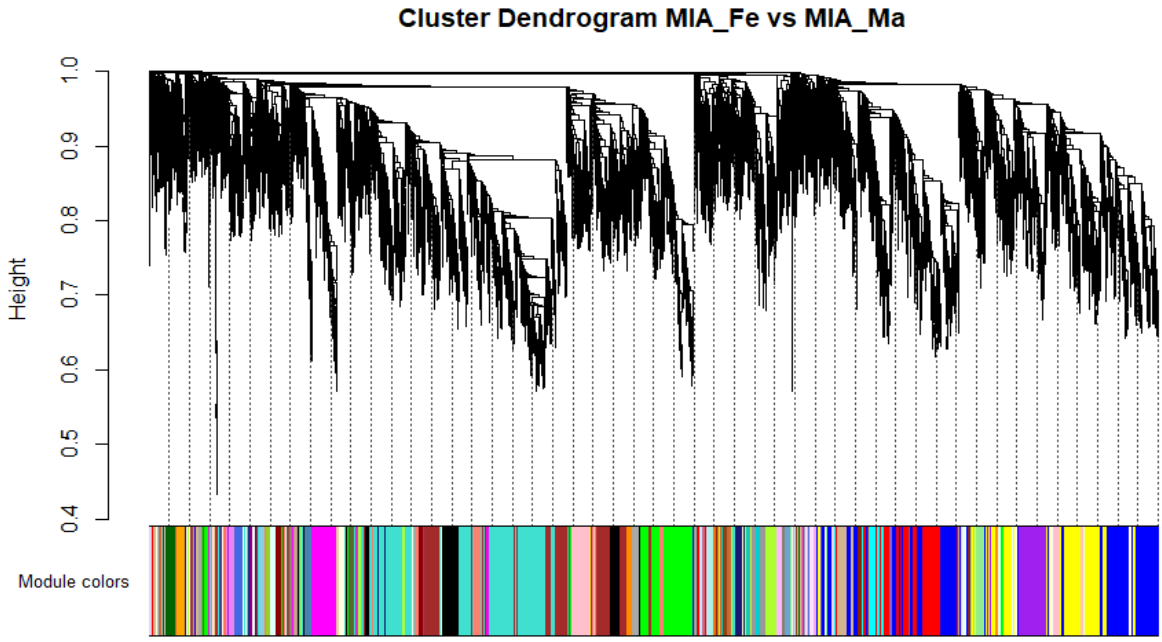

Figure 2.6. Heatmap of treatment correlations (upper cell value) and P-values (lower cell value) between traits (columns) and module eigenvalues (rows) for MPA_Fe vs MPA_Ma (P-value < |0.1|). The color scale denotes the sign and strength of the correlation estimate from –1 (blue) to 1 (red).

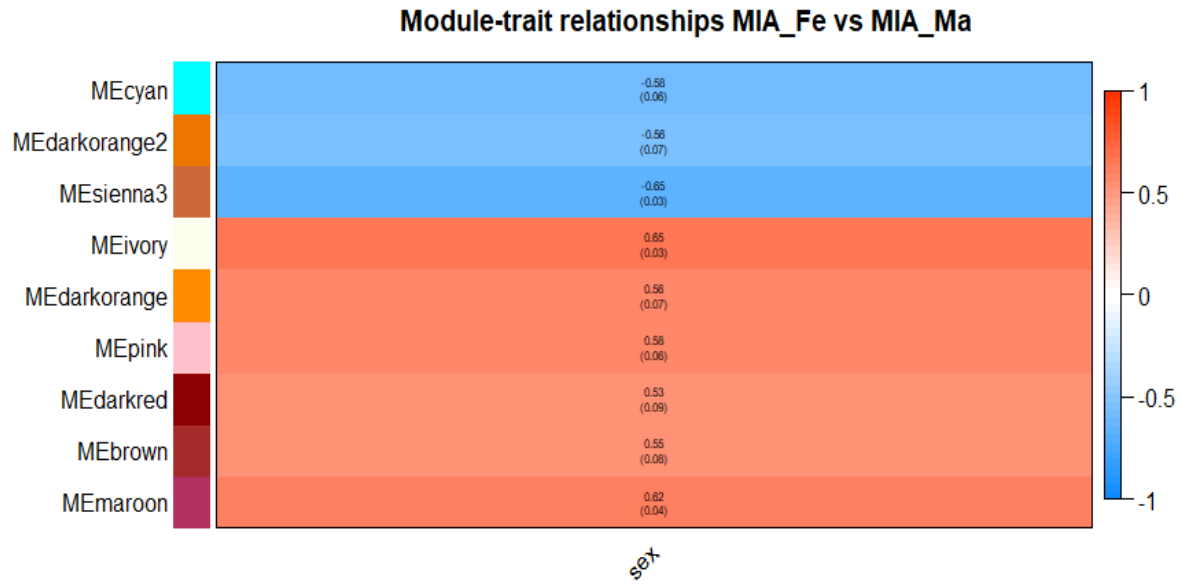

Appendix B: Supplemental Information for Chapter 3

Table 3.3. Extended list of enriched categories from GSEA among genes analyzed for the interaction and main effects of weaning stress, maternal immune activation, and sex (at least one model term significant at P-value < 0.05).

	MIA*Sex			Wean*MIA			Wean*Sex		
KEGG Pathway[a]	NES[b]	P-value	FDR P-valuec	NES	P-value	FDR P-value	NES	P-value	FDR P-value
ssc00020:Citrate cycle (TCA cycle)	-1.6	2.6E-02	2.4E-01	-1.33	1.4E-01	8.3E-01	-1.6	3.4E-02	3.5E-01
ssc00071:Fatty acid degradation	-1.63	1.8E-02	2.7E-01						
ssc00100:Steroid biosynthesis	-1.37	1.4E-01	4.5E-01						
ssc00140:Steroid hormone biosynthesis				1.59	4.1E-02	7.6E-02			
ssc00190:Oxidative phosphorylation	-2.29	0.0E+00	0.0E+00	-1.32	8.8E-02	7.3E-01	-1.92	3.0E-03	1.6E-01
ssc00220:Arginine biosynthesis ssc00270:Cysteine and methionine metabolism ssc00280:Valine, leucine and isoleucine degradation	-1.46	4.6E-02	3.8E-01						
ssc00310:Lysine degradation							1.45	2.7E-02	8.6E-01
ssc00350:Tyrosine metabolism	-1.6	2.7E-02	2.4E-01				-1.32	1.6E-01	5.0E-01
ssc00360:Phenylalanine metabolism	-1.7	2.0E-02	2.0E-01						
ssc00480:Glutathione metabolism	-1.83	4.6E-03	7.3E-02				-1.68	1.7E-02	3.2E-01
ssc00500:Starch and sucrose metabolism				1.49	4.1E-02	1.3E-01			
ssc00512:Mucin type O-glycan biosynthesis							-1.68	2.3E-02	3.0E-01
ssc00531:Glycosaminoglycan degradation				1.5	6.5E-02	1.2E-01			
ssc00565:Ether lipid metabolism									
ssc00590:Arachidonic acid metabolism	-1.63	1.8E-02	2.9E-01						
ssc00790:Folate biosynthesis	-1.63	3.0E-02	2.5E-01				-1.56	4.7E-02	4.1E-01
ssc00900:Terpenoid backbone biosynthesis				-1.32	1.3E-01	8.0E-01			
ssc00982:Drug metabolism	-1.56	3.3E-02	2.8E-01						

Table 3.3 (cont.)

ssc00983:Drug metabolism	-1.66	7.3E-03	2.5E-01				-1.45	6.5E-02	4.2E-01
ssc01100:Metabolic pathways	-1.49	0.0E+00	3.7E-01				-1.35	1.1E-03	4.6E-01
ssc01230:Biosynthesis of amino acids									
ssc03010:Ribosome	-2.45	0.0E+00	0.0E+00				-2.21	0.0E+00	7.4E-02
ssc03060:Protein export	-1.39	1.1E-01	4.3E-01				-1.54	4.9E-02	4.0E-01
ssc03320:PPAR signaling pathway				1.45	4.9E-02	1.6E-01			
ssc03410:Base excision repair									
ssc04060:Cytokine-cytokine receptor interaction	-1.39	5.4E-02	4.3E-01	1.4	5.5E-03	2.0E-01	-1.36	4.7E-02	4.4E-01
ssc04062:Chemokine signaling pathway									
ssc04064:NF-kappa B signaling pathway				1.32	8.9E-02	2.7E-01			
ssc04080:Neuroactive ligand-receptor interaction	-1.97	0.0E+00	1.0E-02	-1.53	6.1E-03	9.6E-01	-1.99	0.0E+00	1.3E-01
ssc04141:Protein processing in endoplasmic reticulum							-1.48	2.2E-02	4.1E-01
ssc04145:Phagosome	1.62	0.0E+00	4.9E-02	2.17	0.0E+00	2.8E-04			
ssc04146:Peroxisome	-1.55	1.9E-02	2.9E-01						
ssc04151:PI3K-Akt signaling pathway	-1.36	1.7E-02	4.3E-01						
ssc04260:Cardiac muscle contraction	-1.61	1.7E-02	2.4E-01	-1.41	7.3E-02	9.8E-01	-1.52	3.4E-02	3.6E-01
ssc04270:Vascular smooth muscle contraction							-1.42	4.7E-02	4.1E-01
ssc04310:Wnt signaling pathway	-1.43	3.0E-02	4.0E-01				-1.36	6.3E-02	4.5E-01
ssc04360:Axon guidance				-1.32	6.2E-02	7.4E-01	-1.4	4.6E-02	4.1E-01
ssc04514:Cell adhesion molecules (CAMs)	1.37	2.7E-02	2.0E-01	1.88	0.0E+00	6.7E-03			
ssc04530:Tight junction	-1.43	2.6E-02	4.2E-01						
ssc04610:Complement and coagulation cascades				1.74	5.0E-03	2.7E-02			
ssc04612:Antigen processing and presentation	2.54	0.0E+00	0.0E+00	2.59	0.0E+00	0.0E+00			
ssc04621:NOD-like receptor signaling pathway				1.6	0.0E+00	7.7E-02			
ssc04622:RIG-I-like receptor signaling pathway	1.74	3.1E-03	2.2E-02	1.64	1.6E-02	5.6E-02			

Table 3.3 (cont.)

ssc04623:Cytosolic DNA-sensing pathway	1.37	7.4E-02	2.1E-01	2.06	0.0E+00	5.2E-04			
ssc04630:JAK-STAT signaling pathway	-1.31	1.2E-01	4.5E-01				-1.53	3.1E-02	3.9E-01
ssc04640:Hematopoietic cell lineage	1.49	6.7E-03	1.1E-01	2.06	0.0E+00	5.5E-04			
ssc04650:Natural killer cell mediated cytotoxicity				1.38	4.7E-02	2.2E-01			
ssc04657:IL-17 signaling pathway				1.44	3.7E-02	1.6E-01			
ssc04658:Th1 and Th2 cell differentiation	1.72	0.0E+00	2.4E-02	2.11	0.0E+00	2.4E-04			
ssc04659:Th17 cell differentiation	1.65	7.9E-03	3.9E-02	2.03	0.0E+00	9.3E-04			
ssc04662:B cell receptor signaling pathway									
ssc04664:Fc epsilon RI signaling pathway									
ssc04666:Fc gamma R-mediated phagocytosis									
ssc04668:TNF signaling pathway				1.58	2.7E-03	7.9E-02			
ssc04670:Leukocyte transendothelial migration	-1.33	8.4E-02	4.6E-01						
ssc04672:Intestinal immune network for IgA production	1.79	8.4E-03	1.4E-02	2.14	0.0E+00	2.6E-04			
ssc04714:Thermogenesis	-1.76	0.0E+00	1.2E-01	-1.45	2.3E-02	9.2E-01	-1.67	6.9E-03	2.9E-01
ssc04720:Long-term potentiation							-1.35	9.5E-02	4.5E-01
ssc04723:Retrograde endocannabinoid signaling	-1.41	3.6E-02	4.2E-01	-1.64	4.6E-03	9.3E-01	-1.73	2.9E-03	2.6E-01
ssc04726:Serotonergic synapse									
ssc04728:Dopaminergic synapse							-1.46	4.1E-02	4.4E-01
ssc04730:Long-term depression				-1.51	4.9E-02	8.0E-01			
ssc04740:Olfactory transduction	1.51	1.6E-02	9.4E-02						
ssc04744:Phototransduction							1.34	1.4E-01	9.0E-01
ssc04912:GnRH signaling pathway	-1.37	6.1E-02	4.3E-01				-1.78	1.3E-02	2.2E-01
ssc04913:Ovarian steroidogenesis	-1.54	4.3E-02	3.0E-01				-1.82	8.9E-03	2.0E-01
ssc04916:Melanogenesis	-1.54	2.3E-02	2.9E-01	-1.31	1.0E-01	6.9E-01	-1.56	3.1E-02	3.9E-01
ssc04917:Prolactin signaling pathway	-1.59	1.0E-02	2.4E-01				-2.05	6.6E-03	2.1E-01
ssc04918:Thyroid hormone synthesis	-1.49	3.1E-02	3.6E-01				-1.64	1.7E-02	3.0E-01

Table 3.3 (cont.)

ssc04920:Adipocytokine signaling pathway	-1.37	7.9E-02	4.4E-01				-1.64	2.1E-02	3.1E-01
ssc04921:Oxytocin signaling pathway				-1.36	6.3E-02	9.6E-01			
ssc04923:Regulation of lipolysis in adipocytes	-1.62	2.4E-02	2.6E-01				-1.92	6.8E-03	1.4E-01
ssc04927:Cortisol synthesis and secretion							-1.44	4.4E-02	4.2E-01
ssc04932:Non-alcoholic fatty liver disease (NAFLD)	-2.11	0.0E+00	1.4E-03	-1.61	6.3E-03	8.4E-01	-2.01	0.0E+00	1.8E-01
ssc04934:Cushing syndrome	-1.39	4.3E-02	4.2E-01	-1.33	7.7E-02	8.7E-01	-1.43	3.8E-02	4.1E-01
ssc04940:Type I diabetes mellitus	2.44	0.0E+00	0.0E+00	2.4	0.0E+00	0.0E+00			
ssc04950:Maturity onset diabetes of the young	-1.46	8.3E-02	4.0E-01						
ssc04961:Endocrine and other factor-regulated calcium reabsorption	-1.33	1.1E-01	4.5E-01				-1.52	3.1E-02	3.7E-01
ssc05010:Alzheimer disease	-2	0.0E+00	8.0E-03	-1.35	5.4E-02	9.4E-01	-1.92	1.5E-03	1.3E-01
ssc05012:Parkinson disease	-2.15	0.0E+00	1.1E-03	-1.46	3.6E-02	9.4E-01	-2	0.0E+00	1.4E-01
ssc05016:Huntington disease	-1.37	4.4E-02	4.3E-01						
ssc05020:Prion diseases				1.52	4.7E-02	1.1E-01			
ssc05030:Cocaine addiction	-1.46	4.5E-02	3.9E-01				-1.46	6.3E-02	4.2E-01
ssc05033:Nicotine addiction				-1.53	3.3E-02	8.2E-01	-1.49	6.0E-02	4.1E-01
ssc05034:Alcoholism	-1.35	7.1E-02	4.4E-01				-1.43	4.6E-02	4.4E-01
ssc05133:Pertussis				1.45	4.4E-02	1.6E-01	1.43	2.4E-02	7.7E-01
ssc05140:Leishmaniasis	1.84	0.0E+00	9.9E-03	1.93	0.0E+00	3.2E-03			
ssc05142:Chagas disease (American trypanosomiasis)									
ssc05143:African trypanosomiasis	-1.62	2.6E-02	2.4E-01	1.48	5.0E-02	1.3E-01	-1.54	5.2E-02	3.8E-01
ssc05145:Toxoplasmosis	1.66	4.0E-03	3.8E-02	1.68	0.0E+00	4.2E-02			
ssc05146:Amoebiasis									
ssc05150:Staphylococcus aureus infection	2.13	0.0E+00	1.6E-04	2.46	0.0E+00	0.0E+00			
ssc05152:Tuberculosis	1.44	8.4E-03	1.4E-01	1.74	2.8E-03	2.7E-02			
ssc05160:Hepatitis C				1.54	5.3E-03	9.6E-02			
ssc05162:Measles				1.69	0.0E+00	4.1E-02			

Table 3.3 (cont.)

ssc05163:Human cytomegalovirus infection				1.32	2.7E-02	2.6E-01			
ssc05164:Influenza A	1.98	0.0E+00	2.9E-03	2.08	0.0E+00	2.8E-04			
ssc05166:Human T-cell leukemia virus 1 infection				1.59	0.0E+00	7.7E-02			
ssc05168:Herpes simplex infection	2.05	0.0E+00	1.5E-03	2.21	0.0E+00	2.0E-04			
ssc05169:Epstein-Barr virus infection	1.6	0.0E+00	5.4E-02	2.09	0.0E+00	2.2E-04			
ssc05170:Human immunodeficiency virus 1 infection				1.34	2.6E-02	2.5E-01			
ssc05200:Pathways in cancer									
ssc05217:Basal cell carcinoma	-1.5	3.9E-02	3.7E-01						
ssc05310:Asthma	1.88	2.4E-03	7.6E-03	2.22	0.0E+00	2.5E-04			
ssc05320:Autoimmune thyroid disease	1.61	1.5E-02	5.1E-02	2.43	0.0E+00	0.0E+00	-1.54	5.2E-02	4.2E-01
ssc05321:Inflammatory bowel disease (IBD)	2.03	0.0E+00	1.5E-03	2	0.0E+00	1.7E-03			
ssc05322:Systemic lupus erythematosus	1.87	0.0E+00	8.1E-03	2.35	0.0E+00	0.0E+00			
ssc05323:Rheumatoid arthritis	1.59	1.0E-02	5.5E-02	2.21	0.0E+00	2.2E-04			
ssc05330:Allograft rejection	2.14	0.0E+00	2.0E-04	2.44	0.0E+00	0.0E+00			
ssc05332:Graft-versus-host disease	2.32	0.0E+00	0.0E+00	2.39	0.0E+00	0.0E+00			
ssc05340:Primary immunodeficiency				1.58	2.8E-02	7.7E-02			
ssc05414:Dilated cardiomyopathy (DCM)									
ssc05416:Viral myocarditis	1.96	0.0E+00	3.1E-03	2.42	0.0E+00	0.0E+00			
ssc05418:Fluid shear stress and atherosclerosis	-1.43	2.9E-02	4.2E-01				-1.41	4.3E-02	4.0E-01

Table 3.3 (cont.)

	Sex			Wean			MIA		
KEGG Pathway[a]	NES	P-value	FDR P-value	NES	P-value	FDR P-value	NES	P-value	FDR P-value
ssc00020:Citrate cycle (TCA cycle)	1.61	5.9E-02	9.5E-01						
ssc00071:Fatty acid degradation							-1.34	1.2E-01	4.5E-01
ssc00100:Steroid biosynthesis				-1.79	5.8E-03	4.4E-02			
ssc00140:Steroid hormone biosynthesis							1.65	1.3E-02	5.7E-01
ssc00190:Oxidative phosphorylation	1.48	7.2E-02	6.6E-01				-1.34	6.7E-02	4.5E-01
ssc00220:Arginine biosynthesis				-1.75	6.4E-03	3.8E-02			
ssc00270:Cysteine and methionine metabolism				1.55	3.8E-02	7.7E-01			
ssc00280:Valine, leucine and isoleucine degradation									
ssc00310:Lysine degradation									
ssc00350:Tyrosine metabolism	1.31	1.6E-01	7.2E-01						
ssc00360:Phenylalanine metabolism	1.46	9.2E-02	6.7E-01						
ssc00480:Glutathione metabolism	1.37	1.1E-01	7.1E-01						
ssc00500:Starch and sucrose metabolism									
ssc00512:Mucin type O-glycan biosynthesis				1.46	6.9E-02	7.3E-01			
ssc00531:Glycosaminoglycan degradation									
ssc00565:Ether lipid metabolism				-1.56	1.6E-02	1.2E-01			
ssc00590:Arachidonic acid metabolism							-1.56	3.3E-02	2.1E-01
ssc00790:Folate biosynthesis	1.34	1.6E-01	7.4E-01						
ssc00900:Terpenoid backbone biosynthesis				-1.62	1.2E-02	8.8E-02			
ssc00982:Drug metabolism									
ssc00983:Drug metabolism									
ssc01100:Metabolic pathways									
ssc01230:Biosynthesis of amino acids				-1.44	2.3E-02	2.1E-01			
ssc03010:Ribosome	1.37	1.2E-01	7.0E-01	2.2	0.0E+00	5.4E-02	-1.95	1.6E-03	7.8E-02
ssc03060:Protein export	1.39	1.4E-01	7.0E-01						
ssc03320:PPAR signaling pathway									
ssc03410:Base excision repair				-1.5	3.2E-02	1.5E-01			
ssc04060:Cytokine-cytokine receptor interaction	1.6	3.4E-02	7.3E-01				-1.54	2.2E-02	2.4E-01

Table 3.3 (cont.)

ssc04062:Chemokine signaling pathway							-1.57	1.2E-02	2.2E-01
ssc04064:NF-kappa B signaling pathway							-1.71	1.7E-03	1.2E-01
ssc04080:Neuroactive ligand-receptor interaction				1.47	1.1E-02	7.9E-01	-1.38	4.5E-02	4.0E-01
ssc04141:Protein processing in endoplasmic reticulum	1.34	1.3E-01	7.3E-01						
ssc04145:Phagosome				-1.42	1.7E-02	2.3E-01	-1.89	1.5E-03	7.0E-02
ssc04146:Peroxisome									
ssc04151:PI3K-Akt signaling pathway	1.6	1.1E-02	7.7E-01				-1.32	4.0E-02	4.9E-01
ssc04260:Cardiac muscle contraction									
ssc04270:Vascular smooth muscle contraction									
ssc04310:Wnt signaling pathway	1.53	5.2E-02	6.7E-01	1.31	9.4E-02	5.2E-01			
ssc04360:Axon guidance	1.38	8.4E-02	7.1E-01						
ssc04514:Cell adhesion molecules (CAMs)				-1.54	6.4E-03	1.3E-01	-1.83	1.6E-03	9.3E-02
ssc04530:Tight junction									
ssc04610:Complement and coagulation cascades									
ssc04612:Antigen processing and presentation	-1.73	6.2E-03	1.5E-01	-2.18	0.0E+00	0.0E+00	-1.64	1.8E-02	1.6E-01
ssc04621:NOD-like receptor signaling pathway				-1.35	2.8E-02	3.2E-01	-1.47	3.0E-02	2.9E-01
ssc04622:RIG-I-like receptor signaling pathway									
ssc04623:Cytosolic DNA-sensing pathway				-1.59	2.0E-02	1.1E-01			
ssc04630:JAK-STAT signaling pathway	1.62	5.0E-02	9.7E-01						
ssc04640:Hematopoietic cell lineage				-1.62	5.9E-03	8.4E-02	-1.99	0.0E+00	8.1E-02
ssc04650:Natural killer cell mediated cytotoxicity							-1.59	1.8E-02	2.0E-01
ssc04657:IL-17 signaling pathway									
ssc04658:Th1 and Th2 cell differentiation				-1.58	1.0E-02	1.0E-01	-1.5	3.7E-02	2.7E-01
ssc04659:Th17 cell differentiation				-1.52	1.4E-02	1.4E-01	-1.46	4.1E-02	2.9E-01
ssc04662:B cell receptor signaling pathway							-1.79	1.1E-02	9.2E-02
ssc04664:Fc epsilon RI signaling pathway							-1.83	5.0E-03	7.9E-02
ssc04666:Fc gamma R-mediated phagocytosis							-1.72	4.8E-03	1.1E-01
ssc04668:TNF signaling pathway									
ssc04670:Leukocyte transendothelial migration	1.42	7.5E-02	6.7E-01				-1.53	3.4E-02	2.4E-01
ssc04672:Intestinal immune network for IgA production				-1.77	4.0E-03	3.7E-02	-1.79	7.3E-03	9.6E-02

Table 3.3 (cont.)

ssc04714:Thermogenesis									
ssc04720:Long-term potentiation				1.51	3.7E-02	7.4E-01			
ssc04723:Retrograde endocannabinoid signaling				1.64	9.0E-03	6.3E-01			
ssc04726:Serotonergic synapse				1.39	4.4E-02	6.8E-01			
ssc04728:Dopaminergic synapse									
ssc04730:Long-term depression									
ssc04740:Olfactory transduction	-1.61	1.2E-02	1.0E-01				1.51	1.5E-02	9.1E-01
ssc04744:Phototransduction	-1.7	1.6E-02	7.0E-02	-1.42	9.4E-02	2.2E-01			
ssc04912:GnRH signaling pathway									
ssc04913:Ovarian steroidogenesis	1.9	2.3E-02	8.8E-01						
ssc04916:Melanogenesis									
ssc04917:Prolactin signaling pathway	1.96	1.5E-03	7.7E-01						
ssc04918:Thyroid hormone synthesis				1.34	9.5E-02	5.6E-01			
ssc04920:Adipocytokine signaling pathway	1.45	9.4E-02	6.5E-01						
ssc04921:Oxytocin signaling pathway				1.42	4.2E-02	7.3E-01			
ssc04923:Regulation of lipolysis in adipocytes				1.64	2.4E-02	7.6E-01			
ssc04927:Cortisol synthesis and secretion	1.49	7.3E-02	6.9E-01						
ssc04932:Non-alcoholic fatty liver disease (NAFLD)	1.49	6.2E-02	6.8E-01				-1.76	4.7E-03	9.7E-02
ssc04934:Cushing syndrome	1.59	3.3E-02	7.0E-01						
ssc04940:Type I diabetes mellitus	-1.72	5.0E-03	8.5E-02	-2.14	0.0E+00	2.3E-04	-1.7	1.4E-02	1.2E-01
ssc04950:Maturity onset diabetes of the young							-1.65	1.8E-02	1.6E-01
ssc04961:Endocrine and other factor-regulated calcium reabsorption	1.45	1.0E-01	6.6E-01						
ssc05010:Alzheimer disease									
ssc05012:Parkinson disease	1.55	5.0E-02	7.0E-01				-1.43	4.3E-02	3.5E-01
ssc05016:Huntington disease				-1.49	4.3E-03	1.5E-01			
ssc05020:Prion diseases									
ssc05030:Cocaine addiction	1.31	1.5E-01	7.0E-01						
ssc05033:Nicotine addiction	1.31	1.7E-01	7.4E-01						
ssc05034:Alcoholism									

Table 3.3 (cont.)

ssc05133:Pertussis							-1.4	5.7E-02	3.8E-01
ssc05140:Leishmaniasis							-1.91	0.0E+00	9.0E-02
ssc05142:Chagas disease (American trypanosomiasis)							-1.49	2.7E-02	2.8E-01
ssc05143:African trypanosomiasis	1.61	5.8E-02	8.4E-01	1.55	4.6E-02	8.9E-01	-1.57	2.9E-02	2.2E-01
ssc05145:Toxoplasmosis				-1.32	7.4E-02	3.6E-01	-1.46	3.0E-02	3.0E-01
ssc05146:Amoebiasis	1.61	4.3E-02	7.8E-01				-1.56	2.3E-02	2.1E-01
ssc05150:Staphylococcus aureus infection				-1.76	6.1E-03	3.8E-02	-1.99	0.0E+00	1.2E-01
ssc05152:Tuberculosis							-1.63	1.4E-02	1.6E-01
ssc05160:Hepatitis C				-1.56	1.0E-02	1.2E-01			
ssc05162:Measles							-1.9	0.0E+00	8.0E-02
ssc05163:Human cytomegalovirus infection									
ssc05164:Influenza A				-1.69	0.0E+00	5.4E-02	-1.73	3.1E-03	1.2E-01
ssc05166:Human T-cell leukemia virus 1 infection							-1.36	4.7E-02	4.5E-01
ssc05168:Herpes simplex infection				-1.72	2.2E-03	4.5E-02	-1.65	9.2E-03	1.6E-01
ssc05169:Epstein-Barr virus infection				-1.77	0.0E+00	4.0E-02	-1.87	0.0E+00	7.3E-02
ssc05170:Human immunodeficiency virus 1 infection							-1.36	4.5E-02	4.5E-01
ssc05200:Pathways in cancer	1.42	2.3E-02	6.8E-01						
ssc05217:Basal cell carcinoma	1.61	5.3E-02	8.9E-01						
ssc05310:Asthma				-1.78	1.4E-02	4.0E-02	-1.78	3.8E-03	8.8E-02
ssc05320:Autoimmune thyroid disease	1.43	1.1E-01	6.8E-01	-2.12	0.0E+00	3.7E-04	-1.9	1.7E-03	7.3E-02
ssc05321:Inflammatory bowel disease (IBD)				-1.59	1.6E-02	1.1E-01	-1.34	1.1E-01	4.5E-01
ssc05322:Systemic lupus erythematosus				-1.68	6.3E-03	5.7E-02	-1.5	2.5E-02	2.7E-01
ssc05323:Rheumatoid arthritis							-1.65	1.2E-02	1.5E-01
ssc05330:Allograft rejection	-1.4	9.5E-02	4.0E-01	-2.17	0.0E+00	0.0E+00	-1.96	0.0E+00	8.1E-02
ssc05332:Graft-versus-host disease	-1.67	1.8E-02	7.5E-02	-2.24	0.0E+00	0.0E+00	-1.73	9.0E-03	1.1E-01
ssc05340:Primary immunodeficiency				-1.34	1.2E-01	3.3E-01	-2.12	1.8E-03	4.1E-02
ssc05414:Dilated cardiomyopathy (DCM)							-1.53	3.3E-02	2.4E-01
ssc05416:Viral myocarditis				-1.89	2.1E-03	1.5E-02	-1.83	7.0E-03	8.5E-02
ssc05418:Fluid shear stress and atherosclerosis	1.36	1.1E-01	7.0E-01						

Table 3.3 (cont.)

[a]KEGG pathway identifier.

[b]normalized enrichment score; positive value indicate enrichment among genes over-expressed in pigs from control gilts exposed to weaning stress (CON_WEAN) and from PRRSV-challenged gilts nursing (MPA_NURS); negative values indicate enrichment among genes over-expressed in pigs from control gilts nursing (CON_NURS) and from PRRSV-challenged gilts exposed to weaning stress (MPA_WEAN).

[c]False Discovery Rate adjusted P-value.

[d]P-value < 0.00001

Table 3.4. P-value (P), FDR-adjusted P-value (FDR) and gene expression profiles (log2(fold change) between pig groups) of functionally annotated genes that presented at least one significant interaction (*) of main effect of weaning, maternal immune activation (MIA), or sex at FDR-adjusted P-value < 0.1.

	MIA	MIA	Sex	Sex	Weaning	Weaning
Symbol	P	FDR	P	FDR	P	FDR
LOC110257905	4.E-01	1.E+00	1.E-36	2.E-32	4.E-01	1.E+00
PYURF	4.E-25	7.E-21	2.E-20	3.E-17	2.E-20	4.E-16
EIF1AY	9.E-03	1.E+00	6.E-34	5.E-30	2.E-01	1.E+00
EIF2S3Y	6.E-02	1.E+00	2.E-32	8.E-29	4.E-01	1.E+00
GH1	8.E-01	1.E+00	2.E-32	8.E-29	4.E-01	1.E+00
DDX3Y	1.E-01	1.E+00	9.E-32	3.E-28	3.E-01	1.E+00
LOC100625207	3.E-01	1.E+00	2.E-27	4.E-24	9.E-01	1.E+00
LOC110255257	8.E-01	1.E+00	2.E-24	3.E-21	1.E-01	1.E+00
LOC110257883	2.E-01	1.E+00	2.E-24	3.E-21	1.E+00	1.E+00
LOC110255204	6.E-09	2.E-05	8.E-02	1.E+00	7.E-14	6.E-10
LOC110255320	1.E+00	1.E+00	5.E-22	9.E-19	1.E+00	1.E+00
VHZ	8.E-20	7.E-16	8.E-04	3.E-01	4.E-04	9.E-01
CGA	9.E-01	1.E+00	3.E-19	4.E-16	4.E-01	1.E+00
OTX2	9.E-10	4.E-06	2.E-09	2.E-06	2.E-01	1.E+00
LOC110257894	9.E-01	1.E+00	7.E-14	1.E-10	9.E-01	1.E+00
SIX1	5.E-01	1.E+00	1.E-13	1.E-10	2.E-04	5.E-01
RGS16	7.E-07	1.E-03	3.E-09	3.E-06	9.E-01	1.E+00
LOC110257896	9.E-01	1.E+00	1.E-13	2.E-10	8.E-01	1.E+00
LOC110260685	4.E-01	1.E+00	5.E-03	1.E+00	3.E-01	1.E+00
IGHG	9.E-11	5.E-07	3.E-01	1.E+00	5.E-01	1.E+00
CHRNA2	2.E-07	4.E-04	3.E-05	1.E-02	7.E-01	1.E+00
NTS	4.E-05	4.E-02	2.E-04	8.E-02	3.E-01	1.E+00
AHNAK2	8.E-05	7.E-02	5.E-05	3.E-02	2.E-01	1.E+00
CALB1	1.E-04	8.E-02	2.E-06	1.E-03	4.E-01	1.E+00
PCP4	4.E-04	2.E-01	1.E-05	7.E-03	1.E+00	1.E+00
FOXB1	2.E-05	2.E-02	6.E-05	3.E-02	6.E-01	1.E+00
DLK1	6.E-03	1.E+00	2.E-06	2.E-03	1.E+00	1.E+00
KRT8	1.E-02	1.E+00	3.E-09	3.E-06	1.E-05	5.E-02
NEXN	1.E-04	9.E-02	5.E-06	3.E-03	6.E-01	1.E+00
LHB	3.E-01	1.E+00	1.E-08	1.E-05	6.E-01	1.E+00
ZFY	1.E+00	1.E+00	2.E-08	1.E-05	7.E-01	1.E+00
CD5L	3.E-08	8.E-05	4.E-03	1.E+00	6.E-01	1.E+00
LHX9	8.E-04	5.E-01	6.E-07	4.E-04	5.E-01	1.E+00
LOC110258704	3.E-08	8.E-05	9.E-02	1.E+00	2.E-01	1.E+00
POMC	9.E-01	1.E+00	4.E-08	3.E-05	8.E-01	1.E+00

Table 3.4 (cont.)

ACP7	2.E-07	4.E-04	3.E-04	1.E-01	1.E-02	1.E+00
LOC100152327	1.E-07	3.E-04	7.E-01	1.E+00	6.E-01	1.E+00
ISM1	2.E-03	1.E+00	7.E-06	4.E-03	6.E-01	1.E+00
FAM83B	2.E-02	1.E+00	6.E-07	5.E-04	1.E-03	1.E+00
POU1F1	8.E-01	1.E+00	2.E-07	2.E-04	6.E-01	1.E+00
NTNG1	2.E-03	8.E-01	1.E-04	5.E-02	5.E-01	1.E+00
PRG4	2.E-02	1.E+00	1.E-03	4.E-01	5.E-07	3.E-03
C3H16orf89	6.E-07	9.E-04	5.E-01	1.E+00	1.E-01	1.E+00
DKK2	5.E-04	3.E-01	4.E-04	1.E-01	6.E-01	1.E+00
VILL	3.E-04	2.E-01	9.E-05	4.E-02	6.E-01	1.E+00
E2F7	5.E-03	1.E+00	1.E-05	7.E-03	5.E-01	1.E+00
C7	3.E-06	4.E-03	4.E-01	1.E+00	3.E-01	1.E+00
MARCO	4.E-06	5.E-03	1.E-01	1.E+00	5.E-01	1.E+00
CEACAM16	2.E-02	1.E+00	3.E-04	1.E-01	9.E-01	1.E+00
GRID2IP	1.E-03	7.E-01	1.E-04	5.E-02	4.E-01	1.E+00
FAM163A	1.E-03	7.E-01	8.E-04	3.E-01	6.E-02	1.E+00
SLC2A7	7.E-06	7.E-03	3.E-01	1.E+00	2.E-01	1.E+00
PLXDC1	4.E-03	1.E+00	6.E-03	1.E+00	7.E-01	1.E+00
UBD	8.E-01	1.E+00	9.E-02	1.E+00	3.E-03	1.E+00
MFAP5	3.E-01	1.E+00	2.E-02	1.E+00	2.E-05	5.E-02
LOC110256276	3.E-02	1.E+00	2.E-02	1.E+00	2.E-01	1.E+00
CPS1	8.E-01	1.E+00	4.E-03	1.E+00	1.E-03	1.E+00
SFRP5	7.E-01	1.E+00	2.E-03	6.E-01	2.E-05	6.E-02
SLC4A1	4.E-03	1.E+00	1.E-03	4.E-01	2.E-02	1.E+00
LOC100525692	1.E-01	1.E+00	2.E-01	1.E+00	2.E-01	1.E+00
CPNE9	4.E-02	1.E+00	2.E-04	7.E-02	8.E-01	1.E+00
EPGN	7.E-03	1.E+00	2.E-03	5.E-01	1.E+00	1.E+00
EPCAM	3.E-01	1.E+00	5.E-05	3.E-02	3.E-01	1.E+00
VIPR2	8.E-03	1.E+00	1.E-03	4.E-01	4.E-01	1.E+00
LOC106505355	7.E-05	7.E-02	7.E-01	1.E+00	6.E-01	1.E+00
MSX1	8.E-01	1.E+00	9.E-05	4.E-02	1.E-01	1.E+00
LOC106504234	7.E-01	1.E+00	4.E-01	1.E+00	4.E-03	1.E+00
SYNDIG1L	2.E-02	1.E+00	3.E-03	9.E-01	8.E-01	1.E+00
LOC110261683	2.E-04	2.E-01	2.E-01	1.E+00	2.E-02	1.E+00
LDLRAD2	1.E-01	1.E+00	7.E-01	1.E+00	1.E-01	1.E+00

Table 3.4 (cont.)

	MIA*Sex	MIA*Sex	Weaning*MIA	Weaning*MIA	Weaning*Sex	Weaning*Sex
Symbol	P	FDR	P	FDR	P	FDR
LOC110257905	3.E-01	1.E+00	9.E-01	1.E+00	4.E-01	1.E+00
PYURF	4.E-15	2.E-11	2.E-17	2.E-13	2.E-36	4.E-32
EIF1AY	1.E-02	1.E+00	1.E-01	1.E+00	2.E-01	1.E+00
EIF2S3Y	9.E-02	1.E+00	8.E-01	1.E+00	5.E-01	1.E+00
GH1	2.E-19	3.E-15	8.E-01	1.E+00	7.E-22	5.E-18
DDX3Y	1.E-01	1.E+00	4.E-01	1.E+00	3.E-01	1.E+00
LOC100625207	4.E-01	1.E+00	3.E-01	1.E+00	1.E+00	1.E+00
LOC110255257	8.E-01	1.E+00	1.E-01	1.E+00	1.E-01	1.E+00
LOC110257883	2.E-01	1.E+00	1.E+00	1.E+00	1.E+00	1.E+00
LOC110255204	3.E-17	2.E-13	1.E-23	2.E-19	8.E-07	3.E-03
LOC110255320	1.E+00	1.E+00	1.E+00	1.E+00	1.E+00	1.E+00
VHZ	1.E-05	8.E-03	2.E-06	5.E-03	2.E-02	1.E+00
CGA	2.E-13	5.E-10	5.E-01	1.E+00	1.E-14	8.E-11
OTX2	6.E-17	3.E-13	3.E-08	1.E-04	5.E-06	1.E-02
LOC110257894	9.E-01	1.E+00	9.E-01	1.E+00	1.E+00	1.E+00
SIX1	3.E-08	3.E-05	2.E-01	1.E+00	9.E-09	4.E-05
RGS16	1.E-13	4.E-10	1.E-04	2.E-01	1.E-05	2.E-02
LOC110257896	8.E-01	1.E+00	1.E+00	1.E+00	7.E-01	1.E+00
LOC110260685	4.E-04	1.E-01	2.E-11	1.E-07	2.E-01	1.E+00
IGHG	5.E-02	1.E+00	3.E-01	1.E+00	9.E-01	1.E+00
CHRNA2	1.E-10	3.E-07	1.E-04	2.E-01	1.E-03	1.E+00
NTS	1.E-09	2.E-06	2.E-02	1.E+00	5.E-03	1.E+00
AHNAK2	1.E-09	2.E-06	8.E-03	1.E+00	2.E-02	1.E+00
CALB1	1.E-09	2.E-06	2.E-02	1.E+00	1.E-03	8.E-01
PCP4	2.E-09	2.E-06	8.E-03	1.E+00	1.E-03	8.E-01
FOXB1	2.E-09	2.E-06	7.E-02	1.E+00	2.E-02	1.E+00
DLK1	2.E-09	3.E-06	5.E-01	1.E+00	3.E-03	1.E+00
KRT8	7.E-05	3.E-02	3.E-01	1.E+00	2.E-04	2.E-01
NEXN	7.E-09	8.E-06	1.E-03	1.E+00	6.E-04	6.E-01
LHB	1.E-04	6.E-02	5.E-01	1.E+00	8.E-05	1.E-01
ZFY	8.E-01	1.E+00	8.E-01	1.E+00	1.E+00	1.E+00
CD5L	1.E-02	1.E+00	4.E-01	1.E+00	2.E-01	1.E+00
LHX9	3.E-08	3.E-05	1.E-02	1.E+00	1.E-03	8.E-01
LOC110258704	3.E-01	1.E+00	2.E-01	1.E+00	2.E-01	1.E+00
POMC	7.E-06	4.E-03	8.E-01	1.E+00	2.E-05	3.E-02
ACP7	5.E-07	4.E-04	4.E-08	1.E-04	1.E-05	2.E-02
LOC100152327	2.E-02	1.E+00	2.E-01	1.E+00	5.E-01	1.E+00
ISM1	2.E-07	1.E-04	8.E-03	1.E+00	4.E-04	4.E-01
FAM83B	2.E-07	2.E-04	9.E-04	1.E+00	8.E-06	2.E-02
POU1F1	8.E-04	3.E-01	7.E-01	1.E+00	5.E-05	7.E-02

Table 3.4 (cont.)

NTNG1	4.E-07	3.E-04	1.E-02	1.E+00	7.E-03	1.E+00
PRG4	2.E-01	1.E+00	5.E-01	1.E+00	2.E-01	1.E+00
C3H16orf89	8.E-01	1.E+00	7.E-04	9.E-01	5.E-01	1.E+00
DKK2	1.E-06	1.E-03	6.E-03	1.E+00	6.E-03	1.E+00
VILL	2.E-06	1.E-03	2.E-02	1.E+00	9.E-03	1.E+00
E2F7	2.E-06	1.E-03	6.E-02	1.E+00	3.E-03	1.E+00
C7	6.E-01	1.E+00	3.E-03	1.E+00	2.E-01	1.E+00
MARCO	6.E-01	1.E+00	4.E-01	1.E+00	3.E-01	1.E+00
CEACAM16	4.E-06	3.E-03	3.E-02	1.E+00	2.E-02	1.E+00
GRID2IP	5.E-06	3.E-03	2.E-01	1.E+00	4.E-02	1.E+00
FAM163A	5.E-06	3.E-03	2.E-03	1.E+00	3.E-03	1.E+00
SLC2A7	5.E-01	1.E+00	3.E-03	1.E+00	5.E-01	1.E+00
PLXDC1	2.E-05	9.E-03	4.E-03	1.E+00	2.E-02	1.E+00
UBD	1.E-02	1.E+00	2.E-05	3.E-02	6.E-02	1.E+00
MFAP5	5.E-02	1.E+00	8.E-01	1.E+00	1.E-01	1.E+00
LOC110256276	2.E-01	1.E+00	2.E-05	3.E-02	3.E-01	1.E+00
CPS1	3.E-02	1.E+00	4.E-02	1.E+00	2.E-05	3.E-02
SFRP5	7.E-02	1.E+00	6.E-01	1.E+00	6.E-02	1.E+00
SLC4A1	3.E-03	8.E-01	9.E-03	1.E+00	2.E-05	3.E-02
LOC100525692	3.E-05	2.E-02	2.E-01	1.E+00	7.E-01	1.E+00
CPNE9	3.E-05	2.E-02	1.E-01	1.E+00	5.E-03	1.E+00
EPGN	5.E-05	3.E-02	5.E-02	1.E+00	3.E-02	1.E+00
EPCAM	4.E-03	9.E-01	4.E-01	1.E+00	8.E-03	1.E+00
VIPR2	6.E-05	3.E-02	1.E-01	1.E+00	2.E-02	1.E+00
LOC106505355	3.E-02	1.E+00	9.E-01	1.E+00	6.E-01	1.E+00
MSX1	3.E-03	8.E-01	3.E-01	1.E+00	2.E-03	1.E+00
LOC106504234	1.E-01	1.E+00	9.E-05	2.E-01	2.E-02	1.E+00
SYNDIG1L	1.E-04	5.E-02	2.E-01	1.E+00	2.E-02	1.E+00
LOC110261683	1.E-04	7.E-02	2.E-02	1.E+00	1.E-01	1.E+00
LDLRAD2	2.E-04	7.E-02	9.E-04	1.E+00	5.E-02	1.E+00

Table 3.4 (cont.)

	MIA*Weaning				Weaning*Sex				MIA*Sex			
Symbol	CN-CW	CN-PN	CW-PW	PN-PW	NF-NM	NF-WF	NM-WM	WF-WM	CF-CM	CF-PF	CM-PM	PF-PM
LOC110257905	0.16	0.08	-0.08	0.00	-12.56	-1.17	0.08	-11.30	-12.62	-1.26	0.13	-11.23
PYURF	-0.06	-2.35	-0.24	2.05	-0.46	0.09	9.74	9.19	-0.15	-2.03	-1.07	0.82
EIF1AY	-0.15	-0.07	0.03	-0.05	-11.49	0.29	-0.11	-11.89	-13.01	-1.95	0.09	-10.96
EIF2S3Y	-0.13	-0.14	-0.02	-0.02	-10.85	0.54	-0.08	-11.47	-12.35	-1.83	0.04	-10.48
GH1	8.90	9.21	-1.04	-1.34	-10.02	-0.44	7.79	-1.80	-9.61	0.40	7.79	-2.22
DDX3Y	-0.20	-0.19	-0.04	-0.05	-11.16	0.49	-0.13	-11.78	-12.84	-2.08	0.00	-10.76
LOC100625207	-0.19	-0.26	0.04	0.11	-9.51	0.66	-0.04	-10.21	-9.98	-0.27	0.01	-9.69
LOC110255257	-0.15	-0.19	0.21	0.25	-9.78	0.06	0.04	-9.79	-10.50	-1.11	0.12	-9.27
LOC110257883	-0.31	-0.41	0.11	0.21	-10.36	0.76	-0.05	-11.17	-11.13	-0.75	-0.04	-10.41
LOC110255204	-5.03	-3.44	5.61	4.02	5.12	-1.58	-1.60	5.11	5.15	1.45	1.10	4.81
LOC110255320	-0.22	-0.34	-0.19	-0.07	-10.37	0.00	-0.15	-10.52	-10.36	0.00	-0.16	-10.52
VHZ	-1.69	-6.10	-3.43	0.99	1.72	2.00	-0.78	-1.06	-1.45	-5.85	-3.61	0.79
CGA	5.77	6.12	0.49	0.13	-6.10	-0.24	6.39	0.52	-5.86	0.27	6.49	0.36
OTX2	2.42	-0.12	0.98	3.52	-0.08	2.84	2.94	0.02	-2.91	-2.88	3.47	3.44
LOC110257894	-0.12	-0.28	0.06	0.21	-5.73	0.01	0.04	-5.69	-5.69	0.04	0.00	-5.73
SIX1	2.07	4.32	0.90	-1.35	-4.57	-2.03	2.59	0.06	-3.13	0.45	3.79	0.21
RGS16	3.21	0.68	-0.07	2.45	-0.89	2.54	3.13	-0.30	-3.25	-2.44	3.06	2.24
LOC110257896	-0.26	-0.35	0.04	0.14	-5.85	0.31	-0.07	-6.23	-5.92	0.19	-0.04	-6.15
LOC110260685	-0.48	-0.11	3.78	3.41	2.93	0.56	-0.06	2.32	2.37	0.88	1.72	3.22
IGHG	-0.51	-3.86	-4.66	-1.30	0.85	-1.50	-1.09	1.26	-0.75	-5.38	-3.27	1.36
CHRNA2	1.78	-0.72	-0.14	2.36	0.52	2.30	1.81	0.03	-1.88	-2.52	1.79	2.44
NTS	1.06	-0.18	0.05	1.29	0.20	0.88	1.58	0.90	-1.43	-1.78	2.47	2.81
AHNAK2	2.28	0.11	0.05	2.23	-0.12	2.37	2.17	-0.32	-2.13	-1.98	2.38	2.23
CALB1	1.66	0.55	-0.26	0.86	-0.69	0.92	1.61	0.00	-2.17	-1.66	2.02	1.52
PCP4	2.05	0.54	0.21	1.72	-0.54	1.49	2.32	0.29	-2.03	-1.51	2.61	2.09
FOXB1	1.20	-0.15	-0.41	0.94	0.08	0.88	1.24	0.44	-1.87	-2.17	2.04	2.34
DLK1	2.05	1.32	-0.40	0.33	-1.22	0.38	2.14	0.54	-2.42	-1.53	2.92	2.03
KRT8	-0.11	4.87	1.53	-3.45	-3.68	-3.05	0.39	-0.25	-1.88	0.70	3.47	0.89
NEXN	1.85	0.39	0.28	1.75	-0.56	1.51	2.08	0.02	-2.05	-1.54	2.20	1.69
LHB	3.13	3.35	0.16	-0.05	-3.22	0.13	3.24	-0.12	-3.16	0.32	3.36	-0.12
ZFY	-0.31	-0.41	0.05	0.16	-4.02	-0.12	-0.08	-3.98	-3.91	0.11	-0.09	-4.10
CD5L	0.55	-2.65	-2.69	0.50	-0.12	0.18	0.70	0.40	-1.41	-3.71	-1.86	0.44
LHX9	1.79	0.94	0.40	1.26	-1.19	0.91	2.10	0.00	-2.37	-1.29	2.48	1.40
LOC110258704	-0.20	-4.09	-4.24	-0.35	-0.61	-0.14	-0.60	-1.06	-0.66	-4.08	-4.23	-0.81
POMC	2.76	2.93	0.17	-0.01	-2.80	0.02	3.02	0.21	-2.79	0.06	3.19	0.33
ACP7	0.58	-1.20	-0.28	1.51	0.60	1.53	0.65	-0.29	-0.65	-1.63	-0.01	0.97
LOC100152327	-0.06	-2.84	-3.96	-1.19	1.45	-1.09	-1.40	1.14	-0.54	-4.44	-2.36	1.53
ISM1	1.86	0.82	0.44	1.48	-0.95	1.05	2.31	0.31	-1.97	-1.06	2.36	1.45
FAM83B	0.65	1.58	1.32	0.39	-1.66	-0.71	1.59	0.64	-1.34	0.27	2.58	0.98
POU1F1	2.37	2.49	0.29	0.18	-2.70	-0.11	2.65	0.06	-2.49	0.33	2.55	-0.27

Table 3.4 (cont.)

NTNG1	1.16	0.41	0.53	1.29	-0.47	0.91	1.52	0.13	-1.60	-1.11	2.09	1.60
PRG4	-2.67	2.86	2.39	-3.14	-1.84	-3.53	-2.28	-0.59	-1.22	1.10	3.64	1.32
C3H16orf89	-1.34	4.08	1.87	-3.55	-0.23	-1.38	-1.60	-0.45	-0.88	1.04	3.55	1.63
DKK2	1.32	0.00	0.11	1.42	-0.16	1.24	1.50	0.10	-1.43	-1.35	1.53	1.45
VILL	1.29	0.06	-0.07	1.16	-0.36	1.03	1.41	0.01	-1.72	-1.55	1.49	1.32
E2F7	2.33	0.82	-0.21	1.31	-1.02	1.44	2.20	-0.26	-2.20	-1.21	1.94	0.95
C7	-1.16	3.44	1.53	-3.07	0.64	-1.01	-1.79	-0.13	-0.28	1.19	2.66	1.20
MARCO	0.17	-4.15	-4.95	-0.63	-1.98	-1.67	-0.29	-0.60	-0.71	-4.39	-4.68	-1.00
CEACAM16	1.59	0.74	0.63	1.48	-0.68	1.19	1.89	0.01	-1.68	-0.84	2.27	1.43
GRID2IP	1.91	0.27	-0.35	1.29	-0.54	1.40	1.77	-0.16	-2.00	-1.62	1.60	1.22
FAM163A	0.46	0.04	0.63	1.04	-0.17	0.39	1.08	0.52	-0.91	-0.79	1.56	1.44
SLC2A7	-1.18	4.11	1.82	-3.47	-0.48	-1.17	-1.48	-0.79	-1.13	1.10	3.11	0.88
PLXDC1	0.97	-0.02	0.75	1.74	0.07	1.19	1.44	0.32	-0.99	-0.95	1.71	1.68
UBD	1.28	-1.02	-3.76	-1.46	-0.41	-1.24	-0.84	-0.01	0.62	-2.06	-2.89	-0.20
MFAP5	-2.05	1.87	1.09	-2.83	-0.97	-2.79	-1.76	0.06	-0.41	0.70	1.55	0.44
LOC110256276	-0.51	-1.08	1.88	2.44	2.05	0.81	0.47	1.72	1.94	-0.06	-0.09	1.91
CPS1	0.14	-0.52	-0.23	0.43	0.64	1.03	-0.41	-0.80	0.05	-0.34	-0.42	-0.04
SFRP5	-1.71	1.38	1.05	-2.04	-1.43	-2.63	-1.23	-0.03	-0.70	0.48	1.57	0.39
SLC4A1	0.51	-0.27	-0.30	0.48	-0.62	-0.15	1.11	0.63	-0.44	-0.61	0.07	0.23
LOC100525692	-0.95	-0.25	0.66	-0.04	2.21	-0.22	-1.47	0.96	0.51	-0.39	2.13	3.03
CPNE9	1.86	0.90	0.07	1.03	-0.96	0.93	2.02	0.13	-1.75	-0.78	1.93	0.96
EPGN	1.21	0.22	0.13	1.12	-0.32	1.03	1.31	-0.05	-1.35	-1.04	1.41	1.10
EPCAM	1.01	1.17	0.19	0.03	-1.65	-0.32	1.22	-0.11	-1.67	-0.26	1.44	0.03
VIPR2	0.85	0.23	-0.17	0.45	-0.37	0.36	0.95	0.22	-1.17	-1.03	1.18	1.04
LOC106505355	0.08	1.59	1.47	-0.03	-0.08	0.53	-0.20	-0.81	-0.03	3.12	0.85	-2.30
MSX1	0.81	1.64	0.67	-0.15	-1.71	-0.60	1.26	0.15	-1.37	0.35	1.83	0.11
LOC106504234	0.71	-1.17	-3.17	-1.30	-0.57	-1.17	-0.81	-0.21	-0.21	-2.24	-2.31	-0.28
SYNDIG1L	1.15	0.36	-0.13	0.67	-0.35	0.60	1.27	0.32	-1.13	-0.91	1.35	1.13
LOC110261683	-0.68	-1.11	-0.39	0.04	1.10	-0.07	-0.64	0.53	-0.03	-1.30	0.14	1.41
LDLRAD2	-0.42	-0.13	1.38	1.09	1.58	0.24	0.00	1.34	1.14	0.29	1.11	1.96

P = P-value ; FDR = FDR-adjusted P-value (FDR)

Interaction (*) of main effect of weaning, maternal immune activation (MIA), and sex

C=control, P = MIA, F = female, M = male, W = weaned, N = nursed.